

https://dspace.org/

Exploring holographic dualities

Tribelhorn, Laila

2019
https://hdl.handle.net/10539/27930

Downloaded from a DSpace repository. https://dspace.org/

Exploring Holographic Dualities

Laila Tribelhorn* 567662
Faculty of Science, School of Physics
University of the Witwatersrand

Supervised by Professor R. de Mello Koch†

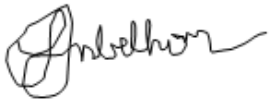
A thesis submitted to the University of the Witwatersrand in fulfilment of the requirements for candidacy for the degree of Doctor of Philosophy.
Johannesburg, 2019



* laila.tribelhorn@students.wits.ac.za
† robert.demellokoch@wits.ac.za

Declaration

I, Laila Tribelhorn, declare that the novel work presented in this thesis is my own unless otherwise stated. This work has not been submitted before for examination in any other university.



January, 2019

Acknowledgements

This work is indebted to the guidance of my supervisor, Robert de Mello Koch. His knowledge of and passion for the field has been an infinite source of motivation and inspiration and his tireless dedication has been invaluable. I am forever grateful for the opportunity.

I would like to thank the NRF for sponsoring this research and the university of the Witwatersrand for making it possible.

Contents

1 Introduction **1**

2 Background **3**
2.1 Matrix Models . . . 6
2.1.1 Ribbon Graphs . . . 6
2.1.2 The N Dependence of a Diagram . . . 13
2.1.3 Complex Matrix Model . . . 14
2.2 CFTs . . . 17
2.2.1 Conformal Symmetry . . . 17
2.2.2 State-Operator Correspondence . . . 18
2.2.3 The CFT Data . . . 19
2.3 Large N and the Duality . . . 21
2.3.1 Factorisation . . . 21
2.3.2 Triangulating a Surface . . . 22
2.4 $AdS_5 \times S^5$ in Brief . . . 25
2.4.1 Deriving the Metric . . . 25
2.4.2 Operator-State Mapping . . . 31
2.4.3 Connection with Young Diagrams . . . 32
2.5 Objects in the String Theory . . . 34
2.5.1 The Relativistic String . . . 34
2.5.2 D-branes . . . 35
2.5.3 Giant Gravitons in AdS . . . 36
2.6 Supergravity . . . 46
2.6.1 Basics of Supersymmetry and Gravity . . . 46
2.6.2 Supergravity and the Duality . . . 51

3 Eigenvalue Dynamics for Multimatrix Models **54**
3.1 Introduction . . . 54
3.2 $AdS_5 \times S^5$ Background . . . 59
3.3 Other Backgrounds . . . 68
3.4 Connection to Supergravity . . . 71
3.5 Summary and Outlook . . . 75

4 Exciting LLM Geometries **77**
4.1 Introduction . . . 77
4.2 Free CFT . . . 81
4.2.1 Background Dependence . . . 82
4.2.2 Excitations of $AdS_5 \times S^5$ . . . 86
4.2.3 Exitations of an LLM Geometry . . . 89
4.3 Weak Coupling CFT . . . 94
4.3.1 One Loop Mixing of Local Operators . . . 95
4.3.2 Mixing with delocalised Operators . . . 98
4.4 Strong Coupling CFT . . . 100
4.5 Summary and Outlook . . . 103

5 Gauge Invariants in Tensor Models **106**
5.1 Introduction . . . 106
5.2 Construction of Gauge Invariant Operators . . . 108
5.2.1 Counting and construction for bosonic tensors . . . 109
5.2.2 Counting and construction for fermionic tensors . . . 112
5.3 Correlators of Gauge Invariant Operators . . . 114
5.3.1 Bosonic Correlators . . . 114
5.3.2 Fermionic Correlators . . . 116
5.4 Algebra of the Gauge Invariant Operators . . . 117
5.5 Collective Field Theory . . . 119
5.6 Summary and Outlook . . . 124

6 Conclusions **126**

A Inequivalent, Irreducible Representations **128**

B Symmetric group and Representation Theory **130**

C Schur Polynomials **133**

D Gauss Graph Operators **137**

E Ratios of Hooks **139**

F Ratios of Factors **141**

G Delocalised Trace Structures are Preserved **142**

H Localised and Delocalised Mixing at One Loop **145**

I Correcting the Planar Limit **146**

J Check of Counting Formulas **147**

K Examples of Operators and Correlators **150**

L Identities Needed to Derive the Collective Field Theory Hamiltonian **152**

1 Introduction

The holographic principle states that the description of a quantum gravity in a volume of space can be encoded in a quantum field theory defined on the boundary of the region. This principle is evident in the study of black holes, where the maximal entropy scales like area and not volume. This means information relevant to the interior of the black hole is stored on the surface. The most successful realisation of the holographic principle is the AdS/CFT correspondence, motivated by the study of D branes. This holographic duality is an example of an equivalence between a theory with quantum gravity in a $(d+1)$ dimensional spacetime and a non-gravitational system on its boundary defined in d dimensions.

Holography has led to a huge paradigm shift in the search for a consistent theory of quantum gravity. Gauge/gravity dualities have posed an interesting field of study as they facilitate a novel and useful way to study string theories but, at the same time, they unearth some deeper questions about fundamental theories of nature. Understanding these dualities and testing them is of chief concern in this thesis and we review the relevant background needed to do so in Chapter 2.

In general, the mechanism we take is to probe beyond what is known and to extend that understanding to more general cases if possible. In particular, the planar limit of AdS/CFT is integrable and so it is natural to investigate whether this integrability persists beyond the planar limit and, if not, in what settings integrability breaks down. To go beyond the planar limit, we must consider operators with dimensions that scale with N in the large N limit. These limits are necessary to understand the AdS/CFT correspondence since operators whose dimensions scale like N are dual to giant graviton branes and operators whose dimensions scale like N^2 are dual to new geometries in supergravity.

In particular, in Chapter 4 we study string excitations of new geometries. This is done in allusion to the single trace correlators of planar $\mathcal{N}=4$ super Yang-Mills (SYM) which can be mapped to an integrable spin chain, leading to S-matrix calculations which affirm the duality. Such a mapping will naively be spoiled in the non-planar limit but we find a subset of excitations which can be identified with excitations of the vacuum, making use of the restricted Schur polynomial basis which is orthogonal. We consider planar excitations to facilitate comparison between correlators in the planar and non-planar sectors.

Carrying out the large N expansion for most matrix models is still beyond our current capabilities. A class of models for which the expansion is possible is the complex matrix model for a single matrix. In these cases, calculations can be reduced to the study eigenvalue dynamics which facilitates a huge reduction in the degrees of freedom. The physics of the planar limit can be formulated by using the density of eigenvalues as a dynamical variable and the resulting collective field theory has found application in descriptions of LLM geometries. These are supergravity geometries dual to the $\frac{1}{2}$-BPS states of $\mathcal{N}=4$ SYM.

Supergravity is a low energy limit of the string theory. At scales much lower than the string energy scale we find this theory decouples from the string theory. An interesting question arises

here in light of what AdS/CFT has taught us and motivated by the single matrix case: is there a similar decoupling in the field theory? Can we match states in supergravity with operators of a certain class in the CFT? Understanding how this works and attempting to answer these questions is an important goal of this thesis and one of the ways we will attempt to explore holography in these settings. In Chapter 3 we extend the relationship between eigenvalue dynamics and supergravity to the two matrix model. This involves constructing an eigenvalue picture for the model and motivating an AdS/CFT interpretation.

Collective field theory descriptions have been insightful to our understanding of holography. It is not clear why a fundamental theory of gravity should be dual to an effective theory without gravity or how gravity manifests from a strongly coupled gauge theory, despite our understanding of the mapping between CFT operators and supergravity geometries. It has been shown that by reorganising a field theory in terms of the gauge invariant observables, the same expansion parameter emerges that we have when studying gravity at strong coupling. This gives some insight into how to treat the CFT, which naturally has the field theory coupling as the loop expansion parameter.

A collective field theory approach to the study of $\mathcal{N} = 4$ SYM is particularly difficult because the space of gauge invariants is large and we do not expect to be able to construct the dynamics of these invariants. However, vector models are much simpler than matrix models and their collective dynamics can be built explicitly. The vector field description has been useful to the study of the SYK model, a model which may be a simple solvable example of holography. The large N physics of SYK is identical to a tensor model. Tensor models are easier to work with than vector models, and possibly have a richer space of gauge invariants than vector models. For these reasons, we aim to construct the gauge invariants of bosonic and fermionic tensor models in Chapter 5, in the hope that they are simpler to manage than those of matrix models.

The research appearing in chapters 3 through 5 is novel and can be found published as follows. Chapter 3 is based on work in the article "Eigenvalue Dynamics for Multimatrix Models" which is published in Physical Review D, Volume 96:026011 in 2017. Chapter 4 is based on work appearing in the article "Exciting LLM Geometries" published in the Journal of High Energy Physics, Volume 1807:146 in 2018. Chapter 5 is based on work appearing in the article "Gauge Invariants, Correlators and Holography in Bosonic and Fermionic Tensor models" published in the Journal of High Energy Physics, Volume 1709:011 in 2017.

The findings of this research is summarised in Chapter 6 which concludes the findings of this thesis. Additional technical information related to the background and research chapters can be found in the appendices.

2 Background

This chapter documents the necessary concepts and details needed to tackle the novel research presented in chapters 3 through 5. This should familiarise the reader with the field of interest by marrying literature review with standard concepts which have been learned through the course of this PhD and that are relevant to said research.

It is presently understood that physics can be described by four forces: gravity, the weak force, the strong force and electromagnetism. We understand how the latter three forces induce dynamics on matter, that is we can write down a Lagrangian for them but we only understand gravity partially. Gravity on large length scales is well described by Einstein's theory of general relativity, but not on the much smaller scales where physics is described by quantum theories of mechanics and fields. We know how to include quantum effects into gravity but we cannot go beyond the Planck length. In the language of quantum field theory, gravity is not renormalisable. In the language of general relativity, we cannot trust the theory in regions where the spacetime becomes singular.

Quantum field theories are written in terms of bare parameters. These are not physical. We don't measure these in the lab. In a perturbative study of quantum field theory, divergences appear in diagrams that contain loops. Virtual particles with any momentum allowed by momentum conservation run in these loops, so that sums over all allowed virtual particle states becomes integrals over particle 4-momenta. These integrals are often divergent. In renormalised perturbation theory, we split our parameters into a sum of a physical parameter (which is measured) and a bare parameter (which isn't). The bare parameters appear in our counter terms and these are seen to remove the divergences in our theory so that the physical parameters are finite. The BPHZ theorem (for Bogoliubov, Parasiuk, Hepp and Zimmermann) states that all divergences in a general quantum field theory are removed by counter terms to all orders in the perturbation, so long as the theory is renormalisable [1],[2],[3]. This tries to treat quantum field theory.

Generally, we can also think about quantum field theories as effective theories and we can introduce a momentum cut-off, Λ, such that integrating over momentum when calculating Feynman diagrams does not give us arbitrarily large values. It was Wilson's insight, however, that any quantum field theory (QFT) is intrinsically defined with a cutoff Λ that is physically significant. His insight was that QFT is not a fundamental theory. It is an effective theory with energy scale defined by the length-scale of what we are observing. For example, friction is not understood by considering all the interactions of the atoms of two objects that are moving against each other. We need only understand it macroscopically to make sense of it. The length scales of atoms is simply too small and we instead imagine a collection of atoms and study the effective interaction of that collection. Similarly, QFT breaks down at length scales that are very small:

$$\Lambda = \frac{\hbar}{l}$$

where l is the shortest length scale. New physics is needed to describe what happens beyond this scale.

So QFTs that are understood as fundamental theories of nature need to be renormalisable. We are interested in quantum gravity, and so we can ask whether we can write down a renormalisable QFT that couples to gravity. To this end, consider the Einstein-Hilbert action.

$$\mathcal{S}_{EH} = \frac{1}{16\pi G_N} \int d^d x \sqrt{-g} R$$

where G_N is our coupling to gravity, R is the Ricci scalar and g is the metric determinant. Metric components are unitless. We can see this by considering

$$ds^2 = g_{\mu\nu} dx^\mu dx^\nu$$

The left hand side of the equality has dimensions of L^2 and each dx^μ has dimension L. Thus we see that $g_{\mu\nu}$ has dimension L^0 so it is dimensionless. The Ricci scalar is built out of derivatives and products of Christoffel symbols. For the purpose of dimensional analysis, we only note that these are proportional to the derivative, ∂_μ, squared. Thus, R has dimensions L^{-2}. We integrate over $d^d x$ which has dimension L^d. The action is dimensionless giving us that

$$[G_N] = L^{-\Delta_{G_N}}$$

where $\Delta_{G_N} = d - 2$. If $d > 2$, then $\Delta_{G_N} > 0$. This tells us that G_N is irrelevant. Relevant and marginal operators, $\mathcal{O}_i$, have dimension $\Delta_{\mathcal{O}_i} \leq 0$. Relevant operators grow as we integrate out small distance – high energy – modes (Wilson's idea). Irrelevant operators do not do this. They flow to zero at larger distances – low energy. Thus, Wilson's renormalisation group flow explains why all low energy theories describing nature are renormalisable theories.

The problem with non-renormalisable field theories is that they cannot be continued to high energies without encountering some difficulties. Renormalisable theories require a finite number of fixed parameters to be predictive at every energy because there are a finite number of divergent loop integrals. The loss of predictive power in non-renormalisable theories means that there are many theories with different behaviours at high-energy whose low-energy behaviours can be described by the same theory. If we consider an expansion of the effective Lagrangian of a theory in inverse powers of the momentum cut-off, the terms with the non-renormalisable operators are suppressed at low-energy. The point is that the renormalisable part does not depend on the cut-off. To study a fundamental theory of nature, we need to probe the high-energy scale. This means we have to consider an infinite number of parameters to deal with the UV divergences, which implies that the theory has no predictive power. The fact that quantum gravity is non-renormalisable means that we cannot feasibly study it at high-energy using an effective field theory approach. Thus QFT is not the correct framework to describe quantum gravity.

String theory is a theory of quantum gravity. The AdS/CFT correspondence as proposed in [4] is a duality between type IIB string theory on an $AdS_5 \times S^5$ background and $\mathcal{N} = 4$ Super Yang-Mills (SYM) which is a gauge theory that lives on the boundary. This is an exact equivalence between the two theories which implies we can translate between the theories. Since field theories are much better understood, it is often practical to study the field theory and relate that to the string theory. This thesis aims to explore this holographic duality in

different settings. The holographic principle, which tells us that a quantum theory of gravity must be describable by a boundary theory which does not include gravity, is non-trivial. The gauge/ gravity correspondence itself is interesting because it provides a way to study string theory and thereby learn about quantum gravity. More than that, the holographic nature of this correspondence is intriguing and may ultimately furnish a cornerstone for our understanding of nature.

The space AdS_5 has an $SO(2,4)$ isometry, which is the conformal group in four dimensions. AdS_5 has negative curvature and can be described by embedding a hyperboloid into $\mathbb{R}^{4,2}$. This can be parametrised using global AdS coordinates and conformally compactified such that the induced metric has boundary $\mathbb{R} \times S^3$. This boundary is equal to the conformal compactification of $\mathbb{R}^{3,1}$ which is related to four dimensional Euclidean space through a Wick rotation. The state-operator correspondence of the CFT has important consequences when interpreted in terms of the AdS/CFT duality. By the state-operator correspondence, states of the theory on $\mathbb{R} \times S^3$ are in one-to-one correspondence with operators in $\mathbb{R}^4$: the Hilbert space of states is isomorphic to the Hilbert space of operators. In the radial quantisation of the CFT, we can insert an operator at the origin. This defines a specific CFT state inserted at the infinite past. Evolving this state to finite time corresponds to evolving a Hilbert space defined on a sphere of radius $r \neq 0$ in the CFT. Each constant r slice in the CFT defines a Hilbert space of states. Identifying the $\mathbb{R} \times S^3$ spaces on each side of the duality allows us to identify the gauge theory operators with the string theory states.

In the following sections of this chapter we will be looking at better understanding some of the ingredients we need to talk about and understand the AdS/CFT correspondence. Thereafter we will be able to tackle some concrete questions which is the main motivation of this thesis.

2.1 Matrix Models

Matrix models in 0 dimensions are a good toy model for non-Abelian gauge theories like $\mathcal{N} = 4$ SYM, whose 6 scalar fields are matrices. They allow us to learn enough about the theory so that we can start to look at more realistic problems. The quantum (scalar) fields of $\mathcal{N} = 4$ SYM are $N \times N$ matrices. By taking the trace of products of these fields we get observables. In the planar limit, where the number of fields are fixed or grow at most like $\sqrt{N}$ as $N \to \infty$, the theory simplifies. 't Hooft [5] proposed that gauge theories in the large N limit are equivalent to string theories. By studying matrix models at large N, we learn something about the dynamics of strings and gravitons. We can explore matrix models in detail to get a feel for the machinery used to describe the planar limit. Beyond the planar limit, there are too many Feynman graphs to sum and so we need more advanced machinery to study these limits.

2.1.1 Ribbon Graphs

The Feynman graphs of a matrix model must keep track of the matrix indices. As we will see, this leads to propagators represented by double lines – ribbons. We will be using the path integral formalism and will develop our discussion in 0 dimensions. The simplification of working in 0 dimensions is that the universe has only a single event and so our field assigns a single value to this one event. The path integral reduces to an ordinary integral. The generating functional of a correlation function for a scalar field theory in 0 dimensions is

$$Z[j] = \mathcal{N} \int_{-\infty}^{\infty} d\phi \; e^{-\mathcal{S}+j\phi} \tag{2.1.1.1}$$

where $\mathcal{N}$ is the normalisation and $\mathcal{S}$ is the action for the theory. The reason for introducing this generating functional is that it allows us to calculate correlation functions by taking derivatives of $Z[j]$. The correlation function looks like

$$\langle \phi^n \rangle = \int_{-\infty}^{\infty} d\phi \; e^{-\mathcal{S}} \phi^n \tag{2.1.1.2}$$

In a $3+1$ dimensional QFT, our generating functional looks like

$$Z[J] = \int [D\phi] \; e^{i\mathcal{S} + \int d^4x \; \phi(x) J(x)} \tag{2.1.1.3}$$

and the correlation functions are

$$\begin{aligned} \langle \phi(x_1) \dots \phi(x_n) \rangle &= \int [D\phi] \; \phi(x_1) \dots \phi(x_n) e^{i\mathcal{S}} \\ &= \frac{\delta}{\delta J(x_1)} \dots \frac{\delta}{\delta J(x_n)} Z[J] \Big|_{J=0} \end{aligned} \tag{2.1.1.4}$$

We can analytically continue $t \to it$ taking us to Euclidean space. This results in $i\mathcal{S} \to -\mathcal{S}$ so that the path integral measure starts to resemble the 0 dimensional calculation. We will also

replace our scalar fields with matrix valued fields so that we study fields, M, living in the Lie algebra of $U(N)$. Finally, moving to 0 dimensions gives us

$$Z[J] = \int [dM]\; e^{-\frac{1}{2}Tr(M^2)+Tr(JM)} \tag{2.1.1.5}$$

Let's study M in more detail. It lives in the Lie algebra of $U(N)$ so it is an $N \times N$ hermitian matrix. This tells us the diagonal elements, M_{ii}, are real. The elements in the upper triangle are the complex conjugate of the elements in the lower triangle: $M_{kl} = M^*_{lk}$; $\;k < l$. Then the measure, $[dM]$, requires us to integrate over the N diagonal elements, plus the $\frac{1}{2}N(N-1)$ real parts of the elements above the diagonal (M^r_{kl}) plus the $\frac{1}{2}N(N-1)$ imaginary parts of the elements above the diagonal (M^i_{kl}). This is a total of N^2 real integrals. Our correlation function looks like

$$\begin{aligned}\langle \dots \rangle &\equiv \mathcal{N} \int [dM]\; e^{-\frac{\omega}{2}Tr(M^2)} \dots \\ &= \mathcal{N} \prod_{i=1}^{N} \int_{-\infty}^{\infty} dM_{ii} \prod_{\substack{k,l=1 \\ k>l}}^{N} \int_{-\infty}^{\infty} dM^r_{kl} \int_{-\infty}^{\infty} dM^i_{kl} \dots \end{aligned} \tag{2.1.1.6}$$

We normalise the expectation value of 1 to be 1 so that

$$\mathcal{N} \int [dM]\; e^{-\frac{1}{2}\omega Tr(M^2)} = 1 \tag{2.1.1.7}$$

For arbitrary N,

$$\mathcal{N} = \left(\frac{1}{\sqrt{2}}\right)^N \left(\sqrt{\frac{\omega}{\pi}}\right)^{N^2}$$

Now we are in a position to check whether we can use our generating functional to determine correlators. Consider

$$\langle M_{ij} M_{kl} \rangle = \int [dM]\; e^{-\frac{\omega}{2}} M_{ij} M_{kl} \tag{2.1.1.8}$$

Taking derivatives of Z with respect to J should replace the $M_{ij}M_{kl}$ in our correlator.

$$\begin{aligned}\frac{d}{dJ_{ji}} e^{Tr(JM)} &= e^{Tr(JM)} M_{kl} \delta_{jl} \delta_{ik} = e^{Tr(JM)} M_{ij} \\ \implies \frac{d}{dJ_{ji}} \frac{d}{dJ_{lk}} Z[J]\bigg|_{J=0} &= \langle M_{ij} M_{kl} \rangle \end{aligned} \tag{2.1.1.9}$$

Now that we know we can use our Z to compute correlation functions, we can turn to evaluating $Z[J]$. Consider

$$\begin{aligned}-\frac{\omega}{2}Tr(M^2) + Tr(JM) &= -\frac{\omega}{2} Tr\left(M^2 - 2\frac{JM}{\omega}\right) \\ &= -\frac{\omega}{2} Tr\left[\left(M - \frac{J}{\omega}\right)^2 - \left(\frac{J}{\omega}\right)^2\right] \\ &= -\frac{\omega}{2} Tr\left(M - \frac{J}{\omega}\right)^2 + \frac{1}{2\omega} Tr(J^2) \end{aligned} \tag{2.1.1.10}$$

where we have completed the square in the second line. We can change variables now so that $M' = M - J$ and use the fact that J is not dependent on M (we fix J to be some matrix with elements of fixed value as we integrate over M). Then $[dM] = [dM']$. This leaves us with

$$Z[J] = e^{\frac{1}{2}Tr(J^2)} \tag{2.1.1.11}$$

Now let's calculate the correlator (2.1.1.8).

$$\begin{aligned}\langle M_{ij}M_{kl}\rangle &= \frac{d}{dJ_{ji}}\frac{d}{dJ_{lk}}Z[J]\bigg|_{J=0} \\ &= \frac{1}{2\omega}\frac{d}{dJ_{ij}}(2J_{lk})Z[J]\bigg|_{J=0} \\ &= \frac{1}{\omega}\delta_{il}\delta_{jk}\end{aligned} \tag{2.1.1.12}$$

These calculations can get cumbersome when we want to consider more complicated correlators. Feynman diagrams provide a convenient language for discussing perturbative quantum field theories. This language is common when talking about scalar fields. It turns out there is a Feynman diagram language for matrix model theories and we can draw diagrams for these correlators. In this case, they are called ribbon graphs. Our rules for drawing Feynman diagrams in this theory are first stated and then detailed:

Each ribbon comes with a factor $\frac{1}{\omega}$.
Each edge has a Kronecker delta.

Ribbons are lines that join indices. Ribbon lines of a single ribbon do not cross. We join indices that are the same. Edges refer to the edge of the ribbon. We count edges going from point to point. In this case, points correspond to the indices of our Kronecker deltas.

We can try reproduce our result for $\langle M_{ij}M_{kl}\rangle$ using the ribbon graph method. We start by drawing a horizontal line. On the line we have four points, one for each index. We label them as they appear in our correlator (i then j then k then l). We start at the leftmost point, i. We cannot join it to j as ij appear on the same field. We can only join i to l and j to k if we want uncrossed ribbon lines. Our graph looks like

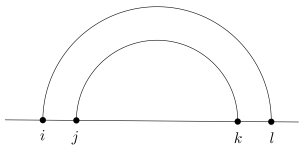


Figure 1: The ribbon graph for $\langle M_{ij}M_{kl}\rangle$

There is only one ribbon, so we acquire a factor $\frac{1}{\omega}$. The outer edge joins i and l so we acquire δ_{il} and a δ_{jk} for the inner edge. Thus

$$\langle M_{ij}M_{kl}\rangle = \frac{1}{\omega}\delta_{il}\delta_{jk}$$

as before.

The physical observables in a non-Abelian gauge theory are invariant under the local gauge symmetry. In our 0 dimensional toy model, we call

$$M \to UMU^\dagger \tag{2.1.1.13}$$

a gauge symmetry. If this transformation leaves our theory invariant, then $M' \equiv UMU^\dagger$ and M generate equivalent $U(N)$ representations and share the same eigenvalues). If M is diagonalisable, then $\mathrm{Tr}(M^n)$ can be written as the sum over i of λ_i^n where λ_i are the eigenvalues of M. Our gauge invariant observables are traces of products of M.

For example, consider

$$\langle \mathrm{Tr}(M^2) \rangle = \langle M_{ij} M_{ji} \rangle = \frac{1}{\omega} \delta_{ii} \delta_{jj} = \frac{N^2}{\omega} \tag{2.1.1.14}$$

Our indices run from $1 \dots N$ hence the N^2. Notice that the answer for our correlator is just a polynomial. This suggests that we can modify our ribbon graph notation to exclude indices. Here are our new rules with this insight:

Link points that are labelled by the same index.
Replace index pairs by a solid line, indicating which indices are summed.
Acquire an N for each closed loop.
Acquire a $\frac{1}{\omega}$ for each ribbon.

For $\langle M_{ij} M_{ji} \rangle$, we start by drawing four points. Our convention will be to connect points that have the same indices with lines on the bottom of our graph. We must connect the outer points and the inner points. This replaces labelling the points with indices which will be cumbersome for larger calculations. We join lines at the top as usual: lines of the same ribbon mustn't cross, otherwise we join however we can until all ribbons in all possible combinations are drawn.

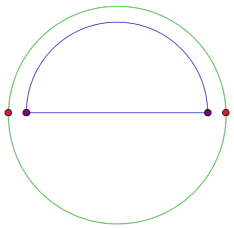


Figure 2: The ribbon graph for $\langle \mathrm{Tr}(M^2) \rangle$

The green line in Figure 2 shows one closed loop and the blue line shows another closed loop. These give us a factor N^2. The points that are coloured in the same are just to reinforce that they represent repeated indices. At the top we have a ribbon, so we gain $\frac{1}{\omega}$.

Consider $\langle \mathrm{Tr}(M^4) \rangle$. Now we will have four pairs of points that need joining. We have only one

way to indicate summed indices but we have multiple ways of connecting ribbons. For example, our first ribbon (on the leftmost side) could be connected to the next pair of dots, or the third pair or the fourth. Once that is connected, the second ribbon can only connect in one way. So we can connect in $3\times1 = 3!!$ ways. In general, for $\langle \mathrm{Tr}(M^{2n})\rangle$ we will have $(2n-1)!!$ diagrams.

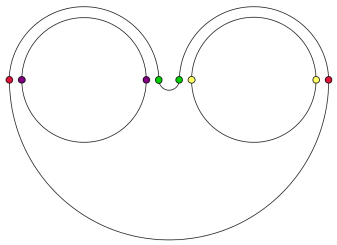


Figure 3: A ribbon graph for $\langle \mathrm{Tr}(M^4)\rangle$

Here are some examples:

$$\begin{aligned}
\langle \mathrm{Tr}(M^2)\rangle &= \frac{N^2}{\omega} \\
\langle \mathrm{Tr}(M^4)\rangle &= \frac{1}{\omega^2}(2N^3+N) \\
\langle \mathrm{Tr}(M^2)\mathrm{Tr}(M^2)\rangle &= \frac{1}{\omega^2}(N^4+2N^2) \\
\langle \mathrm{Tr}(M^2)\mathrm{Tr}(M^4)\rangle &= \frac{1}{\omega^3}(2N^5+9N^3+4N)
\end{aligned} \tag{2.1.1.15}$$

We see something interesting in the limit where we take $N \to \infty$.

$$\begin{aligned}
\langle \mathrm{Tr}(M^2)\rangle &= \frac{N^2}{\omega} \\
\langle \mathrm{Tr}(M^4)\rangle &= \frac{2N^3}{\omega^2}\left(1+\frac{1}{2N^2}\right) \to \frac{2N^3}{\omega^2} \\
\langle \mathrm{Tr}(M^2)\mathrm{Tr}(M^2)\rangle &= \frac{N^4}{\omega^2}\left(1+\frac{2}{N^2}\right) \to \frac{N^4}{\omega^2} \\
\langle \mathrm{Tr}(M^2)\mathrm{Tr}(M^4)\rangle &= \frac{2N^5}{\omega^3}\left(1+\frac{9}{2N^2}+\frac{4}{N^4}\right) \to \frac{2N^5}{\omega^3}
\end{aligned} \tag{2.1.1.16}$$

Remarkably, in this limit, the expectation value of products of our gauge invariant observables are products of their expectation values. That is

$$\begin{aligned}
\langle \mathrm{Tr}(M^2)\rangle\langle \mathrm{Tr}(M^2)\rangle &= \langle \mathrm{Tr}(M^2)\mathrm{Tr}(M^2)\rangle \\
\langle \mathrm{Tr}(M^2)\rangle\langle \mathrm{Tr}(M^4)\rangle &= \langle \mathrm{Tr}(M^2)\mathrm{Tr}(M^4)\rangle
\end{aligned} \tag{2.1.1.17}$$

This is called factorisation. The fact that it holds tells us that taking $N \to \infty$, which was 't Hooft's idea [5], is taking a classical limit of the theory. See Section 2.3.1 for a more detailed explanation of factorisation and its implications for our theory.

Up till this point we have only considered the free field theory. We will now consider adding an interaction term. The concepts are the same as the scalar field theory (which we are more familiar with), and we add a coupling term of strength g to the exponential. Now correlators are given by

$$\langle \dots \rangle = \mathcal{N} \int [dM] e^{-\frac{\omega}{2}\mathrm{Tr}(M^2) - g\mathrm{Tr}(M^4)} \dots \tag{2.1.1.18}$$

We can complete the square in the exponent, as before, to obtain a Gaussian integral which we know how to do. We keep the same normalisation as before. The difference now comes in with the interaction term which we expand using a Taylor series. Our generating functional is

$$\begin{aligned} Z[J] &= \sum_{q=0}^{\infty} \left(-g \frac{d}{dJ_{ba}} \frac{d}{dJ_{cb}} \frac{d}{dJ_{dc}} \frac{d}{dJ_{ad}} \right)^q \frac{\mathcal{N}}{q!} \int [dM] e^{\frac{\omega}{2}\mathrm{Tr}(M^2) + \frac{1}{2\omega}\mathrm{Tr}(J^2)} \\ &= \sum_{q=0}^{\infty} \frac{1}{q!} \left(-g \frac{d}{dJ_{ba}} \frac{d}{dJ_{cb}} \frac{d}{dJ_{dc}} \frac{d}{dJ_{ad}} \right)^q e^{\frac{1}{2\omega}\mathrm{Tr}(J^2)} \end{aligned} \tag{2.1.1.19}$$

where we have used the earlier result that

$$\frac{d}{dJ_{ij}} \leftrightarrow M_{ji}$$

We can see that we will have many more terms than we did for the free theory. In fact, due to the interaction vertex, we have 15 diagrams for $\langle \mathrm{Tr}(M^2) \rangle$ at order g whereas we only had 1 diagram for the same correlator in the free theory. In the scalar field theory, we know that adding loops comes with factors of $\hbar$. The more loops we have, the further we move away from the classical limit. As we add interaction vertices, i.e.: increase the allowed orders of g, we form an increasing number of loops. Often it is sufficient to say the coupling is weak and neglect these higher order terms.

Consider $\langle \mathrm{Tr}(M^2) \rangle$. The method outlined above gives us

$$\langle \mathrm{Tr}(M^2) \rangle = \left[1 - g \left(\frac{2N^3}{\omega^2} + \frac{N}{\omega^2} \right) \right] \frac{N^2}{\omega} - g \frac{8N^3}{\omega^3} - g \frac{4N}{\omega^3} \tag{2.1.1.20}$$

The vacuum diagrams are the diagrams which do not connect the pair of dots representing our matrix elements with the interaction vertex and are written in parenthesis above. Normalising our partition function for the interacting theory will naturally remove these vacuum graphs.

Before we had normalised $Z[g = 0, J = 0] = 1$. We will now use $Z'[g, J] = (Z[g, J = 0])^{-1} Z[g, J]$. Call the normalised partition function $Z[g, J]$ instead of $Z'[g, J]$ for convenience. So if we want to work out correlators in the interacting theory that are normalised to exclude vacuum graphs, then we work out the non-normalised correlators and divide by the partition

function of the non-normalised theory at $J = 0$. For example

$$\begin{aligned}\langle \mathrm{Tr}(M^2)\rangle &= \frac{d}{dJ_{ji}}\frac{d}{dJ_{ij}}Z(J)\bigg|_{J=0} \\ &= \frac{1}{Z'(J=0)}\frac{d}{dJ_{ji}}\frac{d}{dJ_{ij}}Z'(J)\bigg|_{J=0} \\ &= \frac{1}{\omega^3}\frac{N^2[\omega^2 - g(2N^3+N)] - 8gN^3 - 4gN}{\frac{\omega^2 - g(2N^3+N)}{\omega^2}}\end{aligned} \tag{2.1.1.21}$$

Here we have only gone up to first order in g. To be more explicit for the denominator, recall that

$$Z'[J] = \sum_{q=0}^{\infty}\frac{1}{q!}\left(-g\frac{d}{dJ_{ba}}\frac{d}{dJ_{cb}}\frac{d}{dJ_{dc}}\frac{d}{dJ_{ad}}\right)^q \mathcal{N}\int [dM]e^{\frac{\omega}{2}\mathrm{Tr}(M^2)} \tag{2.1.1.22}$$

When $q = 0$ the only term we have is

$$\mathcal{N}\int [dM]e^{\frac{\omega}{2}\mathrm{Tr}(M^2)} = 1 \tag{2.1.1.23}$$

from our original definition of $\mathcal{N}$. When $q = 1$ we have the above term plus

$$-g\langle M_{ab}M_{bc}M_{cd}M_{da}\rangle = -g\langle \mathrm{Tr}(M^4)\rangle = -g(2N^3+N)\frac{1}{\omega^2} \tag{2.1.1.24}$$

Thus, our normalised correlator, (2.1.1.21), is

$$\begin{aligned}\langle \mathrm{Tr}(M^2)\rangle &= \frac{1}{\omega^3}\left\{N^2[\omega^2 - g(2N^3+N)] - 8gN^3 - 4gN\right\}\left\{1 + \frac{g(2N^3+N)}{\omega^2} - \mathcal{O}(g^2)\right\} \\ &= \frac{1}{\omega^3}\left\{[\omega^2 + g(2N^3+N) - g(2N^3+N)] - 8gN^3 - 4gN\right\} + \mathcal{O}(g^2) \\ &= \frac{N^2}{\omega} - \frac{g}{\omega^3}(8N^3+4N)\end{aligned} \tag{2.1.1.25}$$

Comparing this with (2.1.1.20) we see the vacuum diagrams have indeed been removed.

For the free theory, we saw that we could take $N \to \infty$ and treat $\frac{1}{N}$ as a small parameter to get the classical limit: factorisation held. In scalar field theories, we usually consider the coupling to be weak and this is why higher order terms are less relevant. In light of this idea, we choose to assume g is small and take $N \to \infty$. To this end, we consider $\langle \mathrm{Tr}(M^2)\rangle$ again, but this time up to order g^2.

$$\begin{aligned}\langle \mathrm{Tr}(M^2)\rangle &= \frac{N^2}{\omega} - \frac{g}{\omega^3}(8N^3+4N) + \frac{g^2}{\omega^5}(144N^4+224N^2) \\ &\approx \frac{N^2}{\omega} - \frac{gN^3}{\omega^3}\left(8 + \frac{4}{N^2}\right) + \frac{g^2N^4}{\omega^5}\left(144 + \frac{224}{N^2}\right)\end{aligned} \tag{2.1.1.26}$$

There does not appear to be a good and consistent way of taking $N \to \infty$ since the term with the highest power in N is a term with the highest power in g. Even if we consider the coupling to be weak, we can't seem to make sense of the large powers of N. We don't have a good concept of

what it means to be weakly coupled here. That is, we must now ask whether $\frac{1}{g}$ or N dominates.

We proceed by introducing a double scaling limit. We take $N \to \infty$ and $g \to 0$. We know that "$0 \cdot \infty$" is an indeterminate form so we define our scaling to go such that $\lambda = gN$ is fixed. Further, we choose λ to be small. Now we have

$$\begin{aligned}\langle \mathrm{Tr}(M^2) \rangle &= \frac{N^2}{\omega} - \frac{N^2}{\omega^3}\left(8\lambda + \frac{4\lambda}{N^2}\right) + \frac{N^2}{\omega^5}\left(144\lambda^2 + \frac{224\lambda^2}{N^2}\right) \\ &\approx \frac{N^2}{\omega} - \frac{8\lambda N^2}{\omega^3} + \frac{144\lambda^2 N^2}{\omega^5}\end{aligned} \tag{2.1.1.27}$$

In the first line we can see that the leading term is of order N^2 and that holds for each term in the perturbation series (for each power of λ).

λ is called the 't Hooft coupling. We can do an expansion in this coupling since each term looks like some function of λ. In general, for an observable O,

$$\langle O \rangle = \sum_{n=0}^{\infty} f_n(\lambda) N^{2-2n} \tag{2.1.1.28}$$

We can see from the correlator we calculated that $f_n(\lambda)$ is not a trivial function, especially at higher orders of λ. This choice of coupling has not reduced the complexity of our calculation. We also have preserved the structure of terms so, like the free theory, we have terms that go like $\frac{1}{N^2}$ that will fall away at large N. This is interesting because it introduces $\frac{1}{N^2}$ as a new coupling constant. See Section 2.3.1 for more detail.

2.1.2 The N Dependence of a Diagram

We have seen that organising our counting in terms of N is important because at large N only the leading terms survive at fixed 't Hooft coupling. To reduce our work, it is useful to determine the N dependence of each diagram so that we can omit counting the diagrams which are subleading in N. We start by rescaling our matrix fields and determining the rescaled partition function.

$$\begin{aligned} & M = \sqrt{N} M' \\ & \implies \frac{\omega}{2}\mathrm{Tr}(M^2) = \frac{N\omega}{2}\mathrm{Tr}(M'^2) \\ & \implies g\mathrm{Tr}(M^4) = gN^2\mathrm{Tr}(M'^4) = N\lambda\mathrm{Tr}(M'^4) && \because \lambda = gN \\ & \implies \int [dM'] e^{-\frac{N\omega}{2}\mathrm{Tr}(M'^2)} \sum_{q=0}^{\infty} \left(-N\lambda\mathrm{Tr}(M'^4)\right)^q \frac{1}{q!} = Z[0] \end{aligned} \tag{2.1.2.1}$$

It looks like we have made the transformation $\omega \to N\omega$. Correlators transform as

$$\langle M_{ij} M_{kl} \rangle = \frac{\delta_{ij}\delta_{kl}}{\omega} \to \frac{\delta_{ij}\delta_{kl}}{N\omega}$$

Usually we would assign a factor $-g$ for each vertex. Now we assign a $-\lambda N$ to each vertex. We can expand the sum in the partition function, $Z[0]$, to get

$$Z[0] = \int [dM'] e^{-\frac{N\omega}{2}\mathrm{Tr}(M'^2)} \left(1 - \lambda N \mathrm{Tr}(M'^4) + \frac{\lambda^2 N^2}{2}(\mathrm{Tr}(M'^4))^2 + \mathcal{O}(\lambda^3)\right) \tag{2.1.2.2}$$

The first order in λ gives us three diagrams. Two of them have three closed loops, one vertex and two ribbons. So these two diagrams each contribute a factor

$$\left(\frac{1}{N\omega}\right)^2 (-\lambda N) N^3$$

according to our Feynman rules. We introduce some new terminology here. Each loop encloses/ borders a surface. We call these surfaces faces. We count ribbons by starting and ending on a vertex (we know how to count ribbons in the free theory already). We call ribbons the edges of the faces. Vertices do not get a name change. In the new terminology we get an N for each face, a $\frac{1}{N\omega}$ for each edge and a $-\lambda N$ for each vertex. In general, a diagram will contribute a factor

$$\left(\frac{1}{N\omega}\right)^E (-\lambda N)^V (N)^F \tag{2.1.2.3}$$

to the sum. We are now in a position to state the N dependence of a graph with E edges, F faces and V vertices. It is N^{F+V-E}. The quantity $F + V - E$ is a topological invariant called the Euler characteristic. To better understand this topological interpretation, see Section 2.3.2.

2.1.3 Complex Matrix Model

Up to now we have studied matrix models in 0 dimensions where our operators were Hermitian. This was a toy model for a non-Abelian gauge theory like $\mathcal{N} = 4$ SYM. Whilst this taught us most of the intuition we need, we need to modify the model in order to account for the fact that operators in $\mathcal{N} = 4$ SYM are built from complex fields. In particular, the half BPS operators[1] are built from a single complex matrix. In this discussion, we will call this matrix Z. The methodology is very similar to what we have had before and so this discussion is less detailed.

Consider the Hermitian matrices M_1 and M_2. Define

$$Z = \frac{M_1 + iM_2}{\sqrt{2}} \qquad\qquad Z^\dagger = \frac{M_1 - iM_2}{\sqrt{2}} \tag{2.1.3.1}$$

Our new correlation function is

$$\begin{aligned} \langle \dots \rangle &= \int [dZ dZ^\dagger]\, e^{-\omega \mathrm{Tr}(ZZ^\dagger)} \dots \\ &= \int [dM_1][dM_2]\, e^{-\frac{\omega}{2}[\mathrm{Tr}(M_1^2)+\mathrm{Tr}(M_2^2)]} \dots \end{aligned} \tag{2.1.3.2}$$

[1] To be half BPS means the operators are invariant under half the supersymmetries of the theory. In this theory, the four types of supercharges (hence $\mathcal{N} = 4$) generate the superymmetry. Half BPS means that half of these supercharges commute with the fields. A consequence of this is that two and three point correlation functions are given exactly by their free field limits.

where $\langle 1 \rangle = 1$. We introduce the generating function

$$Z[J_1, J_2] = \int [dM_1][dM_2]\; e^{-\frac{\omega}{2}[\mathrm{Tr}(M_1^2)+\mathrm{Tr}(M_2^2)]+\mathrm{Tr}(J_1 M_1)+\mathrm{Tr}(J_2 M_2)} \tag{2.1.3.3}$$

We know from previous sections that

$$\langle (M_a)_{ij}(M_b)_{kl} \rangle = \frac{d}{d(J_a)_{ji}} \frac{d}{d(J_b)_{lk}} Z[J]\bigg|_{J=0}$$

where a and b run over 1 and 2. Like before, we complete the square in the numerator of our partition function but for both M_1 and M_2 separately. We then shift the measure of our integral and use our normalisation condition to obtain

$$Z[J_1, J_2] = e^{\frac{1}{2\omega}[\mathrm{Tr}(J_1^2)+\mathrm{Tr}(J_2^2)]} \tag{2.1.3.4}$$

We are now in a position to calculate the two point function. Using $Z_{ij} = (M_1)_{ij} + i(M_2)_{ij}$ and $Z^\dagger_{kl} = (M_1)_{kl} - i(M_2)_{kl}$ we get the following results:

$$\begin{aligned} \langle Z_{ij} Z^\dagger_{kl} \rangle &= \frac{1}{\omega} \delta_{ij}\delta_{kl} \\ \langle Z_{ij} Z_{kl} \rangle &= 0 = \langle Z^\dagger_{ij} Z^\dagger_{kl} \rangle \end{aligned} \tag{2.1.3.5}$$

This tells us that we must add a new rule when drawing our Feynman diagrams. We must differentiate between which pairs of dots represent the indices of Z and which pair of dots represent the indices of $Z^\dagger$. Ribbons that start on dots for the Zs must end on dots for the $Z^\dagger$s. This reduces the allowed combinations we can have and so the number of graphs we have for this model is less than in an Hermitian matrix model. Recall that physical observables are given by expectation values of traces of operators. In general,

$$\langle \mathrm{Tr}(Z^J)\mathrm{Tr}(Z^{\dagger J}) \rangle = \text{a sum of } J! \text{ graphs}$$

The leading term plus first two correction terms for the above correlator is

$$\langle \mathrm{Tr}(Z^J)\mathrm{Tr}(Z^{\dagger J}) \rangle = JN^J + \frac{J^4 N^{J-2}}{6} + \frac{J^5 N^{J-2}}{24} \tag{2.1.3.6}$$

This is the genus 0 (sphere), genus 1 (torus) and genus 2 (double torus) contribution to the sum. If we hold the scale dimension of our operators fixed at $\mathcal{O}(1)$, then we can neglect the higher genus contributions as we take $N \to \infty$. If the number of fields in each trace grows as we take $N \to \infty$ then we can no longer ignore terms corresponding to the higher genus ribbon graphs. We make this transition precisely when we let J grow like $\sqrt{N}$, i.e.: this is the transition point between the planar and non-planar limit of the theory. We can see this by looking at (2.1.3.6) and noticing that when $J = \mathcal{O}(N)$, the genus 1 and genus 0 contributions are of the same order in N.

Ultimately, we want to study the non-planar limit of the theory as this is where new physics is emergent. We learn from the above discussion that the non-planar limit is a much more difficult problem to study than the planar limit. In fact, when we study the non-planar limit, different

trace structures mix. The operators $Z, Z^\dagger$ have scaling dimension 1.[2] Now we can define the normalised operator as follows:

$$O_n \equiv \frac{1}{\sqrt{nN^n}}\mathrm{Tr}(Z^n) \tag{2.1.3.7}$$

Correlators then look like

$$\langle O_n O_m^\dagger \rangle = \delta_{nm}\left(1 + \mathcal{O}\left(\frac{1}{N^2}\right)\right) \tag{2.1.3.8}$$

A multitrace correlator would look as follows in this notation:

$$\langle O_n O_m O_{n+m}^\dagger \rangle = \frac{\sqrt{nm(n+m)}}{N}\left(1 + O\left(\frac{1}{N^2}\right)\right) \tag{2.1.3.9}$$

If the dimensions of our operators scale like $\mathcal{O}(1)$, then the above correlator goes to zero as $N \to \infty$. This tells us that different multitrace structures do not mix in the planar limit and so we only have to study single trace operators. When our operators have scale dimension of $\mathcal{O}(N)$ then the above correlator cannot be neglected so we must consider all possible multitrace structures.

To get around the problem of summing such a large number of diagrams, we use an alternative method to sum ribbon graphs. This method involves finding a basis of operators that diagonalise the two point function, the restricted Schur polynomial basis, and we see that this is equivalent to finding a set of projectors on the vector space $V_N^{\otimes n}$ (where $Z^{\otimes n}$ lives). This allows us to replace a question in quantum field theory by one in group theory. This basis is introduced in Appendix C and it is the primary tool we use to study physics beyond the planar limit and conduct the investigation into holography presented in this thesis.

[2] If you look at the kinetic term in a dimensionless ($c = \hbar = 1$) action then these fields must have dimension L^{-1}.

2.2 CFTs

Not only is $\mathcal{N}=4$ SYM a matrix model, it has vanishing β function and is therefore a conformal field theory at the quantum level. Usually classical scale invariance is broken when we renormalise but theories with vanishing β function are counter examples because they are either at fixed points of the renormalisation group or there is no RG flow. The latter is the case for $\mathcal{N}=4$ SYM because the β function is zero for arbitrary coupling.

CFTs have a range of interesting properties, one of which is that any CFT can be specified by what is called the CFT data. The conformal symmetry constrains the system to the extent that only the conformal dimensions of the operators and the OPE coefficients are needed to completely specify all correlators. We will elucidate this in this section and build an intuition for what it means to be a CFT. These properties not only help us understand one side of the AdS/CFT correspondence, but we will use them directly in Chapter 4.

Another goal of this section is to illustrate how the the state-operator correspondence arises from using the conformal symmetry of a CFT. This is applied to the AdS/CFT mapping between states, discussed in Section 2.4, and is what allows us to map operators in the field theory to states in the string theory. In particular, the Schur polynomials with $\mathcal{O}(N)$ scaling dimensions are dual to giant gravitons and the Schur polynomials with $\mathcal{O}(N^2)$ scaling dimensions are dual to new geometries.

2.2.1 Conformal Symmetry

Conformal field theories are theories that have a conformal symmetry. These are interesting theories to study because they have the most symmetry possible without being trivial, so there is much that we can potentially learn from them. We will see later in the section that CFTs are specified by two lists of numbers. This is very different to what we are used to, which is writing down a Lagrangian to specify the theory. When we study CFTs, we can compute correlators without ever looking at a Lagrangian.

Conformal transformations preserve angles. This requires the metric to transform with the factor $g_{\mu\nu} \to \Omega^2 g_{\mu\nu}$. This means the spacetime interval only transforms by the overall factor Ω^2 so the null intervals are preserved as well as the timelike/ spacelike character of the separation between points i.e.: we preserve the causal structure. The infinitesimal parameter in these types of transformations is the conformal Killing vector, ξ^μ, which obeys the conformal Killing equation $\nabla_\mu \xi_\nu + \nabla_\nu \xi_\mu = \frac{2}{d}\nabla_\tau \xi^\tau g_{\mu\nu}$ where we consider the infinitesimal scaling $\Omega(x) = 1+\omega(x)$.

The generators for this symmetry group include the Poincaré generators (Lorentz, $M_{\mu\nu}$, and spacetime translations, P_μ), the generator for scaling, D, and the special conformal generators, K_μ. In total we have $\frac{d(d-1)}{2}+d+1+d = \frac{(d+2)(d+1)}{2}$ independent conformal transformations. This is the number of independent components of an antisymmetric matrix that is $(d+2)\times(d+2)$. Indeed, we can define the algebra as Lorentzian in $d+2$ dimensions which we know has antisymmetric generators. Of the two new classes of generators we have introduced, scaling is

the easiest to understand. Special conformal transformations are a little more complicated. They are composed of successive transformation: inversion then translation the inversion. As such the generator of infinitesimal special conformal transformation looks more elaborate. The algebra obeyed by these generators is as follows:

$$\begin{aligned}
[P_\alpha, M_{\mu\nu}] &= i\eta_{\alpha\mu}P_\nu - i\eta_{\alpha\nu}P_\mu \\
[K_\alpha, M_{\mu\nu}] &= i\eta_{\alpha\mu}K_\nu - i\eta_{\alpha\nu}K_\mu \\
[M_{\alpha\beta}, M_{\mu\nu}] &= i\eta_{\alpha\mu}M_{\nu\beta} - i\eta_{\alpha\nu}M_{\mu\beta} + i\eta_{\beta\mu}M_{\alpha\nu} - i\eta_{\beta\mu}M_{\alpha\mu} \\
[D, P_\mu] &= iP_\mu \\
[D, K_\mu] &= -iK_\mu \\
[P_\mu, K_\mu] &= 2i\eta_{\mu\nu}D + 2iM_{\mu\nu} \\
[D, M_{\mu\nu}] &= 0
\end{aligned} \tag{2.2.1.1}$$

Dimensional analysis of the above tells us what dimensions these generators should have. For example, we know spacetime translations are generated by linear momentum which has dimension L^{-1}. This is all we need to know and can infer from the first the commutator that Lorentz generators are dimensionless and so on. The commutator of the vector generators with D looks like the oscillator algebra with P_μ the creation operator and K_μ the annihilation operator. These operators have different length dimension though. We ask ourselves at this point in what regime could they be related by daggering? Dimensional analysis hints that in this regime daggering has to be related to inversion. The last commutation relation tells us that we can simultaneously diagonalise D and $M_{\mu\nu}$. An easier way to write the above algebra is as follows. We identify the generators with components of new generators L_{AB} where $L_{\mu\nu} = M_{\mu\nu}$, $L_{d,d+1} = D$, $L_{\mu d} = \frac{1}{2}(P_\mu + K_\mu)$ and $L_{\mu d+1} = \frac{1}{2}(P_\mu = K_\mu)$. Then the L_{AB} obey the algebra of the Lorentz generators but generalised to the $d+2$ dimensional space and the algebra is $so(2,d)$.

2.2.2 State-Operator Correspondence

For the AdS/CFT correspondence, we study $\mathcal{N} = 4$ SYM on $\mathbb{R} \times S^3$. To get from $\mathbb{M}_4$ to $\mathbb{R} \times S^3$ we perform a Wick rotation and a conformal transformation, identifying the radius in $\mathbb{E}_4$ with time slices on the cylinder: $r = e^\tau$. At each time, so at each S^3 slice of the cylinder, we have a Hilbert space of states. This means that we need to know the fields everywhere along the S^3 to specify a state. In $\mathbb{E}_4$, at each radius there is a surface with a Hilbert space. The Hilbert space at the origin is conformally related to the Hilbert space of the S^3 at time $\tau = -\infty$, which is on the boundary of the cylinder. Usually when we quantise, different Hilbert spaces are related by a unitary transformation with the time evolution operator. The type of scheme described above is called radial quantisation. Different spheres/ Hilbert spaces are now related by scaling which is a conformal transformation.

In Euclidean space, unitary operators become operators with reflection positivity. This implies daggering is related to inversions since we have $r = e^\tau \implies r^\dagger = e^{-\tau} = r^{-1}$. This is necessary to keep us in the same Hilbert space. But $P_\mu^\dagger = IP_\mu I = K_\mu$ so we can identify these

as ladder operators in this scheme as suggested in the previous section. This is also why we label states by their scaling dimension and spin. There is an operator of lowest dimensions called the primary operator. This means that if we act with K_μ on this operator, we will get zero. We can organise the irreps of a CFT into the primary fields and their descendants, which are obtained by acting on the primary field with P_μ.

States are distributed over space but operators are localised. Naturally, the origin is localised because it is a point. We can insert an operator with dimension Δ at the origin on the vacuum state. Then $O_\Delta(x=0)|0\rangle = |\Delta\rangle$, since $D|\Delta\rangle = i\Delta|\Delta\rangle$. If we insert the operator elsewhere we have

$$O_\Delta(x)|0\rangle = e^{iP\cdot x}O_\Delta(x=0)e^{-iP\cdot x}|0\rangle = \sum_{n=0}^{\infty}\frac{(-1)^n}{n!}(P\cdot x)^n O_\Delta(x=0)|0\rangle$$

since the vacuum is invariant under all conformal transformations. We see we have a superposition of states with different eigenvalues. If we insert a primary operator at the origin, we will get a state that is annihilated by K_μ and vice versa. These operators and states are in a 1-1 correspondence and this is the state-operator correspondence.

2.2.3 The CFT Data

We now briefly outline some properties of CFT which we will use in Chapter 4. Recall that the Maldacena-Zhiboedov theorem [6] says that conformal symmetry is the most amount of symmetry we can hope to put into a theory without having something trivial. This conformal invariance completely determines the two and three point functions up to the spectrum of primary operators (labelled by dimension and spin) and the OPE coefficients. This means we can figure out what these correlators look like by requiring they are invariant under the symmetries. By doing this, we find the following general forms. The two point function for a scalar field looks like

$$\langle O_{\Delta_1}(x_1)O_{\Delta_2}(x_2)\rangle = \frac{C\delta_{\Delta_1\Delta_2}}{|x_1-x_2|^{\Delta_1+\Delta_2}} \tag{2.2.3.1}$$

where C is some constant which we can tune to 1 by appropriate choice of basis. The three point function is

$$\langle O_{\Delta_1}(x_1)O_{\Delta_2}(x_2)O_{\Delta_3}(x_3)\rangle = \frac{\lambda_{O_{\Delta_1}O_{\Delta_2}O_{\Delta_3}}}{|x_1-x_2|^{\Delta_1+\Delta_2-\Delta_3}|x_2-x_3|^{\Delta_2+\Delta_3-\Delta_1}|x_1-x_3|^{\Delta_1+\Delta_3-\Delta_2}} \tag{2.2.3.2}$$

When we try to compute the four point function in this manner, we learn that we can include arbitrary functions of conformal cross ratios. These ratios are invariant under the symmetries, so we can only determine the correlator up to some arbitrary function of these ratios. Thus, the four point functions are highly non-trivial.

Operator product expansions take a product of two nearby operators, $O_{\Delta_1}(x)O_{\Delta_2}(0)$ and expresses them as a sum of local operators.

$$O_{\Delta_1}(x)O_{\Delta_2}(0) = \sum_{\text{primaries } O_i}\lambda_{O_{\Delta_1}O_{\Delta_2}O_i}C_{O_i}(x,\partial_y)O_i(y)\big|_{y=0} \tag{2.2.3.3}$$

where the $C_{O_i}(x, \partial_y)$ are determined by conformal invariance. The operator product expansion thus allows us to turn n-point correlation functions into a sum of $n-1$-point correlation functions. The idea is that we approximate two nearby local operators with a sum of operators at one of the points. Proceeding in this way, we can express any CFT n-point function in terms of 3-point functions which are highly constrained, as reviewed above.

To summarise, we have illustrated that all correlation functions in a CFT depend only on the OPE coefficients and the spectrum of the primary operators. This is all the data we need to completely determine the CFT. This is useful for when we come across a theory which we don't have access to the action but we wish to identify, as we will see in Chapter 4.

2.3 Large N and the Duality

2.3.1 Factorisation

Consider some quantum system. This system may be in a number of different states, labelled by i. Suppose we want to perform a measurement. The value of an observable O_I in the state i is $O_I(i)$. The probability to be in this state is μ_i with $\sum_i \mu_i = 1$ (normalisation) and $\mu_i \geq 0 \; \forall i$. Then the expected value of O_I (or the average value) is $\sum_i \mu_i O_I(i)$. Factorisation is the statement that

$$\langle O_{I_1}, \ldots, O_{I_n} \rangle = \langle O_{I_1} \rangle \ldots \langle O_{I_n} \rangle \tag{2.3.1.1}$$

for any observables O_I. We know what the probability to be in the state i is so we can rewrite the left hand side as

$$\langle O_{I_1}, \ldots, O_{I_n} \rangle = \sum_i \mu_i O_{I_1}(i) O_{I_2}(i) \ldots O_{I_n}(i) \tag{2.3.1.2}$$

We can rewrite the right hand side of (2.3.1.1) as

$$\langle O_{I_1} \rangle \ldots \langle O_{I_n} \rangle = \sum_{i_1} \mu_{i_1} O_{I_1}(i_1) \cdot \sum_{i_2} \mu_{i_2} O_{I_2}(i_2) \cdots \sum_{i_n} \mu_{i_n} O_{I_n}(i_n) \tag{2.3.1.3}$$

We see that the left hand side of (2.3.1.1) involves a sum over i, which is a sum over the states of the system. The right hand side, however, involves a sum over i for each expectation value. The only way to achieve equality is if we only have one state participating in the sum. That is, $\mu_i = 1$ for $i = i^*$ and $\mu_i = 0$ for $i \neq i^*$. Now both sides give

$$O_{I_1}(i^*) O_{I_2}(i^*) \ldots O_{I_n}(i^*) \tag{2.3.1.4}$$

We can only be in one state: this is the classical limit. That is, for factorisation to hold our system must be in a classical limit.

The limit as $N \to \infty$ is a classical limit because factorisation holds. In particular, the large N limit of $\mathcal{N} = 4$ SYM is given by the classical limit of type IIB string theory on $AdS_5 \times S^5$.

It is natural to ask what the other terms are that fall away when we take N to be large. If we look back at (2.1.1.16), then we see that the first order correction to this stringy classical limit goes like $\frac{1}{N^2}$. In quantum field theory, the first order quantum correction comes with an $\hbar$. If we relate these ideas then $\frac{1}{N^2} \equiv \hbar_{\text{string}}$. So with strings, just like with field theory, we have quantum corrections or string corrections. It turns out that this is not the only uncertainty we have in string theory.

We are used to having the coupling constant as being a source of fundamental uncertainty and it is related to $\hbar$. For every order in the perturbation (or each vertex in our Feynman diagrams) we introduce an $\hbar$. This is related to an uncertainty in the string theory – the string tension. The fact that we have strings replacing points introduces these new uncertainty because we cannot resolve points in spacetime. The string tension is inversely related to the size of the string and this gives us new uncertainty.

Our theory has gauge group $U(N)$ so our observables are built out of $N \times N$ Hermitian matrices. We know that $\frac{1}{N^2}$ appears as a new source of fundamental uncertainty (in the free and interacting theory), and that the size of our matrices in the field theory controls this uncertainty.

2.3.2 Triangulating a Surface

In Section 2.1.2, we saw that the N dependence of a diagram was given by a number called the Euler characteristic which is a topological invariant. We will now motivate this observation and discuss its implications for the duality between $\mathcal{N} = 4$ SYM and string theory on an asymptotically $AdS_5 \times S^5$ background.

Imagine two loops of ribbon tied to each other. The knot is the vertex. We can arrange these loops onto a sphere so that edges of the ribbon do not cross. This is one of the terms we would get from order λ in the above correlator. It triangulates a 2 dimensional surface, as can be seen in Figure 4. The ribbon divides the surface into patches. These patches are the faces we have introduced above.

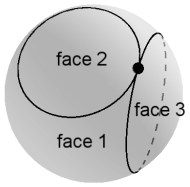


Figure 4: A representation of an $\mathcal{O}(\lambda)$ ribbon graph triangulating a sphere. The ribbons are shown as black lines.

We can imagine more intricate triangulations. Consider some such triangulation. It has four faces when viewed from one side. We can stretch this object horizontally as shown in Figure 5, creating an extra face in the middle. This stretching does not change the topology of the triangulation so the Euler characteristic should be invariant. We want to explicitly verify this.

Notice that, for this section of the triangulation, we started with four faces, five edges and two vertices. After the stretch we have five faces, eight edges and four vertices. Relating

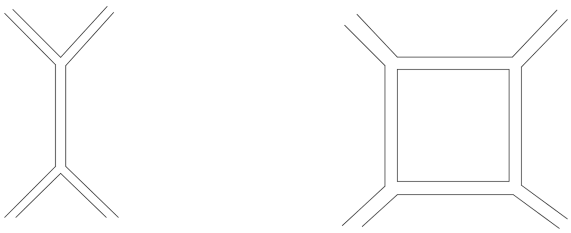


Figure 5: Stretching a piece of the ribbon configuration on one side of a sphere

quantities before and after (indicated with the primed variables) the stretch we have

$$F' = F + 1$$
$$E' = E + 3$$
$$V' = V + 2$$

Thus,

$$F' - E' + V' = F - E + V$$

We could also shrink an edge to nothing. In this case we again find

$$F'' - E'' + V'' = F - E + V$$

and the Euler characteristic is unchanged by the shrinking.

These deformations are all homeomorphisms. They preserve the topological properties of a space. This is why the Euler characteristic is a topological invariant: it does not change under a homeomorphism. This is not only true for the sphere example we have considered above. Some ribbon graphs might triangulate a torus or a pretzel. Intuitively, the more ribbons we have, the harder it becomes to triangulate a surface like a sphere (remember that our ribbons cannot cross on the surface). We see that we need surfaces like a torus, which is a sphere with a handle on it, to give us new ways to place ribbons so that they do not cross.

We do not need the triangulation to calculate what the Euler characteristic is; it can be computed directly from the topology of the surface. Every two dimensional oriented surface is topologically equivalent to a sphere with some handles stuck onto it or some holes cut out of it. So we can think of the torus as being a sphere with a handle on it. By stretching and shrinking our surface in various places, we can imagine moulding this sphere with a handle into a torus shape. The Euler characteristic for a surface has a definition in terms of the number of handles, H, and holes, h: $\chi = 2 - 2H - h$. For a sphere, there are no holes or handles. This gives an Euler characteristic of two. We can check this against the triangulation in Figure 4: $\chi = F - E + V = 3 - 2 + 1 = 2$. A torus has one handle, so it has an Euler characteristic of zero. A pretzel is a sphere with two handles, so it has an Euler characteristic of negative two. Each time we add a handle, our Euler characteristic decreases by two.

Recall that Euler characteristic gives us the N dependence of each ribbon graph. For the

ribbon graph triangulating the sphere in Figure 4, the N dependence is two. The ribbon graph that triangulates a torus is shown in Figure 6. There is only one face (or one closed loop) in this diagram and the N dependence is zero. The surface that has an Euler characteristic of zero is the torus, so this diagram must triangulate the torus. It is remarkable that the topology of the surfaces these ribbon graphs triangulate determine the graphs' N dependence.

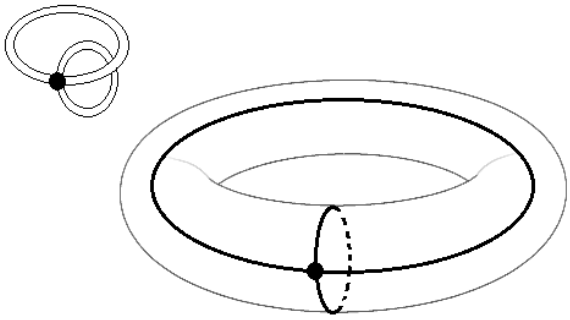


Figure 6: An $\mathcal{O}(\lambda)$ ribbon graph that triangulates a torus

When we study a perturbative quantum field theory, we use Feynman diagrams as a tool to sum terms in the perturbation series. The fact that the N dependence is related to the topology of a surface suggests that summing ribbon graphs has something to do with summing over surfaces. For a non-matrix model theory, like the scalar particle, we perform a path integral quantisation of the theory by summing over all possible worldlines. Similarly for a string theory, we must sum over all possible worldsheets the string can follow in spacetime [3]. The fact that a string traces out a surface as it moves through spacetime draws a link between a matrix model theory, where summing over ribbon graphs is related to summing over surfaces, and a string theory. In particular, $\mathcal{N} = 4$ SYM is a matrix model theory. So we see here further motivation in claiming a duality between $\mathcal{N} = 4$ SYM and a string theory which is realised by the AdS/CFT correspondence. This correspondence is a precise guess for the string theory that is dual to a particular matrix model (type IIB strings on an asymptotically $AdS_5 \times S^5$ background geometry dual to $\mathcal{N} = 4$ SYM).

Looking back at 2.1.1.16, we see that the first correction to the leading order term in our correlation functions went like $\frac{1}{N^2}$. This is a quantum correction to the classical limit (obtained by taking $N \to \infty$) which is related to $\hbar_{\text{string}}$. The Euler characteristic showed us that when the N dependence of our graphs decreased by two, we needed to a glue a handle onto our sphere. This implies that for each $\hbar_{\text{string}}$ we have for the string, we need a higher genus correction. So the genus of our surface tells us the order of the quantum correction. This suggests that we are summing over surfaces and that there is a duality between a matrix model theory and a string theory.

[3] As a particle moves through spacetime, it traces out a line (worldline). A string is one-dimensional, and so it traces out a surface as it moves through spacetime (worldsheet).

2.4 $AdS_5 \times S^5$ in Brief

This section introduces $AdS_5 \times S^5$ and motivates the mapping of states here with states in $\mathcal{N} = 4$ SYM. The state-operator correspondence of the CFT, discussed earlier, then allows us to identify operators in the CFT with states in the gravity. This is important to the goals of this thesis because by matching field theory operators with their string theory duals we are able to say concrete things about holography. We start by looking at the metric for Schwarzschild spacetime to develop our intuition.

2.4.1 Deriving the Metric

The Schwarzschild metric is a solution to the Einstein field equations in the simplest setting (uncharged, non-rotating black holes and a zero cosmological constant).

$$ds^2 = -\left(1 - \frac{2GM}{r}\right) dt^2 + \left(1 - \frac{2GM}{r}\right)^{-1} dr^2 + r^2 d\Omega_2^2 \tag{2.4.1.1}$$

This describes a black hole at the origin. The event horizon is at $r = 2GM$, which we can see because at this radius $g_{00} = 0$. The action is

$$\mathcal{S} = m \int ds = m\sqrt{-g_{\mu\nu}\dot{x}^\mu \dot{x}^\nu} d\tau = \int L dt \tag{2.4.1.2}$$

Here we use an Affine parametrisation

$$-g_{\mu\nu}\dot{x}^\mu \dot{x}^\nu = 1$$

We work out the equations of motion using the Euler-Lagrange equation.

$$\begin{aligned}
\frac{\partial L}{\partial \dot{x}^\alpha} &= -\frac{m}{\sqrt{-g_{\mu\nu}\dot{x}^\mu \dot{x}^\nu}} g_{\alpha\mu}\dot{x}^\mu \\
\implies \frac{d}{dt}\frac{\partial L}{\partial \dot{x}^\alpha} &= -\frac{m}{\sqrt{-g_{\mu\nu}\dot{x}^\mu \dot{x}^\nu}} \left(\frac{\partial g_{\alpha\mu}}{\partial x^\beta}\dot{x}^\beta \dot{x}^\mu + g_{\alpha\mu}\ddot{x}^\mu\right) \\
\frac{dL}{dx^\alpha} &= \frac{m}{2\sqrt{-g_{\mu\nu}\dot{x}^\mu \dot{x}^\nu}} \left(-\frac{\partial g_{\mu\nu}}{\partial x^\alpha}\dot{x}^\mu \dot{x}^\nu\right) \\
\implies \frac{1}{2}\frac{\partial g_{\mu\nu}}{\partial x^\alpha}\dot{x}^\mu \dot{x}^\nu &= \frac{\partial g_{\alpha\mu}}{\partial x^\beta}\dot{x}^\beta \dot{x}^\alpha + g_{\alpha\mu}\ddot{x}^\mu
\end{aligned} \tag{2.4.1.3}$$

where we used the Affine parametrisation to get the last equality. In nearly flat space and in the non-relativistic limit,

$$-g_{\mu\nu}\dot{x}^\mu \dot{x}^\nu = (\dot{x}^0)^2 - \vec{x} \cdot \vec{x} = 1 \tag{2.4.1.4}$$

If we set the speed of light, c, to 1 then $\dot{x}^0 \approx 1$ and $\dot{x}^i \approx 0$. Consider now $\alpha = i$ in (2.4.1.3).

$$\begin{aligned} \frac{1}{2}\frac{\partial g_{\mu\nu}}{\partial x^i}\dot{x}^\mu \dot{x}^\nu &= \frac{\partial g_{ii}}{\partial x^\beta}\dot{x}^\beta \dot{x}^i + g_{ii}\ddot{x}^i \\ \implies g_{ii}\ddot{x}^i &= \frac{1}{2}\frac{\partial g_{00}}{\partial x^i}\dot{x}^0\dot{x}^0 \\ \implies \ddot{x}^i &= \frac{1}{2}\frac{\partial g_{00}}{\partial x^i} = -\frac{\partial}{\partial x^i}\Phi_N \end{aligned} \tag{2.4.1.5}$$

So the Newtonian potential, Φ_N, is $-\frac{1}{2}g_{00}$. In terms of our Schwarzschild metric, $\Phi_N = \frac{1}{2}\left(1 - \frac{2GM}{r}\right)$.

$$\vec{F} = -\nabla\Phi_N = -\left(\frac{\partial}{\partial r}\hat{r} + \frac{1}{r}\frac{\partial}{\partial\theta}\hat{\theta} + \frac{1}{r\sin\theta}\frac{\partial}{\partial\phi}\hat{\phi}\right)\Phi_N = -\frac{GM}{r^2}\hat{r} \tag{2.4.1.6}$$

This tells us that M in the metric is indeed the mass of the black hole. To summarise, we have shown that the g_{00} component of the metric becomes the gravitational potential in the non-relativistic limit and the limit of an almost flat spacetime. This insight is important for the other spacetime metrics we will consider.

Consider a metric on a 10 dimensional spacetime of the form

$$ds^2 = -\frac{dt^2 - d\vec{x}\cdot d\vec{x}}{\sqrt{1+\frac{C}{r^4}}} + \sqrt{1+\frac{C}{r^4}}(dr^2 + r^2 d\Omega_5^2) \tag{2.4.1.7}$$

C is some constant and $d\vec{x}\cdot d\vec{x} = (dx^1)^2 + (dx^2)^2 + (dx^3)^2$. We see as r gets large, the space begins to look flat and we expect to recover Newtonian physics (so as $r \to \infty$ our space starts to look like $\mathcal{M}_{10}$). Thus, in this limit, we can calculate what the Newtonian potential for this space is.

$$\Phi_N = -\frac{1}{2}g_{00} = \frac{1}{2}\left(1+\frac{C}{r^4}\right)^{-\frac{1}{2}} \approx \frac{1}{2}\left(1 - \frac{C}{2r^4}\right) = \frac{1}{2} - \frac{C}{4r^4} \tag{2.4.1.8}$$

Our approximation holds since we are at large r so $\dfrac{1}{r^4}$ is small. For the 4-dimensional Schwarzschild metric, the gravitational potential falls off as $\dfrac{1}{r^2}$ or $\dfrac{1}{r^{d-2}}$. The potential for this 10-dimensional spacetime does not fall of like $\dfrac{1}{r^8}$ as expected. Instead it looks like we are in 6 dimensions. We can interpret this as the metric telling us we are filling $3+1$ dimensions (from the $(dt)^2 - d\vec{x}\cdot d\vec{x}$ terms) so that we have 6 transverse dimensions. The geometry in this limit includes a 5-sphere, S^5, which has an $SO(6)$ rotational invariance. These are rotations in the transverse dimensions. Think of an infinite rod in 3 spatial dimensions. It completely occupies one of the dimensions, so there are only two directions the field can spread in. As a result the electric field sourced by the rod falls off as $\frac{1}{r}$ and not as $\frac{1}{r^2}$. This is analogous to what we have here. It only makes sense to talk about the gravitational potential in the space that isn't already filled.

Looking at our metric, we see that $g_{00} = 0$ at $r = 0$, so there is a horizon at the origin.

This metric describes a black 3-brane. We can probe the metric more by making a few convenient adjustments. For the physics close to the brane we are concerned with small r so we can drop the $+1$ term under the square roots since the term that goes like $\frac{1}{r^4}$ dominates the behaviour. We rename our constant C to C^2. The latter adjustment is perfectly reasonable since C was arbitrary to begin with. Now we have

$$ds^2 = -\frac{r^2}{C}(dt^2 - d\vec{x} \cdot d\vec{x}) + \frac{C}{r^2}dr^2 + Cd\Omega_5^2 \tag{2.4.1.9}$$

This is the metric of $AdS_5 \times S^5$ which is a solution to the Einstein equations with a negative cosmological constant. We can study the potential after this change. We use the relation we derived earlier

$$\Phi \equiv -\frac{1}{2}g_{00} = \frac{r^2}{2C} \tag{2.4.1.10}$$

This is quadratic, just like the potential for the harmonic oscillator. What this means is that, for small r, any object launched radially outward from the brane (at $r = 0$) will ultimately return to the brane. So geodesics on $AdS_5 \times S^5$ will go away from the origin and then come back, just like with the harmonic oscillator.

We make the coordinate transformation

$$t \to \alpha t, \quad \vec{x} \to \alpha \vec{x}, \quad r \to \frac{r}{\alpha}$$

so that our metric is unchanged. In order to leave the metric invariant, we had to have r scaling inversely with $\vec{x}$, so it looks like r is scaling like an energy.

We are interested in studying $AdS_5 \times S^5$, the space in which the type IIB string theory we are interested in lives. A metric on this space is (2.4.1.9), with $C = 1$ and the coordinate transformation $z = \frac{1}{r}$.

$$ds^2 = \frac{1}{z^2}(-dt^2 + d\vec{x} \cdot d\vec{x} + dz^2) + d\Omega_5^2 \tag{2.4.1.11}$$

This is the metric in the Poincaré patch of AdS_5. We have a horizon as $z \to \infty$ and the boundary of the spacetime is at $z = 0$. This metric is defined to cover a patch of AdS_5 only and not the whole spacetime. We have a choice which patch we want to cover, each with its own metric. Our discussion will only consider the above metric and we will see later what portion of the space it covers.

We will explore how this metric can be obtained by embedding AdS_5 into flat space and then we will see how to obtain a metric which describes the whole of the space. We are embedding our curved manifold into a flat space. In curved spaces, the geometry we are used to using in flat space (Euclidean geometry) no longer holds. In particular, the way we measure distances between points is different. We can figure out what the metric in this curved space is if we can figure out how to measure distances between points. That is, we are figuring out how to measure distances between points on the curved space by using the rule (essentially the Pythagoras theorem) that tells us how to measure the distance between points on the flat space.

The AdS_{p+2} geometry has constant negative curvature and its metric describes a hyperbolic

geometry. We want to induce the metric on our manifold by embedding into flat space. Our manifold is a surface in embedding space. Just like we have the equation of a sphere in $(p+2)$ dimensions, $\sum_{i=0}^{p+1}(X^i)^2 = R^2$, we have a negative curvature analogue which describes a hyperboloid

$$(X^0)^2 + (X^{p+2})^2 - \sum_{i=1}^{p+1}(X^i)^2 = R^2 \tag{2.4.1.12}$$

where R is the radius of curvature. Note that when we embed a hyperbolic space into a flat space we appear to gain a timelike dimension: this is required to represent the isometry of the hyperbolic space with the flat embedding space. That is, our embedding space is a $(p+3)$ flat spacetime with two timelike coordinates. Our metric is

$$ds^2 = -(dX^0)^2 - (dX^{p+2})^2 + \sum_{i=1}^{p+1}(dX^i)^2 \tag{2.4.1.13}$$

Note that we are ignoring the sphere part and looking only at AdS_{p+2} spacetime. To get the Poincaré patch, we choose the following coordinates, which satisfy the defining equation for our embedding space (2.4.1.12).

$$\begin{aligned} X^0 &= \frac{R^2}{2r}\left(1 + \frac{r^2}{R^4}(R^2 + \vec{x}\cdot\vec{x} - t^2)\right) \\ X^i &= \frac{r}{R}x^i \qquad\qquad i = 1, \ldots, p \\ X^{p+2} &= \frac{r}{R}t \\ X^{p+1} &= \frac{R^2}{2r}\left(1 - \frac{r^2}{R^4}(R^2 - \vec{x}\cdot\vec{x} + t^2)\right) \end{aligned} \tag{2.4.1.14}$$

We can work out the differentials and plug this into (2.4.1.13) to obtain

$$ds^2 = -\frac{r^2}{R^2}dt^2 + \frac{R^2}{r^2}dr^2 + \frac{r^2}{R^2}d\vec{x}^2 \tag{2.4.1.15}$$

We set $R^2 = 1$ and $z = \frac{1}{r}$ to obtain the AdS part of (2.4.1.11). Our coordinate maps become

$$\begin{aligned} X^0 &= \frac{z}{2}\left(1 + \frac{1 + \vec{x}\cdot\vec{x} - t^2}{z^2}\right) \\ X^i &= \frac{x^i}{z} \qquad\qquad i = 1, \ldots, p \\ X^{p+2} &= \frac{t}{z} \\ X^{p+1} &= \frac{z}{2}\left(1 - \frac{1 - \vec{x}\cdot\vec{x} + t^2}{z^2}\right) \end{aligned} \tag{2.4.1.16}$$

Then

$$\frac{1}{z} = \frac{X^0 - X^{p+2}}{2} \tag{2.4.1.17}$$

The left hand side describes a hyperbola with asymptote along the line $z = 0$. This splits our space up into two regions: $X^0 > X^{p+2}$ and $X^0 < X^{p+2}$. We have to choose which region we

are in by specifying the range of $r = \frac{1}{z}$. This is what we mean by having a patch on the space and this makes it clear that we are choosing which patch to cover. It is most natural to choose $r = \frac{1}{z} \geq 0$ as this looks like a radial coordinate.[4]

We can identify global coordinates, also satisfying (2.4.1.12), that describe the entire AdS_{p+2} space. We use

$$\begin{aligned} X^0 &= R \cosh\rho \cos\tau \\ X^i &= R \sinh\rho \, \eta^i \\ X^{p+2} &= R \cosh\rho \sin\tau \end{aligned} \tag{2.4.1.18}$$

It is convenient to make a coordinate choice where the η^i parametrise a unit sphere. In our case, this sphere is a p-sphere. For example, the unit sphere in 3 dimensions is given by the coordinate transformation $\eta^1 = \cos\theta \sin\phi$, $\eta^2 = \sin\theta \sin\phi$, $\eta^3 = \cos\phi$. This gives the metric $ds^2 = -dt^2 + d\phi^2 + \sin\phi d\theta^2$. Similarly in AdS_5 where our metric has two timelike coordinates, we make a coordinate transformation to spherical coordinates on the X^i for $i = 1 \ldots p+1$. Now we see that the X^i describe a p-sphere with radius $R \sinh\rho$. The components η^i look like

$$\begin{aligned} \eta^1 &= \cos(\theta_1) \\ \eta^2 &= \sin(\theta_1)\cos(\theta_2) \\ \eta^3 &= \sin(\theta_1)\sin(\theta_2)\cos(\theta_3) \\ &\vdots \\ \eta^p &= \sin(\theta_1)\sin(\theta_2)\ldots\sin(\theta_{p-1})\cos(\theta_p) \\ \eta^{p+1} &= \sin(\theta_1)\sin(\theta_2)\ldots\sin(\theta_{p-1})\sin(\theta_p) \end{aligned} \tag{2.4.1.19}$$

Here $\theta_1, \ldots, \theta_{p-1} \in [0, \pi]$ and $\theta_p \in [0, 2\pi]$. Note that $\eta^i \eta_i = 1 \implies d\eta^i \eta_i = \eta^i d\eta_i = 0$.

Now we have everything we need to calculate the induced metric for these coordinates. The result is

$$ds^2_{\text{global}} = R^2(-\cosh^2\rho d\tau^2 + d\rho^2 + \sinh^2\rho d\Omega_p^2) \tag{2.4.1.20}$$

Let's examine whether we really cover the whole space. First, consider that X^0 and X^{p+2} together describe a circle of fixed radius, for ρ constant. As we vary τ we move around the circle and varying ρ changes the radius of the circle with no restriction on how big this radius can be. Now consider X^i. The vector component ensures that we can point in any direction, no matter which value we fix ρ to be. So we truly can get to any point in the space using these coordinates.

We are interested in what happens at the boundary of our space[5]. Looking at our metric, we can examine what happens as ρ gets large. We could do the same for τ but we know $\cos\tau$ and $\sin\tau$ are periodic, so we won't learn anything new.

[4] Recall that the horizon is at $r = 0$ and we reach the boundary of the spacetime as $r \to \infty$

[5] The AdS/ CFT duality conjectures that the CFT lives on the boundary of our space. So we can think of AdS as living inside a box (like the harmonic oscillator): that is where our string theory is. The CFT lives on the surface of that box.

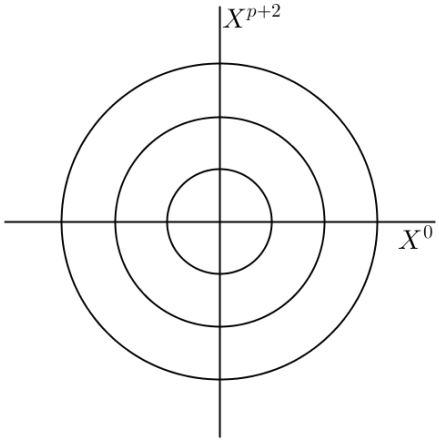


Figure 7: Circles of radius fixed by ρ

For large ρ,

$$\cosh\rho = \frac{e^{\rho}+e^{-\rho}}{2} \approx e^{\rho} \approx \frac{e^{\rho}-e^{-\rho}}{2} = \sinh\rho$$

and so our metric becomes

$$ds^2 = \left(\frac{Re^{\rho}}{2}\right)^2 \left(-d\tau^2 + d\Omega_p^2 + 4e^{-2\rho}d\rho^2\right) \tag{2.4.1.21}$$

The boundary of our manifold is at large ρ. Here any coordinate difference Δx^{μ} leads to a vanishingly small contribution to the proper distance from the ρ coordinate. This can be seen by noticing that Δs^2 is some number multiplied by $(-\Delta\tau^2 + \Delta\Omega_p^2 + 4e^{-2\rho}\Delta\rho^2)$. The coefficient of $\Delta\rho^2$ is exponentially decreasing with increasing ρ and scales this term to be very small at large ρ compared with the other terms. It is thus negligible and our metric at the boundary simplifies.

$$ds^2_{\text{boundary}} = \left(\frac{Re^{\rho}}{2}\right)^2 \left(-d\tau^2 + d\Omega_p^2\right) \tag{2.4.1.22}$$

We see that this metric has the form $\mathbb{R} \times S^p$. So the boundary of our space, AdS_{p+2}, is $\partial AdS_{p+2} = \mathbb{R} \times S^p$. For AdS_5 the boundary is $\mathbb{R} \times S^3$ which what we use for radial quantisation of a 4d CFT. So the boundary of AdS_5 is the same space on which the 4d CFT is defined.

2.4.2 Operator-State Mapping

$\mathcal{N} = 4$ SYM lives on the boundary of the AdS_5 spacetime, which is $\mathbb{R} \times S^3$. We usually define the field theory on Minkowski space, $\mathbb{R}^{1,3}$, and not $\mathbb{R} \times S^3$. However, $\mathbb{R}^{1,3}$ and $\mathbb{R} \times S^3$ are related by a conformal transformation (detailed below). $\mathcal{N} = 4$ SYM is a conformal field theory and any CFT is invariant under conformal transformations. This means that we can define $\mathcal{N} = 4$ SYM on both $\mathbb{R}^{1,3}$ and $\mathbb{R} \times S^3$.

To show that Minkowski spacetime and $\mathbb{R} \times S^3$ are related by a conformal transformation, we can Wick rotate to get the Euclidean signature for the CFT metric.

$$ds^2 = -dt^2 + d\vec{x} \cdot d\vec{x} \to dt_E^2 + d\vec{x} \cdot d\vec{x} = ds_E^2 \tag{2.4.2.1}$$

By a change of coordinates we can obtain

$$ds_E^2 = dr^2 + r^2 d\Omega_3^2 \tag{2.4.2.2}$$

We change variables so that $r = e^\tau \implies dr = e^\tau d\tau$ and then we perform a scale transformation to absorb the e^τ. $\mathcal{N} = 4$ SYM is a CFT and so the above conformal transformation will leave all physical predictions invariant. The metric we obtain

$$ds_E^2 = d\tau^2 + d\Omega_3^2 \tag{2.4.2.3}$$

is $\mathbb{R} \times S^3$. We see that our time coordinate corresponds to $\mathbb{R}$. There is a symmetry for translating in $\mathbb{R}$ in $\mathbb{R} \times S^3$, and rotational invariance associated to the 3-sphere. We can try and match this symmetry in the field theory with one in the string theory. We know that energy is conserved when we have a symmetry in time translations. We have associated the time coordinate in the string theory with the radius in the field theory.

Consider the time translation $\tau \to \tau + a$. We defined $r = e^\tau$. Under this translation, $r \to e^a e^\tau = e^a r$. This is a scale transformation so our conserved quantity is a dimension. If we scale our coordinate x by λ, then our operator scales by a factor λ^{-D} i.e.: $\mathcal{O}(\lambda x) = \lambda^{-D}\mathcal{O}(x)$. So time translations in the string theory correspond to scaling in the field theory (dilatations). This makes sense because in radial quantisation, different Hilbert spaces are related by scaling. Usually for non-CFTs they are related by time translations, implemented by the Hamiltonian. We see that we are matching the Hilbert spaces and this is a concrete example of the AdS/CFT correspondence.

In $\mathcal{N} = 4$ SYM we have $\mathcal{R}$-symmetry which is $SO(6)$ and rotates the supercharges. We have 6 scalar fields, $\phi_1, \ldots, \phi_6$. We build our complex fields by taking $Z = \phi_1 + i\phi_2$, for example. We have conservation of $\mathcal{R}$-charge in the QFT. The space S^5, in $AdS_5 \times S^5$, enjoys an $SO(6)$ isometry given by the group of rotations. We know the conserved quantity associated with rotations is angular momentum. We match these conserved quantities since they both come from the $SO(6)$ symmetry of each theory. Thus, angular momentum in the string theory can be identified with $\mathcal{R}$-charge in the field theory.

We have seen, in Section 2.1, that physical observables are traces of complex fields, Z and

$Z^\dagger$, which are gauge invariant. If we set $c = \hbar = 1$, then the action is dimensionless and the kinetic term gives us

$$\mathcal{S} = \int d^4x \, \mathrm{Tr}(\partial_\mu Z \partial^\mu Z^\dagger)$$

Dimensional analysis tells us $[Z] = [Z^\dagger] = L^{-1}$. However, observables may take the form of something like $\mathrm{Tr}(Z^2)\mathrm{Tr}(Z^3)$. This will have dimension $D = 5$. When we start looking at quantum corrections, D will include the anomalous dimensions.

The $\frac{1}{2}$ BPS operators have scaling dimension that is equal to their $\mathcal{R}$-charge and their two-point correlation functions are protected meaning that they have no anomalous dimensions. This is a consequence of supersymmetry. These operators are built out of a single scalar field. Since their dimension is equal to their $\mathcal{R}$-charge the dual state in the string theory has its energy equal to is angular momentum. In Section 2.5.3 we see how the geometric interpretation of these $\frac{1}{2}$-BPS operators can be identified with gravitons, strings or giant gravitons, depending on their angular momentum. The dual field theory operator for such a state living on the S^5 can be matched with the $\frac{1}{2}$-BPS operators when we identify angular momentum with $\mathcal{R}$-charge.

2.4.3 Connection with Young Diagrams

In [7], Schur polynomials composed of $\mathcal{O}(N)$ fields were proposed as the natural gauge theory duals to $\frac{1}{2}$-BPS giant gravitons. See Appendix C for a review of Schur polynomials. The Schur polynomial operators allow for a natural identification of operators in the gauge theory corresponding to giant gravitons and new background geometries in the string theory side of the AdS/CFT correspondence. In particular, each LLM geometry (which are regular 1/2 BPS solutions to type IIB supergravity that are asymptotically $AdS_5 \times S^5$) corresponds to a specific 1/2 BPS operator. Young diagrams which label Schur polynomials dual to new geometries have $\mathcal{O}(N^2)$ boxes.

Young diagrams that label representations of $U(N)$, which is the gauge group of $\mathcal{N} = 4$ SYM, have a restriction on the length of their columns (no more than N boxes). The fully antisymmetric representation corresponds to a single column of N rows and corresponds to a giant graviton embedded in the S^n part of the $AdS_m \times S^n$ background. We can identify boxes with discrete lumps of angular momenta. This means we have a maximum angular momentum allowed which corresponds to a maximum size of our graviton. In this way, the Young diagram prescription encodes the stringy exclusion principle as we will see in Section 2.5.3.

We can consider also a Young diagram consisting of a single single row of N boxes. This corresponds to a giant graviton expanded in the AdS_m part of the $AdS_m \times S^n$ background. This is the fully symmetric representation. This time, a limit is placed on the number of AdS giants we can have and not the size of the giants. This is because there is no restriction placed on the length of rows by working in a representation of $U(N)$. We can have at most N rows since these representations can have at most N boxes in a column. Thus there are at most N AdS giants.

Young diagrams label representations of the symmetric group (see Appendix B). Since they are composed from a discrete number of boxes, they discretise the geometry of the membrane. This discretisation removes many modes and therefore infinities from the worldvolume theory.

2.5 Objects in the String Theory

The AdS/CFT correspondence is a duality between $\mathcal{N} = 4$ SYM and type IIB string theory on an $AdS_5 \times S^5$ background. This section gives some background on the string theory and D branes which have been instrumental to AdS/CFT. In particular we discuss the giant gravitons, which are $D3$ branes that are dual to operators with large $\mathcal{R}$-charge. Type II superstring theories are defined in $D = 10$ dimensions and are maximally supersymmetric with $\mathcal{N} = 2$ supersymmetry corresponding to 32 supercharges. Type IIB string theory has massless bosonic fields, the spin-2 $G_{\mu\nu}$, the 2-form $B_{\mu\nu}$, the dilaton Φ and Ramond-Ramond gauge fields, C, $C_{\mu\nu}$ and $C_{\mu\nu\rho\sigma}$.

2.5.1 The Relativistic String

Toy Model: relativistic point particle

Before we can develop intuition for understanding the relativistic string, we need to revise our understanding of the relativistic point particle. The key ideas in this treatment extend to the two dimensional counterpart of the point particle: the string. The starting place for writing down the action for the relativistic string comes from our knowledge of special relativity where actions are Lorentz invariant. The action for a relativistic point particle is

$$\mathcal{S} = -m \int_{WL} ds \tag{2.5.1.1}$$

This action is invariant under reparametrisation of the worldline. We can rewrite the action using a parameter, λ, which labels points along the worldline. Spacetime coordinates are a function of λ. Then

$$ds = \sqrt{-g_{\mu\nu} \frac{dx^\mu}{d\lambda} \frac{dx^\nu}{d\lambda}} d\lambda \tag{2.5.1.2}$$

Usually we treat our time coordinate as a parameter and the position coordinates as dynamical degrees of freedom.

Extending the analogy

Strings sweep out a worldsheet in spacetime. This generalises the worldline to two dimensions. Thus we need two parameters. For branes in higher dimensions, we would need to introduce more parameters depending on the dimension of the worldvolume. We usually identify one parameter with a timelike coordinate (like proper time) and the rest with spacelike coordinates on the worldsheet. For closed strings the spacelike coordinate is periodic. For open strings, we need to specify the endpoints of the string with boundary conditions. The key idea for the relativistic point particle action was that it was reparametrisation invariant. If we pick

a new parameter $\tilde{\tau} = \tilde{\tau}(\tau)$, where τ is the old parameter, then the integrand becomes

$$\begin{aligned}\sqrt{-g_{\mu\nu}\frac{dx^\mu}{d\tau}\frac{dx^\nu}{d\tau}}d\tau &= \sqrt{-g_{\mu\nu}\frac{dx^\mu}{d\tilde{\tau}}\frac{d\tilde{\tau}}{d\tau}\frac{dx^\nu}{d\tilde{\tau}}\frac{d\tilde{\tau}}{d\tau}}d\tau \\ &= \sqrt{-g_{\mu\nu}\frac{dx^\mu}{d\tilde{\tau}}\frac{dx^\nu}{d\tilde{\tau}}}d\tilde{\tau} \end{aligned} \tag{2.5.1.3}$$

where we have used the chain rule in the first line. To generalise this result, define $\gamma_{ab} = \frac{\partial x^\mu}{\partial \sigma^a}\frac{\partial x^\nu}{\partial \sigma^b}g_{\mu\nu}$ where $\sigma^a = (\tau, \sigma)$ are worldsheet coordinates. For an action proportional to the area of the worldsheet (as opposed to the length of the worldline), use the determinant of γ_{ab} to define the action

$$\mathcal{S} = -T\int d^2\sigma\sqrt{-\det\gamma} \tag{2.5.1.4}$$

This action is the Nambu-Goto action for the relativistic string and the constant of proportionality, $T(= \frac{1}{2\pi\alpha'})$, is the tension of the string.

2.5.2 D-branes

Open string endpoints are characterised by boundary conditions. Dirichlet boundary conditions give rise to open strings whose endpoints end on objects called D_p-branes (where p is the number of spatial dimensions) which are solitons. D branes are hypersurfaces within the spacetime. The string is free to move in the remaining coordinates. The D brane itself fluctuates within the spacetime. The Nambu-Goto action generalises for branes in higher dimensions. It tells us about fluctuations on the brane. To study dynamics of the brane, we use the Dirac-Born-Infeld action

$$\mathcal{S}_{DBI} = -T_p\int d^{p+1}\sigma\sqrt{-\det(\gamma_{ab} + 2\pi\alpha' F_{ab})} \tag{2.5.2.1}$$

Closed strings are excitations of empty space. Since open strings end on the branes, we can understand them as excitations of the branes. We can study branes by studying open strings. The end points of the string source gauge fields on the brane. When we quantise open strings, there are two massless modes that arise. The first are oscillators longitudinal to the brane which are spin 1 particles. There is a gauge field on the brane associated with these gauge bosons. The second type are oscillators transverse to the brane. They are scalars which we associate with fluctuations transverse to the brane.

In type IIB string theory, only branes with p odd are stable and these are charged under a Ramond-Ramond field. The open strings attached to a single D_p brane have gauge group $U(1)$. A stack of N D_p branes gives rise to gauge group $U(N)$. The $U(1)$ component decouples from the $SU(N)$ fields so that a stack of N D_p branes realises an $SU(N)$ gauge theory in $p+1$ dimensions. In particular, D_3 branes in type IIB string theory have a 4 dimensional worldvolume and 6 scalar fields. This worldvolume gauge theory has a low energy limit that is $\mathcal{N} = 4$ SYM. Note that there are 32 supercharges in type IIB string theory. D_p branes that are flat and infinite are invariant under half these supersymmetries and are thus BPS states. The low-energy

worldvolume dynamics of D_p branes is given by superymmetric versions of Yang-Mills theories which are invariant under 16 supersymmetries.

Operators that are dual to D branes in the field theory have scaling dimensions that grow like N at large N. Operators dual to strings have dimensions that grow like $\sqrt{N}$ and are present in the planar theory. If we want to probe the non-planar limit, and we do, then we study D branes and new geometries which are dual to operators with dimension that grow like N^2.

2.5.3 Giant Gravitons in AdS

A graviton is a point particle that would mediate the gravitational force on the quantum scale. The graviton corresponds to operators in the gauge theory obtained by taking the trace of a product of complex adjoint scalar fields. The gravitons that we get when we take order N fields have the topology of S^3 when we study the $AdS_5 \times S^5$ background and are macroscopic in size. In fact, they have a size of the order of one unit of the spacetime radius. Hence, we call them giant gravitons.

These giant gravitons were discovered in [8] and those findings are reviewed here.

Dipole Analogy

Consider the Lagrangian

$$\mathcal{L} = \frac{m}{2}(\dot{x}_1^i \dot{x}_{1i} + \dot{x}_2^j \dot{x}_{2j}) + \frac{B}{2}\epsilon_{ij}(\dot{x}_1^i x_1^j - \dot{x}_2^i x_2^j) - \frac{k}{2}(x_1 - x_2)^2 \tag{2.5.3.1}$$

This describes two point particles in a magnetic field, $\vec{B}$. They are connected by a spring with spring constant, k. They have the same mass and equal but opposite charge which we've scaled to 1 for simplicity. Suppose that the magnetic field points in the $\hat{z}$ direction. We can then consider the motion of the particles in the x-y plane. Classically, we expect the particles to feel a force (Lorentz force) proportional to the magnetic field and their speed (as well as the size of the charge). Let's forget the spring term for the moment and consider the resultant equations of motion. They are:

$$\begin{aligned} &\frac{d}{dt}\left(\frac{\partial \mathcal{L}}{\partial \dot{x}_1^k}\right) = \frac{\partial \mathcal{L}}{\partial x_1^k} \\ &\implies \frac{d}{dt}\left(m\dot{x}_{1k} + \frac{B}{2}\epsilon_{kj}x_1^j\right) = \frac{B}{2}\epsilon_{ik}\dot{x}_1^i \\ &\implies m\ddot{x}_{1k} = B\epsilon_{ik}\dot{x}_1{}^i \end{aligned} \tag{2.5.3.2}$$

Similarly,

$$m\ddot{x}_{2k} = -B\epsilon_{ik}\dot{x}_2^i \tag{2.5.3.3}$$

This confirms that these charges, when put in a magnetic field and given some momentum, will feel an equal Lorentz force but in opposite directions (positive and negative charges). The Lorentz force is perpendicular to the velocity of the charge and perpendicular to the magnetic field. The more momentum the dipole has, the stronger the Lorentz force that each charge feels. This results in a movement of the two charges away from each other (but perpendicular to the momentum of dipole) so that the dipole is stretched. We know that the particles are coupled by the spring. The spring will limit the ability of the dipole to stretch due to the Lorentz force.

Now send the mass to zero and focus on the magnetic field and spring terms in the Lagrangian. We find that the magnitude of the centre of mass momentum, $|P|$ is proportional to the magnitude of the separation, $\Delta = \frac{x_1 - x_2}{2}$ [6]. Allowing the dipole to move along the surface of a sphere of radius, R, and magnetic flux, N, we see that when the dipole is the size of the sphere ($R = \Delta$), the momentum of the dipole will be at $2BR$ and the angular momentum, $L = PR$, will be at a maximum. It is at a maximum because we are assuming a fixed magnetic field and the largest chord we can draw in a sphere is the diameter. Of course, since Gauss' law tells us the magnetic flux through a closed surface is zero, and we clearly have identified the sphere with having a non-zero magnetic flux, then we must conclude there is a magnetic monopole at the centre of the sphere with strength $2\pi N = \Omega_2 B R^2$ [7]. So the maximum angular momentum is of the order N.

We can make the same argument much more precisely and the steps that follow are based largely on [8].

Since we are working on a sphere, it is natural to work in spherical coordinates. We are on the surface of a 2-sphere so we need to specify two angles (2 coordinates) to specify our position. We need an azimuthal angle, θ, and we have ϕ measuring angular distance from the equator ($\theta \in [0, 2\pi]$ and $\phi \in [-\frac{\pi}{2}, \frac{\pi}{2}]$). We choose to have only the A_θ component of the vector potential nonzero. We want to couple the velocity of the dipole to the magnetic field. Consider the state that has each charge a pole of the sphere. Then they have the same coordinates but with opposite sign for ϕ. This applies whenever the charges are at antipodal points.

Consider $\vec{B} = B\hat{r}$[8]. We know that

$$\begin{aligned} \nabla \times \vec{A} &= \vec{B} \\ \implies \nabla \times (A_x\hat{x} + A_y\hat{y} + A_z\hat{z}) &= B\left(\frac{\partial A_z}{\partial y} - \frac{\partial A_y}{\partial z}\right)\hat{x} + \left(\frac{\partial A_x}{\partial z} - \frac{\partial A_z}{\partial x}\right)\hat{y} + \left(\frac{\partial A_y}{\partial x} - \frac{\partial A_x}{\partial y}\right)\hat{z} \\ &= B\cos\theta\sin\phi\hat{x} + B\sin\theta\sin\phi\hat{y} + B\cos\phi\hat{z} \end{aligned} \tag{2.5.3.4}$$

We also have that

$$\vec{E} = -\nabla\phi - \frac{\partial \vec{A}}{\partial t} \implies \nabla\phi + \vec{E} = -\frac{\partial \vec{A}}{\partial t} \tag{2.5.3.5}$$

[6] Make a change of coordinates to $X = \frac{x_1 + x_2}{2}$ and Δ as above. We find that $\dot{X}^i\Delta^j = \frac{1}{4}(\dot{x}_1^i x_1^j - \dot{x}_2^i x_2^j)$. Using this, the term in the Lagrangian coupling to the magnetic field becomes $2B\epsilon_{ij}\dot{X}^i\Delta^j$. The canonical momentum is $\frac{\partial \mathcal{L}}{\partial \dot{X}^i}$ which we can see is proportional to Δ.

[7] We want a uniform magnetic field on the surface of the sphere. This is achieved by a monopole located at the centre.

[8] We have a magnetic monopole at the centre of the sphere so the field lines point radially outwards

The electromagnetic portion of the Lagrangian is given by

$$\mathcal{L}_B = -q(\vec{A}\cdot\dot{\vec{x}} - \phi) = -q(A_x\dot{x} + A_y\dot{y} + A_z\dot{z} - \phi) \tag{2.5.3.6}$$

which comes from the action

$$\begin{aligned}\mathcal{S}_B &= q\int A_\mu dx^\mu = q\int(\phi dt - \vec{A}d\vec{x}) = q\int\left(\phi dt - \vec{A}\frac{d\vec{x}}{dt}dt\right)\\ &= q\int(\phi - \vec{A}\cdot\dot{\vec{x}})dt\end{aligned} \tag{2.5.3.7}$$

Here we have chosen the convention that q describes a negative test charge. This sign choice should be reflected in our resulting equations of motion.

We are considering charges of mass m with a kinetic energy of $\frac{1}{2}m\dot{\vec{x}}^2$ so we need to add another term to the Lagrangian: the kinetic term. The Lagrangian describing the system is

$$\mathcal{L} = \mathcal{L}_B + \mathcal{L}_T = -q(A_x\dot{x} + A_y\dot{y} + A_z\dot{z} - \phi) + \frac{1}{2}m\dot{\vec{x}}^2 \tag{2.5.3.8}$$

We can check this is indeed the correct Lagrangian by checking if we get the correct equations of motion.

$$\frac{d}{dt}\frac{\partial\mathcal{L}}{\partial\dot{x}} = -q\dot{A}_x + m\ddot{x} = \frac{\partial\mathcal{L}}{\partial x} = q\left(\frac{\partial\phi}{\partial x} - \frac{\partial A_x}{\partial x}\dot{x} - \frac{\partial A_y}{\partial x}y - \frac{\partial\dot{A}_z}{\partial x}\dot{z}\right) \tag{2.5.3.9}$$

$$\frac{d}{dt}\frac{\partial\mathcal{L}}{\partial\dot{y}} = -q\dot{A}_y + m\ddot{y} = \frac{\partial\mathcal{L}}{\partial y} = q\left(\frac{\partial\phi}{\partial y} - \frac{\partial A_x}{\partial y}\dot{x} - \frac{\partial A_y}{\partial y}\dot{y} - \frac{\partial A_z}{\partial y}\dot{z}\right) \tag{2.5.3.10}$$

$$\frac{d}{dt}\frac{\partial\mathcal{L}}{\partial\dot{z}} = -q\dot{A}_z + m\ddot{z} = \frac{\partial\mathcal{L}}{\partial z} = q\left(\frac{\partial\phi}{\partial z} - \frac{\partial A_x}{\partial z}\dot{x} - \frac{\partial A_y}{\partial z}\dot{y} - \frac{\partial A_z}{\partial z}\dot{z}\right) \tag{2.5.3.11}$$

$$\begin{aligned}&\implies \sum_{i=1}^{3}\frac{d}{dt}\frac{\partial\mathcal{L}}{\partial\dot{x}^i} = -q\dot{\vec{A}} + m\ddot{\vec{x}}\\ &= q\nabla\phi - q\dot{x}\left(\frac{\partial A_x}{\partial x} + \frac{\partial A_x}{\partial y} + \frac{\partial A_x}{\partial z}\right) - q\dot{y}\left(\frac{\partial A_y}{\partial x} + \frac{\partial A_y}{\partial y} + \frac{\partial A_y}{\partial z}\right) - q\dot{z}\left(\frac{\partial A_z}{\partial x} + \frac{\partial A_z}{\partial y} + \frac{\partial A_z}{\partial z}\right)\end{aligned} \tag{2.5.3.12}$$

Now we make note of the following:

$$\begin{aligned}\dot{\vec{x}}\times(\nabla\times\vec{A}) &= \nabla(\dot{\vec{x}}\cdot\vec{A}) - \vec{A}(\nabla\dot{\vec{x}})\\ &= \dot{x}\left(\frac{\partial A_x}{\partial x} + \frac{\partial A_x}{\partial y} + \frac{\partial A_x}{\partial z}\right) + \dot{y}\left(\frac{\partial A_y}{\partial x} + \frac{\partial A_y}{\partial y} + \frac{\partial A_y}{\partial z}\right) + \dot{z}\left(\frac{\partial A_z}{\partial x} + \frac{\partial A_z}{\partial y} + \frac{\partial A_z}{\partial z}\right)\end{aligned} \tag{2.5.3.13}$$

Using this, (2.5.3.12) and (2.5.3.5) we obtain

$$\begin{aligned}&-q\dot{\vec{A}} + m\ddot{\vec{x}} = q\nabla\phi + q\vec{E} + m\ddot{\vec{x}} = q\nabla\phi - q\nabla(\dot{\vec{x}}\cdot\vec{A})\\ &\implies m\ddot{\vec{x}} = -q(\dot{\vec{x}}\times\nabla\times\vec{A}) - q\vec{E} = -q(\dot{\vec{x}}\times\vec{B}) - q\vec{E}\end{aligned} \tag{2.5.3.14}$$

which are our equations of motion. They describe the motion of a negative test charge in a magnetic field. Note that the Lorentz force is conventionally written in terms of a positive test charge: the result is simply a sign change.

We repeat the argument for spherical coordinates. We have that

$$\left(\frac{1}{r}\frac{\partial A_\phi}{\partial\theta} - \frac{1}{r\sin\theta}\frac{\partial A_\theta}{\partial\phi}\right)\hat{r} + \left(\frac{1}{r\sin\theta}\frac{\partial A_r}{\partial\phi} - \frac{\partial A_\phi}{\partial r}\right)\hat{\theta} + \left(\frac{\partial A_\theta}{\partial r} - \frac{1}{r}\frac{\partial A_r}{\partial\theta}\right)\hat{\phi} = B\hat{r} \qquad (2.5.3.15)$$

Here $\vec{B} = B\hat{r}$ as before. We'll denote the scalar potential as $\tilde{\phi}$ so as not to confuse this with our coordinate ϕ. In this choice of coordinates our position and velocity vectors are

$$\begin{aligned}\vec{r} &= r\hat{r}\\ \dot{\vec{r}} &= \dot{r}\hat{r} + r\dot{\theta}\hat{\theta} + r\sin\theta\dot{\phi}\hat{\phi}\end{aligned}$$

We get the second line as follows. First, we note that the transformation from Cartesian to spherical coordinates is

$$\begin{aligned}x &= r\cos\phi\sin\theta\\ y &= r\sin\phi\cos\theta\\ z &= r\cos\phi\end{aligned}$$

In spherical coordinates, $\vec{r}$ is our position vector; θ and ϕ are angles. Only the coordinate $r = |\vec{r}|$ has dimensions of length.

$$\vec{r} = x\hat{x} + y\hat{y} + z\hat{z} = r\cos\phi\sin\theta\hat{x} + r\sin\phi\sin\theta\hat{y} + r\cos\theta\hat{z} \qquad (2.5.3.16)$$

We look at how a small change in one of our coordinates will affect our position vector, $\vec{r}$, in terms of Cartesian coordinates and then we divide by that magnitude to get our unit vector. That is

$$\begin{aligned}\hat{r} &= \frac{\frac{\partial\vec{r}}{\partial r}}{\left|\frac{\partial\vec{r}}{\partial r}\right|} = \cos\phi\sin\theta\hat{x} + \sin\phi\sin\theta\hat{y} + \cos\theta\hat{z}\\ \hat{\theta} &= \frac{\frac{\partial\vec{r}}{\partial\theta}}{\left|\frac{\partial\vec{r}}{\partial\theta}\right|} = \frac{r\cos\phi\cos\theta\hat{x} + r\sin\phi\cos\theta\hat{y} - r\sin\theta\hat{z}}{\sqrt{r^2(\cos^2\theta + \sin^2\theta)}} = \cos\phi\cos\theta\hat{x} + \sin\phi\cos\theta\hat{y} - \sin\theta\hat{z}\\ \hat{\phi} &= \frac{\frac{\partial\vec{r}}{\partial\phi}}{\left|\frac{\partial\vec{r}}{\partial\phi}\right|} = \frac{-r\sin\phi\sin\theta\hat{x} + r\cos\phi\sin\theta\hat{y}}{\sqrt{r^2\sin^2\theta}} = -\sin\phi\hat{x} + \cos\phi\hat{y}\end{aligned} \qquad (2.5.3.17)$$

This notation is useful to calculate the velocity vector, $\dot{\vec{r}}$, because we know how to treat Cartesian unit vectors under operations like differentiation.

$$\begin{aligned}\dot{\vec{r}} &= (\dot{r}\cos\phi\sin\theta - r\sin\phi\sin\theta\dot{\phi} + r\cos\phi\cos\theta\dot{\theta})\hat{x} + (\dot{r}\sin\phi\sin\theta + r\cos\phi\sin\theta\dot{\phi} + r\sin\phi\cos\theta\dot{\theta})\hat{y} + (\dot{r}\cos\theta -\\ &= \dot{r}\hat{r} + r\dot{\theta}\hat{\theta} + r\sin\theta\dot{\phi}\hat{\phi}\end{aligned} \qquad (2.5.3.18)$$

We will make use of

$$\begin{aligned}\dot{\vec{r}}\times(\nabla\times\vec{A}) = \nabla(\dot{\vec{r}}\cdot\vec{A}) &= \left(\frac{\partial}{\partial r}\hat{r}+\frac{1}{r}\frac{\partial}{\partial\theta}\hat{\theta}+\frac{1}{r\sin\theta}\frac{\partial}{\partial\phi}\hat{\phi}\right)\left(\dot{r}A_r + r\dot{\theta}A_\theta + r\dot{\phi}\sin\theta A_\phi\right)\\ &= \left(\dot{r}\frac{\partial A_r}{\partial r}+r\frac{\partial A_\theta}{\partial r}\dot{\theta}+A_\theta\dot{\theta}+\sin\theta A_\phi\dot{\phi}+r\sin\theta\frac{\partial A_\phi}{\partial r}\dot{\phi}\right)\hat{r}\\ &+\left(\frac{\dot{r}}{r}\frac{\partial A_r}{\partial\theta}+\frac{\partial A_\theta}{\partial\theta}\dot{\theta}+\sin\theta\frac{\partial A_\phi}{\partial\theta}\dot{\phi}+\cos\theta A_\phi\dot{\phi}\right)\hat{\theta}\\ &+\left(\frac{\dot{r}}{r\sin\theta}\frac{\partial A_r}{\partial\phi}+\frac{1}{\sin\theta}\frac{\partial A_\theta}{\partial\phi}\dot{\theta}+\frac{\partial A_\phi}{\partial\phi}\dot{\phi}\right)\hat{\phi}\end{aligned} \tag{2.5.3.19}$$

Now equations of motion can be calculated as before:

$$\frac{d}{dt}\left(\frac{\partial\mathcal{L}}{\partial\dot{\vec{r}}}\right)=\frac{\partial\mathcal{L}}{\partial\vec{r}} \tag{2.5.3.20}$$

Our kinetic term in the Lagrangian is $\mathcal{L}_T=\frac{1}{2}m\dot{\vec{r}}^2$.

Using the Euler-Lagrange equation we get

$$\begin{aligned}\frac{d}{dt}\left(\frac{\partial\mathcal{L}}{\partial\dot{r}}\right)=q\dot{A}_r+m\ddot{r}=\frac{\partial\mathcal{L}}{\partial r}&=q\left(A_\theta\dot{\theta}+\frac{\partial A_\theta}{\partial r}\dot{\theta}+\sin\theta A_\phi\dot{\phi}+r\sin\theta\frac{\partial A_\phi}{\partial r}\dot{\phi}+\frac{\partial A_r}{\partial r}\dot{r}-\frac{\partial\tilde{\phi}}{\partial r}\right)\\ \frac{d}{dt}\left(\frac{1}{r}\frac{\partial\mathcal{L}}{\partial\dot{\theta}}\right)=q\dot{A}_\theta=\frac{1}{r}\frac{\partial\mathcal{L}}{\partial\theta}&=q\left(\frac{\partial A_\theta}{\partial\theta}\dot{\theta}+\cos\theta A_\phi\dot{\phi}+\sin\theta\frac{\partial A_\phi}{\partial\theta}\dot{\phi}+\frac{1}{r}\frac{\partial A_r}{\partial\theta}\dot{r}-\frac{1}{r}\frac{\partial\tilde{\phi}}{\partial\theta}\right)\\ \frac{d}{dt}\left(\frac{1}{r\sin\theta}\frac{\partial\mathcal{L}}{\partial\dot{\phi}}\right)=q\dot{A}_\phi=\frac{1}{r\sin\theta}\frac{\partial\mathcal{L}}{\partial\phi}&=q\left(\frac{1}{\sin\theta}\frac{\partial A_\theta}{\partial\phi}\dot{\theta}+\frac{\partial A_\phi}{\partial\phi}\dot{\phi}+\frac{1}{r\sin\theta}\frac{\partial A_r}{\partial\phi}\dot{r}-\frac{1}{r\sin\theta}\frac{\partial\tilde{\phi}}{\partial\phi}\right)\\ \implies q\dot{\vec{A}}+m\ddot{\vec{r}}=q(\dot{\vec{r}}\times(\nabla\times\vec{A}))-q\nabla\tilde{\phi}&=q(\dot{\vec{r}}\times\vec{B})-q\nabla\tilde{\phi}\\ \implies q\dot{\vec{r}}\times\vec{B}+q\vec{E}&=m\ddot{\vec{r}}\end{aligned} \tag{2.5.3.21}$$

Here we have used the convention that we are working with a positive test charge and so our equations of motion describe a positive test charge moving in a magnetic field.

Assuming only A_θ is non-zero[9], our Lagrangian is

$$\mathcal{L}=A_\theta r\dot{\theta}=A_\theta R\cos\phi\dot{\theta} \tag{2.5.3.22}$$

We have dropped the kinetic term since it is small compared to the coupling to the magnetic field i.e.: we can send the mass to zero.

We choose

$$A_\theta=N\frac{1-\sin\phi}{2R\cos\phi} \tag{2.5.3.23}$$

[9]We fix our gauge so that A_θ is the only non-zero component of the vector potential. This is possible since our field is uniform on the sphere.

We can check that this is reasonable by noting that $r = R\cos\phi$ (see Figure[8]) and is a maximum, i.e.: $r = R$, when $\phi = 0 + 2k\pi$, $k \in \mathbb{Z}$. Using this, we can take the curl of our vector potential and check that we recover the expression for the flux, which we do.

The electromagnetic term in the Lagrangian looks like

$$\mathcal{L}_B = A_\theta R\cos\phi\dot{\theta} + A_\theta R\cos(-\phi)\dot{\theta} = -N\sin\phi\dot{\theta} \tag{2.5.3.24}$$

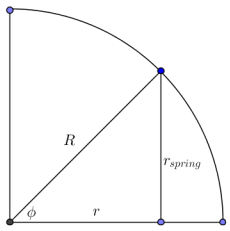


Figure 8: An arc of a great circle cutting the poles of the sphere

The spring coupling term is

$$\mathcal{L}_S = -\frac{k}{2}R^2\sin^2\phi \tag{2.5.3.25}$$

Here we have used the chord length instead of arc length for the purpose of simplification. $\frac{\partial\mathcal{L}_B}{\partial\dot{\theta}}$ gives us the angular momentum. This leads to

$$|L_{max}| = N\sin(\pi/2) = N \tag{2.5.3.26}$$

Embedding in S^4: $AdS_7 \times S^4$

Before considering D3 brane giant gravitons, we will review the case of M2 brane giant gravitons. Consider a relativistic spherical membrane[10] moving in S^4. The membrane has no net charge but it does have a dipole moment. There is a background 4-form field strength which it

[10]This membrane is the giant graviton.

couples to. We can parametrise S^4 such that

$$\begin{aligned} X_1 &= R\cos\theta_1 \\ X_2 &= R\sin\theta_1\cos\theta_2 \\ X_3 &= R\sin\theta_1\sin\theta_2\cos\theta_3 \\ X_4 &= R\sin\theta_1\sin\theta_2\sin\theta_3\cos\theta_4 \\ X_5 &= R\sin\theta_1\sin\theta_2\sin\theta_3\sin\theta_4 \end{aligned} \tag{2.5.3.27}$$

Here θ_4 is the azimuthal angle and goes from 0 to 2π while the other angles go from 0 to π. It is simple to verify that $\sum_{i=1}^{5} X_i^2 = R^2$. Now we embed a spherical membrane into this S^4. We can parametrise this membrane using the azimuthal angle, θ_4, and another angle, choose θ_3. By (2.5.3.27) we see that this means the membrane (or brane) can only move in the $X_1 - X_2$ plane (the only coordinates left that are not involved in our parametrisation of the sphere). It is natural to define $r = R\sin\theta_1\sin\theta_2$ which leaves the 2-sphere

$$\begin{aligned} X_3 &= r\cos\theta_3 \\ X_4 &= r\sin\theta_3\cos\theta_4 \\ X_5 &= r\sin\theta_3\sin\theta_4 \end{aligned} \tag{2.5.3.28}$$

The size of the brane (with radius r) depends on its location in the $X_1 - X_2$ plane (since r depends on θ_1 and θ_2, as does X_1 and X_2. We also have $X_3^2 + X_4^2 + X_5^2 = r^2 \implies X_1^2 + X_2^2 = R^2 - r^2$. That is, r is radius of the brane whilst $\sqrt{R^2 - r^2}$ is the radius of the circle on which the brane orbits. So circles in this plane describe branes of fixed size. In terms of our embedding coordinates,

$$\begin{aligned} X_1 &= \sqrt{R^2 - r^2}\cos\phi \\ X_2 &= \sqrt{R^2 - r^2}\sin\phi \end{aligned} \tag{2.5.3.29}$$

The metric on the 4-sphere (embedded into 5 dimensional Euclidean space) is

$$ds^2 = dX_1^2 + dX_2^2 + dX_3^2 + dX_4^2 + dX_5^2 \tag{2.5.3.30}$$

where (assuming only ϕ is time-dependent)

$$\begin{aligned} dX_1 &= \frac{-r}{\sqrt{R^2 - r^2}}\cos\phi dr - \sqrt{R^2 - r^2}\sin\phi d\phi - \sqrt{R^2 - r^2}\sin\phi\dot{\phi}dt \\ dX_2 &= \frac{-r}{\sqrt{R^2 - r^2}}\sin\phi dr + \sqrt{R^2 - r^2}\cos\phi d\phi + \sqrt{R^2 - r^2}\cos\phi\dot{\phi}dt \\ dX_3 &= \cos\theta_3 dr - r\sin\theta_3 d\theta_3 \\ dX_4 &= \sin\theta_3\cos\theta_4 dr + r\cos\theta_3\cos\theta_4 d\theta_3 - r\sin\theta_3\sin\theta_4 d\theta_4 \\ dX_5 &= \sin\theta_3\sin\theta_4 dr + r\cos\theta_3\sin\theta_4 d\theta_3 + r\sin\theta_3\cos\theta_4 d\theta_4 \end{aligned} \tag{2.5.3.31}$$

This gives us almost all the terms we need to compute the induced metric. That is, we want the metric on the worldvolume from the metric on the spacetime. We compute the elements by

$$g_{ij} = \frac{\partial X^M}{\partial \xi^i}\frac{\partial X^N}{\partial \xi^j}G_{MN} \tag{2.5.3.32}$$

where G_{MN} is the metric on the spacetime and g_{ij} is the metric induced on the worldvolume. We already have the transformations for r, θ_3, θ_4 and ϕ. The induced metric is

$$g_{tt} = \left(\frac{\partial X_1}{\partial t}\right)^2 G_{X_1X_1} + \left(\frac{\partial X_2}{\partial t}\right)^2 G_{X_2X_2} + \cdots + \left(\frac{\partial X_5}{\partial t}\right)^2 G_{X_5X_5} + \left(\frac{\partial \tau}{\partial t}\right)^2 G_{\tau\tau} \tag{2.5.3.33}$$

Our brane must be positioned in the full 11 dimensional space. We choose to put it at the origin of AdS_7 which leads to the simplification $G_{\tau\tau} = -1$. Thus $g_{tt} = -1 + (R^2 - r^2)\sin^2\phi\dot{\phi}^2 + (R^2 - r^2)\cos^2\phi\dot{\phi}^2$. The induced metric is

$$ds^2 = \frac{R^2}{R^2 - r^2}dr^2 + (R^2 - r^2)d\phi^2 + r^2 d\theta_3^2 + r^2\sin^2\theta_3 d\theta_4^2 + (-1 + (R^2 - r^2)\dot{\phi}^2)dt^2 \tag{2.5.3.34}$$

$$\implies \sqrt{-g} = Rr^2\sin\theta_3\sqrt{1 - (R^2 - r^2)\dot{\phi}^2} \tag{2.5.3.35}$$

We can now compute the kinetic-like term of the action, which is given by the Dirac-Born-Infeld action.

$$\begin{aligned} S_{DBI} &= -T\int r^2\sqrt{1 - (R^2 - r^2)\dot{\phi}^2}dtd\theta_3d\theta_4 \\ &= -T\Omega_2\int r^2\sqrt{1 - (R^2 - r^2)\dot{\phi}^2}dt \end{aligned} \tag{2.5.3.36}$$

where T is the tension of the membrane and is given by $T = \frac{1}{4\pi^2 l_p^3}$.

The term that couples to the background field is called the Chern-Simons coupling. Each orbit, the brane sweeps out a 3-dimensional surface in S^4 (the worldvolume of the brane after 1 orbit). This surface forms a boundary of a 4-manifold, call it Σ. If we integrate the flux over this surface, then we obtain the contribution of the 4-form field strength to the action of the brane per orbit. The background flux, $F \equiv dC$, is the constant flux density, B, multiplied by the infinitesimal volume element on S^4. This gives us

$$S_B = \oint_{\text{wv}} C = \int_\Sigma F = B\text{vol}(\Sigma) \tag{2.5.3.37}$$

This volume is given by

$$\text{vol}(\Sigma) = R\Omega_2\int_0^{2\pi} d\phi\int_0^r r'^2 dr' = \frac{8\pi^2}{3}Rr^3 \tag{2.5.3.38}$$

We make the ansatz that $\phi = \omega_0 t$ so that $\omega_0 = \dot{\phi}$. If T is the period of the orbit of the brane, then $\omega_0 T = 2\pi$.

$$\mathcal{L}_B = \frac{\dot{\phi}}{2\pi}B\Omega_4 Rr^3 \tag{2.5.3.39}$$

We can see check if we get the correct action back.

$$\begin{aligned}\mathcal{S}_B &= B\frac{8\pi^2}{3}Rr^3 = B\Omega_4 Rr^3 \\ &= \int_{t_{\text{initial}}}^{t_{\text{final}}} dt\mathcal{L} \\ &= \int_{t_{\text{initial}}}^{t_{\text{final}}} \frac{\dot{\phi}}{2\pi}B\Omega_4 Rr^3 = \int_0^T \frac{d(\omega_0 t)}{dt}\frac{B\Omega_4 Rr^2}{2\pi}dt \\ &= \frac{\omega_0 T}{2\pi}\mathcal{S}_B = \mathcal{S}_B \end{aligned} \tag{2.5.3.40}$$

Here we have integrated over one period of the orbit of the brane. We can do this because we calculated the Chern-Simons term in the action by using Stoke's theorem. Stoke's theorem required us to integrate over a closed path which is the boundary of some surface. In our case, this surface was precisely the orbit of the brane.

Quantisation of the flux requires that

$$\Omega_4 BR^4 = 2\pi N \implies B = \frac{2\pi N}{R^4\Omega_4} \implies \mathcal{L}_B = \dot{\phi}N\frac{r^3}{R^3} \tag{2.5.3.41}$$

Defining $m = \Omega_2 T r^2$ we have the full Lagrangian

$$\mathcal{L} = -m\sqrt{1-\dot{\phi}^2(R^2-r^2)} + N\frac{r^3}{R^3}\dot{\phi} \tag{2.5.3.42}$$

The angular momentum is

$$L = \frac{\partial\mathcal{L}}{\partial\dot{\phi}} = \frac{m\dot{\phi}(R^2-r^2)}{\sqrt{1-\dot{\phi}^2(R^2-r^2)}} + mr \tag{2.5.3.43}$$

where the definition of the membrane tension and $R = l_p(\pi N)^{\frac{1}{3}}$ give $\frac{N}{R^3} = T\Omega_2$. This function is strictly increasing for $r > 0$ so it is clear that the angular momentum has a minimum at $r = 0$ (the smallest the membrane can be) and a maximum at $r = R$ (the maximum size the membrane can be). This gives us that $L_{max} = N$, just like in the dipole case. This fact, and the behaviour of $L(r)$ in general, implies that the angular momentum of the membrane is greater at larger r or, rather, that the membrane size increases with increasing angular momentum. The membrane must fit in S^4 and so it cannot be bigger than R.

This cut-off on the angular momentum is the stringy exclusion principle. Some states that we would expect are missing due to this upper bound placed on the momentum. Since there is a largest momentum, there is also a smallest distance such that we can no longer resolve points on the sphere.

For the energy, we get

$$E = \dot{\phi}L - \mathcal{L} = \sqrt{\left(\frac{Nr^2}{R^3}\right)^2 + \frac{(L - Nr^3/R^3)^2}{R^2 - r^2}} \tag{2.5.3.44}$$

We can examine what happens to the energy as $r \to R$ and at $L = N$. The second term inside the square root is an indeterminate form in this limit but we see the r^3 term in the numerator increases to R more rapidly then the quadratic r^2 in the denominator. So the numerator tends to zero faster than the denominator and that whole term is zero in the above limit. This leaves us with

$$E|_{r=R} = \frac{N}{R} \tag{2.5.3.45}$$

This is in agreement with the energy of a Kaluza-Klein graviton with angular momentum L. We also note that the Kaluza-Klein graviton has a maximum angular momentum in accordance with the stringy exclusion principle.[11]

The extension to $AdS_5 \times S^5$ follows quite similarly and the angular momentum in this case is given by

$$L = \frac{m\dot{\phi}(R^2 - r^2)}{\sqrt{1 - \dot{\phi}^2(R^2 - r^2)}} + N\frac{r^4}{R^4} \tag{2.5.3.46}$$

where $m = T\Omega_3 r^3$. The behaviour of this function is in complete agreement with the previous case, with angular momentum increasing the size of our graviton to the maximum value R.

[11] We have compactified on the sphere. Our single field in the full spacetime has reduced to many fields in the reduced spacetime, without losing dependence on the quantum numbers of the full space. This is Kaluza-Klein reduction.

2.6 Supergravity

The research presented in this PhD studies the large N limit in non-planar settings. We saw in Section 2.3.1 that quantum fluctuations for matrix theories go like $\frac{1}{N^2}$ and these are dual to $\hbar$ corrections in the quantum gravity. When N is large, the fluctuations are suppressed so that the large N limit of $\mathcal{N} = 4$ SYM is dual to classical type IIB string theory on an $AdS_5 \times S^5$ background. Recall that the 't Hooft coupling is $\lambda = g_{YM}^2 N$. This is related to the string coupling

$$\lambda = g_s N = \frac{1}{4\pi} \left(\frac{R}{l_s} \right)^4$$

so that strong coupling in the field theory at large N means weak coupling for the string. The second equality tells us that for weak coupling in the string theory, the radius of curvature of the bulk space is much larger than the string length. This means the string is not sensitive to the curvature of the space i.e.: spacetime looks flat. This twofold simplification of the string theory in this limit is known as the low energy limit of the gravity and open and closed strings decouple from each other in this limit.

In the following sections we describe supergravity in general using supersymmetry as a starting point, instead of starting with the string theory, to illuminate how gravity naturally arises in these settings. We show how studying the low energy theory motivated by the AdS/CFT correspondence leads us to the $\frac{1}{2}$-BPS states. We then go on to talk about the LLM geometries, which are a specific supergravity solution that maps the $\frac{1}{2}$-BPS states of a single matrix model to the supergravity solution. This mapping is used in Chapter 4 and motivates the study in Chapter 3.

2.6.1 Basics of Supersymmetry and Gravity

String theory does not have the non-renormalisation issues that quantising classical gravity has. SUGRA, a supersymmetric theory of gravity, has some of the UV divergences cancelled by supersymmetry. Since SUGRA is a low energy theory of strings, we can think of it as an effective string theory.

Gravity is a local theory. What this means is that at each point in spacetime the curvature may vary. This is because heavy objects curve the spacetime, and so the curvature must depend on where these objects are. We know, also, that local symmetries are gauge symmetries. Global symmetries and local symmetries differ by how the transformation is implemented. A global transformation is implemented the same way at every point in the spacetime, whereas a local symmetry is implemented depending on the spacetime point. Global symmetries correspond to conservation laws (Noether's theorem). These symmetry transformations map solutions to the equations of motion of the theory into another solution: the action changes by a surface term which leaves the equations of motion invariant. These are important for physics to make sense: the actual laws of physics do not change under translations or rotations. They are symmetries

of the laws of nature.

What about local gauge symmetries? These are not symmetries at all. They do not change the state of the system i.e.: they do not map solutions of the equations of motion into other solutions of the equations of motion. It is a statement about the redundancy of our description: we capture the same physical state many times. Electromagnetism has the gauge symmetry

$$A_\mu \to A_\mu + \partial_\mu \chi \tag{2.6.1.1}$$

This transformation does not change the electric and magnetic fields.

$$\begin{aligned}
\vec{E} &= -\vec{\nabla}\phi - \partial_t \vec{A} \quad &\to -\vec{\nabla}(\phi + \partial_t \chi) - \partial_t(\vec{A} - \vec{\nabla}\chi) \\
&&= -\vec{\nabla}\phi - \partial_t \vec{A} - \vec{\nabla}\partial_t \chi + \partial_t \vec{\nabla}\chi \\
&&= \vec{E} \\
\vec{B} &= \vec{\nabla} \times \vec{A} &\to \vec{\nabla} \times (\vec{A} - \vec{\nabla}\chi) \\
&&= \vec{\nabla} \times \vec{A} \\
&&= \vec{B}
\end{aligned}$$

One might wonder at this point why gauge symmetry is there at all. It is a redundant description. However, gauge symmetry plays an important role in rectifying the tension between special relativity and quantum mechanics that comes about when one tries to quantise classical electromagnetism. When one quantises using canonical quantisation, a mode expansion of the field ($A_\mu(x)$ for electromagnetism) is performed.

$$A_\mu(x) = \int \frac{d^3k}{(2\pi)^3 2\omega_{\vec{k}}} (e^{-ik\cdot x}\alpha_\mu(k) + e^{ik\cdot x}\alpha_\mu^\dagger(k)) \tag{2.6.1.2}$$

This gives the creation and annihilation operators which are specified with a commutator.

$$[\alpha_\mu(k), \alpha_\nu^\dagger(p)] = \pm(2\pi)^3 2\omega_k \delta(\vec{k} - \vec{p})\eta_{\mu\nu} \tag{2.6.1.3}$$

Lorentz invariance forces the appearance of the metric. But the metric has at least one negative component. This means we can build states (using the creation operator) that will have negative norm. This ruins quantum mechanics. If we want all states to have positive norm then we must replace $\eta_{\mu\nu}$ with $\delta_{\mu\nu}$ which is not invariant under a Lorentz transformation. So we must choose between quantum mechanics and special relativity. Nature is undoubtedly Lorentz invariant, so instead we must try to reason how we can get rid of these states with negative norm.

Gauge invariance means that the same physical state can be represented by a (gauge) transformation. We don't have a new physical state, just a redundant fluctuation. At the quantum level, certain states are not physical. These are the states with negative norm. It appears that gauge invariance is making a statement about these fields. There are a number of approaches we can take when quantising a theory with a local symmetry. For the case of electromagnetism we learn that only the transverse modes of A_μ are non-zero. This is precisely why we observe photons to have only transverse (2) polarisations. By appropriate gauge fixing, we pick out the physical states (with positive norm). So gauge invariance is extremely important when we quantise as it allows us to remove the unphysical (negative norm) states from our theory. If we

want to make a global symmetry local, we need to define a covariant derivative, which is the usual derivative plus a term containing the gauge field $(\partial_\mu - iA_\mu)$, so that our action will be invariant under the transformation. We also promote the field to be dynamical (respecting the gauge symmetry) to get a consistent theory.

We can think of gravity as being a gauge theory. We have a metric, $g_{\mu\nu}(x)$, which tells us how to measure lengths in the space we are working in. The line element

$$ds^2 = g_{\mu\nu}(x)dx^\mu dx^\nu \tag{2.6.1.4}$$

is Lorentz invariant. It is physical. We know physics is coordinate invariant, and so the line element must also be invariant under a coordinate transformation. This means that

$$ds^2 = g_{\mu\nu}(x)dx^\mu dx^\nu = ds'^2 = g'_{\mu\nu}(x')dx'^\mu dx'^\nu \tag{2.6.1.5}$$

so that the metric changes under a coordinate transformation. Thus, different metrics can describe the same space. This is hinting towards the fact that we have a redundant description. By changing the metric via a coordinate transformation, we have not moved to a new space. Locally, we can always make a coordinate transformation to Minkowski space ($g_{\mu\nu} \to \eta_{\mu\nu}$) so the metric is not a good indication of curvature around a point. In curved spaces, we replace the usual derivative with the covariant derivative. This is defined in terms of the Christoffel symbols: $\partial_\mu g_{\rho\sigma} - \Gamma^\nu_{\rho\mu} g_{\nu\sigma} - \Gamma^\nu_{\sigma\mu} g_{\nu\rho}$. Comparing this with the gauge theory case, it is clear that the Christoffel symbols are playing the role of the gauge field. These symbols are not unique and can locally be put to zero by an appropriate coordinate transformation. This has to be the case by the equivalence principle.

When we make a global transformation local, the covariant derivative must be used in order to leave the action invariant under the transformation. The Christoffel symbols appear above because, in a curved space, we cannot follow Euclidean geometry intuition in adding or translating vectors and we need to account for the change in coordinate basis around each point. We can think about the covariant derivative acting on different fields, which will bring us back to local transformations.

We know the line element is a Lorentz scalar, so it is invariant under a global Lorentz transformation. What happens when we make this transformation local? We can always transform locally to flat space. We can rewrite the metric as

$$g_{\mu\nu}(x) = \epsilon^a_\mu(x)\epsilon^b_\nu(x)\eta_{ab} \tag{2.6.1.6}$$

Here flat space indices, a and b, are contracted so that locally we have a Lorentz scalar. The new vector we have introduced is called the vielbein. It looks like we have performed a change of coordinates

$$\begin{aligned} d\xi^a &= \frac{\partial \xi^a}{\partial x^\mu} dx^\mu \equiv \epsilon^a_\mu(x) dx^\mu \\ dx^\mu &= \frac{\partial x^\mu}{\partial \xi^a} d\xi^a \equiv \epsilon^\mu_a(x) d\xi^a \end{aligned} \tag{2.6.1.7}$$

however we cannot go from a curved space to Minkowski space by changing coordinates. There is no way to integrate this so that it makes sense globally. Studying the above equations, we note

$$ds'^2 = \eta_{ab} d\xi^a d\xi^b = \eta_{ab}\epsilon^a_\mu(x)\epsilon^b_\nu(x)dx^\mu dx^\nu = g_{\mu\nu}(x)dx^\mu dx^\nu = ds^2 \tag{2.6.1.8}$$

From (2.6.1.7) we also see that

$$\epsilon^a_\mu \epsilon^\mu_b = \delta^a_b \qquad\qquad \epsilon^a_\mu \epsilon^\nu_a = g^\nu_\mu \tag{2.6.1.9}$$

To ensure we have local Lorentz invariance under an arbitrary choice of vielbein, we must introduce a gauge field (as usual) to define the covariant derivative [9]. The gauge field for the Lorentz group is called the spin connection. For a Lorentz transformation, the transformation parameter is ω_{ab} which contracts with the Lorentz generator M^{ab}. Gauge fields have an extra index μ (recall that the gauge field for the scalar field is A_μ). Thus the gauge field we must introduce is $(\omega_\mu)_{ab}$. For translations, the parameter is ϵ^a which contracts with the generator of translations P_a so that the gauge field for translations is $(\epsilon_\mu)^a$ which is the vielbein. For a vector in curved space, the covariant derivative would look like

$$D_\mu V^\alpha = \partial_\mu V^\alpha + \Gamma^\alpha_{\mu\nu} V^\nu \tag{2.6.1.10}$$

where the Christoffel symbol is the usual gravity gauge field and V^α is an arbitrary vector. We want local Lorentz invariance (in the space labelled by lower case Roman letters) so the vectors/ tensors the covariant derivative will act upon will have free indices in the flat frame indices. We can use the vielbein to transform a vector in the curved space, V^ν, to a vector in the flat space, $\epsilon^a_\nu V^\nu$. Recall that the spin connection is a gauge field so that

$$D_\mu(\epsilon^a_\nu V^\nu) = \partial_\mu(\epsilon^a_\nu V^\nu) + (\omega_\mu)^a_b(\epsilon^b_\nu V^\nu) \tag{2.6.1.11}$$

In order to obtain a consistent form of the covariant derivative, we must satisfy

$$D_\mu(\epsilon^a_\nu V^\nu) = \epsilon^a_\nu D_\mu V^\nu \tag{2.6.1.12}$$

so that the covariant derivative of the vielbein is zero (by the product rule). Since the vielbein has two indices, we need a gauge field (connection term) for each index. We have used the spin connection to transform the flat space indices, and the Christoffel symbol, as usual, will be used for the curved space index. Then

$$D_\mu \epsilon^a_\nu = \partial_\mu \epsilon^a_\nu - \Gamma^\alpha_{\mu\nu}\epsilon^a_\alpha + \omega^a_{\mu b}\epsilon^b_\nu \tag{2.6.1.13}$$

The minus sign in front of the Christoffel symbol appears because the derivative is acting on the dual vector. By requiring that the above equation is zero, we can actually solve for the spin connection in terms of the vielbein. We use a metric compatible covariant derivative so that $D_\alpha g_{\mu\nu} = 0 \implies D_\alpha \epsilon^a_\mu = 0$.

$$\begin{aligned}
&D_\mu \epsilon^a_\nu(x) = 0 \\
\implies\ &\omega^{ac}_\mu = \epsilon^a_\alpha \Gamma^\alpha_{\mu\nu}\epsilon^{\nu c} - \epsilon^{\nu c}\partial_\mu \epsilon^a_\nu \\
&\quad = \frac{\epsilon^a_\alpha}{2}\left[\epsilon^{\alpha b}\partial_\nu \epsilon_{b\mu} + \epsilon^\alpha_a \epsilon^{a\sigma}\epsilon_{b\mu}\partial_\nu \epsilon^b_\sigma + \epsilon^{\alpha b}\partial_\mu \epsilon b\nu + \epsilon^\alpha_a \epsilon^{a\sigma}\epsilon_{b\nu}\partial_\mu \epsilon^b_\sigma - \epsilon^\alpha_a \epsilon^{a\sigma}\epsilon^b_\mu \partial_\sigma \epsilon_{b\nu} - \epsilon^\alpha_a \epsilon^{a\sigma}\epsilon_{b\nu}\partial_\sigma \epsilon^b_\mu\right]\epsilon^{\nu c} \\
&\qquad - \epsilon^{\nu c}\partial_\mu \epsilon^a_\nu \\
&\quad = \frac{1}{2}\left[\epsilon^{\nu c}(\partial_\nu \epsilon^a_\mu - \partial_\mu \epsilon^a_\nu) + \epsilon^{a\sigma}(\partial_\mu \epsilon^c_\sigma - \partial_\sigma \epsilon^c_\mu) + \epsilon^{a\sigma}\epsilon^{\nu c}(\partial_\nu \epsilon^b_\sigma - \partial_\sigma \epsilon^b_\nu)\epsilon_{b\mu}\right]
\end{aligned} \tag{2.6.1.14}$$

The covariant derivative acting on a spinor looks a little different, and that is because we need to contract the free flat indices with the generator of Lorentz transformations for spinors. This is $\frac{1}{2}S_{ab} = \frac{1}{4}[\gamma_a, \gamma_b]$. Then

$$D_\mu(\psi) = \partial_\mu\psi + \frac{1}{4}\omega_\mu^{ab}S_{ab}\psi \tag{2.6.1.15}$$

We have seen how to go from a global to a local Lorentz symmetry. We can do something similar for supersymmetry, First, we will recap a few things about supersymmetry.

We are comfortable defining our theory by the Lie algebra of our generators. In supersymmetry, the generators close a graded Lie algebra: some of the usual commutation relations are replaced by the anticommutator brackets. This change is necessary to generalise the Poincaré symmetry (Lorentz and translations) of spacetime. The Coleman-Mandula theorem forbade this generalisation on the assumption the generators will close the usual Lie algebra (not the graded Lie algebra). The generators of the supersymmetry algebra are Q_α^i, and the commutator between them, $\{Q_\alpha^i, Q_\beta^j\}$, will give the other generators (M_{ab} for Lorentz, P_a for translations and T_r for internal symmetries). Since we have an anticommutator, it is natural to identify these new generators with spinors, with α a spinor index and i labelling the generator. We say these Q_α^i are odd, and the other generators are even. Then the algebra is an anti-commutation relation for the odd generators and the usual commutator for any other combination of generators. We know that an odd number times an odd number will give us an even number, so $\{Q_\alpha^i, Q_\beta^j\}$ will give us an even generator. Following that logic, only commutator of this type $[P_a, Q_\alpha^i]$, $[M_{ab}, Q_\alpha^i]$ and $[T_r, Q_\alpha^i]$ will give us back the supersymmetry generators.

Since $[M_{ab}, Q_\alpha^i] \neq 0$, supersymmetry generators are in a representative of the Lorentz group. A boson field multiplied with a spinor field gives a spinor field. So the supersymmetry generators transform bosons into fermions (spinors) and vice versa, which is where the even-odd grading comes from. For example, consider two supersymmetry (SUSY) transformations. B denotes a boson field and F denotes a fermion field. Indices are not displayed for simplicity but ε represents the SUSY transformation ε_α^i.

$$\delta_1 B = \bar{\varepsilon}_1 F \qquad\qquad \delta_2 = \varepsilon_2 \partial B \tag{2.6.1.16}$$

The derivative appears for dimensional correctness. In mass units, $[B] = 1$, $[F] = \frac{3}{2}$ and $[\partial] = 1$. The above then gives us that $[\varepsilon] = -\frac{1}{2}$. This then tells us that

$$[\delta_1, \delta_2] \propto \partial_\mu B \tag{2.6.1.17}$$

Thus

$$\{Q, \bar{Q}\} \propto P_\mu \tag{2.6.1.18}$$

If we make our transformations local and in particular the translation generator, P_μ, local then we have coordinate invariance: any local translation is a symmetry of the theory. But coordinate invariance is a property of general relativity, so this local SUSY means we have included gravity so that local SUSY is supergravity. By studying the symmetry locally, we must automatically include gravity.

We can implement this local SUSY transformation explicitly as follows. The parameter of

the infinitesimal global supersymmetry transformation is ε^i_α. It is a spinor. If we make the transformation local, then we will have to introduce a gauge field and define a covariant derivative. The gauge field must carry a spinor index, since we are dealing with spinors, and also a Lorentz index for the curved space. This gauge field is denoted by $\psi_{\mu\alpha}$ (α is the spinor index) and is called the gravitino, since we are dealing with gravity.

Fermions and bosons are related by supersymmetry. We can ask what a supersymmetry transformation does to the gravitino. Since we have a local theory (gravity) then we must match the gravitino to the fields we previously considered when studying local Lorentz invariance in a curved space. The vielbein has one curved index and so it emerges as the correct candidate. Thus we have

$$\delta\psi^\mu_\alpha = \frac{1}{k}\partial^\mu\epsilon_\alpha \tag{2.6.1.19}$$

where k appears to get the correct dimensions. To make a gauge theory of supersymmetry, we need a covariant derivative and we need to promote the gravitino to a dynamical field. Consider the following Lagrangian

$$\mathcal{L} = -(\partial^\mu\phi^*)(\partial_\mu\phi) - \frac{1}{2}\bar{\psi}\gamma^\mu\partial_\mu\psi \tag{2.6.1.20}$$

This is invariant under a global SUSY transformation with the fields transforming as

$$\delta\phi = \epsilon\psi \qquad\qquad \delta\psi = -i\sigma^\mu\bar{\epsilon}\partial_\mu\phi \tag{2.6.1.21}$$

If we promote the transformation parameter ϵ to $\epsilon(x)$, then the Lagrangian is not invariant under the local transformation. Using the covariant derivative and adding the dynamical term for the gravitino, $-k(\partial_\mu\phi^*\psi^\alpha + \frac{1}{2}\psi^\beta(\sigma_\mu\bar{\sigma}^\nu)^\alpha_\beta\partial_\nu\phi^*)\psi^\mu_\alpha$, we find that [10]

$$\delta\mathcal{L}' = ik\bar{\psi}_\mu\gamma_\nu\epsilon\bar{\psi}\gamma^\mu\partial^\nu\psi \tag{2.6.1.22}$$

where

$$i\bar{\psi}\gamma^\mu\partial^\nu\psi = T^{\mu\nu} \tag{2.6.1.23}$$

which is the energy momentum tensor. So we need to add one more term to get an invariant action. This term is $-g_{\mu\nu}T^{\mu\nu}$ with the metric transforming as $\delta g_{\mu\nu} = k\bar{\psi}_\mu\gamma_\nu\epsilon$. The fact that the metric transforms tells us this is a theory of gravity. Thus we have explicitly shown that a locally supersymmetric theory must include gravity and we call this theory supergravity.

2.6.2 Supergravity and the Duality

Recall that in string theory, closed and open strings are the fundamental objects. Open strings have endpoints on objects called D-branes, while closed strings are independent of the branes. A D-brane generalises the concept of a point particle to higher dimensions. A D0 brane is a point particle, a D1 brane looks like a line (i.e.: a string), a D2 brane[12] looks like a 2 dimensional object (i.e.: a membrane) and so forth.

[12]D3 branes feature in Type IIB string theory and will play an important role in what follows.

The low energy effective action of a closed string describes gravitons. For the open string, the action describes a spin 1 gauge theory. If we think about how this relates to our D-branes, then we see that the theory that describes the physics on the brane is a gauge theory. We can turn questions we have about these branes into questions about strings. For example, if we want to know how two branes interact then we can consider a string exchanged between the two branes. We might wonder if the brane has mass. Then we can think about a string interacting with the brane. This must be a gravitational interaction – the strength of which we can relate to mass. In this way, any question we have about the D-brane can be phrased as a question about strings and answered using string theory. In order to do brane physics, we do not need to add new degrees of freedom.

In the supergravity, we have objects called p-branes, where p is the dimension of the object. They are like black holes but they are infinitely long cylinders or planes or hyperplanes with a horizon. The event horizon in a spacetime is where the metric component g_{00} is zero. So while an observer will measure time passing, the proper time is frozen ($g_{00}(dx^0)^2 = d\tau^2$). A 3-brane is a 3 dimensional object surrounded by a horizon.

In the low energy theory (supergravity), we have small momenta and therefore long wavelengths. Rayleigh's criterion places a limit on the resolution ability of any imaging process to be on the order of the wavelength of the wave used to measure it. This is best understood in the case of single slit diffraction. Diffraction imposes a limit on our ability to resolve images. The defining equation for the first minimum in a diffraction pattern is given by

$$\sin\theta_m = \frac{\lambda}{a_0}$$

where λ is the wavelength of the source and a_0 is the size of the aperture. This equation tells us that we will see a diffraction pattern when $\lambda < a_0$ and that when $\lambda = a_0$ the first minimum is at $\frac{\pi}{2}$. This tells us that, for long wavelength waves, the wave is spread out so much that we cannot resolve maxima and minima and so we cannot say where the source of the wave is.

Thus the long wavelengths in the supergravity mean that the supergravity modes don't see the modes on the D-brane and so the branes do not interact with the closed strings. The low energy Lagrangian density is thus split into a gravitational part on $\mathcal{M}_{10}$ and a gauge theory part (Supersymmetric Yang-Mills), with no interactions mixing them.

The same can be said about interactions in the p-brane description at low-energy. However, the geometry in this description is not flat. Far away from the p-branes, the space looks flat and we have supergravity on $\mathcal{M}_{10}$. Near to the p-branes, the gravitational potential is a deep well (it looks like an attractive force) and so the energies of our string modes are red-shifted. This means that all the modes are at a low energy, so we have to retain a complete description of the string – not just the supergravity modes. The Lagrangian density is thus split into gravity on $\mathcal{M}_{10}$ and into type IIB strings on $AdS_5 \times S^5$.

If D-branes are the same as p-branes then the above two descriptions must agree (we iden-

tify 10d supergavity in both descriptions) and

$$\mathcal{L}_{\mathcal{N}=4\text{SYM}} \equiv \mathcal{L}^{\text{IIB strings}}_{AdS_5\times S^5} \tag{2.6.2.1}$$

This claims an equivalence between $\mathcal{N}=4$ SYM and a string theory on $AdS_5 \times S^5$. The left hand side is a flat space theory of particles. It has the gauge group $U(N)$. The right hand side is a string theory in higher dimensions, so it has many more degrees of freedom arising from these extra dimensions. We can try to build a dictionary that maps quantities in either theory to each other. In particular, we are interested in finding the low energy limit of the field theory which is equivalent to supergravity: the low energy limit of string theory.

When we study the field theory at large ('t Hooft) coupling, then the curvature is small on the string side[13]. It is difficult to study a theory with strong coupling because we cannot study it perturbatively. The beauty of supersymmetry is that it protects some quantities from corrections. This means we can study them at weak coupling and assume that they will remain the same at strong coupling. These are the BPS states whose conformal dimensions is equal to their $\mathcal{R}$ charge. To be in the $\frac{1}{2}$-BPS sector means that half of the supersymmetries are preserved and it is the most amount of supersymmetry we have after the vacuum. These $\frac{1}{2}$-BPS states are supergravity states.

[13] $g^2_{YM}N = \lambda = \frac{R^4}{l_s^4}$ where λ is the 't Hooft coupling, R is the radius of AdS_5 and l_s is the string length.

3 Eigenvalue Dynamics for Multimatrix Models

This chapter is based on the work presented in [11]. Motivated primarily by the work done in [12], we attempt to extend a supergravity interpretation of eigenvalue dynamics in the two matrix sector of the field theory. We perform explicit computations for operators belonging to the $SU(2)$ sector and match them with correlators computed with our proposed eigenvalue prescription. We recover the supergravity boundary condition by showing the eigenvalues condense on the surface that defines a wall between two boundary conditions.

3.1 Introduction

The large N expansion continues to be a promising approach towards the strong coupling dynamics of quantum field theories. For example, 't Hooft's proposal that the large N expansions of Yang-Mills theories are equivalent to the usual perturbation expansion in terms of topologies of worldsheets in string theory[5] has been realized concretely in the AdS/CFT correspondence[4]. Besides the usual planar limit where classical operator dimensions are held fixed as we take $N \to \infty$, there are non-planar large N limits of the theory [13] defined by considering operators with a bare dimension that is allowed to scale with N as we take $N \to \infty$. These limits are also relevant for the AdS/CFT correspondence. Indeed, operators with a dimension that scales as N include operators relevant for the description of giant graviton branes[8, 14, 15] while operators with a dimension of order N^2 include operators that correspond to new geometries in supergravity[12, 7, 16]. Despite these convincing motivations carrying out the large N expansion for most matrix models is still beyond our current capabilities.

One class of models for which the large N expansion can be computed are the singlet sector of matrix quantum mechanics of a single hermitian matrix[17]. We can also consider a complex matrix model as long as we restrict ourselves to potentials that are analytic in Z (summed with the dagger of this which needs to be added to get a real potential) and observables constructed out of traces of a product of Zs or out of a product of $Z^\dagger$s[18]. In these situations we can reduce the problem to eigenvalue dynamics. This is a huge reduction in degrees of freedom since we have reduced from $O(N^2)$ degrees of freedom, associated to the matrix itself, to $O(N)$ eigenvalue degrees of freedom. Studying saddle points of the original matrix action does not reproduce the large N values of observables. This is a consequence of the large number of degrees of freedom: we expect fluctuations to be suppressed by $1/N^2$ so that if N^2 variables in total are fluctuating, then we can have fluctuations of size $1/N^2 \times N^2 \sim 1$ which are not suppressed as $N \to \infty$. In terms of eigenvalues there are only N variables fluctuating so that fluctuations are bounded by $N \times 1/N^2 \sim 1/N$ which vanishes as $N \to \infty$. Thus, classical eigenvalue dynamics captures the large N limit. For example, one can formulate the physics of the planar limit by using the density of eigenvalues as a dynamical variable. The resulting collective field theory defines a field theory that explicitly has $1/N$ as a coupling constant[19, 20]. It has found both application in the context of the $c = 1$ string[21, 22, 23] and in descriptions of the LLM geometries[24].

Standard arguments show that eigenvalue dynamics corresponds to a familiar system: non-interacting fermions in an external potential[17]. This makes the description extremely convenient because the fermion dynamics is rather simple. This eigenvalue dynamics is also a very natural description of the large N but non-planar limits discussed above. Giant graviton branes which have expanded into the AdS_5 of the spacetime correspond to highly excited fermions or, equivalently, to single highly excited eigenvalues: the giant graviton is an eigenvalue[14, 16]. Giant graviton branes which have expanded into the S^5 of the spacetime correspond to holes in the Fermi sea, and hence to collective excitations of the eigenvalues where many eigenvalues are excited[16]. Half-BPS geometries also have a natural interpretation in terms of the eigenvalue dynamics: every fermion state can be identified with a particular supergravity geometry[7, 16]. The map between the two descriptions was discovered by Lin, Lunin and Maldacena in [12]. The fermion state can be specified by stating which states in phase space are occupied by a fermion, so we can divide phase space up into occupied and unoccupied states. By requiring regularity of the corresponding supergravity solution exactly the same structure arises: the complete set of regular solutions are specified by boundary conditions obtained by dividing a certain plane into black (identified with occupied states in the fermion phase space) and white (unoccupied states) regions. See [12] for the details.

Our main goal in this chapter is to ask if a similar eigenvalue description can be constructed for a two matrix model. Further, if such a construction exists, does it have a natural AdS/CFT interpretation? Work with a similar motivation but focusing on a different set of questions has appeared in[25, 26, 27, 28, 29]. We will consider the dynamics of two complex matrices, corresponding to the $SU(2)$ sector of $\mathcal{N} = 4$ super Yang-Mills theory. Further we consider the theory on $R \times S^3$ and expand all fields in spherical harmonics of the S^3. We will consider only the lowest s-wave components of these expansions so that the matrices are constant on the S^3. The reduction to the s-wave will be motivated below. In this way we find a matrix model quantum mechanics of two complex matrices. Expectation values are computed as follows

$$\langle \cdots \rangle = \int [dZ dZ^\dagger dY dY^\dagger] e^{-S} \cdots \tag{3.1.1}$$

At first sight it appears that any attempts to reduce (3.1.1) to an eigenvalue description are doomed to fail: the integral in (3.1.1) runs over two independent complex matrices Z and Y which will almost never be simultaneously diagonalizable. However, perhaps there is a class of questions, generalizing the singlet sector of a single hermitian matrix model, that can be studied using eigenvalue dynamics. To explore this possibility, let's review the arguments that lead to eigenvalue dynamics for a single complex matrix Z. We can use the Schur decomposition[18, 30, 31],

$$Z = U^\dagger D U \tag{3.1.2}$$

with U a unitary matrix and D is an upper triangular matrix, to explicitly change variables. Since we only consider observables that depend on the eigenvalues (the diagonal elements of D) we can integrate U and the off diagonal elements of D out of the model, leaving only the eigenvalues. The result of the integrations over U and the off diagonal elements of D is a non trivial Jacobian. Denoting the eigenvalues of Z by z_i, those of $Z^\dagger$ are given by complex

conjugation, $\bar{z}_i$. The resulting Jacobian is[18]

$$J = \Delta(z)\Delta(\bar{z}) \tag{3.1.3}$$

where

$$\begin{aligned}\Delta(z) &= \begin{vmatrix} 1 & 1 & \cdots & 1 \\ z_1 & z_2 & \cdots & z_N \\ \vdots & \vdots & \vdots\vdots\vdots & \vdots \\ z_1^{N-1} & z_2^{N-1} & \cdots & z_N^{N-1} \end{vmatrix} \\ &= \prod_{j>k}^{N}(z_j - z_k)\end{aligned} \tag{3.1.4}$$

is the usual Van der Monde determinant. A standard argument now maps this into non-interacting fermion dynamics[17]. Trying to apply a very direct change of variables argument to the two matrix model problem appears difficult. There is however an approach which both agrees with the above non-interacting fermion dynamics and can be generalized to the two matrix model. The idea is to construct a basis of operators that diagonalizes the inner product of the free theory. The construction of an orthogonal basis, given by the Schur polynomials, was achieved in [7]. Each Schur polynomial $\chi_R(Z)$ is labelled by a Young diagram R with no more than N rows. In [7] the exact (to all order in $1/N$) two point function of Schur polynomials was constructed. The result is

$$\langle \chi_R(Z)\chi_S(Z^\dagger)\rangle = f_R\delta_{RS} \tag{3.1.5}$$

where all spacetime dependence in the correlator has been suppressed. This dependence is trivial as it is completely determined by conformal invariance. The notation f_R denotes the product of the factors of Young diagram R. Remarkably there is an immediate and direct connection to non-interacting fermions: the fermion wave function can be written as

$$\psi_R(\{z_i, \bar{z}_i\}) = \chi_R(Z)\Delta(z)e^{-\frac{1}{2}\sum_i z_i\bar{z}_i} \tag{3.1.6}$$

This relation can be understood as a combination of the state operator correspondence (we associate a Schur polynomial operator on R^4 to a wave function on $R \times S^3$) and the reduction to eigenvalues (which is responsible for the $\Delta(z)$ factor)[16]. In this map the number of boxes in each row of R determines the amount by which each fermion is excited. In this way, each row in the Young diagram corresponds to a fermion and hence to an eigenvalue. Having one very long row corresponds to exciting a single fermion by a large amount, which corresponds to a single large (highly excited) eigenvalue. In the dual AdS gravity, a single long row is a giant graviton brane that has expanded in the AdS_5 space. Having one very long column corresponds to exciting many fermions by a single quantum, which corresponds to many eigenvalues excited by a small amount. In the dual AdS gravity, a single long column is a giant graviton brane that has expanded in the S^5 space.

The first questions we should tackle when approaching the two matrix problem should involve operators built using many Z fields and only a few Y fields. In this case at least a rough

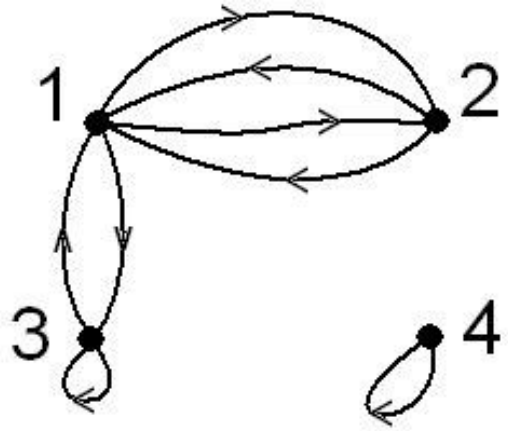


Figure 9: An example of a graph labeling an operator with a definite scaling dimension. Each node corresponds to an eigenvalue. Edges connect the different nodes so that the eigenvalues are interacting.

outline of the one matrix physics should be visible, and experience with the one matrix model will prove to be valuable.

For the case of two matrices we can again construct a basis of operators that again diagonalizes the free field two point function. These operators $\chi_{R,(r,s)ab}(Z,Y)$ are a generalization of the Schur polynomials, called restricted Schur polynomials[32, 33, 34]. They are labelled by three Young diagrams (R,r,s) and two multiplicity labels (a,b). For an operator constructed using n Zs and m Ys, $R \vdash n+m$, $r \vdash n$ and $s \vdash m$. The multiplicity labels distinguish between different copies of the (r,s) irreducible representation of $S_n \times S_m$ that arise when we restrict the irreducible representation R of S_{n+m} to the $S_n \times S_m$ subgroup. The two point function is

$$\langle \chi_{R,(r,s)ab}(Z,Y)\chi_{T,(t,u)cd}(Z^\dagger,Y^\dagger)\rangle = f_R \frac{\text{hooks}_R}{\text{hooks}_r \text{hooks}_s}\delta_{RT}\delta_{rt}\delta_{su}\delta_{ac}\delta_{bd} \tag{3.1.7}$$

where f_R was defined after (3.1.5) and hooks_a denotes the product of the hook lengths associated to Young diagram a. These operators do not have a definite dimension. However, they only mix weakly under the action of the dilatation operator and they form a convenient basis in which to study the spectrum of anomalous dimensions[35]. This action has been diagonalized in a limit in which R has order 1 rows (or columns), $m \ll n$ and n is of order N. Operators of a definite dimension are labelled by graphs composed of nodes that are traversed by oriented edges[36, 37]. There is one node for each row, so that each node corresponds to an eigenvalue. The directed edges start and end on the nodes. There is one edge for each Y field and the number of oriented edges ending on a node must equal the number of oriented edges emanating from a node. See figure 1 for an example of a graph labeling an operator. This picture, derived in the Yang-Mills theory, has an immediate and compelling interpretation in the dual gravity: each node corresponds to a giant graviton brane and the directed edges are open string excitations of these branes. The constraint that the number of edges ending on a node equals the number of edges emanating from the node is simply encoding the Gauss law on the brane world volume, which is topologically an S^3. For this reason the graphs labeling the operators are called Gauss graphs. If we are to obtain a system of non-interacting eigenvalues, we should only consider Gauss graphs that have no directed edges stretching between nodes. See figure

2 for an example. In fact, these all correspond to BPS operators. We thus arrive at a very concrete proposal:

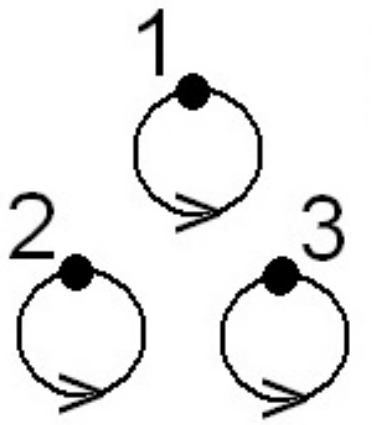


Figure 10: An example of a graph labeling a BPS operator. Each node corresponds to an eigenvalue. There are no edges connecting the different nodes so that these eigenvalues are not interacting.

If there is a free fermion description arising from the eigenvalue dynamics of the two matrix model, it will describe the BPS operators of the $SU(2)$ sector.

The BPS operators are associated to supergravity solutions of string theory. Indeed, the only one-particle states saturating the BPS bound in gravity are associated to massless particles and lie in the supergravity multiplet. Thus, eigenvalue dynamics will reproduce the supergravity dynamics of the gravity dual.

The BPS operators are all constructed from the s-wave of the spherical harmonic expansion on S^3[16]. This is our motivation for only considering operators constructed using the s-wave of the fields Y and Z. One further comment is that it is usually not consistent to simply restrict to a subset of the dynamical degrees of freedom. Indeed, this is only possible if the subset of degrees of freedom dynamically decouples from the rest of the theory. In the case that we are considering this is guaranteed to be the case, in the large N limit, because the Chan-Paton indices of the directed edges are frozen at large N [36].

We should mention that eigenvalue dynamics as dual to supergravity has also been advocated by Berenstein and his collaborators[38, 39, 40, 41, 42, 43, 44]. See also [45, 46, 47, 48] for related studies. Using a combination of numerical and physical arguments, which are rather different to the route we have followed, compelling evidence for this proposal has already been found. The basic idea is that at strong coupling the commutator squared term in the action forces the Higgs fields to commute and hence, at strong coupling, the Higgs fields of the theory should be simultaneously diagonalizable. In this case, an eigenvalue description is possible. Notice that our argument is a weak coupling argument, based on diagonalization of the one loop dilatation operator, that comes to precisely the same conclusion. In this chapter we will make some exact analytic statements that agree with and, in our opinion, refine some of the physical picture of

the above studies. For example, we will start to make precise statements about what eigenvalue dynamics does and does not correctly reproduce.

3.2 $AdS_5 \times S^5$ Background

To motivate our proposal for eigenvalue dynamics, we will review the $\frac{1}{2}$-BPS sector stressing the logic that we will subsequently use. The way in which a direct change of variables is used to derive the eigenvalue dynamics can be motivated by considering a correlation function of some arbitrary observables $\cdots$ that are functions only of the eigenvalues. Because we are considering BPS operators, correlators computed in the free field theory agree with the same computations at strong coupling[49], so that we now work in the free field theory. Performing the change of variables we find

$$\begin{aligned}\langle \cdots \rangle &= \int [dZ dZ^\dagger] e^{-\mathrm{Tr} ZZ^\dagger} \cdots \\ &= \int \prod_{i=1}^{N} dz_i d\bar{z}_i e^{-\sum_k z_z \bar{z}_k} \Delta(z)\Delta(\bar{z}) \cdots \\ &= \int \prod_{i=1}^{N} dz_i d\bar{z}_i |\psi_{\rm gs}(\{z_i, \bar{z}_i\})|^2 \cdots\end{aligned}$$

where the groundstate wave function is given by

$$\psi_{\rm gs}(\{z_i, \bar{z}_i\}) = \Delta(z) e^{-\frac{1}{2}\sum_i z_i \bar{z}_i} \tag{3.2.1}$$

We will shortly qualify the adjective "groundstate". Under the state-operator correspondence, this wave function is the state corresponding to the identity operator. The above transformation is equivalent to the identification

$$[dZ] e^{-\frac{1}{2}\mathrm{Tr}(ZZ^\dagger)} \leftrightarrow c \prod_{i=1}^{N} dz_i \, \psi_{\rm gs}(\{z_i, \bar{z}_i\}) \tag{3.2.2}$$

where c is a constant that arises from integrating over $U, U^\dagger$ and the off diagonal elements of D in (3.1.2). The role of each of the elements of the wave function is now clear:

1. Under the state operator correspondence, dimensions of operators map to energies of states. The dimensions of BPS operators are not corrected, i.e. they take their free field values. This implies an evenly spaced spectrum and hence a harmonic oscillator wave function. This explains the $e^{-\frac{1}{2}\sum_i z_i \bar{z}_i}$ factor. It also suggests that the wavefunction will be a polynomial times this Gaussian factor.

2. There is a gauge symmetry $Z \to UZU^\dagger$ that is able to permute the eigenvalues. Consequently we are discussing identical particles. Two matrices drawn at random from the complex Gaussian ensemble will not have degenerate eigenvalues, so we choose the particles to be fermions. This matches the fact that the wave function is a Slater determinant.

3. Under the transformation $Z \to e^{i\theta} Z$, dZ transforms with charge N^2. Since $\prod_i dz_i$ has charge N, $c\psi_{\rm gs}(\{z_i, \bar{z}_i\})$ must have charge $N(N-1)$. The constant c is obtained by integrating over the off diagonal elements of D in (3.1.2). Thus, c has charge $\frac{1}{2}N(N-1)$ and $\psi_{\rm gs}(\{z_i, \bar{z}_i\})$ itself has the same charge[14].

4. If we assign the dimension $\big[Z\big] = L$ it is clear that both $\psi_{\rm gs}(\{z_i, \bar{z}_i\})$ and c must have dimension $\frac{1}{2}N(N-1)$.

The wave function (3.2.1) satisfies these properties. Further, if we require that the wavefunction is a polynomial in the eigenvalues z_i times the exponential $e^{-\frac{1}{2}\sum_i z_i \bar{z}_i}$, then (3.2.1) is the state of lowest energy (we did not write down a Hamiltonian, but any other wave function has more nodes and hence a higher energy) so it deserves to be called the ground state. The wave function (3.2.1) is the state corresponding to the $\mathrm{AdS}_5 \times \mathrm{S}^5$ spacetime in the $\frac{1}{2}$-BPS sector.

The above discussion can be generalized to write down a wave function corresponding to the $\mathrm{AdS}_5 \times \mathrm{S}^5$ spacetime in the $SU(2)$ sector. The equation (3.2.2) is generalized to

$$[dZdY] e^{-\frac{1}{2}\mathrm{Tr}(ZZ^\dagger) - \frac{1}{2}\mathrm{Tr}(YY^\dagger)} \to c \prod_{i=1}^{N} dz_i dy_i \, \Psi_{\rm gs}(\{z_i, \bar{z}_i, y_i, \bar{y}_i\}) \tag{3.2.3}$$

where c is again a constant coming from integrating the non-eigenvalue variables out. The wave function must obey the following properties:

1. Our wave functions again describe states that correspond to BPS operators. The dimensions of the BPS operators take their free field values, implying an evenly spaced spectrum and hence a harmonic oscillator wave function. This suggests the wave function is a polynomial times the Gaussian factor $e^{-\frac{1}{2}\sum_i z_i \bar{z}_i - \frac{1}{2}\sum_i y_i \bar{y}_i}$ factor.

2. There is a gauge symmetry $Z \to UZU^\dagger$ and $Y \to UYU^\dagger$ that is able to permute the eigenvalues. Consequently we are discussing N identical particles. Matrices drawn at random will not have degenerate eigenvalues, so we choose the particles to be fermions. Thus we expect the wave function is a Slater determinant.

3. Under the transformation $Z \to e^{i\theta} Z$ and $Y \to Y$ the measure $dZdY$ transforms with charge N^2. Since $\prod_i dz_i dy_i$ has charge N and c has charge $\frac{1}{2}N(N-1)$, the wave function $\Psi_{\rm gs}(\{z_i, \bar{z}_i, y_i, \bar{y}_i\})$ must have charge $\frac{1}{2}N(N-1)$. Similarly, under the transformation $Z \to Z$ and $Y \to e^{i\theta} Y$ the measure $dZdY$ transforms with charge N^2. Since $\prod_i dz_i dy_i$ has charge N and again c has charge $\frac{1}{2}N(N-1)$, the wave function $\Psi_{\rm gs}(\{z_i, \bar{z}_i, y_i, \bar{y}_i\})$ should have charge $\frac{1}{2}N(N-1)$.

4. If we assign the dimension $\big[Z\big] = L = \big[Y\big]$ it is clear that both $\Psi_{\rm gs}(\{z_i, \bar{z}_i, y_i, \bar{y}_i\})$ and c must have dimension $N(N-1)$.

5. The probability density associated to a single particle $\rho_{\rm gs}(z_1, \bar{z}_1, y_1, \bar{y}_1)$ must have an $SO(4)$ symmetry, i.e. it should be a function of $|z_i|^2 + |y_i|^2$.

[14] We are assuming that any non-trivial measure depends only on the eigenvalues. This is a guess and we do not know a proof of this. We will make this assumption for the two matrix model as well.

The single particle probability density referred to in point 5 above is given, for any state $\Psi(\{z_i, \bar{z}_i, y_i, \bar{y}_i\})$ as usual, by

$$\rho(z_1, \bar{z}_1, y_1, \bar{y}_1) = \int \prod_{i=2}^{N} dz_i d\bar{z}_i dy_i d\bar{y}_i |\Psi(\{z_i, \bar{z}_i, y_i, \bar{y}_i\})|^2 \tag{3.2.4}$$

There is a good reason why the single particle probability density is an interesting quantity to look at: at short distances the eigenvalues feel a repulsion from the Slater determinant, which vanishes when two eigenvalues are equal. At long distances the confining harmonic oscillator potential dominates, ensuring the eigenvalues are clumped together in some finite region and do not wander off to infinity. In the end we expect that at large N the locus where the eigenvalues lie defines a specific surface, generalizing the idea of a density of eigenvalues for the single matrix model. This large N surface is captured by $\rho(z_1, \bar{z}_1, y_1, \bar{y}_1)$. We will make this connection more explicit in a later section.

There appears to be a unique wave function singled out by the above requirements. It is given by

$$\Psi_{\rm gs}(\{z_i, \bar{z}_i, y_i, \bar{y}_i\}) = \mathcal{N}\Delta(z, y) e^{-\frac{1}{2}\sum_k z_z \bar{z}_k - \frac{1}{2}\sum_k y_z \bar{y}_k} \tag{3.2.5}$$

where

$$\begin{aligned} \Delta(z,y) &= \begin{vmatrix} y_1^{N-1} & y_2^{N-1} & \cdots & y_N^{N-1} \\ z_1 y_1^{N-2} & z_2 y_2^{N-2} & \cdots & z_N y_N^{N-2} \\ \vdots & \vdots & \vdots\vdots\vdots & \vdots \\ z_1^{N-2} y_1 & z_2^{N-2} y_2 & \cdots & z_N^{N-2} y_N \\ z_1^{N-1} & z_2^{N-1} & \cdots & z_N^{N-1} \end{vmatrix} \\ &= \prod_{j>k}^{N} (z_j y_k - y_j z_k) \end{aligned} \tag{3.2.6}$$

generalizes the usual Van der Monde determinant and $\mathcal{N}$ is fixed by normalizing the wave function. Normalizing the wave function in the state picture corresponds to choosing a normalization in the original matrix model so that the expectation value of 1 is 1.

We can provide detailed tests of this wave function by using the equation

$$\int [dY dZ dY^\dagger dZ^\dagger] e^{-{\rm Tr}(ZZ^\dagger) - {\rm Tr}(YY^\dagger)} \cdots = \int \prod_{i=1}^{N} dz_i d\bar{z}_i dy_i d\bar{y}_i |\Psi_{\rm gs}(\{z_i, \bar{z}_i, y_i, \bar{y}_i\})|^2 \cdots \tag{3.2.7}$$

to compute correlators of observables (denoted by $\cdots$ above) that depend only on the eigenvalues. We have already argued above that we expect that these observables are the BPS operators of the CFT. As a first example, consider correlators of traces $O_J = {\rm Tr}(Z^J)$. These can be computed exactly in the matrix model, using a variety of different techniques - see for example [18, 50, 30]. The result is

$$\langle {\rm Tr}(Z^J) {\rm Tr}(Z^{\dagger J}) \rangle = \frac{1}{J+1} \Big[\frac{(J+N)!}{(N-1)!} - \frac{N!}{(N-J-1)!} \Big] \tag{3.2.8}$$

if $J < N$ and

$$\langle \mathrm{Tr}(Z^J)\mathrm{Tr}(Z^{\dagger J})\rangle = \frac{1}{J+1}\frac{(J+N)!}{(N-1)!} \tag{3.2.9}$$

if $J \geq N$. These expressions could easily be expanded to generate the $1/N$ expansion if we wanted to do that. We would now like to consider the eigenvalue computation. It is useful to write the wave function as

$$\Psi_{\mathrm{gs}}(\{z_i, \bar{z}_i, y_i, \bar{y}_i\}) = \frac{\pi^{-N}}{\sqrt{N!}}\epsilon^{a_1 a_2 \cdots a_n}\frac{z^0_{a_1} y^{N-1}_{a_1}}{\sqrt{0!(N-1)!}} \cdots \frac{z^{k-1}_{a_k} y^{N-k}_{a_k}}{\sqrt{(k-1)!(N-k)!}} \cdots$$
$$\cdots \frac{z^{N-1}_{a_N} y^0_{a_N}}{\sqrt{(N-1)!0!}} e^{-\frac{1}{2}\sum_q z_q \bar{z}_q - \frac{1}{2}\sum_q y_q \bar{y}_q} \tag{3.2.10}$$

The gauge invariant observable in this case is given by

$$\mathrm{Tr}(Z^J)\mathrm{Tr}(Z^{\dagger J}) = \sum_{i=1}^{N} z_i \sum_{j=1}^{N} \bar{z}_j \tag{3.2.11}$$

It is now straightforward to find

$$\int \prod_{i=1}^{N} dz_i d\bar{z}_i dy_i d\bar{y}_i |\Psi(\{z_i, \bar{z}_i, y_i, \bar{y}_i\})|^2 \sum_i z_i^J \sum_j \bar{z}_j^J = \frac{1}{J+1}\frac{(J+N)!}{(N-1)!} \tag{3.2.12}$$

When evaluating the above integral, only the terms with $i = j$ contribute. From this result we see that we have not reproduced traces with $J < N$ correctly - we don't even get the leading large N behavior right. We have, however, correctly reproduced the exact answer (to all orders in $1/N$) of the two point function for all single traces of dimension N or greater. For $J > N$ there are trace relations of the form

$$\mathrm{Tr}(Z^J) = \sum_{i,j,\ldots,k} c_{ij\ldots k}\mathrm{Tr}(Z^i)\mathrm{Tr}(Z^j)\cdots\mathrm{Tr}(Z^k) \tag{3.2.13}$$

$i, j, ..., k \leq N$ and $i + j + \cdots + k = J$. The fact that we reproduce two point correlators of traces with $J > N$ exactly implies that we also start to reproduce sums of products of traces of less than N fields. This suggests that the important thing is not the trace structure of the operator, but rather the dimension of the state.

The fact that we only reproduce observables that have a large enough dimension is not too surprising. Indeed, supergravity can't be expected to correctly describe the back reaction of a single graviton or a single string. To produce a state in the CFT dual to a geometry that is different from the AdS vacuum one needs to allow a number of AdS giant gravitons (eigenvalues) to condense. The eigenvalue dynamics is correctly reproducing the two point function of traces when their energy is greater than that required to blow up into an AdS giant graviton.

With a very simple extension of the above argument we can argue that we also correctly reproduce the correlator $\langle \mathrm{Tr}(Y^J)\mathrm{Tr}(Y^{\dagger J})\rangle$ with $J \geq N$. A much more interesting class of observables

to consider are mixed traces, which contain both Y and Z fields. To build BPS operators using both Y and Z fields we need to construct symmetrized traces. A very convenient way to perform this construction is as follows

$$\mathcal{O}_{J,K} = \frac{J!}{(J+K)!}\mathrm{Tr}\left(Y\frac{\partial}{\partial Z}\right)^K \mathrm{Tr}(Z^{J+K}) \tag{3.2.14}$$

The normalization up front is just the inverse of the number of terms that appear. With this normalization, the translation between the matrix model observable and an eigenvalue observable is

$$\mathcal{O}_{J,K} \leftrightarrow \sum_i z_i^J y_i^K \tag{3.2.15}$$

Since we could not find this computation in the literature, we will now explain how to evaluate the matrix model two point function exactly, in the free field theory limit. Since the dimension of BPS operators are not corrected, this answer is in fact exact. To start, perform the contraction over the $Y, Y^\dagger$ fields

$$\begin{aligned}\langle \mathcal{O}_{J,K}\mathcal{O}^\dagger_{J,K}\rangle &= \left(\frac{J!}{(J+K)!}\right)^2 \langle \mathrm{Tr}\left(Y\frac{\partial}{\partial Z}\right)^K \mathrm{Tr}(Z^{J+K})\mathrm{Tr}\left(Y^\dagger\frac{\partial}{\partial Z^\dagger}\right)^K \mathrm{Tr}(Z^{\dagger\, J+K})\rangle \\ &= \left(\frac{J!}{(J+K)!}\right)^2 K!\langle \mathrm{Tr}\left(\frac{\partial}{\partial Z}\frac{\partial}{\partial Z^\dagger}\right)^K \mathrm{Tr}(Z^{J+K})\mathrm{Tr}(Z^{\dagger\, J+K})\rangle \end{aligned} \tag{3.2.16}$$

Given the form of the matrix model two point function

$$\langle Z_{ij} Z^\dagger_{kl}\rangle = \delta_{il}\delta_{jk} \tag{3.2.17}$$

we know that we can write any free field theory correlator as

$$\langle \cdots \rangle = e^{\mathrm{Tr}\left(\frac{\partial}{\partial Z}\frac{\partial}{\partial Z^\dagger}\right)} \cdots \Big|_{Z=Z^\dagger=0} \tag{3.2.18}$$

Using this identity we now find

$$\langle \mathcal{O}_{J,K}\mathcal{O}^\dagger_{J,K}\rangle = \left(\frac{J!}{(J+K)!}\right)^2 K!\frac{(J+K)!}{J!}\langle \mathrm{Tr}(Z^{J+K})\mathrm{Tr}(Z^{\dagger\, J+K})\rangle \tag{3.2.19}$$

Thus, the result of the matrix model computation is

$$\langle \mathcal{O}_{J,K}\mathcal{O}^\dagger_{J,K}\rangle = \frac{J!K!}{(J+K+1)!}\left[\frac{(J+K+N)!}{(N-1)!} - \frac{N!}{(N-J-K-1)!}\right] \tag{3.2.20}$$

if $J+K<N$ and

$$\langle \mathcal{O}_{J,K}\mathcal{O}^\dagger_{J,K}\rangle = \frac{J!K!}{(J+K+1)!}\frac{(J+K+N)!}{(N-1)!} \tag{3.2.21}$$

if $J+K \geq N$. Notice that for these two matrix observables we again get a change in the form of the correlator as the dimension of the trace passes N.

Next, consider the eigenvalue computation. We need to perform the integral

$$\langle \mathcal{O}_{J,K}\mathcal{O}^\dagger_{J,K}\rangle = \int \prod_{i=1}^{N} dz_i d\bar{z}_i dy_i d\bar{y}_i |\Psi_{\rm gs}(\{z_i,\bar{z}_i,y_i,\bar{y}_i\})|^2 \sum_{k=1}^{N} z_k^J y_k^K \sum_{j=1}^{N} \bar{z}_j^J \bar{y}_j^K \tag{3.2.22}$$

After some straightforward manipulations we have

$$\langle \mathcal{O}_{J,K}\mathcal{O}^\dagger_{J,K}\rangle = \pi^{-2N} \int \prod_{i=1}^{N} dz_i d\bar{z}_i dy_i d\bar{y}_i \frac{|z_1|^0|y_1|^{2N-2}}{0!(N-1)!}\cdots\frac{|z_k|^{2k-2}|y_k|^{2N-2k}}{(k-1)!(N-k)!}\cdots \\ \frac{|z_N|^{2N-2}|y_N|^0}{(N-1)!0!}\times e^{-\sum_q z_q\bar{z}_q-\sum_q y_q\bar{y}_q}\sum_{k,j=1}^{N} z_k^J y_k^K \bar{z}_j^J \bar{y}_j^K \tag{3.2.23}$$

Only terms with $k=j$ contribute so that

$$\langle \mathcal{O}_{J,K}\mathcal{O}^\dagger_{J,K}\rangle = \sum_{k=1}^{N}\frac{(N-k+K)!}{(N-k)!}\frac{(J+k-1)!}{(k-1)!} = \frac{K!J!}{(K+J+1)!}\frac{(J+K+N)!}{(N-1)!} \tag{3.2.24}$$

Thus, we again correctly reproduce the exact (to all orders in $1/N$) answer for the two point function of single trace operators of dimension N or greater.

It is also interesting to consider multi trace correlators. We will start with the correlator between a double trace and a single trace and we will again start with the matrix model computation

$$\langle O_{J_1,K_1}O_{J_2,K_2}O^\dagger_{J_1+J_2,K_1+K_2}\rangle = \frac{J_1!}{(J_1+K_1)!}\frac{J_2!}{(J_2+K_2)!}\frac{(J_1+J_2)!}{(J_1+K_1+J_2+K_2)!}\times \\ \langle {\rm Tr}\left(Y\frac{\partial}{\partial Z}\right)^{K_1}{\rm Tr}(Z^{J_1+K_1}){\rm Tr}\left(Y\frac{\partial}{\partial Z}\right)^{K_2}{\rm Tr}(Z^{J_2+K_2}){\rm Tr}\left(Y^\dagger\frac{\partial}{\partial Z^\dagger}\right)^{K_1+K_2}{\rm Tr}(Z^{\dagger J_1+K_1 J_2+K_2})\rangle \tag{3.2.25}$$

We could easily set $K_1=K_2=0$ and obtain traces involving only a single matrix. Begin by contracting all $Y, Y^\dagger$ fields to obtain

$$\langle O_{J_1,K_1}O_{J_2,K_2}O^\dagger_{J_1+J_2,K_1+K_2}\rangle = \frac{J_1!}{(J_1+K_1)!}\frac{J_2!}{(J_2+K_2)!}\frac{(J_1+J_2)!}{(J_1+K_1+J_2+K_2)!}(K_1+K_2)!\times \\ \langle \frac{\partial}{\partial Z_{i_1j_1}}\cdots\frac{\partial}{\partial Z_{i_{K_1}j_{K_1}}}{\rm Tr}(Z^{J_1+K_1})\frac{\partial}{\partial Z_{i_{K_1+1}j_{K_1+1}}}\cdots\frac{\partial}{\partial Z_{i_{K_1+K_2}j_{K_1+K_2}}}{\rm Tr}(Z^{J_2+K_2}) \\ \frac{\partial}{\partial Z^\dagger_{j_1i_1}}\cdots\frac{\partial}{\partial Z^\dagger_{j_{K_1+K_2}i_{K_1+K_2}}}{\rm Tr}(Z^{\dagger J_1+K_1+J_2+K_2})\rangle \tag{3.2.26}$$

It is now useful to integrate by parts with respect to $Z^\dagger$, using the identity

$$\langle \frac{\partial}{\partial Z_{ij}} f(Z)\, g(Z)\, \frac{\partial}{\partial Z^\dagger_{ji}} h(Z^\dagger)\rangle = n_f \langle f(Z)\, g(Z)\, h(Z^\dagger)\rangle \tag{3.2.27}$$

where $f(Z)$ is of degree n_f in Z. Repeatedly using this identity, we find

$$\begin{aligned}\langle O_{J_1,K_1} O_{J_2,K_2} O^\dagger_{J_1+J_2,K_1+K_2}\rangle &= \frac{J_1!}{(J_1+K_1)!}\frac{J_2!}{(J_2+K_2)!}\frac{(J_1+J_2)!}{(J_1+K_1+J_2+K_2)!}(K_1+K_2)!\times \\ &\frac{(J_1+K_1)!}{J_1!}\frac{(J_2+K_2)!}{J_2!}\langle \mathrm{Tr}(Z^{J_1+K_1})\mathrm{Tr}(Z^{J_2+K_2})\mathrm{Tr}(Z^{\dagger J_1+K_1+J_2+K_2})\rangle \\ &= \frac{(J_1+J_2)!(K_1+K_2)!}{(J_1+K_1+J_2+K_2)!}\langle \mathrm{Tr}(Z^{J_1+K_1})\mathrm{Tr}(Z^{J_2+K_2})\mathrm{Tr}(Z^{\dagger J_1+K_1+J_2+K_2})\rangle\end{aligned} \tag{3.2.28}$$

This last correlator is easily computed. For example, if $J_1+K_1<N$ and $J_2+K_2<N$ we have

$$\begin{aligned}\langle O_{J_1,K_1} O_{J_2,K_2} O^\dagger_{J_1+J_2,K_1+K_2}\rangle = \frac{(J_1+J_2)!(K_1+K_2)!}{(J_1+K_1+J_2+K_2+1)!}\Big[&\frac{(J_1+K_1+J_2+K_2+N)!}{(N-1)!} \\ +\frac{N!}{(N-J_1-K_1-J_2-K_2-1)!} &- \frac{(N+J_1+K_1)!}{(N-J_2-K_2-1)!} \\ &- \frac{(N+J_2+K_2)!}{(N-J_1-K_1-1)!}\Big]\end{aligned} \tag{3.2.29}$$

and if $J_1+K_1\geq N$ and $J_2+K_2\geq N$ we have

$$\langle O_{J_1,K_1} O_{J_2,K_2} O^\dagger_{J_1+J_2,K_1+K_2}\rangle = \frac{(J_1+J_2)!(K_1+K_2)!}{(J_1+K_1+J_2+K_2+1)!}\frac{(J_1+K_1+J_2+K_2+N)!}{(N-1)!} \tag{3.2.30}$$

It is a simple exercise to check that, in terms of eigenvalues, we have

$$\begin{aligned}\langle \mathcal{O}_{J_1,K_1} \mathcal{O}_{J_2,K_2} \mathcal{O}^\dagger_{J_1+J_2,K_1+K_2}\rangle &= \int \prod_{i=1}^N dz_i d\bar{z}_i dy_i d\bar{y}_i |\Psi_{\rm gs}(\{z_i,\bar{z}_i,y_i,\bar{y}_i\})|^2 \\ &\quad \times \sum_{k=1}^N z_k^{J_1} y_k^{K_1} \sum_{l=1}^N z_l^{J_2} y_l^{K_2} \sum_{j=1}^N \bar{z}_j^{J_1+J_2} \bar{y}_j^{K_1+K_2} \\ &= \frac{(J_1+J_2)!(K_1+K_2)!}{(J_1+K_1+J_2+K_2+1)!}\frac{(J_1+K_1+J_2+K_2+N)!}{(N-1)!}\end{aligned} \tag{3.2.31}$$

so that once again we have reproduced the exact answer as long as the dimension of each trace is not less than N. The agreement that we have observed for multi trace correlators continues as follows: as long as the dimension of each trace is greater than $N-1$ the matrix model and the eigenvalue descriptions agree and both give

$$\langle O_{J_1,K_1} O_{J_2,K_2} \cdots O_{J_n,K_n} O^\dagger_{J,K}\rangle = \frac{J!K!}{(J+K+1)!}\frac{(J+K+N)!}{(N-1)!}\delta_{J_1+\cdots+J_n,J}\delta_{K_1+\cdots+K_n,K} \tag{3.2.32}$$

for the exact value of this correlator. We have limited our selves to a single daggered observable in the above expression for purely technical reasons: it is only in this case that we can compute

the matrix model correlator using the identity (3.2.27). It would be interesting to develop analytic methods that allow more general computations.

Finally, we can also test multi trace correlators with a dimension of order N^2. A particularly simple operator is the Schur polynomial labelled by a Young diagram R with N rows and M columns. For this R we have

$$\chi_R(Z) = (\det Z)^M = z_1^M z_2^M \cdots z_N^M \tag{3.2.33}$$

$$\chi_R(Z^\dagger) = (\det Z^\dagger)^M = \bar{z}_1^M \bar{z}_2^M \cdots \bar{z}_N^M \tag{3.2.34}$$

The dual LLM geometry is labelled by an annulus boundary condition that has an inner radius of $\sqrt{M}$ and an outer radius of $\sqrt{M+N}$. The two point correlator of this Schur polynomial is

$$\begin{aligned}
\langle \chi_R(Z)\chi_R(Z^\dagger)\rangle &= \int \prod_{i=1}^N dz_i d\bar{z}_i dy_i d\bar{y}_i \chi_R(Z)\chi_R(Z^\dagger)|\Psi_{\rm gs}(\{z_i,\bar{z}_i,y_i,\bar{y}_i\})|^2 \\
&= \pi^{-2N}\int \prod_{i=1}^N dz_i d\bar{z}_i dy_i d\bar{y}_i \frac{|z_1|^{0+2M}|y_1|^{2N-2}}{0!(N-1)!}\cdots \frac{|z_k|^{2k-2+2M}|y_k|^{2N-2k}}{(k-1)!(N-k)!} \\
&\times \quad \cdots \frac{|z_N|^{2N-2+2M}|y_N|^0}{(N-1)!0!} \times e^{-\sum_q z_q\bar{z}_q - \sum_q y_q\bar{y}_q} \\
&= \prod_{i=1}^N \frac{(i-1+M)!}{(i-1)!}
\end{aligned} \tag{3.2.35}$$

which is again the exact answer for this correlator.

After this warm up example we will now make a few comments that are relevant for the general case. The details are much more messy, so we will not manage to make very precise statements. We have however included this discussion as it does provide a guide as to when eigenvalue dynamics is applicable. A Schur polynomial labelled with a Young diagram R that has row lengths r_i is given in terms of eigenvalues as (our labeling of the rows is defined by $r_1 \geq r_2 \geq \cdots \geq r_N$)

$$\chi_R(Z) = \frac{\epsilon_{a_1 a_2 \cdots a_N} z_{a_1}^{N-1+r_1} z_{a_2}^{N-2+r_2} \cdots z_{a_N}^{r_N}}{\epsilon_{b_1 b_2 \cdots b_N} z_{b_1}^{N-1} z_{b_2}^{N-2} \cdots z_{b_{N-1}}} \tag{3.2.36}$$

Using this expression, we can easily write the exact two point function as follows

$$\begin{aligned}
\langle \chi_R(Z)\chi_R(Z^\dagger)\rangle &= \frac{1}{N!\pi^N}\int \prod_{i=1}^N dz_i d\bar{z}_i \epsilon_{a_1 a_2\cdots a_N} z_{a_1}^{N-1+r_1} z_{a_2}^{N-2+r_2}\cdots z_{a_N}^{r_N} \\
&\qquad \times \epsilon_{b_1 b_2 \cdots b_N} \bar{z}_{b_1}^{N-1+r_1} \bar{z}_{b_2}^{N-2+r_2} \cdots \bar{z}_{b_N}^{r_N} e^{-\sum_k z_k \bar{z}_k} \\
&= \prod_{j=0}^{N-1} \frac{(j+r_{N-j})!}{j!} = f_R
\end{aligned} \tag{3.2.37}$$

Using our wave function we can compute the two point function of Schur polynomials. The result is

$$\begin{aligned}\langle \chi_R(Z)\chi_R(Z^\dagger)\rangle &= \int \prod_{i=1}^{N} dz_i d\bar{z}_i dy_i d\bar{y}_i \chi_R(Z)\chi_R(Z^\dagger)|\Psi_{\rm gs}(\{z_i,\bar{z}_i,y_i,\bar{y}_i\})|^2 \\ &= \frac{1}{N!\pi^N}\int \prod_{i=1}^{N} dz_i d\bar{z}_i \epsilon_{a_1 a_2\cdots a_N}|z_{a_1}|^{2N-2}|z_{a_2}|^{2N-4}\cdots|z_{a_{N-1}}|^2 \\ &\quad \times \frac{\epsilon_{b_1 b_2\cdots b_N} z_{b_1}^{N-1+r_1} z_{b_2}^{N-2+r_2}\cdots z_{b_N}^{r_N}}{\epsilon_{c_1 c_2\cdots c_N} z_{c_1}^{N-1} z_{c_2}^{N-2}\cdots z_{a_{N-1}}} \\ &\quad \times \frac{\epsilon_{d_1 d_2\cdots d_N} \bar{z}_{d_1}^{N-1+r_1} \bar{z}_{d_2}^{N-2+r_2}\cdots \bar{z}_{d_N}^{r_N}}{\epsilon_{e_1 e_2\cdots e_N} \bar{z}_{e_1}^{N-1} \bar{z}_{e_2}^{N-2}\cdots \bar{z}_{e_{N-1}}} e^{-\sum_k z_k \bar{z}_k}\end{aligned} \tag{3.2.38}$$

When the integration over the angles θ_i associated to $z_i = r_i e^{i\theta_i}$ are performed, a non-zero result is only obtained if powers of the z_i match the powers of the $\bar{z}_i$. The difference between the above expression and the exact answer is simply that in the eigenvalue expression these powers are separately set to be equal in the measure and in the product of Schur polynomials - there are two matchings, while in the exact answer the power of z_i arising from the product of the measure and the product of Schur polynomials is matched to the power of $\bar{z}_i$ from the product of the measure and the product of Schur polynomials - there is a single matching happening. Thus, the eigenvalue computation may miss some terms that are present in the exact answer[15]. For Young diagrams with a few corners and $O(N^2)$ boxes (the annulus above is a good example) the eigenvalues clump into groupings, with each grouping collecting eigenvalues of a similar size corresponding to rows with a similar row length[48]. This happens because the product of the Gaussian fall off $e^{-z\bar{z}}$ and a polynomial of fixed degree $|z^2|^n$ is sharply peaked at $|z| = n$. Thus, for example if $r_i \approx M_1$ for $i = 1, 2, \cdots, \frac{N}{2}$ and $r_i \approx M_2$ for $i = 1 + \frac{N}{2}, 2 + \frac{N}{2}, \cdots, N$ with M_1 and M_2 well separated ($M_1 - M_2 \geq O(N)$), under the integral we can replace

$$\frac{\epsilon_{b_1 b_2\cdots b_N} z_{b_1}^{N-1+r_1} z_{b_2}^{N-2+r_2}\cdots z_{b_N}^{r_N}}{\epsilon_{c_1 c_2\cdots c_N} z_{c_1}^{N-1} z_{c_2}^{N-2}\cdots z_{a_{N-1}}} \to \prod_{i=1}^{\frac{N}{2}} z_{a_i}^{M_1} z_{a_{i+\frac{N}{2}}}^{M_2} \tag{3.2.39}$$

After making a replacement of this type, we recover the exact answer. This replacement is not exact - we need to appeal to large N to justify it. It would be very interesting to explore this point further and to quantify in general (if possible) what the corrections to the above replacement are. For Young diagrams with many corners, row lengths are not well separated and there is no similar grouping that occurs, so that the eigenvalue description will not agree with the exact result, even at large N. A good example of a geometry with many corners is the superstar[51]. The corresponding LLM boundary condition is a number of very thin concentric annuli, so that we effectively obtain a gray disk, signaling a singular supergravity geometry. It is then perhaps not surprising that the eigenvalue dynamics does not correctly reproduce this two point correlator.

Having discussed the two point function of Schur polynomials in detail, the product rule

$$\chi_R(Z)\chi_S(Z) = \sum_T f_{RST}\chi_T(Z) \tag{3.2.40}$$

[15]This is the reason why (3.2.12) only captures one of the terms present in the two point function for $J < N$.

with f_{RST} a Littlewood-Richardson coefficient, implies that there is no need to consider correlation functions of products of Schur polynomials.

3.3 Other Backgrounds

In the $\frac{1}{2}$ BPS sector there is a wave function corresponding to every LLM geometry. The (not normalized) wave function has already been given in (3.1.6). In this section we consider the problem of writing eigenvalue wave functions that correspond to geometries other than $AdS_5 \times S^5$. The simplest geometry we can consider is the annulus geometry considered in the previous section, where we argued that the eigenvalue dynamics reproduces the exact correlator of the Schur polynomials dual to this geometry. Our proposal for the state that corresponds to this LLM spacetime is

$$\Psi_{\rm LLM}(\{z_i,\bar{z}_i,y_i,\bar{y}_i\}) = \frac{\pi^{-N}}{\sqrt{N!}}\epsilon^{a_1 a_2\cdots a_n}\frac{z_{a_1}^M y_{a_1}^{N-1}}{\sqrt{M!(N-1)!}}\cdots\frac{z_{a_k}^{k-1+M}y_{a_k}^{N-k}}{\sqrt{(k-1+M)!(N-k)!}} \cdots\frac{z_{a_N}^{N-1+M}y_{a_N}^{0}}{\sqrt{(N-1+M)!0!}}e^{-\frac{1}{2}\sum_q z_q\bar{z}_q-\frac{1}{2}\sum_q y_q\bar{y}_q} \tag{3.3.1}$$

This is simply obtained by multiplying the ground state wave function by the relevant Schur polynomial and normalizing the resulting state. The connection between matrix model correlators and expectation values computed using the above wave function is the following[16]

$$\begin{aligned}\langle\cdots\rangle_{\rm LLM} &= \frac{\langle\cdots\ \chi_R(Z)\chi_R(Z^\dagger)\rangle}{\langle\chi_R(Z)\chi_R(Z^\dagger)\rangle}\\ &= \int\prod_{i=1}^N dz_i d\bar{z}_i dy_i d\bar{y}_i|\Psi_{\rm LLM}(\{z_i,\bar{z}_i,y_i,\bar{y}_i\})|^2\ \cdots\end{aligned} \tag{3.3.2}$$

We can use this wave function to compute correlators that we are interested in. Traces involving only Zs for example lead to

$$\begin{aligned}\langle{\rm Tr}(Z^J){\rm Tr}(Z^{\dagger J})\rangle_{\rm LLM} &= \int\prod_{i=1}^N dz_i d\bar{z}_i dy_i d\bar{y}_i|\Psi_{\rm LLM}(\{z_i,\bar{z}_i,y_i,\bar{y}_i\})|^2\sum_{k=1}^N z_k^J\sum_{l=1}^N\bar{z}_l^J\\ &= \sum_{k=0}^{N-1}\frac{(J+k+M)!}{(k+M)!}\\ &= \frac{1}{J+1}\left[\frac{(J+M+N)!}{(M+N-1)!}-\frac{(J+M)!}{(M-1)!}\right]\end{aligned} \tag{3.3.3}$$

which agrees with the exact result, as long as $J > N-1$. Thus, in this background, eigenvalue dynamics is correctly reproducing the same set of correlators as in the original $AdS_5 \times S^5$

[16]The new normalization for matrix model correlators is needed to ensure that the identity operator has expectation value 1. This matches the normalization adopted in the eigenvalue description.

background. Traces involving only Y fields are also correctly reproduced

$$\langle \mathrm{Tr}(Y^J)\mathrm{Tr}(Y^{\dagger J})\rangle_{\mathrm{LLM}} = \int \prod_{i=1}^{N} dz_i d\bar{z}_i dy_i d\bar{y}_i |\Psi_{\mathrm{LLM}}(\{z_i,\bar{z}_i,y_i,\bar{y}_i\})|^2 \sum_{k=1}^{N} y_k^J \sum_{l=1}^{N} \bar{y}_l^J$$
$$= \frac{1}{J+1}\frac{(J+N)!}{(N-1)!} \tag{3.3.4}$$

where $J \geq N$. Notice that these results are again exact, i.e. we reproduce the matrix model correlators to all orders in $1/N$. Finally, let's consider the most interesting case of traces involving both matrices. The LLM wave function we have proposed does not reproduce the exact matrix model computation. The matrix model computation gives

$$\begin{aligned}
\langle \mathcal{O}_{J,K}\mathcal{O}^\dagger_{J,K}\rangle_{\mathrm{LLM}} &= \left(\frac{J!}{(J+K)!}\right)^2 \langle \mathrm{Tr}\left(Y\frac{\partial}{\partial Z}\right)^K \mathrm{Tr}(Z^{J+K})\mathrm{Tr}\left(Y^\dagger\frac{\partial}{\partial Z^\dagger}\right)^K \mathrm{Tr}(Z^{\dagger\, J+K})\rangle_{\mathrm{LLM}} \\
&= \left(\frac{J!}{(J+K)!}\right)^2 K!\langle \mathrm{Tr}\left(\frac{\partial}{\partial Z}\frac{\partial}{\partial Z^\dagger}\right)^K \mathrm{Tr}(Z^{J+K})\mathrm{Tr}(Z^{\dagger\, J+K})\rangle_{\mathrm{LLM}} \\
&= \left(\frac{J!}{(J+K)!}\right)^2 K!\frac{(J+K)!}{J!}\langle \mathrm{Tr}(Z^{J+K})\mathrm{Tr}(Z^{\dagger\, J+K})\rangle_{\mathrm{LLM}} \\
&= \frac{J!K!}{(J+K+1)!}\left[\frac{(J+K+M+N)!}{(M+N-1)!} - \frac{(J+K+M)!}{(M-1)!}\right]
\end{aligned} \tag{3.3.5}$$

if $J+K \geq N$. Next, consider the eigenvalue computation. We need to perform the integral

$$\begin{aligned}
\langle \mathcal{O}_{J,K}\mathcal{O}^\dagger_{J,K}\rangle_{\mathrm{LLM,eigen}} &= \int \prod_{i=1}^{N} dz_i d\bar{z}_i dy_i d\bar{y}_i |\Psi_{\mathrm{LLM}}(\{z_i,\bar{z}_i,y_i,\bar{y}_i\})|^2 \sum_{k=1}^{N} z_k^J y_k^K \sum_{j=1}^{N} \bar{z}_j^J \bar{y}_j^K \\
&= \sum_{k=1}^{N} \frac{(N-k+K)!}{(N-k)!}\frac{(J+M+k-1)!}{(M+k-1)!}
\end{aligned} \tag{3.3.6}$$

It is not completely trivial to compare (3.3.5) and (3.3.6), but it is already clear that they do not reproduce exactly the same answer. To simplify the discussion, let's consider the case that $M = O(\sqrt{N})$. In this case, in the large N limit, we can drop the second term in (3.3.5) to obtain

$$\langle \mathcal{O}_{J,K}\mathcal{O}^\dagger_{J,K}\rangle_{\mathrm{LLM}} = \frac{J!K!}{(J+K+1)!}\frac{(J+K+M+N)!}{(M+N-1)!}(1+\cdots) \tag{3.3.7}$$

where $\cdots$ stand for terms that vanish as $N \to \infty$. In the sum appearing in (3.3.6), change variables from k to $k'-M$ and again appeal to large N to write

$$\begin{aligned}
\langle \mathcal{O}_{J,K}\mathcal{O}^\dagger_{J,K}\rangle_{\mathrm{LLM,eigen}} &= \sum_{k'=M+1}^{M+N} \frac{(N+M-k'+K)!}{(N+M-k')!}\frac{(J+k'-1)!}{(k'-1)!} \\
&= \sum_{k'=1}^{M+N} \frac{(N+M-k'+K)!}{(N+M-k')!}\frac{(J+k'-1)!}{(k'-1)!}(1+\cdots) \\
&= \frac{J!K!}{(J+K+1)!}\frac{(J+K+M+N)!}{(M+N-1)!}(1+\cdots)
\end{aligned} \tag{3.3.8}$$

In the last two lines above $\cdots$ again stands for terms that vanish as $N \to \infty$. Thus, we find agreement between (3.3.5) and (3.3.6). It is again convincing to see genuine multi matrix observables reproduced by the eigenvalue dynamics. Notice that in this case the agreement is not exact, but rather is realized to the large N limit. This is what we expect for the generic situation - the $AdS_5 \times S^5$ case is highly symmetric and the fact that eigenvalue dynamics reproduces so many observables exactly is a consequence of this symmetry. We only expect eigenvalue dynamics to reproduce classical gravity, which should emerge from the CFT at $N = \infty$.

Much of our intuition came from thinking about the Gauss graph operators constructed in [36, 37]. It is natural to ask if we can write down wave functions dual to the Gauss graph operators. The simplest possibility is to consider a Gauss graph operator obtained by exciting a single eigenvalue by J levels, and then attaching a total of K Y strings to it. The extreme simplicity of this case follows because we can write the (normalized) Gauss graph operator in terms of a familiar Schur polynomial as

$$\hat{O} = \sqrt{\frac{J!K!}{(J+K)!}\frac{(N-1)!}{(N+J+K-1)!}}\mathrm{Tr}\left(Y\frac{\partial}{\partial Z}\right)^K \chi_{(J+K)}(Z) \tag{3.3.9}$$

where we have used the notation (n) to denote a Young diagram with a single row of n boxes. Consider the correlator

$$\begin{aligned}\langle \hat{O}\mathrm{Tr}(Y^\dagger)^K \mathrm{Tr}(Z^{\dagger J})\rangle &= \langle \mathrm{Tr}\left(\frac{\partial}{\partial Y}\right)^K \hat{O}\mathrm{Tr}(Z^{\dagger J})\rangle \\ &= \sqrt{\frac{J!K!}{(J+K)!}\frac{(N+J+K-1)!}{(N-1)!}}\end{aligned} \tag{3.3.10}$$

This answer is exact, in the free field theory. In what limit should we compare this answer to eigenvalue dynamics? Our intuition is coming from the $\frac{1}{2}$- BPS sector where we know that rows of Schur polynomials correspond to eigenvalues and we know exactly how to write the corresponding wave function. If we only want small perturbations of this picture, we should keep $K \ll J$. In this case we should simplify

$$\begin{aligned}\frac{J!K!}{(J+K)!} &\to \frac{1}{J^K} \\ \frac{(N+J+K-1)!}{(N-1)!} &= \frac{(N+J+K-1)!}{(N+J-1)!}\frac{(N+J-1)!}{(N-1)!} \\ &\to (N+J-1)^K \frac{(N+J-1)!}{(N-1)!}\end{aligned} \tag{3.3.11}$$

How should we scale J as we take $N \to \infty$? The Schur polynomials are a sum over all possible matrix trace structures. We want these sums to be dominated by traces with a large number of matrices (N or more) in each trace. To accomplish this we will scale $J = O(N^{1+\epsilon})$ with $\epsilon > 0$. In this case, at large N, we can replace

$$\frac{1}{J^K}(N+J-1)^K \to 1 \tag{3.3.12}$$

and hence, the result that should be reproduced by the eigenvalue dynamics is given by

$$\langle \hat{O}\mathrm{Tr}(Y^\dagger)^K \mathrm{Tr}(Z^{\dagger J})\rangle = \sqrt{K!\frac{(N+J-1)!}{(N-1)!}} \tag{3.3.13}$$

In the eigenvalue computation, we will use the wave function of the ground state and the wave function of the Gauss graph operator ($\Psi_{\mathrm{GG}}(\{z_i,\bar{z}_i,y_i,\bar{y}_i\})$) to compute the amplitude

$$\int \prod_{i=1}^{N} dz_i d\bar{z}_i dy_i d\bar{y}_i \Psi^*_{\mathrm{gs}}(\{z_i,\bar{z}_i,y_i,\bar{y}_i\})(\sum_i \bar{y}_i)^K \sum_j \bar{z}_j^J \Psi_{\mathrm{GG}}(\{z_i,\bar{z}_i,y_i,\bar{y}_i\}) \tag{3.3.14}$$

We expect the amplitude (3.3.14) to reproduce (3.3.13). Our proposal for the wave function corresponding to the above Gauss graph operator is

$$\begin{aligned}\Psi_{GG}(\{z_i,\bar{z}_i,y_i,\bar{y}_i\}) = \frac{\pi^{-N}}{\sqrt{N!}}\epsilon^{a_1a_2\cdots a_n}\frac{z_{a_1}^0 y_{a_1}^{N-1}}{\sqrt{0!(N-1)!}}\cdots\frac{z_{a_k}^{k-1}y_{a_k}^{N-k}}{\sqrt{(k-1)!(N-k)!}}\cdots \\ \cdots\frac{z_{a_{N-1}}^{N-2}y_{a_{N-1}}}{\sqrt{(N-2)!1!}}\frac{z_{a_N}^{J+N-1}y_{a_N}^K}{\sqrt{(J+N-1)!K!}}e^{-\frac{1}{2}\sum_q z_q\bar{z}_q-\frac{1}{2}\sum_q y_q\bar{y}_q}\end{aligned} \tag{3.3.15}$$

The eigenvalue with the largest power of z (i.e. z_{a_N}) was the fermion at the very top of the Fermi sea. It has been excited by J powers of z and K powers of y. It is now trivial to verify that (3.3.14) does indeed reproduce (3.3.13).

Finally, the state with three eigenvalues excited by $J_1 > J_2 > J_3$ and with $K_1 > K_2 > K_3$ strings attached to each eigenvalue is given by

$$\begin{aligned}\Psi_{GG}(\{z_i,\bar{z}_i,y_i,\bar{y}_i\}) = \frac{\pi^{-N}}{\sqrt{N!}}\epsilon^{a_1a_2\cdots a_n}\frac{z_{a_1}^0 y_{a_1}^{N-1}}{\sqrt{0!(N-1)!}}\cdots\frac{z_{a_k}^{k-1}y_{a_k}^{N-k}}{\sqrt{(k-1)!(N-k)!}}\cdots \\ \cdots\frac{z_{a_{N-3}}^{N-4}y_{a_{N-3}}^3}{\sqrt{(N-4)!3!}}\frac{z_{a_{N-2}}^{J_3+N-3}y_{a_{N-2}}^{2+K_3}}{\sqrt{(J_3+N-3)!(2+K_3)!}}\frac{z_{a_{N-1}}^{J_2+N-2}y_{a_{N-1}}^{K_2+1}}{\sqrt{(J_2+N-2)!(K_2+1)!}} \\ \times\frac{z_{a_N}^{J_1+N-1}y_{a_N}^{K_1}}{\sqrt{(J_1+N-1)!K_1!}}e^{-\frac{1}{2}\sum_q z_q\bar{z}_q-\frac{1}{2}\sum_q y_q\bar{y}_q}\end{aligned} \tag{3.3.16}$$

The generalization to any Gauss graph operator is now clear.

3.4 Connection to Supergravity

In this section we would like to explore the possibility that the eigenvalue dynamics of the $SU(2)$ sector has a natural interpretation in supergravity. The relevant supergravity solutions have been considered in [52, 53, 54, 55].

There are 6 adjoint scalars in the $\mathcal{N} = 4$ super Yang-Mills theory that can be assembled into the following three complex combinations

$$Z = \phi^1 + i\phi^2 \qquad Y = \phi^3 + i\phi^4 \qquad X = \phi^5 + i\phi^6 \tag{3.4.1}$$

The operators we consider are constructed using only Z and Y so that they are invariant under the $U(1)$ which rotates ϕ^5 and ϕ^6. Further, since our operators are BPS they are built only from the s-wave spherical harmonic components of Y and Z, so that they are invariant under the $SO(4)$ symmetry which acts on the S^3 of the $R \times S^3$ spacetime on which the CFT is defined. Local supersymmetric geometries with $SO(4) \times U(1)$ isometries have the form[52, 55]

$$ds_{10}^2 = -h^{-2}(dt + \omega)^2 + h^2\Big[\frac{2}{Z + \frac{1}{2}}\partial_a\bar{\partial}_b K dz^a d\bar{z}^b + dy^2\Big] + y(e^G d\Omega_3^2 + e^{-G}d\psi^2) \tag{3.4.2}$$

$$d\omega = \frac{i}{y}\Big(\partial_a\bar{\partial}_b\partial_y K dz^a d\bar{z}^b - \partial_a Z dz^a dy + \bar{\partial}_a Z d\bar{z}_a dy\Big) \tag{3.4.3}$$

Here z^1 and z^2 is a pair of complex coordinates and K is a Kahler potential which may depend on y, z^a and $\bar{z}^a$. y^2 is the product of warp factors for S^3 and S^1. Thus we must be careful and impose the correct boundary conditions at the $y = 0$ hypersurface if we are to avoid singularities. The $y = 0$ hypersurface includes the four dimensional space with coordinates given by the z^a. These boundary conditions require that when the S^3 contracts to zero, we need $Z = -\frac{1}{2}$ and when the ψ-circle collapses we need $Z = \frac{1}{2}$[52, 55]. There is a surface separating these two regions, and hence, defining the supergravity solution. So far the discussion given closely matches what is found for the $\frac{1}{2}$-BPS supergravity solutions. In that case the $y = 0$ hypersurface includes a two dimensional space which is similarly divided into two regions, giving the black droplets on a white plane. The edges of the droplets are completely arbitrary, which is an important difference from the case we are considering. The surface defining local supersymmetric geometries with $SO(4) \times U(1)$ isometries is not completely arbitrary - it too has to satisfy some additional constraints as spelled out in [55]. It is natural to ask if the surface defining the supergravity solution is visible in the eigenvalue dynamics?

To answer this question we will now review how the surface defining the local supersymmetric geometries with $SO(4) \times U(1)$ isometries corresponding to the $\frac{1}{2}$-BPS LLM geometries is constructed. According to [55], the boundary condition for these geometries have walls between the two boundary conditions determined by the equation[17]

$$z^2\bar{z}^2 = e^{-2\hat{D}(z^1,\bar{z}^1)} \tag{3.4.4}$$

where $\hat{D}(z^1, \bar{z}^1)$ is determined by expanding the function D as follows (it is the y coordinate that we set to zero to get the LLM plane)

$$D = \log(y) + \hat{D}(z, \bar{z}) + O(x) \tag{3.4.5}$$

The function D is determined by the equations

$$y\partial_y D = \frac{1}{2} - Z \qquad V = -i(dz\partial_z - d\bar{z}\partial_{\bar{z}})D \tag{3.4.6}$$

[17] This next equation is (6.35) of [55]. We will relate z^1 and z^2 to z_i (the eigenvalues of Z) and y_i (the eigenvalues of Y) when we make the correspondence to eigenvalues.

where $Z(y, z^1, \bar{z}^1)$ is the function obeying Laplace's equation that determines the LLM solution and $V(y, z^1, \bar{z}^1)$ is the one form appearing in the combination $(dt + V)^2$ in the LLM metric.

Consider an annulus that has an outer edge at radius $M + N$ and an inner edge at a radius M. This solution has (these solutions were constructed in the original LLM paper [12])

$$\begin{aligned} Z(y, z^1, \bar{z}^1) = -\frac{1}{2}\Bigg(& \frac{|z^1|^2 + y^2 - M + 1}{\sqrt{(|z^1|^2 + y^2 + M - 1)^2 - 4|z^1|^2(M-1)}} \\ & + \frac{|z^1|^2 + y^2 - M - N}{\sqrt{(|z^1|^2 + y^2 + M + N)^2 - 4|z^1|^2(M+N)}}\Bigg) \\ V(y, z^1, \bar{z}^1) = \frac{d\phi}{2}\Bigg(& \frac{|z^1|^2 + y^2 + M - 1}{\sqrt{(|z^1|^2 + y^2 + M - 1)^2 - 4|z^1|^2(M-1)}} \\ & + \frac{|z^1|^2 + y^2 + M + N}{\sqrt{(|z^1|^2 + y^2 + M + N)^2 - 4|z^1|^2(M+N)}}\Bigg) \end{aligned}$$

Evaluating at $y = 0$, the second of (3.4.6) says

$$V = -i(dz\partial_z - d\bar{z}\partial_{\bar{z}})\hat{D} \tag{3.4.7}$$

Setting $z^1 = re^{-i\phi}$ and assuming that $\hat{D}$ depends only on r we find

$$r\frac{\partial \hat{D}}{\partial r} = -\frac{M+N}{r^2 - M - N} + \frac{M-1}{r^2 - M + 1} \tag{3.4.8}$$

which is solved by

$$\hat{D} = \frac{1}{2}\log\frac{|z^1\bar{z}^1 - M + 1|}{|z^1\bar{z}^1 - M - N|} \tag{3.4.9}$$

Thus, the wall between the two boundary conditions is given by

$$|z^2|^2 = \frac{M + N - 1 - z^1\bar{z}^1}{z^1\bar{z}^1 - M + 1} \tag{3.4.10}$$

The same analysis applied to the $AdS_5 \times S^5$ solution gives

$$|z^1|^2 + |z^2|^2 = N - 1 \tag{3.4.11}$$

For the pair of geometries described above, we know the wave function in the eigenvalue description. We will now return to the eigenvalue description and see how these surfaces are related to the eigenvalue wave functions.

At large N, since fluctuations are controlled by $1/N^2$, we expect a definite eigenvalue distribution. These eigenvalues will trace out a surface specified by the support of the single fermion probability density

$$\rho(z_1, \bar{z}_1, y_1, \bar{y}_1) = \int \prod_{i=2}^{N} dz_i d\bar{z}_i dy_i d\bar{y}_i |\Psi(\{z_i, \bar{z}_i, y_i, \bar{y}_i\})|^2 \tag{3.4.12}$$

Denote the points lying on this surface using coordinates z, y.

Using the wave function $\Psi_{\rm gs}(\{z_i, \bar{z}_i, y_i, \bar{y}_i\})$ corresponding to the $AdS_5 \times S^5$ spacetime, the probability density for a single eigenvalue is

$$\rho(z, \bar{z}, y, \bar{y}) = \frac{1}{N\pi^2} \sum_{i=0}^{N-1} \frac{(z\bar{z})^i}{i!} \frac{(y\bar{y})^{N-i-1}}{(N-i-1)!} e^{-z\bar{z}-y\bar{y}} \tag{3.4.13}$$

As y and z vary, the dominant contribution comes from a term with a specific value for i. When the ith term dominates the sum, the value of the eigenvalue coordinate is given by

$$\begin{aligned} \frac{(z\bar{z})^i}{i!} = 1 \qquad & |z|^{2i} = i! \approx i^i \\ \frac{(y\bar{y})^{N-i-1}}{(N-i-1)!} = 1 \qquad & |y|^{2(N-i-1)} = (N-i-1)! \approx (N-i-1)^{N-i-1} \end{aligned} \tag{3.4.14}$$

This leads to the following points

$$|z_{(i)}|^2 = i \qquad |y_{(i)}|^2 = N-i-1 \qquad i = 0, 1, 2, ..., N-1 \tag{3.4.15}$$

Thus, if we identify the points $z_{(i)}, y_{(i)}$ and the supergravity coordinate z^1, z^2 as follows

$$z^2 = y_{(i)} \qquad z^1 = z_{(i)} \tag{3.4.16}$$

we find

$$|z^1|^2 + |z^2|^2 = i + (N-i-1) = N-1 \tag{3.4.17}$$

so that the eigenvalues condense on the surface that defines the wall between the two boundary conditions.

Let's now compute the positions of our eigenvalues, using $\Psi_{\rm LLM}(\{z_i, \bar{z}_i, y_i, \bar{y}_i\})$. The probability density for a single eigenvalue is easily obtained by computing the following integral

$$\begin{aligned} \rho(z_1, \bar{z}_1, y_1, \bar{y}_1) &= \int \prod_{i=2}^{N} dz_i d\bar{z}_i dy_i d\bar{y}_i |\Psi_{\rm LLM}(\{z_i, \bar{z}_i, y_i, \bar{y}_i\})|^2 \\ &= \frac{1}{N\pi^2} \sum_{i=0}^{N-1} \frac{(z_1\bar{z}_1)^{M+i}}{(M+i)!} \frac{(y_1\bar{y}_1)^{N-i-1}}{(N-i-1)!} e^{-z_1\bar{z}_1 - y_1\bar{y}_1} \end{aligned} \tag{3.4.18}$$

Following the analysis we performed above, we find that the complete set of points on the eigenvalue surface is given by

$$|z_{(i)}|^2 = (M+i) \qquad |y_{(i)}|^2 = N-i-1 \qquad i = 0, 1, 2, ..., N-1 \tag{3.4.19}$$

Thus, if we identify the points $z_{(i)}, y_{(i)}$ and the supergravity coordinate z^1, z^2 as follows

$$z^2 = \frac{y_{(i)}}{\sqrt{|z_{(i)}|^2 - M + 1}} \qquad z^1 = z_{(i)} \tag{3.4.20}$$

we find that (3.4.10) gives

$$\frac{|y^{(i)}|^2}{i+1} = \frac{M+N-1-|z^{(i)}|^2}{|z^{(i)}|^2-M+1} \tag{3.4.21}$$

in complete agreement with where our wave function is localised. This again shows that the eigenvalues are collecting on the surface that defines the wall between the two boundary conditions. Although these examples are rather simple, they teach us something important: the map between the eigenvalues and the supergravity coordinates depends on the specific geometry we consider.

The fact that eigenvalues condense on the surface that defines the wall between the two boundary conditions is something that was already anticipated by Berenstein and Cotta in [40]. The proposal of [40] identifies the support of the eigenvalue distribution with the degeneration locus of the three sphere in the full ten dimensional metric. Our results appear to be in perfect accord with this proposal.

3.5 Summary and Outlook

There are a number of definite conclusions resulting from our study. One of our key results is that we have found substantial evidence for the proposal that there is a sector of the two matrix model that is described (sometimes exactly) by eigenvalue dynamics. This is rather non-trivial since, as we have already noted, it is simply not true that the two matrices can be simultaneously diagonalized. The fact that we have reproduced correlators of operators that involve products of both matrices in a single trace is convincing evidence that we are reproducing genuine two matrix observables. The observables we can reproduce correspond to BPS operators. In the dual gravity these operators map to supergravity states corresponding to classical geometries. The local supersymmetric geometries with $SO(4)\times U(1)$ isometries are determined by a surface that defines the boundary conditions needed to obtain a non-singular supergravity solution. At large N where we expect classical geometry, the eigenvalues condense on this surface. In this way the supergravity boundary conditions appear to match the large N eigenvalue description perfectly.

The eigenvalue dynamics appears to provide some sort of a coarse grained description. Correlators of operators dual to states with a very small energy are not reproduced correctly: for example the energy of states dual to single traces has to be above some threshold (N) before they are correctly reproduced. For complicated operators with a detailed multi trace structure we would thus expect to get the gross features correct, but we may miss certain finer details - see the discussion after (3.2.38). Developing this point of view, perhaps using the ideas outlined in [45], may provide a deeper understanding of the eigenvalue wave functions.

The eigenvalue description we have developed here is explicit enough that we could formulate the dynamics in terms of the density of eigenvalues. This would provide a field theory that has $1/N$ appearing explicitly as a coupling. It would be very interesting to work out, for example, what the generalization of the Das-Jevicki Hamiltonian[56] is.

The picture of eigenvalue dynamics that we are finding here is almost identical to the proposal discussed by Berenstein and his collaborators[38, 39, 40, 41, 42, 43, 44], developed using numerical methods and clever heuristic arguments. The idea of these works is that the eigenvalues represent microscopic degrees of freedom. At large N one can move to collective degrees of freedom that represent the 10 dimensional geometry of the dual gravitational description. This is indeed what we are seeing. They have also considered cases with reduced supersymmetry and orbifold geometries[57, 58, 59]. These are natural examples to consider using the ideas and methods we have developed in this thesis. Developing other examples of eigenvalue dynamics will allow us to further test the proposals for wave functions and the large N distributions of eigenvalues put forward in this thesis.

An important question that should be tackled is to ask how one could derive (and not guess) the wave functions we have described. Progress with this question is likley to give some insights into how it is even possible to have a consistent eigenvalue dynamics. One would like to know when an eigenvalue description is relevant and to what classes of observables it is applicable.

Another important question is to consider the extension to more matrices, including gauge and fermion degrees of freedom. The Gauss graph labeling of operators continues to work when we include gauge fields and fermions[60, 61], so that our argument goes through without modification and we again expect that eigenvalue dynamics in these more general settings will be an effective approach to compute these more general correlators of BPS operators. Another important extension is to consider the eigenvalue dynamics, perturbed by off diagonal elements, which should allow one to start including stringy degrees of freedom. Can this be done in a controlled systematic fashion? In this context, the studies carried out in [62, 63, 64], will be relevant.

4 Exciting LLM Geometries

This chapter is based on work in [65]. We are looking to find new integrable subsectors of the CFT. We show how to construct operators that represent excitations of LLM geometries. The Young diagram labelling we use proves especially useful. At low energy, the excitations give rise to an emergent Yang-Mills theory localised at a corner of the Young diagram. This shows the emergent theory is decoupled at large N which is important to demonstrate integrability. In the planar limit, we are able to show that these gauge theories are $\mathcal{N} = 4$ SYM.

4.1 Introduction

The map between the planar limit of $\mathcal{N} = 4$ super Yang-Mills theory and an integrable spin chain[66] has been a surprisingly rich idea. Single trace operators in the conformal field theory (CFT) are identified with states of the spin chain, and the dilatation operator of the CFT with the Hamiltonian of the spin chain. This allows the exact computation of anomalous dimensions and hence precision tests[67, 68] of the duality with string theory on $AdS_5 \times S^5$[4, 69, 70]. Excitations of the closed string are identified as magnons. The magnons are visible in the dual string theory description[71, 72]. After projecting the closed string solution to a plane (the so called bubbling plane [12]) and using coordinates suited to 1/2 BPS supergravity geometries, the string worldsheet traces out a polygon[72]. The sides of the polygon are the magnons. Geometrical properties of these sides (their length and orientation) determine the conserved charges (momentum and energy) labeling the magnon. The S-matrix for magnon scattering is determined up to a single overall phase simply by kinematics[73]. Integrability then fixes this phase. The S-matrix computed in string theory is in exact agreement with the S-matrix computed in the CFT.

How much, if anything, of this story survives for string excitations of new geometries? The geometries that we have in mind are the LLM geometries[12]. An LLM geometry is dual to an operator with a dimension that grows as N^2 in the large N limit. Consequently, correlators of operators with dimensions of order N^2 encode the physics of excitations of these geometries. For operators with such a large dimension the planar approximation is not justified[13]. Consequently, mixing between different trace structures is not suppressed. The identification between single trace operators in the CFT and spin chain states is spoiled and it seems that the link to an integrable spin chain is lost. In this introduction we will give some physical arguments which suggest that, at least for a subset of excitations, this is not the case. The rest of the chapter then carries out detailed CFT computations that confirm the details of this physical picture.

The LLM geometries are dual to a 1/2 BPS sector of the CFT. This 1/2 BPS sector contains all gauge invariant operators built from a single complex matrix Z. Since we study single matrix dynamics, there is a simple free fermion description, obtained by working in terms of the eigenvalues of Z[74, 7]. There is also a closely related description which employs Schur polynomials in Z[7, 16]. We mainly use this second description as we know how to generalize

it when including more matrices[33, 34]. This is needed when studying small fluctuations of the LLM geometries. A Schur polynomial dual to an LLM geometry is labelled by a Young diagram with order N^2 boxes[12]. An operator dual to a smooth supergravity geometry has a Young diagram with $O(1)$ corners and the distance between any two adjacent corners (that is, the number of rows or columns ending on the side between the two corners) is order N. The string theory understanding of this geometry is that it is the state obtained from back reaction of condensed giant gravitons[8, 14, 15]. The translation between the CFT and string theory descriptions is direct: we read the rows of the Young diagram as dual giant gravitons or the columns as giant gravitons[7].

To excite the geometry in the CFT description, add boxes at a particular corner of the Young diagram describing the LLM geometry[48, 75, 76]. In string theory we understand this as exciting the giants that condensed to produce the geometry. The description of worldvolume excitations of these D3 brane giant gravitons is in terms of some open string field theory whose low energy limit gives rise to a new emergent Yang-Mills theory[77, 32]. Relative to the original Yang-Mills theory we started with, the space of the giant's worldvolume is an emergent space. The new emergent Yang-Mills theory may itself have a holographic description so we might have new holographic dualities in this large charge limit[77].

The intuitive picture sketched above suggests that excitations arising from any particular corner give rise to a distinct super Yang-Mills theory. We will study the planar limit of these emergent gauge theories, to provide detailed support for this intuition. To restrict to the planar limit consider excitations with a bare dimension of at most $O(\sqrt{N})$, i.e. add at most $O(\sqrt{N})$ boxes to any given corner. Concretely we will demonstrate three things

1. An isomorphism between the planar Hilbert space of the original $\mathcal{N} = 4$ super Yang-Mills theory and the planar Hilbert space of the emergent gauge theory arising at a corner. When restricted to the 1/2 BPS sector, these Hilbert spaces are in fact a generalization of the code subspaces constructed by [78] (see also [79, 80, 81]).

2. Three point functions of operators in the planar emergent gauge theory vanish. We demonstrate this in the free field theory. In the planar limit of matrix models the vanishing follows because to mix three single traces we have to break some index loops which costs (at least) a factor of N. This is a general conclusion true for both free and interacting matrix models. Consequently we conjecture that our free field theory result holds after interactions are turned on. Since operator product expansion (OPE) coefficients can be read from the three point functions, this implies the OPE coefficients of the planar emergent gauge theory vanish.

3. The correct spectrum of planar anomalous dimensions of the emergent gauge theory. We know the planar spectrum of anomalous dimensions of $\mathcal{N} = 4$ super Yang-Mills theory. We find the same spectrum for the emergent gauge theory. This demonstrates integrability for the emergent gauge theories.

Notice that since any CFT is determined by its spectrum of anomalous dimensions and OPE coefficients, and that in the strict planar limit all OPE coefficients vanish, this demonstrates that the planar limit of the emergent gauge theories are planar $\mathcal{N} = 4$ super Yang-Mills theory.

We will see that although these different emergent gauge theories all share the same coupling constant (which is expected since this coupling is equal to the string coupling constant of the original string theory on $AdS_5 \times S^5$), they generically have distinct gauge groups $U(N_{\text{eff}})$. The rank of the gauge group N_{eff} receives contributions both from the flux of the original N D3 branes that gives rise to the $\mathcal{N} = 4$ super Yang-Mills theory we start with and from the giants which have condensed. By considering a large charge state, its possible to have an emergent gauge theory with gauge group that has rank larger than N.

What we are finding is that a subset of the excitations of large charge states of the $\mathcal{N} = 4$ super Yang-Mills theory are equivalent to excitations of the vacuum. There are of course excitations that go beyond the planar limit of the emergent gauge theory. The excitation is constructed by adding boxes to the Young diagram describing the LLM geometry. We might add so many boxes that we reach beyond two corners of the Young diagram defining the LLM geometry. The excitation is "too big" to sit on the Young diagram and in this way we can detect features of the background Young diagram. These excitations are obtained by adding $\sim N$ boxes and hence do not belong to the planar limit of the emergent gauge theory - they are giant graviton like operators of the emergent theory. There are also excitations constructed by adding order $\sqrt{N}$ boxes, with the boxes added at different corners[82, 75, 76]. These (delocalised) states can be described as strings with magnon excitations that stretch between two corners. We will show that at large N these states are decoupled from (localised) states in the planar Hilbert space of the emergent gauge theory, so that if we start from a state in the planar Hilbert space, the large N dynamics will not take us out of this space. This is an important point to demonstrate since the coupling of the planar Hilbert space of the emergent gauge theory to other degrees of freedom will almost certainly ruin integrability.

The free fermion description of the system is a powerful description because of its simplicity. The large charge state corresponds to exciting the fermions as illustrated in Fig 11. The idea that a subset of the excitations of large charge states of the CFT are equivalent to excitations of the vacuum has a natural interpretation in this free fermion language. We are saying that exciting any edge of the blocks appearing in the excited state is equivalent to exciting the edge of the original Fermi sea. The only difference between the different blocks is their extent. By restricting to the planar limit we consider excitations that are not able to detect that the Fermi sea is not infinite, so the extent of each block is irrelevant.

We will be using group representation theory methods to approach the problem of computing correlators of operators with a bare dimension of order N^2. This approach has been developed in a series of articles[7],[62]-[83],[33],[34], which has developed a number of bases for the local operators of the theory. These bases diagonalize the two point function of the free theory to all orders in $1/N$, and they mix weakly at weak coupling[63, 35, 84]. They therefore provide a very convenient tool with which to tackle the large N but non-planar limit of the CFT.

The representation theory methods sum the complete set of ribbon graphs. In this approach, operators are constructed using projection operators[18] of the symmetric group so that the gauge

[18]These operators are actually intertwiners since they map between different copies of the representations involved. For simplicity though the reader may think of them as projectors which are more familiar.

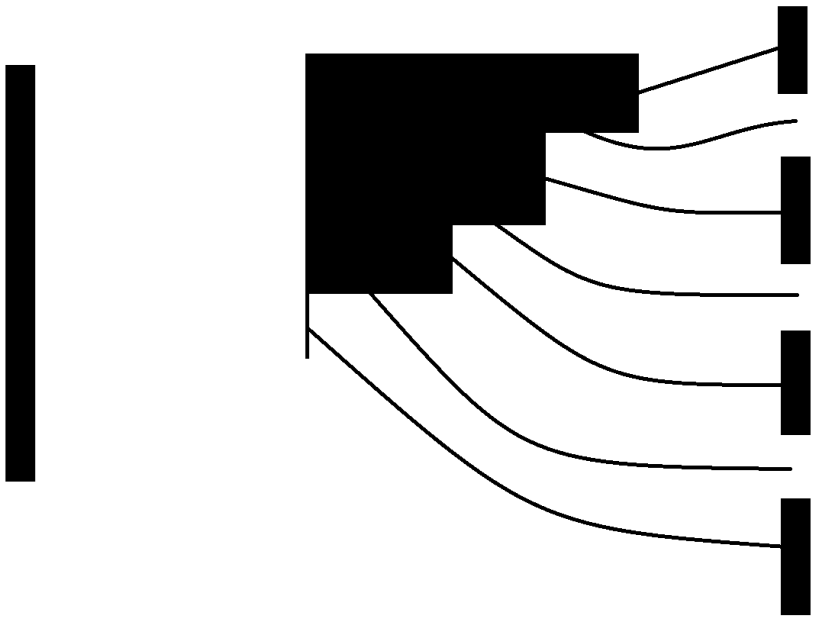


Figure 11: The free fermion description of a state labelled by a Young diagram. On the left we have the Fermi sea corresponding to the $AdS_5 \times S^5$ geometry. The states are simply filled from the lowest to highest energy with no unoccupied states. On the right, the Young diagram corresponding to a particular LLM geometry is shown. Each vertical edge of the Young diagram maps into occupied states while the horizontal edges map into unoccupied states. The number of fermions that were not excited at all is equal to the number of rows with no boxes. Thus, the excited state has broken the Fermi sea up into a series of occupied blocks.

invariant operators are labelled with irreducible representations of the group. Summing the ribbon diagrams of the free theory becomes multiplying these projectors and then taking a trace. At loop level, we evaluate the dilatation operator D. Evaluating matrix elements of D amounts to computing the trace of the product of commutators of elements of the symmetric group with projection operators. The central technical achievement is that in the end computing correlators, i.e. summing the ribbon graphs, is reduced to well defined (but technically involved) problems in group representation theory. A helpful point of view in making sense of the details, which we introduce and develop in this thesis, entails classifying the various ingredients of the computation as background independent or background dependent. By something that is background independent, we mean something that would take the same value on any inward pointing corner of any Young diagram dual to an LLM geometry, or even in the absence of a background, i.e. in the planar limit of the original CFT. These are quantities that take the same value regardless of which collection of branes we excite, and this is what we signify in the terminology "background independent". A quantity that is background dependent does depend on the collection of branes we excite. As we discuss in section 4.2, after making this distinction it is clear that the Hilbert spaces of the planar limit of the emergent gauge theory at any corner are isomorphic to each other and to the planar Hilbert space of the theory in the absence of a background.

One of the original motivations for this study are the results [75, 76, 85] which suggest the

existence of new integrable subsectors of the CFT. We want to explore (and further establish) the existence of these integrable subsectors. As discussed above, a key issue is to understand if the integrable sectors are decoupled from the nonintegrable sectors. It is useful to bear in mind that integrability in the planar limit also depends on a decoupling between different subspaces: it makes use of the fact that different trace structures don't mix. Thanks to this decoupling, it is consistent to focus on the space of single trace operators and it is in this subspace that its possible to construct a bijection between operators and the states of an integrable spin chain. The statement of this decoupling is coded into the planar correlation functions: correlators of operators with different trace structures vanish as $N \to \infty$. Motivated with this insight we focus on correlation functions of the large N but non-planar limits to establish the decoupling between integrable and non-integrable subsectors. This is discussed in section 2, where we obtain a simple formula for the correlators in the planar limit of the free emergent gauge theory in terms of correlators of the free planar CFT without background. Consequently the decoupling we establish is closely related to the absence of mixing between different trace structures in the planar limit.

We extend these results to the weakly interacting CFT in section 3, giving arguments that the spectrum of planar anomalous dimensions of the emergent gauge theory match the spectrum of planar anomalous dimensions of the original $\mathcal{N} = 4$ super Yang-Mills theory. We revisit the issue of coupling between integrable and non-integrable subsectors, arriving at the conclusion that the two are decoupled even after interactions are turned on.

In section 4 we consider the strongly coupled CFT, using the dual string description. We explain why the excitations considered should be understood as open string excitations localised on the world volume of giant graviton branes. We also suggest how to describe closed string excitations of the large charge state we consider. In section 5 we summarize and discuss a number of promising directions in which to extend this work.

4.2 Free CFT

Our basic goal is to organize and study excitations of an LLM background, using the dual $\mathcal{N} = 4$ super Yang-Mills theory. Any LLM geometry is specified by a boundary condition, given by coloring the bubbling plane into black and white regions[12]. The LLM backgrounds we consider have boundary conditions given by concentric annuli, possibly with a central black disk. The LLM geometry is described by a CFT operator with a bare dimension of order N^2. Concretely, it is a Schur polynomial[7] labelled by a Young diagram with $O(N^2)$ boxes and $O(1)$ corners. Large N correlators of these operators are not captured by summing only planar diagrams, so we talk about the large N but non-planar limit of the theory. The excitation is described by adding J boxes to the background, with $J^2 \ll N$. Consequently, we can ignore back reaction of the excitation on the LLM geometry.

The CFT operators corresponding to the background and excitation are given by restricted Schur polynomials[33, 34]. Construction of these operators and their correlators becomes an

exercise in group representation theory. In section 4.2.1 we discuss elements of this description, placing an emphasis on if the quantity being considered depends on or is independent of the collection of branes being excited. This distinction will clarify general patterns in the CFT computations that follow.

We begin our study in the free field theory. The Hilbert space of possible excitations can be written as a direct sum of subspaces. There are subspaces that collect the excitations localised at the outer or inner edge of a given annulus, or at the outer edge of the central disk. The excitations are obtained by adding boxes to the Young diagram describing the background, at a specific location. They are also localised in the dual gravitational description, at a specific radius on the bubbling plane[75, 76]. Each localised Hilbert space is labelled by the edge at which it is localised. There are also delocalised excitations, where the description of the excitation involves adding boxes at different locations on the background Young diagram[75, 76]. We will not have much to say about delocalised excitations.

The excitations belonging to the localised Hilbert spaces play a central role in our study. These are the Hilbert spaces of the emergent gauge theories. We give a bijection between the states belonging to the planar Hilbert space of an emergent gauge theory, and the states of the planar limit of the original CFT without background. To show that the bijection takes on a physical meaning, we argue that correlation functions of operators that are in bijection are related in a particularly simple way, in the large N limit. This result is significant because the basic observables of any quantum field theory are its correlation functions and many properties of the theory can be phrased as statements about correlation functions. Thanks to the map between correlation functions, any statement about the planar limit that can be phrased in terms of correlators, immediately becomes a statement about the planar emergent gauge theories that arise in the large N but non-planar limits we consider.

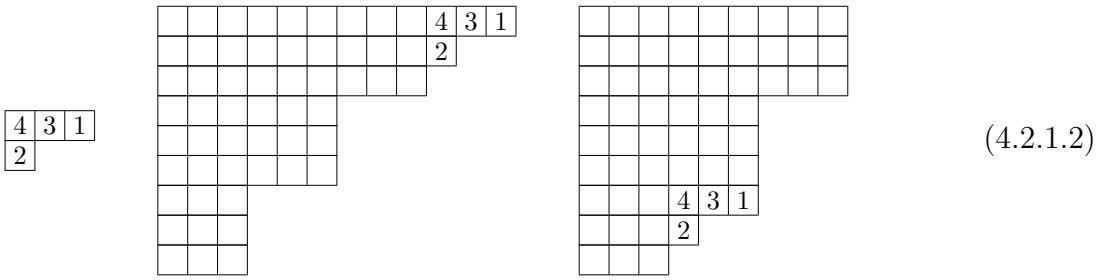
4.2.1 Background Dependence

Irreducible representations of the symmetric group S_n are labelled by Young diagrams with n boxes. States in the carrier space of the representation are labelled by standard tableau, in which we populate the boxes with numbers $\{1, 2, ..., n\}$ such that the numbers are decreasing along the rows (from left to right) and along the columns (from top to bottom). A representation for S_n is given by specifying the action of any element $\sigma \in S_n$ on the standard tableau. We will use Young's orthogonal representation. For example, here is the action of the two cycle $\sigma = (12) \in S_4$ on a specific tableau

$$(12)\ \begin{array}{|c|c|c|}\hline 4&3&1\\\hline 2\\\cline{1-1}\end{array} = \frac{1}{3}\ \begin{array}{|c|c|c|}\hline 4&3&1\\\hline 2\\\cline{1-1}\end{array} + \sqrt{1-\left(\frac{1}{3}\right)^2}\ \begin{array}{|c|c|c|}\hline 4&3&2\\\hline 1\\\cline{1-1}\end{array} \tag{4.2.1.1}$$

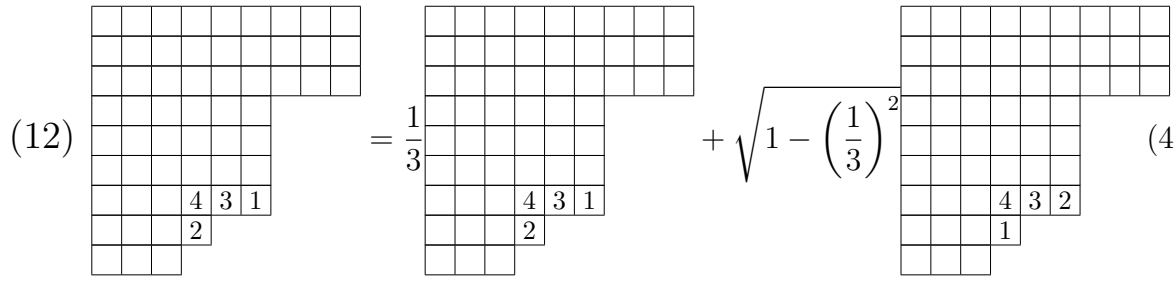
The number $\frac{1}{3}$ that appears in the above equation is counting the number of boxes in the shortest path from the box labelled 1 to the box labelled 2. The only thing that matters is the relative position of boxes 1 and 2. Consequently, σ has the same action on all three states

shown below.



(4.2.1.2)

For example



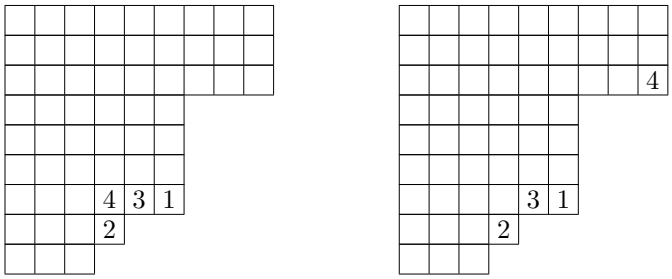
(4.2.1.3)

This demonstrates that the action of the symmetric group on the boxes belonging to the excitation is background independent. In what follows we will use R (or r) to denote the Young diagram describing the excitation and $+R$ (or $+r$) to denote the Young diagram after it has been placed at an inward pointing corner of the Young diagram for the LLM geometry.

When our excitation has more than one type of field, the gauge invariant operator is constructed by restricting to the subgroup that permutes fields of a specific type. For example, if we have n Z fields and m Y fields, we would start with an irreducible representation $R \vdash n+m$ of S_{n+m} and restrict to some representation (r, s), $r \vdash n$, $s \vdash m$, of the $S_n \times S_m$ subgroup. Upon restricting (r, s) may appear more than once, so we need a multiplicity label α to distinguish the different copies. Since we use only the action of the symmetric group to perform the restrictions, the multiplicity labels are also background independent. To diagonalize the one loop dilatation operator [36, 37] traded the multiplicity labels for directed graphs recording how open strings are connected between giant gravitons. These graphs summarize basic physics coming from the Gauss Law on the brane worldvolume that is true for any collection of compact branes. This is why the multiplicity labels are background independent.

There is a potential fly in the ointment that deserves discussion. In the absence of the background, R is used to put the Zs and Ys together while r is used to organize the Zs and s the Ys. In the presence of the background, constructed using Zs, we must replace $R \to +R$ and $r \to +r$, while s is unchanged. The first m boxes labelled in the standard tableau made by filling R are Y fields, and are among the impurity boxes added to the background Young diagram. The remaining boxes are then labelled in all possible ways to give the states of the

subspace. Imagine that $n = m = 2$. Two possible labeling are as follows



(4.2.1.4)

On the left we have the usual action of the symmetric group on the added boxes. For the state on the right, we find a different answer. At large N, when the number of boxes in the shortest path linking distant box 4 to any local labelled box (where the excitation was added) is of order N, any permutation swapping box 4 with another box, will just swap the two labels. This is orthogonal to the state before the swap. We will always land up taking a trace over group elements of the subgroup that permutes excitation boxes. For the traces we need only states on the left contribute. As a consequence, although the action of the symmetric group on impurities is not background independent traces over these elements are[19]. Notice that the problem of resolving multiplicities is phrased entirely in terms of the subgroup acting on Y fields i.e. we can set the problem up so that the multiplicities are associated to representation s. For this reason the above potential spanner in the works doesn't threaten our conclusion that multiplicity labels are background independent.

The operators which generalize the Schur polynomials when more than one type of field is present are called restricted Schur polynomials[62, 33]. The Schur polynomial is constructed using characters of the symmetric group. The restricted Schur polynomial is constructed using a restricted character $\chi_{R,(r,s),\alpha\beta}(\sigma)$ [62]. Recall that the character $\chi_R(\sigma)$ is given as a trace over the matrix $\Gamma_R(\sigma)$ representing σ in irreducible representation R. For the restricted character we restrict the trace to the subspace carrying the representation of the subgroup (r, s). Because there are different copies of (r, s) in the game, there are many ways to do this. The restricted character $\chi_{R,(r,s)\alpha\beta}(\sigma)$ is given by summing the row index of $\Gamma_R(\sigma)$ over the α copy of (r, s) and the column label over the β copy of (r, s). This can be accomplished by making use of an intertwining map $P_{R,(r,s)\alpha\beta}$ which maps from the α copy of (r, s) to the β copy of (r, s). This map can be constructed using only elements of the symmetric group that act on the impurities. In terms of $P_{R,(r,s)\alpha\beta}$ we have

$$\chi_{R,(r,s)\alpha\beta}(\sigma) = \mathrm{Tr}\left(P_{R,(r,s)\alpha\beta}\,\Gamma_R(\sigma)\right) \tag{4.2.1.5}$$

In the presence of the background this becomes

$$\chi_{+R,(+r,s)\alpha\beta}(\sigma) = \mathrm{Tr}\left(P_{+R,(+r,s)\alpha\beta}\,\Gamma_{+R}(\sigma)\right) \tag{4.2.1.6}$$

where σ is the same permutation as in (4.2.1.5). It is clear that the restricted character is background independent, up to the remark of footnote 2.

[19] This is of course up to a factor which is determined by the dimension of the irreducible representation of the background. This factor is from summing over all the possible standard tableau obtained by filling boxes associated to the background.

The operators of the planar limit are dual to strings and gravitons in the $AdS_5 \times S^5$ geometry. Since the restricted Schur polynomials provide a basis, any such operator can be expressed as a linear combination of restricted Schurs. For simplicity we will discuss operators constructed from two complex matrices Z and Y, but it will be clear that our conclusions generalize for an arbitrary local operator. The definition of the restricted Schur polynomial is[33]

$$\chi_{R,(r,s)\alpha\beta}(Z,Y) = \frac{1}{n!m!} \sum_{\sigma \in S_{n+m}} \chi_{R,(r,s),\alpha\beta}(\sigma) Y^{i_1}_{i_{\sigma(1)}} \cdots Y^{i_m}_{i_{\sigma(m)}} Z^{i_{m+1}}_{i_{\sigma(m+1)}} \cdots Z^{i_{n+m}}_{i_{\sigma(n+m)}} . \tag{4.2.1.7}$$

An arbitrary operator O_A can be expanded in the basis of restricted Schur polynomials as follows[34]

$$O_A = \sum_{R,r,s,\alpha,\beta} a^{(A)}_{R,(r,s),\alpha,\beta} \chi_{R,(r,s)\alpha\beta}(Z,Y,X,\cdots) \tag{4.2.1.8}$$

We will argue that the expansion coefficients $a^{(A)}_{R,(r,s),\alpha,\beta}$ are background independent. Imagine that O_A is the operator in the planar Hilbert space corresponding to some specific state, labelled by its dimension, $\mathcal{R}$-charge and whatever other labels we need to specify it completely. The operator in the planar Hilbert space of the emergent gauge theory, dual to the state that shares the same labels, is given by

$$O_{+A} = \sum_{R,r,s,\alpha,\beta} a^{(A)}_{R,(r,s),\alpha,\beta} \chi_{+R,(+r,s)\alpha\beta}(Z,Y,X,\cdots) \tag{4.2.1.9}$$

It is in this sense that the expansion coefficients are background independent. We will argue for (4.2.1.9) below by demonstrating that with this rule the correlation functions of the set of operators $\{O_{+A}\}$ are given in terms of those of $\{O_A\}$, essentially by replacing $N \to N_{\text{eff}}$. The two operators should then represent the same physical state since the physical interpretation of any operator is coded into its correlation functions.

We now consider quantities that are background dependent. The two point function of restricted Schur polynomials includes a product of the factors of the Young diagram. A box in row i and column j of a Young diagram has factor $N - i + j$. This quantity clearly depends sensitively on where you are located within the Young diagram and is not simply a function of the relative position of two boxes. The factors of the boxes added at different corners will depend on the corner and on the details of the shape of the Young diagram. We will see in what follows that all of the N dependence of the correlators comes from factors, so that moving between different corners shifts $N \to N_{\text{eff}}$, which changes the rank of the emergent gauge group. The only difference between the planar limit of the emergent gauge theories at each corner is this shift in N.

A second ingredient in the two point function of restricted Schur polynomials, is a ratio of the product of the hook lengths of the Young diagram. Assume that we have a total of C outward pointing corners and further that our localised excitation is stacked in the ith corner. In the Appendix E we prove the following result

$$\frac{\text{hooks}_{+R}}{\text{hooks}_{+r}} = \frac{\text{hooks}_R}{\text{hooks}_r} (\eta_B)^{|R|-|r|} \left(1 + O\left(\frac{1}{N}\right)\right) \tag{4.2.1.10}$$

where $|R|$ stands for the number of boxes in the Young diagram R and

$$\eta_B = \prod_{j=1}^{i} \frac{L(j,i)}{L(j,i)-N_j} \prod_{l=i+1}^{C} \frac{L(i+1,l)}{L(c+1,l)-M_l} \tag{4.2.1.11}$$

$$L(a,b) = \sum_{k=a}^{b} (N_k + M_k) \tag{4.2.1.12}$$

The notation in the above formulas is defined in Figure 12. Formula (4.2.1.10) is telling us that although $\text{hooks}_{+R}/\text{hooks}_{+r}$ depends on the background this dependence is a simple multiplicative factor that is sensitive to the shape of the Young diagram for the LLM geometry and the number of fields in the excitation that are not Z fields. Its dependence on R and r nicely matches $\text{hooks}_R/\text{hooks}_r$. Note that (4.2.1.10) is not exact - it receives $\frac{1}{N}$ corrections.

Our discussion in this section has focused on operators constructed using only 2 fields, Z and Y. The generalization is straight forward. For k different species of fields (which may include additional scalars, fermions or covariant derivatives), with n_k fields of each species, we consider a subgroup $S_{n_1} \times S_{n_2} \times \cdots \times S_{n_k}$ of $S_{n_1+n_2+\cdots+n_k}$. By including enough different species we can describe any operator in the planar limit of the CFT. It is again clear that although the action of the symmetric group on impurities is not background independent, traces over these elements are and that multiplicity labels and expansion coefficients are again background independent.

4.2.2 Excitations of $AdS_5 \times S^5$

Start in the simplest setting in which no giant graviton branes have condensed and consider excitations that are dual to operators with a bare dimension of order J with $J^2 \ll N$. This corresponds to the planar limit of the $\mathcal{N}=4$ super Yang-Mills. In this limit there are important simplifications. First, different trace structures don't mix[20]. This is phrased as a statement about correlation functions. To see this, consider loops constructed from a single complex adjoint matrix Z. In terms of the normalized traces $O_J \equiv \text{Tr}(Z^J)/\sqrt{JN^J}$ we have

$$\begin{aligned} \langle O_J^\dagger(x_1) O_J(x_2)\rangle &= \frac{1}{|x_1-x_2|^{2J}} + O\left(\frac{J^2}{N}\right) \\ \langle O_{J_1+J_2}^\dagger(x_1) O_{J_1}(x_2) O_{J_2}(x_2)\rangle &= \frac{\sqrt{J_1 J_2 (J_1+J_2)}}{N|x_1-x_2|^{2J_1+2J_2}} + \ldots \\ &\to 0 \qquad \text{as} \qquad N\to\infty \end{aligned} \tag{4.2.2.1}$$

The two point function of single traces is of order 1, while the two point function of a double trace with a single trace operator goes to zero. We have considered mixing between single

[20] For a careful study of this point see [86].

and double traces, but the conclusion is general: to mix different trace structures, we break color index loops to match traces structures and every time we break an index loop it costs a factor of N. The fact that different trace structures do not mix in the planar limit is an important result, ultimately responsible for the existence of the spin chain language. Indeed, the absence of mixing implies it is consistent to restrict to single trace operators and each single trace operator can be identified with a specific spin chain state. We will derive a formula for the correlation functions of certain excitations of a (heavy) operator with an enormous $\sim N^2$ dimension in terms of the correlation functions of the planar limit. As a consequence of this formula, we will see that simplifications of the planar limit encoded in correlation functions are then automatically present in correlation functions of certain excitations of the background.

We will make extensive use of the two point function of the restricted Schur polynomial, given by[33]

$$\langle \chi_{R,(r,s)\alpha\beta}(Z,Y)\chi_{T,(t,u)\delta\gamma}(Z,Y)^\dagger\rangle = \delta_{RS}\delta_{rt}\delta_{su}\delta_{\alpha\delta}\delta_{\beta\gamma}\frac{f_R \text{hooks}_R}{\text{hooks}_r \text{hooks}_s} \tag{4.2.2.2}$$

In the above formula f_R stands for the product of factors of Young diagram R, while hooks_R stands for the product of hook lengths of Young diagram R. This result is exact for the free field theory, i.e. all ribbon diagrams have been summed. Thus, the above formula is reliable for correlators of operators regardless of their dimension. This is why its useful to express our computations in the restricted Schur polynomial language: we can tackle both the planar correlators (with dimension $\leq O(\sqrt{N})$) and correlators in the background of a heavy operator (with dimension of $O(N^2)$) using a single formalism.

The computation of correlation functions most useful for our goals, starts by expressing the operators of interest as linear combinations of restricted Schur polynomials. This is always possible because the restricted Schur polynomials furnish a basis for the local gauge invariant operators of the theory. An arbitrary operator O_A

$$O_A = \text{Tr}(\sigma Y^{\otimes m}\otimes Z^{\otimes n}) = Y^{i_1}_{i_{\sigma(1)}}\cdots Y^{i_m}_{i_{\sigma(m)}} Z^{i_{m+1}}_{i_{\sigma(m+1)}}\cdots Z^{i_{n+m}}_{i_{\sigma(n+m)}} \tag{4.2.2.3}$$

can be written as a linear combination of restricted Schur polynomials as follows

$$O_A = \sum_{R,r,s,\alpha,\beta} a^{(A)}_{R,(r,s),\alpha,\beta}\chi_{R,(r,s)\alpha\beta}(Z,Y,X,\cdots) \tag{4.2.2.4}$$

By changing the permutation σ appearing in (4.2.2.3) we can obtain any desired multi trace structure. Taking linear combinations of these terms, we can easily construct, for example, the operators that would map into the states of the spin chain. Explicit formulas for the coefficients are known

$$\text{Tr}(\sigma Z^{\otimes n}Y^{\otimes m}) = \sum_{T,(t,u)\alpha\beta}\frac{d_T n!m!}{d_t d_u (n+m)!}\chi_{T,(t,u)\alpha\beta}(\sigma^{-1})\chi_{T,(t,u)\beta\alpha}(Z,Y) \tag{4.2.2.5}$$

We will not however need the precise values of the $a^{(A)}_{R,\{r\},\alpha}$. Formula (4.2.2.5) does however make it clear that these coefficients are symmetric group data and consequently, they are independent

of N. Using the known two point function for the restricted Schur polynomial, we find in the free field theory, that

$$\langle O_A(x_1)O_B(x_2)^\dagger\rangle = \sum_{R,r,s,\alpha} \frac{a^{(A)}_{R,(r,s),\alpha,\beta} a^{(B)*}_{R,(r,s),\alpha,\beta} \text{hooks}_R f_R}{\text{hooks}_r \text{hooks}_s} \frac{1}{|x_1-x_2|^{2J}} \tag{4.2.2.6}$$

The above result is exact and its an ingredient in the proof of the identity relating planar correlation functions of $\mathcal{N}=4$ super Yang-Mills theory to the correlations functions of the emergent gauge theories that arise in large N but non-planar limits. The planar approximation to the correlation function in free field theory is obtained by truncating the above exact result to its leading term in a large N expansion.

Up to now we have focused on operators constructed using only the Z and Y fields. The most general operator will be constructed from adjoint scalars, adjoint fermions or covariant derivatives of these fields. The construction of restricted Schur polynomials with an arbitrary number of species of adjoint scalars and an arbitrary number of species of adjoint fermions was given in [61]. The construction of restricted Schur polynomials using covariant derivatives has been described in [60]. Each power of the covariant derivative $D^p_\mu Z$ must be treated as a new species of field. If the operator we consider is constructed using a total of k species of fields, then the restricted Schur polynomial becomes $\chi_{R,\{r\},\alpha\beta}$, with $\{r\}$ a collection of k Young diagrams, one for each species. If we use n_i fields of species i the corresponding Young diagram r_i has n_i boxes. Young diagram r_1 corresponds to the Z field. Young diagram R has $n_1+n_2+...+n_k$ boxes. The additional labels contained in α and β are again discrete labels distinguishing operators that carry the same $R,\{r\}$ labels. The formulas we have given above now generalize as follows

$$\langle \chi_{R,\{r\}\alpha\beta}(Z,Y)\chi_{T,\{t\}\delta\gamma}(Z,Y)^\dagger\rangle = \delta_{RS}\delta_{\{r\},\{t\}}\delta_{\alpha\delta}\delta_{\beta\gamma}\frac{f_R \text{hooks}_R}{\prod_r \text{hooks}_r} \tag{4.2.2.7}$$

$$O_A = \sum_{R,r,s,\alpha,\beta} a^{(A)}_{R,\{r_1,r_2,\cdots\},\alpha,\beta}\chi_{R,\{r_1,r_2,\cdots\}\alpha\beta}(Z,Y,X,\cdots) \tag{4.2.2.8}$$

and

$$\langle O_A(x_1)O_B(x_2)^\dagger\rangle = \sum_{R,r,s,\alpha} \frac{a^{(A)}_{R,\{r\},\alpha,\beta} a^{(B)*}_{R,\{r\},\alpha,\beta} \text{hooks}_R f_R}{\prod_r \text{hooks}_r} \frac{1}{|x_1-x_2|^{2J}} \tag{4.2.2.9}$$

In the above formulas, $\delta_{\{r\},\{t\}}$ is 1 if the complete ordered sets of Young diagrams $\{r\}$ and $\{t\}$ are equal, and it is zero otherwise. The planar approximation is again obtained by truncating to the leading term in a large N expansion. This completes our discussion of the planar correlation functions.

4.2.3 Exitations of an LLM Geometry

The LLM geometries that we consider are described by Schur polynomials $\chi_B(Z)$ of the complex matrix Z labelled by a Young diagram B with $O(N^2)$ boxes and $O(1)$ outward pointing corners. An example of a possible Young diagram B, with 5 outward pointing corners is shown in Figure 12.

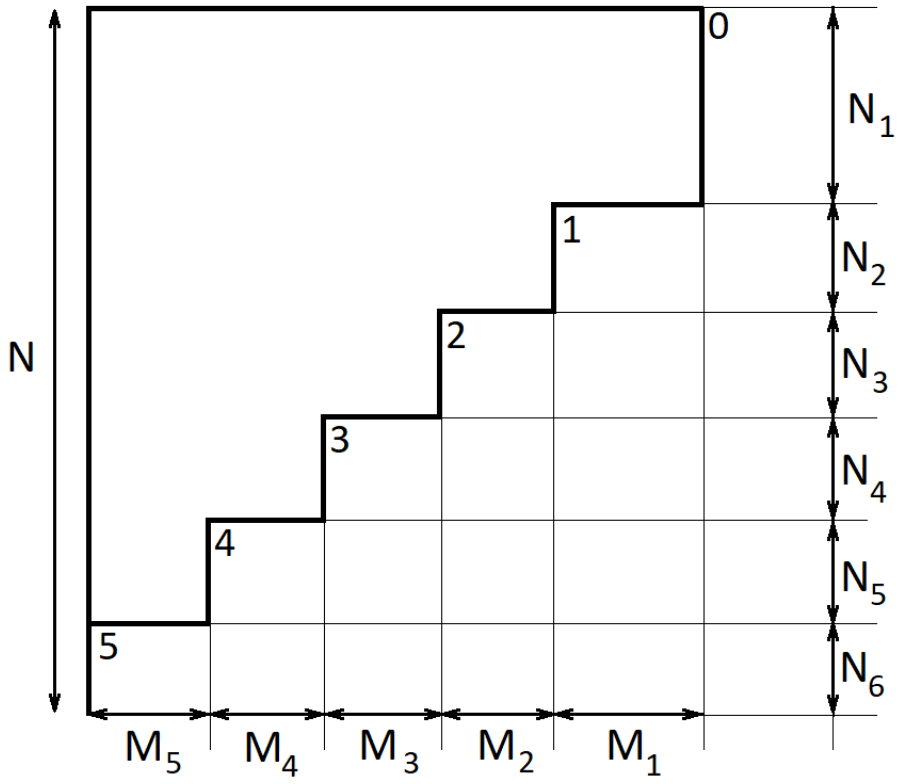


Figure 12: A possible label B for a Schur polynomial describing an LLM background. Note that $\sum_{i=1}^{6} N_i = N$.

All of the horizontal edges M_i, and vertical edges N_i have a length of $O(N)$. Excitations are obtained by adding $J = O(\sqrt{N})$ boxes to B. These new boxes could be stacked at any of the inward pointing corners, below or to the right[21] of B. The possible locations for the new boxes are labelled 0 to 5 in Figure 12. We will distinguish between excitations constructed by adding all extra boxes at a single inward pointing corner (*localised* excitations) and excitations constructed by adding extra boxes at more than one corner (*delocalised* excitations). In the free field theory, thanks to the fact that the two point function of the restricted Schur polynomial is diagonal in all of its labels, the local and delocalised excitations are orthogonal[22]. Denote the

[21] We could also create excitations by eroding the outward pointing corners. We will not study these excitations here.

[22] When we make this comment we have the operator/state correspondence of the CFT in mind. According to the correspondence, the inner product of two states is related to the correlators of the corresponding operators.

Hilbert space of small fluctuations about the LLM geometry by $\mathcal{H}_{\text{CFT;LLM}}$. This Hilbert space can be decomposed as a direct sum as follows

$$\mathcal{H}_{\text{CFT;LLM}} = \mathcal{H}_{\text{CFT;Local}} \bigoplus \mathcal{H}_{\text{CFT;Delocalized}} \tag{4.2.3.1}$$

Our study will focus on the local excitations. The Hilbert space of local excitations can further be refined as a direct sum of subspaces, one for each corner of the background Young diagram

$$\mathcal{H}_{\text{CFT;Local}} = \bigoplus_i \mathcal{H}^{(i)}_{\text{CFT}} \tag{4.2.3.2}$$

where i runs over inward pointing corners with the understanding that below or to the right[23] of B count as corners. Each factor $\mathcal{H}^{(i)}_{\text{CFT}}$ in the above sum is the Hilbert space of an emergent gauge theory and is isomorphic to the space of local operators in the planar limit of the original CFT, as we now explain. We do this by giving the bijection between operators of dimension J with $J^2 \ll N$ and operators in $\mathcal{H}^{(i)}_{\text{CFT}}$. The bijection maps the operator given in (4.2.2.8) above into

$$O^{(B)}_A = \sum_{R,r,s,\alpha,\beta} a^{(A)}_{R,\{r_1,r_2,\cdots\},\alpha,\beta} \chi_{+R,\{+r_1,r_2,\cdots\}\alpha\beta}(Z,Y,X,\cdots) \tag{4.2.3.3}$$

The coefficients of the expansion appearing in (4.2.2.8) are identical to the coefficients appearing in (4.2.3.3). It is only the R and r_1 labels in the restricted Schur polynomials in (4.2.2.8) and (4.2.3.3) that have changed. The Young diagram $+R$ is obtained by stacking R at the ith corner of B and similarly, the Young diagram $+r$ is obtained by stacking r at the ith corner of B. For an example of how this works, see Figure 13.

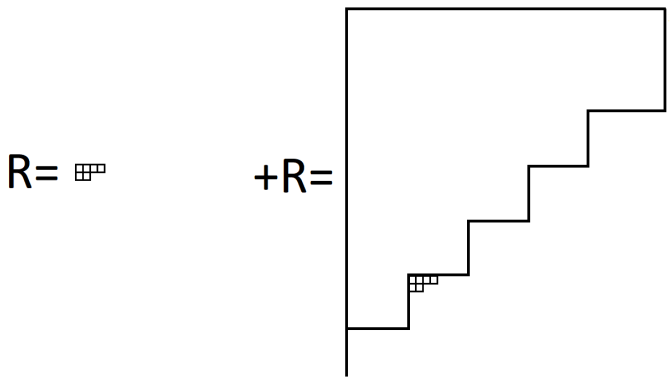


Figure 13: To obtain $+R$ from R we stack R at one of the inward pointing corners of B.

This mapping is a bijection. Operators with distinct labels are orthogonal. Operators with distinct labels before the map have distinct labels after the map. Thus, the mapping is injective. Any operator with a bare dimension J and $J^2 \ll N$ can be mapped to an excitation of the background B. What is important here is that, since each edge of the Young diagram has

[23] The locations labelled 0 and 5 in Figure 12.

a length of order N, there is no danger that when we stack R it will not fit onto the corner. Of course, the converse is also true: any excitation of the background can be mapped to an operator of dimension J by deleting the boxes in $+R$ and $+r_1$ which belong to B. Thus, the map is surjective. This demonstrates that our mapping is a bijection.

In the remainder of this section we will argue that the correlation functions of operators that are in bijection are related in a particularly simple way, in the large N limit. We would like to normalize our correlators so that

$$\langle 1 \rangle_B = 1 \tag{4.2.3.4}$$

We know that 1 maps into $\chi_B(Z)$ and that

$$\langle \chi_B(Z) \chi_B(Z)^\dagger \rangle = f_B \frac{1}{|x_1 - x_2|^{2|B|}} \tag{4.2.3.5}$$

where $|B|$ is the free field dimension of $\chi_B(Z)$. Consequently we will include an extra factor of $|x_1 - x_2|^{2|B|} f_B^{-1}$ to ensure that our correlators are correctly normalized

$$\langle \cdots \rangle_B = \frac{\langle \cdots \rangle}{f_B} |x_1 - x_2|^{2|B|} \tag{4.2.3.6}$$

Using the two point function of the restricted Schur polynomial, we obtain the following result

$$\langle O_A^{(B)}(x_1) O_B^{(B)}(x_2)^\dagger \rangle_B = \sum_{R,r,s,\alpha} \frac{a^{(A)}_{R,(r,s),\alpha,\beta} a^{(B)*}_{R,(r,s),\alpha,\beta} \, \text{hooks}_{+R} \, f_{+R}}{f_B \, \text{hooks}_{+r_1} \prod_{i>2} \text{hooks}_{r_i}} \frac{1}{|x_1 - x_2|^{2J}} \tag{4.2.3.7}$$

Assume that we have a total of C outward pointing corners and further that our localised excitation is stacked in the ith corner. Applying the identity (4.2.1.10) we find

$$\langle O_A^{(B)}(x_1) O_B^{(B)}(x_2)^\dagger \rangle_B = (\eta_B)^{n_I} \sum_{R,r,s,\alpha} \frac{a^{(A)}_{R,(r,s),\alpha,\beta} a^{(B)*}_{R,(r,s),\alpha,\beta} \, \text{hooks}_R}{\prod_i \text{hooks}_{r_i}} \frac{f_{+R}}{f_B} \frac{1}{|x_1 - x_2|^{2J}} \left(1 + O\left(\frac{1}{N} \right) \right) \tag{4.2.3.8}$$

(4.2.1.10) is not exact - it includes $\frac{1}{N}$ corrections and this is the only source of $\frac{1}{N}$ corrections in our final result. We have assumed[24] that every term in the sum has the same total number of fields and the same number of Z fields, i.e. that each term has the same value for $|R| - |r_1| \equiv n_I$. The subscript I on n_I stands for "impurity" since its common to refer to fields in our excitation that are not Z fields as impurities. We would now like to compare this to the result that we obtained for the planar correlators, which is

$$\langle O_A(x_1) O_B(x_2)^\dagger \rangle = \sum_{R,r,s,\alpha} \frac{a^{(A)}_{R,(r,s),\alpha,\beta} a^{(B)*}_{R,(r,s),\alpha,\beta} \text{hooks}_R f_R}{\text{hooks}_r \text{hooks}_s} \frac{1}{|x_1 - x_2|^{2J}}$$

[24] This assumption is not necessary. By rescaling each impurity field by $\sqrt{\eta_B}$ we could remove the η_B dependence in these formulas.

$$\equiv \quad F_{AB}(N)\frac{1}{|x_1-x_2|^{2J}} \tag{4.2.3.9}$$

The two results are nearly identical. The only difference, apart from the overall factor $(\eta_B)^{n_I}$, is that f_R in the planar result is replaced by $\frac{f_{+R}}{f_B}$ in the emergent gauge theory result. Now, recall that f_R is the product of factors in Young diagram R and that a box in row j and column k has factor $N-j+k$. Consequently

$$f_R(N) = \prod_{(j,k)\in R}(N-j+k) \tag{4.2.3.10}$$

In the ratio $\frac{f_{+R}}{f_B}$ factors of boxes that are common to $+R$ and B cancel. After performing these cancellations we find

$$\frac{f_{+R}}{f_B} = f_R(N_{\text{eff}}) = \prod_{(j,k)\in R}(N_{\text{eff}}-j+k) \tag{4.2.3.11}$$

where

$$N_{\text{eff}} = N - \sum_{a=1}^{i} N_a + \sum_{b=i+1}^{C} M_b \tag{4.2.3.12}$$

This last formula is explained in Figure 12 and Appendix F. N_{eff} is the factor of the first excitation box added to the background Young diagram. Finally, recalling that the only source of N dependence is in f_R (for the planar correlators) or $\frac{f_{+R}}{f_B}$ (for the emergent gauge theory correlators) we finally obtain

$$\begin{aligned}\langle O_A(x_1)O_B(x_2)^\dagger\rangle &= F_{AB}(N)\frac{1}{|x_1-x_2|^{2J}}\\ \langle O_A(x_1)O_B(x_2)^\dagger\rangle_B &= F_{AB}(N_{\text{eff}})\frac{(\eta_B)^{n_I}}{|x_1-x_2|^{2J}}\left(1+O\left(\frac{1}{N}\right)\right)\end{aligned} \tag{4.2.3.13}$$

This demonstrates a remarkable relationship between correlators in the planar and non-planar limits.

This result has a number of immediate applications. As we have stressed above, the fact that operators with different trace structures don't mix in the planar limit is a statement about correlators. This no-mixing result allows focus on the single trace operators which is needed to develop the spin chain connection for the planar CFT. Our result (4.2.3.13) immediately implies that operators that are the image of operators with different trace structures, will not mix. Thus, we too can focus on the image of single trace operators and then develop a spin chain description of the planar limit of the emergent gauge theory. States of the spin chain that were identified with a given operator in the planar limit will now be identified with the image of the same operator.

Three point functions of single trace operators are suppressed in the planar limit of the original CFT. Is there a similar statement for three point functions of single trace operators in the emergent gauge theory? In any Poincare invariant CFT the spacetime dependence of the three point

function is fixed by conformal invariance. We can thus simply factor this dependence out and consider the problem of the combinatorics of the Wick contractions. This is also a complicated problem, but for some well chosen examples it can be solved. Consider the following correlator

$$\langle \mathrm{Tr}\,(Z^{n_1}Y^{n_2}\cdots)\mathrm{Tr}\,(Z^{m_1}Y^{m_2}\cdots)\mathrm{Tr}\,(Z^{\dagger p_1}Y^{\dagger p_2}\cdots)\rangle \tag{4.2.3.14}$$

The Wick contractions are all between the first trace and the third trace, and between the second trace and the third trace. In particular, there are no contractions between the first and second traces. For the combinatorics of the Wick contractions, we can treat the double trace $\mathrm{Tr}\,(Z^{n_1}Y^{n_2}\cdots)\mathrm{Tr}\,(Z^{m_1}Y^{m_2}\cdots)$ as a single operator and apply the bijection and treat $\mathrm{Tr}\,(Z^{\dagger p_1}Y^{\dagger p_2}\cdots)$ as a single operator and apply the bijection. Thus, we have reduced the computation to a two point function. This two point correlator correctly sums the contractions between the three traces with each other and with the background. The result (4.2.3.13) then implies that this correlator, which is giving the three point function, is suppressed in the planar limit of the emergent gauge theory. Since OPE coefficients are read from three point functions, the OPE coefficients vanish in the planar limit of both $\mathcal{N}=4$ super Yang-Mills and the emergent gauge theory. We have proved this in the free field theory, for a specific class of correlators. We *conjecture* that it holds quite generally and continues to hold when interactions are turned on. The usual suppression holds because we need to break index loops (which costs N^{-1} for each loop we break) to find a non-zero correlator between three single traces. This does not rely on any detailed structure of the interaction and is quite generally true for a matrix model. Of course, this is one point in our analysis that could be improved.

Our argument in this section considers only the local operators. One might wonder if mixing between different trace structures of delocalised operators is also suppressed or not. In this case the argument is more involved. It is unlikely that there is a simple relationship between correlators of delocalised operator and correlators computed in the planar limit. Explicit computations using concrete examples support the conclusion that again, different trace structures don't mix. See Appendix G for a discussion of this point.

To summarize, we have arrived at a rather detailed picture of the structure of the Hilbert space. We have decomposed the Hilbert space of excitations of the LLM geometry into a direct sum

$$\mathcal{H}_{\mathrm{CFT;LLM}} = \left(\bigoplus_i \mathcal{H}^{(i)}_{\mathrm{CFT}}\right)\bigoplus \mathcal{H}_{\mathrm{CFT;Delocalized}} \tag{4.2.3.15}$$

Restricted Schur polynomials are orthogonal if their labels don't match. This immediately implies that in the free field theory operators belonging to different Hilbert spaces in the above sum have vanishing two point functions and hence that the corresponding subspaces are orthogonal. We have further argued that each subspace can be decomposed into a direct sum of orthogonal components, with each component collecting operators of a definite "trace structure". Here the trace structure is read from the preimage of the operator under the bijection (4.2.3.3). At large N these different trace structures do not mix.

Our study has focused on the free field theory. Of course, the bijection we have defined holds for any coupling. The free field limit has been used to obtain the relationship between correlators

of operators and correlators of their images. It is this discussion that we will extend to weak coupling in the next section.

4.3 Weak Coupling CFT

We expect that the gravitational physics dual to the CFT is coded into the large N correlators. Consequently, it is attractive if we can find relationships between correlators of the planar limit and correlators in the background of a heavy operator. In the previous section we have exhibited relationships of this type, all in the free limit of the CFT. We expect the dual gravitational description is simplest when the CFT is strongly coupled. It is natural to ask if the simple relations between correlation functions exhibited in the free theory survive when interactions are added. Answering this question is the goal of the current section. We start with a careful discussion of the one loop dilatation operator, which develops the relation between correlators at one loop. This argument also gives insight into why the relationship we have uncovered between correlators holds even when higher loop corrections are included.

The article [75] argued that matrix elements of the planar dilation operator are identical to matrix elements of the dilatation operator computed using local excitations, localised at corner[25] i of the Young diagram for the LLM geometry, after replacing $\lambda = g_{YM}^2 N$ by $\lambda_{\text{eff}} = g_{YM}^2 N_{\text{eff}}$ where N_{eff} is the factor of the first box added to corner i. This again amounts to replacing $N \to N_{\text{eff}}$ so it is the rule we derived in Section 4.2.3. We will revisit this argument below adding two new improvements

1. By carefully tracking what is background independent and what is not we will develop a much simpler technical analysis.

2. We will phrase the result using the bijection we developed in Section 4.2.3. The advantage of the rephrasing is that it supports the conclusion that the planar limit of the emergent gauge theory is planar $\mathcal{N} = 4$ super Yang-Mills.

The final result is remarkable: in the large N but non-planar limit we need to sum a huge set of Feynman diagrams. The net effect of summing the huge set of non-planar diagrams, is a simple rescaling of the 't Hooft coupling. This is in complete harmony with the physical argument we developed in the introduction.

The fact that we simply need to rescale the 't Hooft coupling has far reaching consequences: since the dilatation operator in the planar CFT matches the Hamiltonian of an integrable spin chain, we know that the dilatation operator describing the anomalous dimensions of the emergent gauge theory will also match the integrable spin chain. As long as the dilatation operator does not mix operators that belong to the Hilbert space $\mathcal{H}_{\text{CFT}}^{(i)}$ with operators that don't belong to this space, we conclude that there are integrable subsectors in the large N but non-planar limit we consider. Demonstrating the absence of this mixing is one of the main goals of this

[25] These operators belong to $\mathcal{H}_{\text{CFT}}^{(i)}$

section.

Before turning to a detailed technical analysis we will briefly review the evidence supporting the above result. It implies that the anomalous dimensions of the operators of the planar emergent gauge theory are determined in terms of the corresponding dimensions computed in the planar CFT. Explicit computations of anomalous dimensions of the emergent CFT, when developed in a perturbative expansion, confirm this prediction both in the weak coupling CFT and at strong coupling using the dual string theory[82, 75]. Using the $su(2|2)$ symmetry enjoyed by the $su(3|2)$ subspace of local excitations, the two magnon S-matrix has been determined and it agrees up to two loops with a weak coupling computation performed in the CFT[76]. The first finite size corrections to both the magnon and the dyonic magnon have been computed by constructing solutions to the Nambu-Goto action that carry finite angular momentum. These computations[76] again show that the net affect of the background is a scaling of the 't Hooft coupling. This constitutes strong coupling evidence for our result. Since these corrections are sensitive to the overall phase of the S-matrix, which is not determined by kinematics (i.e. the $su(2|2)^2$ symmetry of the theory), this is a non-trivial test. Finally, strings spinning on the three sphere that belongs to AdS_5 have been considered in [85]. These strings are dual to operators belonging to the $SL(2)$ sector of the gauge theory. Once again, the net affect of the background is a scaling of the 't Hooft coupling as predicted[85].

In the subsection that follows we revisit the analysis of [75], phrasing things in terms of the bijection of section 4.2.3 and paying attention the background dependence of the various ingredients in the analysis. This significantly simplifies the original analysis. We pay careful attention to operator mixing, to give evidence supporting the conclusion that the integrable subsectors are decoupled at large N. This closes an important hole in the analysis of [75]. Finally, we consider how the one loop discussion generalizes when we include higher loops.

4.3.1 One Loop Mixing of Local Operators

From now on we normalize the two point function of our operators to 1. To simplify the discussion again focus on operators constructed using only Z and Y fields. It is a simple generalization to include more fields. Consider the mixing between two restricted Schur polynomials, $O_{+R,(+r,s)\mu_1\mu_2}(Z,Y)$ and $O_{+T,(+t,u)\nu_1\nu_2}(Z,Y)$. The capital letter O for the restricted Schur polynomial instead of the χ stresses the fact we are considering normalized operators

$$\langle O_{+R,(+r,s)\mu_1\mu_2}(Z,Y)^\dagger O_{+T,(+t,u)\nu_1\nu_2}(Z,Y)\rangle = \delta_{+R,+T}\delta_{+r,+t}\delta_{su}\delta_{\mu_1\nu_1}\delta_{\mu_2\nu_2} \tag{4.3.1.1}$$

These operators are the image under the bijection of $O_{R,(r,s)\mu_1\mu_2}(Z,Y)$ and $O_{T,(t,u)\nu_1\nu_2}(Z,Y)$. The operators $O_{+R,(+r,s)\mu_1\mu_2}(Z,Y)$ provide a basis for $\mathcal{H}^{(i)}_{\rm CFT}$. The starting point of our analysis is the one loop dilatation operator in this basis[35]

$$DO_{+R,(+r,s)\mu_1\mu_2}(Z,Y) = \sum_{T,(t,u)\nu_1\nu_2} N_{+R,(+r,s)\mu_1\mu_2;+T,(+t,u)\nu_1\nu_2} O_{+T,(+t,u)\nu_1\nu_2}(Z,Y) \tag{4.3.1.2}$$

where

$$N_{+R,(+r,s)\mu_1\mu_2;+T,(+t,u)\nu_1\nu_2} = -\frac{g_{YM}^2}{8\pi^2}\sum_{+R'}\frac{c_{+R,+R'}d_{+T}nm}{d_{+R'}d_{+t}d_u(n+m)}\sqrt{\frac{f_{+T}\text{hooks}_{+T}\text{hooks}_{+r}\text{hooks}_s}{f_{+R}\text{hooks}_{+R}\text{hooks}_{+t}\text{hooks}_u}}$$
$$\text{Tr}\left(\left[(1,m+1),P_{+R,(+r,s)\mu_1\mu_2}\right]I_{+R'+T'}\left[(1,m+1),P_{+T,(+t,u)\nu_2\nu_1}\right]I_{+T'+R'}\right) \tag{4.3.1.3}$$

In the above expression Young diagram $+R'$ is obtained by dropping one box from $+R$ and $c_{+R,+R'}$ is the factor of the box that is dropped. Also, d_r is the dimension of symmetric group irreducible representation r. Use n to denote the total number of Z fields in $O_{+R,(+r,s)\mu_1\mu_2}$ and n_B to denote the number of Z fields in the background. Also, n_Z denotes the number of Z fields in $O_{R,(r,s)\mu_1\mu_2}$ and m denotes the number of Y fields. We have $n = n_B + n_Z$. The above result (4.3.1.2),(4.3.1.3) was derived using the convention that the Y fields occupy slots 1 to m exactly as shown in (4.2.1.7). In the standard tableau labeling of the states in $+R$, the Y's would be associated to the boxes labelled 1 to m. This result is the exact one loop result - we have not made use of any of the simplifications that come from taking $N \to \infty$. Notice that the N dependence of the matrix elements appears in $c_{+R,+R'}$, f_{+R} or f_{+T}. This immediately implies that we will again have a dependence on N_{eff} and not on N.

To proceed further, begin by discussing the intertwining map $P_{+R,(+r,s)\mu_1\mu_2}$. Our goal is to give a careful argument concluding that $P_{+R,(+r,s)\mu_1\mu_2}$ is background independent. This map acts within a direct sum of the carrier space of $+T$ and the carrier space of $+R$. It gives zero on $+T$ and projects the row and column labels of the $+R$ subspace to an (r,s) irreducible representation of $S_n \times S_m$. Our convention is that the first boxes removed are associated to Y. This projection operator simply has to assemble these boxes into an irreducible representation s of S_m. The remaining boxes are already in $+r$. Thus, the projection operator is

$$P_{+R,(+r,s)} = \frac{1}{m!}\sum_{\sigma\in S_m}\chi_s(\sigma)\Gamma_{+R}(\sigma) \tag{4.3.1.4}$$

In writing the above projection operator it is understood that we are acting in the subspace of $+R$ in which states are labelled by standard tableau such that labels 1,...,m only fill boxes that belong to $+R$ and not to $+r$. This is the subspace in which the remaining boxes are already in $+r$. To get the intertwining map, restrict the above row and column labels. The key point is that the projection operator acts only on boxes associated to the Y fields. Restricting indices to get the intertwining map will not change this so that the intertwining map $P_{+R,(+r,s)\alpha\beta}$ only has a nontrivial action on the Y boxes, that is, on the boxes that are removed from $+R$ to get $+r$. With the discussion of Section 4.2.1 in mind, its clear that $P_{+R,(+r,s)\alpha\beta}$ is background independent.

To evaluate the matrix elements of the dilatation operator, we need to perform the following trace

$$\text{Tr}\left(\left[(1,m+1),P_{+R,(+r,s)\mu_1\mu_2}\right]I_{+R'+T'}\left[(1,m+1),P_{+T,(+t,u)\nu_2\nu_1}\right]I_{+T'+R'}\right) \tag{4.3.1.5}$$

The intertwining maps $I_{+R'+T'}$ and $I_{+T'+R'}$ map from the subspace $+R'$ obtained by dropping a single box from $+R$, to the subspace $+T'$ obtained by dropping a single box from $+T$. As a

result, these maps act only on the box in the standard tableau labelled 1 which is associated to a Y and hence these maps are background independent. The results of Section 4.2.1 imply that the above trace is background independent. Lets pursue this further in our current example. The intertwining maps $P_{+R,(+r,s)\mu_1\mu_2}$ and $P_{+T,(+t,u)\nu_2\nu_1}$ act only on the boxes labelled 1 to m - all Y boxes, and the permutation $(1, m+1)$ acts only on boxes labelled 1 or $m+1$. One is a Y box, one is a Z box and both belong to the excitation. Consequently, in the above trace the very vast majority of boxes - those with labels $> m+1$ and there are $O(N^2)$ of them - are simply spectators and can be traced over. Recall that we are focusing on operators that belong to a given emergent gauge theory. The non-trivial structure of the matrix elements is determined by the Young diagrams R, r and s and it will agree with the non-trivial structure of the planar matrix elements - this is the background independence. The only difference between the planar result for the trace and what we consider above, is that the sum over the inert boxes produces a factor $d_{+r'_i}$ where $+r'_i$ is obtained by dropping a box from row i of r in $+r$ while in the planar case we get a factor of $d_{r'_i}$. If we now consider mixing with operators outside of the emergent gauge theory, in principle we could drop a box from $+r$ at any location - even a corner that is distinct from where our excitation is located. These matrix elements arise when there is mixing with states that don't belong to the integrable subsector. We will consider these corrections in detail in the next section. Our conclusion is that these matrix elements vanish at large N. Using this result, we can restrict to mixing between operators that belong to the planar limit of the emergent gauge theory. Consequently, the bijection of section 4.2.3 relates these operators to two operators, $O_{R,(r,s)\mu_1\mu_2}(Z,Y)$ and $O_{T,(t,u)\nu_1\nu_2}(Z,Y)$ defined in the planar CFT. We will now derive a relationship between the matrix elements for mixing $O_{+R,(+r,s)\mu_1\mu_2}(Z,Y)$ and $O_{+T,(+t,u)\nu_1\nu_2}(Z,Y)$ and those for mixing $O_{R,(r,s)\mu_1\mu_2}(Z,Y)$ and $O_{T,(t,u)\nu_1\nu_2}(Z,Y)$. This extends the free field theory relationship between correlators obtained in Section 4.2.3, to one loop. The argument is[26]

$$
\begin{aligned}
&-\frac{g_{YM}^2}{8\pi^2}\sum_{+R'}\frac{c_{+R,+R'}d_{+T}nm}{d_{+R'}d_{+t}d_u(n+m)}\sqrt{\frac{f_{+T}\text{hooks}_{+T}\text{hooks}_{+r}\text{hooks}_s}{f_{+R}\text{hooks}_{+R}\text{hooks}_{+t}\text{hooks}_u}}\\
&\qquad\text{Tr}\left(\left[(1,m+1),P_{+R,(+r,s)\mu_1\mu_2}\right]I_{+R'+T'}\left[(1,m+1),P_{+T,(+t,u)\nu_2\nu_1}\right]I_{+T'+R'}\right)\\
&=-\frac{g_{YM}^2}{8\pi^2}\sum_{+R'}\sum_i\frac{c_{+R,+R'}m}{d_u}\frac{\sqrt{\text{hooks}_{+r}\text{hooks}_{+t}}}{\text{hooks}_{+r'_i}}\frac{\text{hooks}_{+R'}}{\sqrt{\text{hooks}_{+T}\text{hooks}_{+R}}}\sqrt{\frac{f_{+T}\text{hooks}_s}{f_{+R}\text{hooks}_u}}\\
&\qquad\text{Tr}_{+i}\left(\left[(1,m+1),P_{+R,(+r,s)\mu_1\mu_2}\right]I_{+R'+T'}\left[(1,m+1),P_{+T,(+t,u)\nu_2\nu_1}\right]I_{+T'+R'}\right)\\
&=-\frac{g_{YM}^2}{8\pi^2}\sum_{+R'}\sum_i\frac{c_{+R,+R'}m}{d_u}\frac{\sqrt{\text{hooks}_{r}\text{hooks}_{t}}}{\text{hooks}_{r'_i}}\frac{\text{hooks}_{R'}}{\sqrt{\text{hooks}_{T}\text{hooks}_{R}}}\sqrt{\frac{f_{+T}\text{hooks}_s}{f_{+R}\text{hooks}_u}}\\
&\qquad\text{Tr}_{i}\left(\left[(1,m+1),P_{+R,(+r,s)\mu_1\mu_2}\right]I_{+R'+T'}\left[(1,m+1),P_{+T,(+t,u)\nu_2\nu_1}\right]I_{+T'+R'}\right)\\
&=-\frac{g_{YM}^2}{8\pi^2}\sum_{+R'}\sum_i\frac{c_{+R,+R'}m}{d_u}\frac{\sqrt{\text{hooks}_{r}\text{hooks}_{t}}}{\text{hooks}_{r'_i}}\frac{\text{hooks}_{R'}}{\sqrt{\text{hooks}_{T}\text{hooks}_{R}}}\sqrt{\frac{f_{+T}\text{hooks}_s}{f_{+R}\text{hooks}_u}}\\
&\qquad\text{Tr}_{i}\left(\left[(1,m+1),P_{R,(r,s)\mu_1\mu_2}\right]I_{R'T'}\left[(1,m+1),P_{T,(t,u)\nu_2\nu_1}\right]I_{T'R'}\right)
\end{aligned}
$$

[26]Recall that $d_r = n!/\text{hooks}_r$ for any irrep r of S_n. In what follows Tr_i indicates that we have traced over r_i and Tr_{+i} indicates that we have traced over $+r_i$.

$$= -\frac{g_{YM}^2}{8\pi^2}\sum_{R'}\frac{c_{+R,+R'}d_T n_Z m}{d_{R'}d_t d_u(n_Z+m)}\sqrt{\frac{f_{+T}\text{hooks}_T\text{hooks}_r\text{hooks}_s}{f_{+R}\text{hooks}_R\text{hooks}_t\text{hooks}_u}}$$
$$\text{Tr}\left(\left[(1,m+1),P_{R,(r,s)\mu_1\mu_2}\right]I_{R'T'}\left[(1,m+1),P_{T,(t,u)\nu_2\nu_1}\right]I_{T'R'}\right) \quad (4.3.1.6)$$

In moving to the third line above we have used the formula (4.2.1.10) proved in Appendix E. This is the only step in the above computation that is not exact, but relies on the large N limit. Notice that the only difference between the last line above and the matrix elements of the dilatation operator in the planar limit is that N is replaced with N_{eff}. This is then a simple proof that at large N, the matrix elements of the one loop dilatation operator with respect to states of the emergent gauge theory are given by replacing $N \to N_{\text{eff}}$ in the matrix elements of the planar dilatation operator, taken with respect to the preimages of these states.

How does this generalize to higher loops? The two loop dilatation operator has been considered in [87] and from that analysis it is clear what the general results are. The structure of the matrix elements are very similar to the form shown in (4.3.1.3). One again lands up computing a trace. The same intertwining maps $P_{+R,(+r,s)\mu_1\mu_2}$ and $P_{+T,(+t,u)\nu_1\nu_2}$ appear in the trace. The maps $I_{R'T'}, I_{T'R'}$ are replaced at L loops by maps which map from a representation $R^{(L)}$ obtained by dropping L boxes from R to a representation $T^{(L)}$ obtained by dropping L boxes from T. There are also again permutations that act on the boxes associated to the excitation. Finally, the trace is multiplied by the square root of the factors of the boxes dropped from R and T. Arguing as we did above, its clear that the trace is background independent and the product of factors implies that the simple rule $N \to N_{\text{eff}}$ again applies. These observations imply that our one loop conclusion goes through when higher loop corrections are included.

To summarize, we have found integrable subsectors in the large N but non-planar limit that we are considering. Each integrable subsector is an emergent gauge theory, with its own gauge group $U(N_{\text{eff}})$. To complete this discussion, in the next section we will consider the mixing between the integrable and non-integrable subsectors.

4.3.2 Mixing with delocalised Operators

The operators that belong to the planar limit of a given emergent gauge theory are localised at a given corner and define an integrable subsector of the theory. There are operators that are not localised at one corner - they straddle two or more corners. If these delocalised operators mix with the localised operators they will almost certainly ruin integrability of the emergent gauge theory. In this section we consider the mixing between localised and delocalised operators. Our main result is that

$$\langle\phi|D|\psi\rangle = 0 \qquad |\phi\rangle \in \mathcal{H}_{\text{CFT;Local}} \quad |\psi\rangle \in \mathcal{H}_{\text{CFT;Delocalized}} \quad (4.3.2.1)$$

at large N.

We make extensive of two basic observations. First, in computing the matrix element (4.3.1.3),

it is clear that the reason why two different states can have a non-zero matrix element, is because the permutation group element $(1, m+1)$ acts to change the identity of the state. It is thus important to have a good understanding of the action of this permutation on a standard tableau. Since we are computing a trace which has the same value in any equivalent representation, we can carry this computation out in any convenient representation. In what follows, we will use Young's orthogonal representation. This representation is specified by giving the action of adjacent swaps which are two cycles of the form $(i, i+1)$. Given the matrices representing the complete set of adjacent swaps, it is easy to generate the rest of the group. Let $|\psi\rangle$ denote a valid standard tableau and let $|\psi\rangle_{i\leftrightarrow i+1}$ denote the state obtained from $|\psi\rangle$ by swapping i and $i+1$. The content of the box labelled i, denoted $c(i)$ is given by $b-a$ if the box is in row a and column b. Our convention for the standard tableau labeling is spelled out in the following example

$$\begin{array}{|c|c|c|c|c|}\hline 5&4&3&2&1\\\hline\end{array} \tag{4.3.2.2}$$

The rule specifying the matrix representing the adjacent swap is

$$(i,i+1)|\psi\rangle = \frac{1}{c(i)-c(i+1)}|\psi\rangle + \sqrt{1-\frac{1}{(c(i)-c(i+1))^2}}|\psi\rangle_{i\leftrightarrow i+1} \tag{4.3.2.3}$$

If boxes i and $i+1$ are located at different corners, the first term above is of order N^{-1} and can be neglected in the large N limit while the coefficient of the second term is 1, to the same accuracy.

The second observation is a relationship between the loop order and the number of boxes that can differ in the Young diagram labels of the operators that are mixing. To add loop effects, we consider Feynman diagrams with a certain number of vertices included in the diagram. Contracting two fields in a restricted Schur polynomial with a vertex has the effect of setting the indices of two different fields equal. This Kronecker delta function restricts the sum over permutations in (4.2.1.7) from S_{n+m} to S_{n+m-1}. Two operators which begin as distinct representations of S_{n+m} may well produce the same representation of S_{n+m-1}. For this to happen, their Young diagram labels must differ in the placement of at most one box. This is manifest in the matrix element (4.3.1.3), because the maps $I_{T'R'}$ which appear are only non-zero if T' (obtained by dropping one box from T) has the same shape as R' (obtained by dropping one box from R). At L loops we have added L vertices which lands up restricting the sum in (4.2.1.7) from S_{n+m} to S_{n+m-L}. In this case operators that differ by at most L boxes will mix.

As a warm up example, consider the mixing of localised operators that belong to different corners

$$\langle\phi|D|\psi\rangle = 0 \qquad |\phi\rangle \in \mathcal{H}^{(i)}_{\text{CFT}} \quad |\psi\rangle \in \mathcal{H}^{(j)}_{\text{CFT}} \tag{4.3.2.4}$$

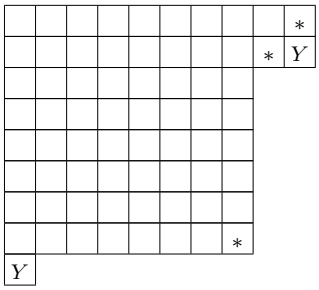
with $j \neq i$. This represents a mixing between states of two different planar emergent gauge theories, i.e. two distinct integrable subsectors. For concreteness imagine that these two operators are the images of $R(r,s)\alpha\beta$ and $T(t,u)\gamma\delta$ under the bijection described in section 4.2.3. These two operators disagree in the placement of $J \sim O(\sqrt{N})$ boxes, since the excitation which has J boxes is located at corner i for state $|\phi\rangle$ and at corner j for state $|\psi\rangle$. Thus, these two operators will start to mix at the J loop order. Further, for a non-zero intertwining map $I_{R^{(J)},T^{(J)}}$ we need to drop the boxes that disagree between the two operators[27]. This implies

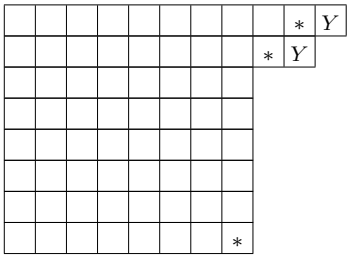
[27]We use $R^{(J)}$ to denote a Young diagram obtained by dropping J boxes from R and similarly for $T^{(J)}$.

that, after expressing permutations that appear in the dilatation operator in terms of adjacent swaps, only the first term on the right hand side of (4.3.2.3) contributes. We need to swap all of the distant and local boxes which leads to a suppression of $O(N^{-1})$, for every box in the excitation. Consequently this mixing is completely suppressed at large N and (4.3.2.4) holds.

We are now ready to tackle (4.3.2.1). Consider a localised excitation, located at corner i. We study the mixing of this localised excitation with a delocalised excitation, that has k boxes at corner $j \neq i$ and is otherwise located at corner i. These two operators disagree in the placement of at least k boxes and so the first time they can possibly mix is at k loops. To get a non-zero answer, for the interwining map, we need to drop the boxes that don't agree and this means that we must keep terms in which distant boxes remain distant. This again amounts to retaining the first term on the right hand side of (4.3.2.3) and hence a suppression of $O(N^{-1})$, for every distant box. Consequently this mixing is suppressed as $\sim N^{-k}$ at large N. This demonstrates that (4.3.2.1) holds at large N.

We will end this section with a simple example illustrating the above argument. The operators which mix are labelled by the Young diagrams shown in (4.3.2.5). They have a total of 2 Y fields and many Z fields.

$A =$ 

$B =$ 

(4.3.2.5)

A and B are the Young diagrams for the excitations in the background. They both have $O(N^2)$ boxes. The boxes labelled with a Y correspond to Y fields and they may be labelled 1. The boxes with a $*$ are Z fields and may be labelled with $m+1=3$. For a non-zero answer, the states in A which contribute have the bottom Y labelled with a 1. Only in this case can we match the shape of B, after one box - the upper Y box - is dropped. Using Dirac notation, the structure of the terms contributing to (4.3.1.5) are

$$\sum_{i,j} \langle A', i | P_{+R,(+r,s)\mu_1\mu_2}(1, m+1) | A', j \rangle \langle B', j | P_{+T,(+t,u)\nu_1\nu_2}(1, m+1) | B', i \rangle \tag{4.3.2.6}$$

It is clear that the only way that $\langle A', i | P_{+R,(+r,s)\mu_1\mu_2}(1, m+1) | A', j \rangle$ can be non-zero is if we keep the first term in (4.3.2.3) when the permutation acts. Since the only boxes labelled with $m+1$ (the starred boxes) are distant from the bottom Y box in A, this is suppressed as $\frac{1}{N}$.

4.4 Strong Coupling CFT

In this section we want to explore the string theory interpretation of our results, adding to the discussion of the introduction. The excitations we have considered in the CFT are all dual to

excitations of the D3-brane giant gravitons that condensed to produce the geometry. These are all open string excitations and we have demonstrated that they lead to emergent gauge theories. In this section we will motivate why adding boxes to the Young diagrams give excitations that are localised to the brane, that is, why they are open strings. There are also closed string excitations in the dual string theory. We will give an example of a closed string excitation. For relevant earlier literature see [47, 88, 89, 90].

Why does adding extra boxes to a Young diagram as we have done above, lead to open strings excitations? We can also phrase this question as: Why does adding extra boxes to a Young diagram lead to excitations localised on the branes? Recall that there is an intimate connection between the entanglement of the underlying degrees of freedom and the geometry of spacetime. This is manifested in the Ryu-Takayanagi formula for entanglement entropy in terms of the area of a minimal surface[91]. Further, Van Raamsdonk has conjectured that the amount of entanglement between two regions is related to the distance between them: the more the entanglement the less the distance between the two regions[92]. For a recent relevant discussion see [81]. To apply this to our set up, recall that the Young diagram is an instruction for how an operator composed of many fields is to be constructed. Each box corresponds to a distinct field and the indices of fields in the same row are to be symmetrized, while the indices of fields in the same column are to be antisymmetrized. This will in the end produce a highly entangled state, with fields corresponding to boxes that are nearby on the Young diagram being more entangled than boxes that are more distant. The Young diagram becomes a convenient way to visualize the entanglement so that boxes that are nearby on the Young diagram, are nearby in spacetime. To make these comments more precise we would need a better understanding of entanglement for multi part quantum systems.

If this interpretation is correct, then to produce a closed string excitation (which is not localised on the brane), we should construct an operator whose indices are not symmetrized or antisymmetrized with indices of the fields making up the background. An example of such an operator is given by $O_{\{k\}} = \mathrm{Tr}\,(Y^{k_1}X^{k_2}Y^{k_3}\cdots)$. Since this is a closed string state, we expect that the mixing of this operator with the background will correspond to closed string absorption by a brane. Intuition from a single brane suggests that this is highly suppressed because $g_s \sim O(N^{-1})$ at large N. However, we are dealing with $O(N)$ branes so that we can't neglect mixing of $O_{\{k\}}$ with the background. If this mixing were suppressed, we would be dealing with an $SU(2)$ sector of the planar Yang-Mills theory which is integrable. We will explore this issue at strong coupling using string theory.

The state dual to $O_{\{k\}}$ should be a closed string moving in an LLM geometry. The general LLM geometry is described by the metric[12] $(i,j=1,2)$

$$ds^2 = -y(e^G+e^{-G})(dt+V_i dx^i)^2 + \frac{1}{y(e^G+e^{-G})}(dy^2+dx^i dx^i) + ye^G d\Omega_3 + ye^{-G}d\tilde{\Omega}_3^2 \quad (4.4.0.1)$$

where

$$z = \tilde{z} + \frac{1}{2} = \frac{1}{2}\tanh(G) \qquad y\partial_y V_i = \epsilon_{ij}\partial_j \tilde{z} \qquad y(\partial_i V_j - \partial_j V_i) = \epsilon_{ij}\partial_y \tilde{z} \quad (4.4.0.2)$$

The metric is determined by the function z which depends on the three coordinates y, x^1 and x^2 and is obtained by solving Laplace's equation

$$\partial_i \partial_i z + y \partial_y \frac{\partial_y z}{y} = 0. \tag{4.4.0.3}$$

In what follows we often trade x^1, x^2 for a radius and an angle, r and φ. Our focus is on geometries given by concentric black annuli on the bubbling plane. For a set of rings with a total of E edges with radii R_l $l = 1, 2, ..., E$ the geometry is determined by the functions[12]

$$\tilde{z} = \sum_{l=1}^{E} \frac{(-1)^{E-l}}{2} \left(\frac{r^2 + y^2 - R_l^2}{\sqrt{(r^2 + y^2 + R_l^2)^2 - 4r^2 R_l^2}} - 1 \right), \tag{4.4.0.4}$$

$$V_\varphi(x^1, x^2, y) = \sum_{l=1}^{E} \frac{(-1)^{E-l+1}}{2} \left(\frac{r^2 + y^2 + R_l^2}{\sqrt{(r^2 + y^2 + R_l^2)^2 - 4r^2 R_l^2}} - 1 \right). \tag{4.4.0.5}$$

We need the $y = 0$ limit of the metric, which is given by

$$ds^2 = -\frac{1}{b}(dt + V_\varphi d\varphi)^2 + b(dy^2 + y^2 d\tilde{\Omega}_3^2) + b(dr^2 + r^2 d\varphi^2) + \frac{1}{b}\left(\sin^2\psi d\beta^2 + d\psi^2 + \cos^2\psi d\alpha^2\right) \tag{4.4.0.6}$$

with

$$b(r) = \sqrt{\sum_{l=1}^{E} (-1)^{E-l} \frac{R_l^2}{(R_l^2 - r^2)^2}} \tag{4.4.0.7}$$

We look for classical string solutions to the equations of motion following from the Nambu-Goto action

$$S_{NG} = \frac{\sqrt{\lambda}}{2\pi} \int d\tau L_{NG} = \frac{\sqrt{\lambda}}{2\pi} \int d\sigma \int d\tau \sqrt{(\dot{X} \cdot X')^2 - \dot{X}^2 X'^2} \tag{4.4.0.8}$$

The ansatz

$$t = \tau \qquad \psi = \psi(\tau, \sigma) \qquad \alpha = \alpha(\tau, \sigma) \qquad y = 0 \qquad r = 0 \tag{4.4.0.9}$$

with $\tilde{\theta}, \tilde{\varphi}, \tilde{\psi}, \varphi, \beta$ constant leads to a solution. After inserting this into the equations of motion, the resulting equations describe a string moving on

$$ds^2 = \frac{1}{b(0)}\left(-dt^2 + d\psi^2 + \cos^2\psi d\alpha^2\right) \tag{4.4.0.10}$$

This is string theory on $\mathbb{R} \times S^2$ which is integrable. The single magnon solution is given by $t = \tau$, $\alpha = \tau + \sigma$ and

$$\cos\psi = \frac{\cos\psi_0}{\cos\sigma} \qquad -\psi_0 \leq \sigma \leq \psi_0 \tag{4.4.0.11}$$

The energy of this solution is given by

$$\begin{aligned} E &= \frac{\sqrt{\lambda}}{2\pi}\int_{-\psi_0}^{\psi_0} d\sigma \frac{\partial L_{NG}}{\partial \dot{t}} \\ &= \frac{\sqrt{\lambda}}{\pi}\frac{1}{b(0)}\cos\psi_0 \end{aligned} \tag{4.4.0.12}$$

This is the energy of a single magnon with $N \to N_{\text{eff}}$ where

$$N_{\text{eff}} = \frac{N_1(M+N_1)(M+N_1+N_2)}{M^2+N_1^2+M(2N_1+N_2)} \tag{4.4.0.13}$$

and $N_1 + N_2 = N$. In writing this formula we specialized to a geometry with a central black disk of area N_1, a white ring of area M and a black ring of area N_2. If we take $N_2 = O(1) = M$ at large N we find $N_{\text{eff}} = N_1 = N(1+O(N^{-1}))$. This is exactly as expected since this boundary condition corresponds to exciting so few giant gravitons that backreaction can be neglected and we must recover the $AdS_5 \times S^5$ result as we have done. The above result shows that the closed string is exploring the geometry at $r = 0$ in the bubbling plane. This region simply can't be explored by adding boxes to any corner of the background Young diagram. The result depends in a nontrivial way on the details of the background, as we might expect for an excitation that is not localised on a specific set of branes. This supports our argument that this is a closed string excitation. For this closed string excitation once again the only change as compared to the planar limit is the replacement $N \to N_{\text{eff}}$. This is probably only a property of the strong coupling limit. Indeed, in the free theory the correlator of the closed string excitation and the background factorizes

$$\langle \chi) B(Z) \chi_B(Z)^\dagger O_{\{k\}} O_{\{k\}}^\dagger \rangle = \langle \chi) B(Z) \chi_B(Z)^\dagger \rangle \langle O_{\{k\}} O_{\{k\}}^\dagger \rangle \tag{4.4.0.14}$$

which is not consistent with a simple $N \to N_{\text{eff}}$ replacement.

4.5 Summary and Outlook

In this thesis we have considered excitations of LLM geometries. The excitations are constructed by adding boxes (representing the excitation) to a Young diagram with $O(N^2)$ boxes (representing the LLM geometry). Adding a box to a row of a Young diagram implies that the indices of the added operator will be symmetrized or antisymmetrized with the indices of adjacent boxes, so that the fields associated to the boxes added are highly entangled with the fields associated to adjacent boxes. Two objects that are entangled are nearby in spacetime, so that we produce excitations that are localised to the brane worldvolume. These excitations are open strings and hence give rise to an emergent gauge theory. We have constructed a bijection between operators in the Hilbert space of planar $\mathcal{N} = 4$ super Yang-Mills and operators in the planar Hilbert space of the emergent gauge theory. Free field correlators of operators that are in bijection are related in a very simple way. This immediately implies that since three point functions of single trace operators are suppressed in the planar limit of the original free CFT,

they are also suppressed in the planar limit of the free emergent gauge theory. Since OPE coefficients are read from three point functions, the OPE coefficients vanish in the planar limit of both free $\mathcal{N} = 4$ super Yang-Mills and the free emergent gauge theory. We have conjectured that this continues to be the case when interactions are turned on. By considering the weak coupling CFT we have also given arguments concluding that the anomalous dimensions match the dimensions of an $\mathcal{N} = 4$ super Yang-Mills with gauge group $U(N_{\text{eff}})$, where N_{eff} is read from the factor of the boxes associated to the excitations. Since any CFT is determined by its OPE coefficients and spectrum of anomalous dimensions, this strongly suggests that the planar limit of the emergent gauge theories are planar $\mathcal{N} = 4$ super Yang-Mills theories.

We have been careful to stress that the planar limit of the emergent gauge theory agrees with planar $\mathcal{N} = 4$ super Yang-Mills. The stronger statement, that the emergent gauge theory is $\mathcal{N} = 4$ super Yang-Mills is not true: there are important differences between the two theories that are only apparent when going beyond the planar limit. The emergent gauge theory has gauge group $U(N_{\text{eff}})$. If this gauge theory really is $\mathcal{N}$=4 super Yang-Mills theory we expect a stringy exclusion principle cutting off the angular momentum of the giant graviton at momentum N_{eff}. In actual fact, the maximum angular momentum for a giant graviton is in general below this and it is set by the shape of the background Young diagram. Similarly, dual giant gravitons can usually have an arbitrarily large angular momentum. In the emergent gauge theory, the dual giant must fit inside the corner at which the emergent gauge theory is located, so there are no dual giant excitations with arbitrarily large momentum. These discrepancies arise because the giant graviton excitations detect the structure of the bubbling plane. They can probe the difference between a black disk in a sea of white or just one ring among many or something else. So even in the large N limit, the emergent gauge theory and $\mathcal{N} = 4$ super Yang-Mills theory are different. They do however share the same planar limit.

An interesting technical result that has been achieved is the description of states when some of the rows of the Young diagram describing the giant graviton branes are equal in length. Previous studies [93, 36, 37] have considered the displaced corners approximation in which the length between any two rows (for a system of dual giant gravitons) scales as N in the large N limit. In this situation, the action of the symmetric group simplifies and explicit formulas for the restricted characters can be developed[93, 36]. Here we have the case that many row lengths are of comparable size. Progress is achieved by uncovering the relationship between the relevant restricted Schur computations and those of the planar limit. We also allowed some Z fields in the excitation which includes the case that the row lengths are similar but not identical.

There are a number of interesting directions that could be pursued. First, perhaps there are new holographic dualities: each emergent gauge theory might itself be dual to an $\text{AdS}_5\times\text{S}^5$ geometry, in a suitable limit. There maybe a limit of the geometry that zooms in on the edge of the black regions in the bubbling plane to give an $\text{AdS}_5\times\text{S}^5$ geometry with N_{eff} units of five form flux. Restricting to excitations that belong to $\mathcal{H}^{(i)}_{\text{CFT}}$ is how we restrict to the integrable subsector in the CFT. The limit that isolates an $\text{AdS}_5\times\text{S}^5$ geometry would restrict us to the integrable subsector in the string theory. This is currently under active investigation [94].

There are a number of questions we could pursue to further explore the dynamics of the emergent gauge theory. As we have mentioned, the worldvolume of the giant gravitons is a distinct

space from the space on which the original CFT is defined. How is locality in this emergent space of the emergent gauge theory realized? This may provide a simple testing ground for ideas addressing the emergence of spacetime. We have argued that there are integrable subsectors in large N but non-planar limits of $\mathcal{N} = 4$ super Yang-Mills. Can we find further evidence for the integrability of these subsectors? Even more important, how can this integrability be exploited to explore the physics of emergent gauge theories in interesting and non-trivial ways? For other promising indications of integrability beyond the planar limit see [95, 96, 97]. Besides the local observables we have considered, the emergent gauge theory will have Wilson loops. It maybe interesting to explore these non-local observables.

The emergent gauge theory that we have explored in this thesis is only a decoupled sector at large N. What are the first corrections which couple the emergent gauge theory to the rest of the theory? Presumably these corrections correspond to closed string absorption/emission by branes. This is something concrete that can be evaluated.

Finally, decoupling limits for gauge theory living on the intersections of giant gravitons have been considered in [98, 99, 100, 101, 102]. It would be interesting to see if the methods developed in this thesis can be used to clarify the emergent gauge theories arising in these cases, which may shed light on the microstates of near-extremal black holes in $AdS_5 \times S^5$.

5 Gauge Invariants in Tensor Models

This chapter is based on work that appears in [103]. Reorganising a field theory in terms of gauge invariant parameters has been insightful in how to treat the CFT so as to better understand how gravity manifests itself from a strongly coupled gauge theory. The space of gauge invariants in $\mathcal{N} = 4$ is huge, however. The SYK model has been a promising candidate for a simple solvable example of holography. Motivated by the close connection between tensor models and SYK, and in the hope the space of gauge invariants will be easier to work with than for a matrix model, we construct the gauge invariants of bosonic and fermionic tendor models. We compute the correlation functions exactly in the free theory and construct the collective theory for the bosonic model. In this way we hope to take a step closer to understanding holography.

5.1 Introduction

The SYK model[104, 105] may provide a simple solvable example of holography[4], realized as an AdS/CFT duality - see [106, 107, 108, 109]. This expectation is motivated by the fact that the model develops an approximate conformal symmetry in the infrared. Exact conformal symmetry is spontaneously and explicitly broken, leading to a pseudo-Goldstone mode. This mode is responsible for the exponential growth of out of time ordered correlators, which saturates the chaos bound[110]. Saturating the bound is a strong hint that the model is dual to something close to Einstein gravity. Much of the progress to date is possible because the large N limit is dominated by a simple class of diagrams. It is because these diagrams can be summed that the model is solvable, even at strong coupling.

The SYK model describes fermions interacting with all-to-all random interactions. However, the large N physics of the SYK model is identical to a tensor model, that has a conventional large N limit[111]. The large N limit of the tensor models is dominated by melonic graphs[112, 113, 114, 115], which can be summed. For interesting related work on holographic tensor models see [116]-[117]. Earlier work on tensor models includes [118]-[119].

The mechanism by which gravitational physics is manifested from a strongly coupled gauge theory remains elusive. The original CFT description has the field theory coupling as the loop expansion parameter. On the other hand, the gravitational description that emerges at strong coupling, must have $1/N$ as the loop counting parameter. This is a highly non-trivial hint into the structure of the holographic reorganization of the CFT. The collective field theory of Jevicki and Sakita[120, 121] achieves exactly this: by formulating the theory in terms of gauge invariant variables, the resulting field theory explicitly has $1/N$ as the loop expansion parameter. The reorganization of the dynamics is highly non-trivial, with non-linear collective dynamics being induced by the Jacobian of the change of variables[120, 121].

It would be very attractive to apply the collective field theory method to CFTs and explore the resulting field theory. In the case of a single matrix, this leads to a string field theory for

the $c = 1$ string[56]. This is a beautiful example of how a quantum mechanical system can develop an extra dimension. In the much more interesting example of $\mathcal{N} = 4$ super Yang-Mills theory[4] (or even QCD) the construction of collective field theory is frustrated by the fact that the space of gauge invariants (loop space) is enormous and an explicit construction of the dynamics of gauge invariants looks hopeless. It turns out that representation theory can provide a systematic approach towards the structure of loop space. Indeed, the use of representation theory in the half-BPS sector[122, 123] leads to a clear connection to free fermions[122, 123, 16] and ultimately to a rather complete understanding of the mapping between the CFT operators and supergravity geometries[12]. This has been extended to more general bosonic sectors[32] -[83] and even for fermions and gauge fields[60, 61]. These bases allow the computations of anomalous dimensions of heavy operators in $\mathcal{N} = 4$ super Yang-Mills[36, 93, 124, 37] (in a large N but non planar limit[13]) that are dual to excited giant gravitons[62]-[82]. Up to now however, even with this improved understanding, it is not obvious how to build the collective field theory of these invariant variables.

Vector models are much simpler. The space of invariants is spanned by a bilocal field and one can explicitly build the collective dynamics[125]. In [126] the idea that the bilocal fields provide a reconstruction of the bulk fields of the dual higher spin gravity[127] was put forwards. Using essentially kinematics [128]-[129] developed a map between the space of bilocals and the dual gravity. The bilocal description has also proved to be very useful for the SYK model itself[107, 109, 130], as well as for descriptions of supersymmetric versions of SYK[131, 132, 133, 134], in which case an elegant bilocal superspace formulation has been developed in [135].

One might hope that the case of tensor models is, in a sense, intermediate between the vector and matrix models. It is possible that the space of gauge invariants is richer than that of vectors, but still not as complex as that of matrices. If this is the case, this may provide a useful lesson towards managing the loop space of multi-matrix models. We explore this possibility in the present chapter.

Our basic goal is to construct the gauge invariants of both bosonic and fermionic tensor models. For bosonic tensor (colored as well as non-colored) models, the paper [136] counted the gauge invariants uncovering a relationship with counting problems of branched covers of the 2-sphere. The rank d of the tensor is related to a number of branch points. Further, formulas for correlators of the tensor model invariants in a permutation basis were obtained. Correlators in the permutation basis have been related to the (Hurwitz) character calculus in [137] (see also [138]). A dual representation theory basis was developed in [139]. Our starting point reconsiders the representation theory basis for the bosonic tensor models, in a way that naturally allows an extension to fermionic tensor models. The basic ideas are explained in the next section, where we obtain counting formulas for the number of gauge invariant operators in bosonic and fermionic tensor models. The counting results for the bosons agree with results presented in [136, 139, 140]. The counting formulas for the fermions are new. In section 3 we consider both the computations of the vacuum expectation values of our gauge invariant operators, as well as two point functions of normal ordered gauge invariant operators. These computations are performed exactly (i.e. to all orders in $1/N$), in the free theory. In section 4 we describe the algebraic structure of the gauge invariants: they form a ring. In section 5, we construct a

collective field theory in terms of a subset of the gauge invariant variables in analogy to the construction for a single matrix model. We exhibit an emergent dimension and show that the Hamiltonian is local in this new dimension. We reproduce large N correlators of the tensor model quantum mechanics from the classical collective field theory. Finally, in section 6 we conclude and mention some possible directions for further investigation.

5.2 Construction of Gauge Invariant Operators

In this section we simply want to count the number of gauge invariant operators that can be constructed, for both bosonic and fermionic tensor models. Once we have understood how to count the number of gauge invariants, a natural construction formula will be evident.

The fields that we consider are tensors, of rank r. We will denote the bosonic tensors by $\phi_{b_1 b_2 \cdots b_r}$ and the fermionic tensors by $\psi_{f_1 f_2 \cdots f_r}$. These fields transform in the fundamental of $G = U(N_1) \times U(N_2) \times \cdots \times U(N_r)$.

Let V_k denote the vector space carrying a copy of the fundamental representation of $U(N_k)$. Fields transforming in the fundamental of $G = U(N_1) \times U(N_2) \times \cdots \times U(N_r)$ belong to $\mathcal{V} \equiv V_1 \times V_2 \times \cdots \times V_r$. To build gauge invariants we will also need fields that transform in the anti-fundamental, denoted $\bar{\phi}^{b_1 b_2 \cdots b_r}$ and $\bar{\psi}^{f_1 f_2 \cdots f_r}$. Gauge invariants are then given by contracting corresponding upper and lower indices. The valid gauge invariants, built using two fields, are given by

$$\bar{\phi}^{b_1 b_2 \cdots b_r} \phi_{b_1 b_2 \cdots b_r} \qquad \bar{\psi}^{f_1 f_2 \cdots f_r} \psi_{f_1 f_2 \cdots f_r} \tag{5.2.0.1}$$

The operators that follow are not observables because they are not gauge invariant

$$\bar{\phi}^{b_1 b_2 \cdots b_r} \phi_{b_2 b_1 \cdots b_r} \qquad \bar{\psi}^{f_1 f_2 f_3 \cdots f_r} \psi_{f_1 f_3 f_2 \cdots f_r} \tag{5.2.0.2}$$

A valid gauge invariant operator is only obtained if we contract corresponding indices of the tensors, since the position of an index signifies which gauge group it belongs to. To simplify the arguments that follow, we now specialize to rank 3 tensors ϕ_{ijk} or ψ_{ijk} with $i = 1, ..., N_1$, $j = 1, ..., N_2$ and $k = 1, ..., N_3$. The generalization to higher rank tensors is completely clear. A comment is in order: the symmetry $U(N) \times U(N) \times U(N)$ can not be realized in any interacting theory, whose large N expansion is dominated by melonic diagrams. The maximal symmetry in this case is only $U(N) \times U(N) \times O(N)$.

We will want to consider products of tensors to build the general gauge invariant operator. Here is an example

$$\phi_{i_1 j_1 k_1} \phi_{i_2 j_2 k_2} \cdots \phi_{i_n j_n k_n} \tag{5.2.0.3}$$

This notation will quickly get out of hand, as the number of indices rapidly proliferates. To avoid this, we will now use the notation first introduced in [122, 123]. The sleek notation uses a capital Roman letter to collect all of the little Roman letter indices, for example I stands for

$i_1, i_2, \cdots, i_n$. We will also use a capital Greek letter to collect the tensors. Thus, for example, we write

$$\Phi_{IJK} = \phi_{i_1 j_1 k_1} \phi_{i_2 j_2 k_2} \cdots \phi_{i_n j_n k_n} \tag{5.2.0.4}$$

Similarly

$$\Psi_{IJK} = \psi_{i_1 j_1 k_1} \psi_{i_2 j_2 k_2} \cdots \psi_{i_n j_n k_n} \tag{5.2.0.5}$$

These fields belong to $\mathcal{V}^{\otimes n}$. There is a natural action of S_n on $\mathcal{V}^{\otimes n}$ defined as follows: For any $\sigma \in S_n$ we have

$$\sigma \cdot \Phi_{IJK} \to \Phi_{\sigma(I)\sigma(J)\sigma(K)} = \phi_{i_{\sigma(1)} j_{\sigma(1)} k_{\sigma(1)}} \phi_{i_{\sigma(2)} j_{\sigma(2)} k_{\sigma(2)}} \cdots \phi_{i_{\sigma(n)} j_{\sigma(n)} k_{\sigma(n)}} \tag{5.2.0.6}$$

We will sometimes call this the diagonal action of S_n since each type of index, i, j or k is permuted in exactly the same way. We could also define an action of $S_n \times S_n \times S_n$ that acts independently on these three indices. The notation distinguishing these two actions is

$$\sigma \cdot \Phi_{IJK} \to \Phi_{\sigma(I)\sigma(J)\sigma(K)} \qquad \sigma \in S_n \tag{5.2.0.7}$$

versus

$$\sigma_1 \circ \sigma_2 \circ \sigma_3 \cdot \Phi_{IJK} \to \Phi_{\sigma_1(I)\sigma_2(J)\sigma_3(K)} \qquad \sigma_1 \circ \sigma_2 \circ \sigma_3 \in S_n \times S_n \times S_n \tag{5.2.0.8}$$

Since the diagonal action swaps the tensors we have

$$\sigma \cdot \Phi_{IJK} = \Phi_{\sigma(I)\sigma(J)\sigma(K)} = \Phi_{IJK} \tag{5.2.0.9}$$

$$\sigma \cdot \Psi_{IJK} = \Psi_{\sigma(I)\sigma(J)\sigma(K)} = \mathrm{sgn}(\sigma) \Psi_{IJK} \tag{5.2.0.10}$$

We know that swapping fermions costs a sign which is what the above equation captures. In the last formula above $\mathrm{sgn}(\sigma)$ denotes the signature of the permutation σ. For example, if $n = 2$ and $\sigma = (12)$ we have

$$\begin{aligned} (12)\psi_{i_1 j_1 k_1} \psi_{i_2 j_2 k_2} &= \psi_{i_2 j_2 k_2} \psi_{i_1 j_1 k_1} \\ &= -\psi_{i_1 j_1 k_1} \psi_{i_2 j_2 k_2} \\ &= \mathrm{sgn}\,(\,(12)\,)\, \psi_{i_1 j_1 k_1} \psi_{i_2 j_2 k_2} \end{aligned} \tag{5.2.0.11}$$

since the fermions are described using Grassman numbers. The equations (5.2.0.9),(5.2.0.10) will be important in the next section.

5.2.1 Counting and construction for bosonic tensors

Our goal in this section is to count the number of gauge invariant operators that can be constructed from the bosonic tensors introduced above. To construct gauge invariants we need to completely contract the indices of Φ_{IJK} with the indices of $\bar{\Phi}^{IJK}$. In general, this

is accomplished using three permutations $\sigma_1, \sigma_2, \sigma_3 \in S_n$ (or equivalently, one permutation $\sigma_1 \circ \sigma_2 \circ \sigma_3 \in S_n \times S_n \times S_n$) as follows

$$\bar{\Phi} \cdot \sigma_1 \circ \sigma_2 \circ \sigma_3 \cdot \Phi = \bar{\Phi}^{IJK} \Phi_{\sigma_1(I)\sigma_2(J)\sigma_3(K)} \tag{5.2.1.1}$$

The invariants given in equation (5.2.1.1) are over complete: the ϕ's and $\bar{\phi}$'s are bosons, so we have the symmetry given in (5.2.0.9) which must be accounted for. Let $\beta_1 \in S_n$ be an arbitrary permutation of the ϕ's and let $\beta_2 \in S_n$ be an arbitrary permutation of the $\bar{\phi}$'s. Then (we act to the right if we act on lower indices and to the left if we act on upper indices)

$$\bar{\Phi} \cdot \sigma_1 \circ \sigma_2 \circ \sigma_3 \cdot \Phi = (\bar{\Phi} \cdot \beta_2) \cdot \sigma_1 \circ \sigma_2 \circ \sigma_3 \cdot (\beta_1 \cdot \Phi) \tag{5.2.1.2}$$

Manipulating this a little, we have[28]

$$\begin{aligned} \Phi_{\sigma_1(I)\sigma_2(J)\sigma_3(K)} \bar{\Phi}^{IJK} &= \Phi_{\sigma_1(\beta_1(I))\sigma_2(\beta_1(J))\sigma_3(\beta_1(K))} \bar{\Phi}^{\beta_2(I)\beta_2(J)\beta_2(K)} \\ &= \Phi_{\beta_2^{-1}(\sigma_1(\beta_1(I)))\beta_2^{-1}(\sigma_2(\beta_1(J)))\beta_2^{-1}(\sigma_3(\beta_1(K)))} \bar{\Phi}^{IJK} \end{aligned} \tag{5.2.1.3}$$

Thus, $(\sigma_1, \sigma_2, \sigma_3)$ and $(\beta_1\sigma_1\beta_2, \beta_1\sigma_2\beta_2, \beta_1\sigma_3\beta_2)$ define the same gauge invariant operator. This implies that we have one gauge invariant operator for each element in the double coset

$$S_n \setminus S_n \times S_n \times S_n / S_n \tag{5.2.1.4}$$

This understanding of the structure of the space of gauge invariant observables was first achieved in [136]. The generalization to other ranks is obvious. For example, rank 5 tensors would be elements of the coset

$$S_n \setminus S_n \times S_n \times S_n \times S_n \times S_n / S_n \tag{5.2.1.5}$$

The number of elements in a double coset $|H_1 \setminus G / H_2|$ is given, by Burnside's Lemma, as

$$|H_1 \setminus G / H_2| = \frac{1}{|H_1||H_2|} \sum_{h_1 \in H_1} \sum_{h_2 \in H_2} \sum_{g \in G} \delta(h_1 g h_2 g^{-1}) \tag{5.2.1.6}$$

Thus, for example, the number $\mathcal{N}_3$ of rank 3 tensors built using n fields is given by

$$\mathcal{N}_3 = \frac{1}{(n!)^2} \sum_{\sigma_1,\sigma_2,\sigma_3 \in S_n} \sum_{\beta_1,\beta_2 \in S_n} \delta(\beta_1\sigma_1\beta_2\sigma_1^{-1}) \delta(\beta_1\sigma_2\beta_2\sigma_2^{-1}) \delta(\beta_1\sigma_3\beta_2\sigma_3^{-1}) \tag{5.2.1.7}$$

To make sure the generalization is clear, we simply quote the count for the number of rank q tensors built using n fields

$$\mathcal{N}_q = \frac{1}{(n!)^2} \sum_{\sigma_1,\cdots,\sigma_q \in S_n} \sum_{\beta_1,\beta_2 \in S_n} \prod_{i=1}^{q} \delta(\beta_1\sigma_i\beta_2\sigma_i^{-1}) \tag{5.2.1.8}$$

The arguments we have just outlined are not the most natural when we generalize to fermionic tensors. To perform the counting in a way that will generalize nicely to the fermionic case, we will change basis. The operators

$$\mathcal{O}(\sigma_1, \sigma_2, \sigma_3) = \bar{\Phi} \cdot \sigma_1 \circ \sigma_2 \circ \sigma_3 \cdot \Phi \tag{5.2.1.9}$$

[28] A useful identity to keep in mind is the following: $\bar{\Phi}^{\gamma^{-1}(K)} \Phi_K = \bar{\Phi}^K \Phi_{\gamma(K)}$. This follows very simply by using the explicit representation $(\sigma)^I_J = \delta^{i_1}_{j_{\sigma(1)}} \cdots \delta^{i_n}_{j_{\sigma(n)}}$.

define the "permutation basis". We will Fourier transform to the representation theory basis as follows

$$(\mathcal{O}_{r_1,r_2,r_3})_{\alpha_1\alpha_2\alpha_3,\beta_1\beta_2\beta_3} = \sum_{\sigma_1,\sigma_2,\sigma_2} \mathcal{O}(\sigma_1,\sigma_2,\sigma_3)\Gamma^{r_1}{}_{\alpha_1\beta_1}(\sigma_1)\Gamma^{r_2}{}_{\alpha_2\beta_2}(\sigma_2)\Gamma^{r_3}{}_{\alpha_3\beta_3}(\sigma_3) \tag{5.2.1.10}$$

All of the representations above are irreducible representations of S_n, i.e. $r_i \vdash n$, $i = 1, 2, 3$. We again have to deal with the symmetry present as a consequence of (5.2.0.9). The simplest way to do this is to couple the row indices to the trivial irreducible representation and to couple the column indices to the trivial irreducible representation of the diagonal S_n. The tensor product of the irreducible representations involved is

$$V_{r_1} \otimes V_{r_2} \otimes V_{r_3} = \bigoplus_r g_{r_1\, r_2\, r_3\, r} V_r \tag{5.2.1.11}$$

The Kronecker coefficients $g_{r_1\, r_2\, r_3\, r}$ are non-negative integers that count how many times irreducible representation r appears in the tensor product $r_1 \otimes r_2 \otimes r_3$. To perform the projection to the trivial, introduce the branching coefficients $B^{\gamma}_{\alpha_1\alpha_2\alpha_3}$ defined by

$$\frac{1}{n!}\sum_{\sigma\in S_n} \Gamma^{r_1}{}_{\alpha_1\beta_1}(\sigma)\Gamma^{r_2}{}_{\alpha_2\beta_2}(\sigma)\Gamma^{r_3}{}_{\alpha_3\beta_3}(\sigma) = \sum_{\gamma} B^{\gamma}_{\alpha_1\alpha_2\alpha_3}B^{\gamma}_{\beta_1\beta_2\beta_3} \tag{5.2.1.12}$$

The branching coefficients provide an orthonormal basis for the subspace of $r_1 \otimes r_2 \otimes r_3$ that carries the trivial representation, i.e.

$$B^{\gamma_1}_{\alpha_1\alpha_2\alpha_3}B^{\gamma_2}_{\alpha_1\alpha_2\alpha_3} = \delta^{\gamma_1\gamma_2} \tag{5.2.1.13}$$

and where we employ the usual convention that repeated indices are summed. The gauge invariant operators are now given by

$$\mathcal{O}^{\gamma_1\gamma_2}_{r_1,r_2,r_3} = B^{\gamma_1}_{\alpha_1\alpha_2\alpha_3}(\mathcal{O}_{r_1,r_2,r_3})_{\alpha_1\alpha_2\alpha_3,\beta_1\beta_2\beta_3}B^{\gamma_2}_{\beta_1\beta_2\beta_3} \tag{5.2.1.14}$$

We will also write this as

$$\mathcal{O}^{\gamma_1\gamma_2}_{r_1,r_2,r_3} = \sum_{\sigma_1\in S_n}\sum_{\sigma_2\in S_n}\sum_{\sigma_3\in S_n} C^{\gamma_1\gamma_2}_{r_1,r_2,r_3}(\sigma_1,\sigma_2,\sigma_3)\mathcal{O}(\sigma_1,\sigma_2,\sigma_3) \tag{5.2.1.15}$$

where

$$C^{\gamma_1\gamma_2}_{r_1,r_2,r_3}(\sigma_1,\sigma_2,\sigma_3) = B^{\gamma_1}_{\alpha_1\alpha_2\alpha_3}\Gamma^{r_1}{}_{\alpha_1\beta_1}(\sigma_1)\Gamma^{r_2}{}_{\alpha_2\beta_2}(\sigma_2)\Gamma^{r_3}{}_{\alpha_3\beta_3}(\sigma_3)B^{\gamma_2}_{\beta_1\beta_2\beta_3} \tag{5.2.1.16}$$

is in fact a restricted character, in the language introduced in [62],[141]. Thus, (5.2.1.15) provides the restricted Schur polynomial basis for the gauge invariant operators of the bosonic tensor model.

Since each multiplicity runs from 1 to $g_{r_1\, r_2\, r_3\, 1}$ and each operator is labeled by a pair of multiplicity labels, this second construction shows that the number of gauge invariant operators, constructed using n ϕ's and n $\bar{\phi}$'s, is given by

$$\sum_{r_i\vdash n\ l(r_i)\leq N_i} g^2_{r_1\, r_2\, r_3\, 1} \tag{5.2.1.17}$$

where we have used 1 to denote the rep labeled by a Young diagram with a single row of n boxes. This is in complete agreement with [140], as already pointed out in [139]. A standard result which follows from the orthogonality of characters is

$$g_{r_1\, r_2\, r_3\, 1} = \frac{1}{n!}\sum_{\sigma\in S_n}\chi_{r_1}(\sigma)\chi_{r_2}(\sigma)\chi_{r_3}(\sigma) = g_{r_1\, r_2\, r_3} \tag{5.2.1.18}$$

Some checks of the counting formula (5.2.1.17) are given in Appendix J.

5.2.2 Counting and construction for fermionic tensors

Our goal in this section is to count the number of gauge invariant operators that can be constructed from the fermionic tensors introduced above. To construct gauge invariants we need to completely contract the indices of Ψ_{IJK} with the indices of $\bar{\Psi}^{IJK}$. In general, this is again accomplished using three permutations $\sigma_1, \sigma_2, \sigma_3 \in S_n$ (or equivalently $\sigma_1\circ\sigma_2\circ\sigma_3 \in S_n\times S_n\times S_n$) as follows

$$\bar{\Psi}\ \cdot\ \sigma_1\circ\sigma_2\circ\sigma_3\ \cdot\ \Psi = \bar{\Psi}^{IJK}\Psi_{\sigma_1(I)\sigma_2(J)\sigma_3(K)} \tag{5.2.2.1}$$

The invariants given in equation (5.2.2.1) are again over complete: the ψ's and $\bar{\psi}$'s are fermions, so we have the symmetry given in (5.2.0.10) which must be accounted for. Following our discussion for the bosons, let $\beta_1 \in S_n$ be an arbitrary permutation of the ψ's and let $\beta_2 \in S_n$ be an arbitrary permutation of the $\bar{\psi}$'s. Then (exactly as for bosonic tensors, we act to the right if we act on lower indices and to the left, if we act on upper indices)

$$\bar{\Psi}\ \cdot\ \sigma_1\circ\sigma_2\circ\sigma_3\ \cdot\ \Psi = \mathrm{sgn}(\beta_1)\mathrm{sgn}(\beta_2)(\bar{\Psi}\cdot\beta_2)\ \cdot\ \sigma_1\circ\sigma_2\circ\sigma_3\ \cdot\ (\beta_1\cdot\Psi) \tag{5.2.2.2}$$

Manipulating this a little, we have

$$\begin{aligned}\Psi_{\sigma_1(I)\sigma_2(J)\sigma_3(K)}\bar{\Psi}^{IJK} &= \mathrm{sgn}(\beta_1)\mathrm{sgn}(\beta_2)\Psi_{\sigma_1(\beta_1(I))\sigma_2(\beta_1(J))\sigma_3(\beta_1(K))}\bar{\Psi}^{\beta_2(I)\beta_2(J)\beta_2(K)}\\ &= \mathrm{sgn}(\beta_1)\mathrm{sgn}(\beta_2)\Psi_{\beta_2^{-1}(\sigma_1(\beta_1(I)))\beta_2^{-1}(\sigma_2(\beta_1(J)))\beta_2^{-1}(\sigma_3(\beta_1(K)))}\bar{\Psi}^{IJK}\end{aligned} \tag{5.2.2.3}$$

We will still have to account for this symmetry. To do this, it again proves useful to change basis. The operators

$$\mathcal{P}(\sigma_1,\sigma_2,\sigma_3) = \bar{\Psi}\ \cdot\ \sigma_1\circ\sigma_2\circ\sigma_3\ \cdot\ \Psi \tag{5.2.2.4}$$

define the "permutation basis". Again, Fourier transform to the representation theory basis as follows

$$(\mathcal{P}_{r_1,r_2,r_3})_{\alpha_1\alpha_2\alpha_3,\beta_1\beta_2\beta_3} =$$

$$\sum_{\sigma_1,\sigma_2,\sigma_2}\mathcal{P}(\sigma_1,\sigma_2,\sigma_3)\Gamma^{r_1}{}_{\alpha_1\beta_1}(\sigma_1)\Gamma^{r_2}{}_{\alpha_2\beta_2}(\sigma_2)\Gamma^{r_3}{}_{\alpha_3\beta_3}(\sigma_3) \tag{5.2.2.5}$$

We now have to deal with the symmetry present as a consequence of (5.2.0.10). The simplest way to do this is to couple the row indices to the antisymmetric irreducible representation and to couple the column indices to the antisymmetric irreducible representation of the diagonal S_n. By the antisymmetric irreducible representation, (denoted (1^n)) we mean the irreducible representation labeled by a Young diagram that has a single column of n boxes. This is a one dimensional representation defined by

$$\Gamma^{(1^n)}(\sigma) = \mathrm{sgn}(\sigma) \tag{5.2.2.6}$$

To perform the projection to the antisymmetric irreducible representation, we again introduce branching coefficients

$$\frac{1}{n!}\sum_{\sigma\in S_n}\Gamma^{r_1}{}_{\alpha_1\beta_1}(\sigma)\Gamma^{r_2}{}_{\alpha_2\beta_2}(\sigma)\Gamma^{r_3}{}_{\alpha_3\beta_3}(\sigma)\mathrm{sgn}(\sigma) = \sum_{\gamma}\tilde{B}^{\gamma}_{\alpha_1\alpha_2\alpha_3}\tilde{B}^{\gamma}_{\beta_1\beta_2\beta_3} \tag{5.2.2.7}$$

We are using a tilde to distinguish the branching coefficients defined using the antisymmetric irreducible representation, from those relevant for the bosons which are defined using the symmetric representation. The branching coefficients again define an orthonormal basis

$$\tilde{B}^{\gamma_1}_{\alpha_1\alpha_2\alpha_3}\tilde{B}^{\gamma_2}_{\alpha_1\alpha_2\alpha_3} = \delta^{\gamma_1\gamma_2} \tag{5.2.2.8}$$

The gauge invariant operators are now given by

$$\mathcal{P}^{\gamma_1\gamma_2}_{r_1,r_2,r_3} = \tilde{B}^{\gamma_1}_{\alpha_1\alpha_2\alpha_3}(\mathcal{P}_{r_1,r_2,r_3})_{\alpha_1\alpha_2\alpha_3,\beta_1\beta_2\beta_3}\tilde{B}^{\gamma_2}_{\beta_1\beta_2\beta_3} \tag{5.2.2.9}$$

Once again, we can write this as

$$\mathcal{P}^{\gamma_1\gamma_2}_{r_1,r_2,r_3} = \sum_{\sigma_1\in S_n}\sum_{\sigma_2\in S_n}\sum_{\sigma_3\in S_n}\tilde{C}^{\gamma_1\gamma_2}_{r_1,r_2,r_3}(\sigma_1,\sigma_2,\sigma_3)\mathcal{P}(\sigma_1,\sigma_2,\sigma_3) \tag{5.2.2.10}$$

where

$$\tilde{C}^{\gamma_1\gamma_2}_{r_1,r_2,r_3}(\sigma_1,\sigma_2,\sigma_3) = \tilde{B}^{\gamma_1}_{\alpha_1\alpha_2\alpha_3}\Gamma^{r_1}{}_{\alpha_1\beta_1}(\sigma_1)\Gamma^{r_2}{}_{\alpha_2\beta_2}(\sigma_2)\Gamma^{r_3}{}_{\alpha_3\beta_3}(\sigma_3)\tilde{B}^{\gamma_2}_{\beta_1\beta_2\beta_3} \tag{5.2.2.11}$$

is again a restricted character. Thus, (5.2.2.10) provides the restricted Schur polynomial basis for the gauge invariant operators of the fermionic tensor model.

This construction shows that the number of gauge invariant operators is given by

$$\sum_{r_i\vdash n\ l(r_i)\leq N_i} g^2_{r_1\,r_2\,r_3\,(1^n)} \tag{5.2.2.12}$$

A standard result which follows from the orthogonality of characters is

$$g_{r_1\,r_2\,r_3\,(1^n)} = \frac{1}{n!}\sum_{\sigma\in S_n}\chi_{r_1}(\sigma)\chi_{r_2}(\sigma)\chi_{r_3}(\sigma)\mathrm{sgn}(\sigma) \tag{5.2.2.13}$$

Some checks of this counting formula are given in Appendix J.

5.3 Correlators of Gauge Invariant Operators

In this section we will compute the correlation functions of the operators defined in the previous section. Since these operators are neutral under the gauge symmetry they can develop a nonzero vacuum expectation value. It is interesting to compute these values as their large N limit must be reproduced by the classical equations of motion of collective field theory. We also compute the two point functions of normal ordered gauge invariant operators. The large N limit of these two point functions must be reproduced by considering quadratic fluctuations about the classical collective configuration.

5.3.1 Bosonic Correlators

The free field two point function is

$$\langle \bar{\phi}^{ijk} \phi_{lmn} \rangle = \delta^i_l \delta^j_m \delta^k_n \tag{5.3.1.1}$$

This is valid both as a formula in a zero dimensional random tensor model, or as an equal time two point function in the tensor model quantum mechanics. Wick's theorem can be written as

$$\begin{aligned} \langle \bar{\Phi}^{IJK} \Phi_{LMN} \rangle &= \sum_{\sigma \in S_n} \prod_{a=1}^{n} \delta^{i_a}_{l_{\sigma(a)}} \delta^{j_a}_{m_{\sigma(a)}} \delta^{k_a}_{n_{\sigma(a)}} \\ &= \sum_{\sigma \in S_n} (\sigma)^I_L (\sigma)^J_M (\sigma)^K_N \end{aligned} \tag{5.3.1.2}$$

There are two interesting correlators to consider: first we could consider the one point functions $\langle \mathcal{O}^{\gamma_1\gamma_2}_{r_1,r_2,r_3} \rangle$; second we could consider the two point function of normal ordered operators $\langle : \mathcal{O}^{\gamma_1\gamma_2}_{r_1 r_2 r_3} :: \mathcal{O}^{\gamma_3\gamma_4}_{s_1 s_2 s_3} : \rangle$.

One point functions: We will use the fact that

$$\mathrm{Tr}_{V_j}(\sigma) = \delta^{i_1}_{i_{\sigma(1)}} \cdots \delta^{i_n}_{i_{\sigma(n)}} = N_j^{C(\sigma)} \tag{5.3.1.3}$$

where $C(\sigma)$ denotes the number of cycles in the permutation σ. In addition, we will use the orthogonality relation

$$\frac{d_r}{n!} \sum_{\sigma \in S_n} \Gamma_r(\sigma)_{ab} \Gamma_s(\sigma^{-1})_{cd} = \delta_{rs} \delta_{bc} \delta_{ad} \tag{5.3.1.4}$$

to obtain

$$\frac{d_r}{n!} \sum_{s \vdash n} \sum_{\sigma_1 \in S_n} \Gamma_r(\sigma_1)_{cd} \chi_s(\sigma \sigma_1^{-1}) = \Gamma_r(\sigma)_{cd} \tag{5.3.1.5}$$

Finally, we will use the relation, valid for Schur polynomials

$$\mathrm{Tr}(\sigma Z) = \sum_R \chi_R(\sigma) \chi_R(Z) \tag{5.3.1.6}$$

evaluated at $Z = 1$ to find

$$\mathrm{Tr}(\sigma) = \frac{1}{n!}\sum_{R\vdash n} d_R \chi_R(\sigma) f_R(N) \tag{5.3.1.7}$$

$f_R(N)$ is the product of the factors of Young diagram R understood as a representation of $U(N)$. Recall that the factor of a box in row i and column j is $N - i + j$. We use $\chi_R(\sigma)$ to denote a character of the symmetric group and $\chi_R(Z)$ to denote a Schur polynomial. The two are distinguished only by their argument, which is either an element of the symmetric group $\sigma \in S_n$ or an $N \times N$ matrix Z. We are now ready to compute the one point function

$$\begin{aligned}
\langle \mathcal{O}^{\gamma_1\gamma_2}_{r_1r_2r_3}\rangle &= \sum_{\sigma_i\in S_n} \langle \bar\Phi\cdot\sigma_1\circ\sigma_2\circ\sigma_3\cdot\Phi\rangle B^{\gamma_1}\Gamma_{r_1}(\sigma_1)\Gamma_{r_2}(\sigma_2)\Gamma_{r_3}(\sigma_3)B^{\gamma_2}\\
&= \sum_{\sigma,\sigma_i\in S_n} N_1^{C(\sigma\sigma_1)}N_2^{C(\sigma\sigma_2)}N_3^{C(\sigma\sigma_3)} B^{\gamma_1}\Gamma_{r_1}(\sigma_1)\Gamma_{r_2}(\sigma_2)\Gamma_{r_3}(\sigma_3)B^{\gamma_2}\\
&= \sum_{\sigma,\sigma_i\in S_n}\sum_{s_i\vdash n}\left(\frac{1}{n!}\right)^3 d_{s_1}\chi_{s_1}(\sigma\sigma_1^{-1})f_{s_1}(N_1) d_{s_2}\chi_{s_2}(\sigma\sigma_2^{-1})f_{s_2}(N_2)\\
&\quad d_{s_3}\chi_{s_3}(\sigma\sigma_3^{-1})f_{s_3}(N_3) B^{\gamma_1}\Gamma_{r_1}(\sigma_1)\Gamma_{r_2}(\sigma_2)\Gamma_{r_3}(\sigma_3)B^{\gamma_2}\\
&= \sum_{\sigma\in S_n} f_{r_1}(N_1)f_{r_2}(N_2)f_{r_3}(N_3) B^{\gamma_1}\Gamma_{r_1}(\sigma)\Gamma_{r_2}(\sigma)\Gamma_{r_3}(\sigma)B^{\gamma_2}\\
&= n! f_{r_1}(N_1)f_{r_2}(N_2)f_{r_3}(N_3)\delta^{\gamma_1\gamma_2}
\end{aligned} \tag{5.3.1.8}$$

See Appendix K for some checks of this formula.

Two point functions of normal ordered operators: Using the identities given above, it is straightforward to compute

$$\begin{aligned}
&\langle :\mathcal{O}^{\gamma_1\gamma_2}_{r_1r_2r_3}:: \mathcal{O}^{\gamma_3\gamma_4}_{s_1s_2s_3}:\rangle = \sum_{\sigma\in S_n}\sum_{\rho\in S_n}\sum_{\sigma_i\in S_n}\sum_{\tau_i\in S_n}\mathrm{Tr}(\sigma_1\sigma\tau_1\rho)\mathrm{Tr}(\sigma_2\sigma\tau_2\rho)\mathrm{Tr}(\sigma_3\sigma\tau_3\rho)\\
&\times B^{\gamma_1}\Gamma_{r_1}(\sigma_1)\Gamma_{r_2}(\sigma_2)\Gamma_{r_3}(\sigma_3)B^{\gamma_2}\ B^{\gamma_3}\Gamma_{s_1}(\tau_1)\Gamma_{s_2}(\tau_2)\Gamma_{s_3}(\tau_3)B^{\gamma_4}\\
&= \sum_{\sigma\rho\sigma_i\tau_i} N^{C(\sigma_1\sigma\tau_1\rho)}N^{C(\sigma_2\sigma\tau_2\rho)}N^{(\sigma_3\sigma\tau_3\rho)}\\
&\times B^{\gamma_1}\Gamma_{r_1}(\sigma_1)\Gamma_{r_2}(\sigma_2)\Gamma_{r_3}(\sigma_3)B^{\gamma_2}\ B^{\gamma_3}\Gamma_{s_1}(\tau_1)\Gamma_{s_2}(\tau_2)\Gamma_{s_3}(\tau_3)B^{\gamma_4}\\
&= \sum_{\sigma\rho\sigma_i\tau_i}\sum_{t_i\vdash n}\left(\frac{1}{n!}\right)^3 d_{t_1}\chi_{t_1}(\sigma_1\sigma\tau_1\rho)f_{t_1}(N_1) d_{t_2}\chi_{t_2}(\sigma_2\sigma\tau_2\rho)f_{t_2}(N_2) d_{t_3}\chi_{t_3}(\sigma_3\sigma\tau_3\rho)f_{t_3}(N_3)\\
&\times B^{\gamma_1}\Gamma_{r_1}(\sigma_1)\Gamma_{r_2}(\sigma_2)\Gamma_{r_3}(\sigma_3)B^{\gamma_2}\ B^{\gamma_3}\Gamma_{s_1}(\tau_1)\Gamma_{s_2}(\tau_2)\Gamma_{s_3}(\tau_3)B^{\gamma_4}\\
&= (n!)^2\delta_{r_1s_1}\delta_{r_2s_2}\delta_{r_3s_3}f_{r_1}(N_1)f_{r_2}(N_2)f_{r_3}(N_3)\frac{n!}{d_{r_1}}\frac{n!}{d_{r_2}}\frac{n!}{d_{r_3}}\delta^{\gamma_1\gamma_4}\delta^{\gamma_2\gamma_3}
\end{aligned} \tag{5.3.1.9}$$

Some checks of this formula are given in Appendix K.

5.3.2 Fermionic Correlators

The relevant two point function for the fermionic tensor model is

$$\langle \bar{\psi}^{ijk} \psi_{lmn} \rangle = \delta^i_l \delta^j_m \delta^k_n \tag{5.3.2.1}$$

This is valid, as for the bosons, both as a formula in a zero dimensional random tensor model, or as an equal time two point function in the tensor model quantum mechanics. Since the fermionic fields anticommute, it is important to spell out the ordering of the fields. Order the fields in the following way

$$\bar{\Psi}^{IJK} \Psi_{LMN} = \bar{\psi}^{i_1 j_1 k_1} \bar{\psi}^{i_2 j_2 k_2} \dots \bar{\psi}^{i_n j_n k_n} \psi_{l_n m_n n_n} \cdots \psi_{l_2 m_2 n_2} \psi_{l_1 m_1 n_1} \tag{5.3.2.2}$$

With this ordering spelled out, a simple application of Wick's theorem now gives

$$\langle \bar{\psi}^{IJK} \psi_{LMN} \rangle = \sum_{\sigma \in S_n} \mathrm{sgn}(\sigma) \sigma^I_L \sigma^J_M \sigma^K_N \tag{5.3.2.3}$$

One point functions: A simple computation shows that

$$\begin{aligned}
\langle \mathcal{P}^{\gamma_1\gamma_2}_{r_1 r_2 r_3} \rangle &= \sum_{\sigma_i \in S_n} \langle \bar{\Psi} \cdot \sigma_1 \circ \sigma_2 \circ \sigma_3 \cdot \Psi \rangle \tilde{B}^{\gamma_1} \Gamma_{r_1}(\sigma_1) \Gamma_{r_2}(\sigma_2) \Gamma_{r_3}(\sigma_3) \tilde{B}^{\gamma_2} \\
&= \sum_{\sigma, \sigma_i \in S_n} \mathrm{sgn}(\sigma) N_1^{C(\sigma\sigma_1)} N_2^{C(\sigma\sigma_2)} N_3^{C(\sigma\sigma_3)} \tilde{B}^{\gamma_1} \Gamma_{r_1}(\sigma_1) \Gamma_{r_2}(\sigma_2) \Gamma_{r_3}(\sigma_3) \tilde{B}^{\gamma_2} \\
&= \sum_{\sigma \in S_n} \mathrm{sgn}(\sigma) f_{r_1}(N_1) f_{r_2}(N_2) f_{r_3}(N_3) \tilde{B}^{\gamma_1} \Gamma_{r_1}(\sigma) \Gamma_{r_2}(\sigma) \Gamma_{r_3}(\sigma) \tilde{B}^{\gamma_2} \\
&= n! f_{r_1}(N_1) f_{r_2}(N_2) f_{r_3}(N_3) \delta^{\gamma_1\gamma_2}
\end{aligned} \tag{5.3.2.4}$$

See Appendix K for examples and checks of this formula.

Two point functions of normal ordered operators: Using the identities given above

$$\begin{aligned}
&\langle : \mathcal{P}^{\gamma_1\gamma_2}_{r_1 r_2 r_3} :: \mathcal{P}^{\gamma_3\gamma_4}_{s_1 s_2 s_3} : \rangle = \sum_{\sigma \in S_n} \sum_{\rho \in S_n} \sum_{\sigma_i \in S_n} \sum_{\tau_i \in S_n} \mathrm{sgn}(\sigma)\mathrm{sgn}(\rho) \mathrm{Tr}(\sigma_1 \sigma \tau_1 \rho) \mathrm{Tr}(\sigma_2 \sigma \tau_2 \rho) \mathrm{Tr}(\sigma_3 \sigma \tau_3 \rho) \\
&\times \tilde{B}^{\gamma_1} \Gamma_{r_1}(\sigma_1) \Gamma_{r_2}(\sigma_2) \Gamma_{r_3}(\sigma_3) \tilde{B}^{\gamma_2} \ \tilde{B}^{\gamma_3} \Gamma_{s_1}(\tau_1) \Gamma_{s_2}(\tau_2) \Gamma_{s_3}(\tau_3) \tilde{B}^{\gamma_4} \\
&= \sum_{\sigma \rho \sigma_i \tau_i} \mathrm{sgn}(\sigma)\mathrm{sgn}(\rho) N^{C(\sigma_1 \sigma \tau_1 \rho)} N^{C(\sigma_2 \sigma \tau_2 \rho)} N^{(\sigma_3 \sigma \tau_3 \rho)} \\
&\times \tilde{B}^{\gamma_1} \Gamma_{r_1}(\sigma_1) \Gamma_{r_2}(\sigma_2) \Gamma_{r_3}(\sigma_3) \tilde{B}^{\gamma_2} \ \tilde{B}^{\gamma_3} \Gamma_{s_1}(\tau_1) \Gamma_{s_2}(\tau_2) \Gamma_{s_3}(\tau_3) \tilde{B}^{\gamma_4} \\
&= (n!)^2 \delta_{r_1 s_1} \delta_{r_2 s_2} \delta_{r_3 s_3} f_{r_1}(N_1) f_{r_2}(N_2) f_{r_3}(N_3) \frac{n!}{d_{r_1}} \frac{n!}{d_{r_2}} \frac{n!}{d_{r_3}} \delta^{\gamma_1\gamma_4} \delta^{\gamma_2\gamma_3}
\end{aligned} \tag{5.3.2.5}$$

Appendix K illustrates and checks this formula in some simple cases.

5.4 Algebra of the Gauge Invariant Operators

The gauge invariant operators that we have introduced above close an interesting algebra: we will argue that the gauge invariant operators have a ring structure. Algebras of gauge invariant operators have also been considered in [142]. To develop the algebra for our tensor model, we will need to develop some properties of the restricted character. We can always assume that we work in an orthogonal representation of the symmetric group. In this case the restricted characters obey

$$C^{\gamma_1\gamma_2}_{r_1r_2r_3}(\sigma_1,\sigma_2,\sigma_3) = C^{\gamma_2\gamma_1}_{r_1r_2r_3}(\sigma_1^{-1},\sigma_2^{-1},\sigma_3^{-1})$$
$$\tilde{C}^{\gamma_1\gamma_2}_{r_1r_2r_3}(\sigma_1,\sigma_2,\sigma_3) = \tilde{C}^{\gamma_2\gamma_1}_{r_1r_2r_3}(\sigma_1^{-1},\sigma_2^{-1},\sigma_3^{-1}) \tag{5.4.1}$$

They also enjoy a "completeness identity" given by

$$\sum_{\sigma_1\in S_n}\sum_{\sigma_2\in S_n}\sum_{\sigma_3\in S_n} C^{\gamma_1\gamma_2}_{r_1r_2r_3}(\sigma_1,\sigma_2,\sigma_3)C^{\gamma_3\gamma_4}_{s_1s_2s_3}(\sigma_1,\sigma_2,\sigma_3) = \frac{n!}{d_{r_1}}\frac{n!}{d_{r_2}}\frac{n!}{d_{r_3}}\delta_{r_1s_1}\delta_{r_2s_2}\delta_{r_3s_3}\delta^{\gamma_1\gamma_3}\delta^{\gamma_2\gamma_4}$$
$$\sum_{\sigma_1\in S_n}\sum_{\sigma_2\in S_n}\sum_{\sigma_3\in S_n} \tilde{C}^{\gamma_1\gamma_2}_{r_1r_2r_3}(\sigma_1,\sigma_2,\sigma_3)\tilde{C}^{\gamma_3\gamma_4}_{s_1s_2s_3}(\sigma_1,\sigma_2,\sigma_3) = \frac{n!}{d_{r_1}}\frac{n!}{d_{r_2}}\frac{n!}{d_{r_3}}\delta_{r_1s_1}\delta_{r_2s_2}\delta_{r_3s_3}\delta^{\gamma_1\gamma_3}\delta^{\gamma_2\gamma_4} \tag{5.4.2}$$

Using these formulas, we find the following interesting Fourier transform pairs

$$\mathcal{O}^{\gamma_1\gamma_2}_{r_1r_2r_3} = \sum_{\sigma_1\in S_n}\sum_{\sigma_2\in S_n}\sum_{\sigma_3\in S_n} C^{\gamma_1\gamma_2}_{r_1r_2r_3}(\sigma_1,\sigma_2,\sigma_3)\mathcal{O}(\sigma_1,\sigma_2,\sigma_3) \tag{5.4.3}$$

$$\mathcal{O}(\sigma_1,\sigma_2,\sigma_3) = \sum_{s_1\vdash n}\sum_{s_2\vdash n}\sum_{s_3\vdash n}\sum_{\gamma_1,\gamma_2}\frac{d_{s_1}}{n!}\frac{d_{s_2}}{n!}\frac{d_{s_3}}{n!}C^{\gamma_1\gamma_2}_{s_1s_2s_3}(\sigma_1,\sigma_2,\sigma_3)\mathcal{O}^{\gamma_1\gamma_2}_{s_1s_2s_3} \tag{5.4.4}$$

$$\mathcal{P}^{\gamma_1\gamma_2}_{r_1r_2r_3} = \sum_{\sigma_1\in S_n}\sum_{\sigma_2\in S_n}\sum_{\sigma_3\in S_n} \tilde{C}^{\gamma_1\gamma_2}_{r_1r_2r_3}(\sigma_1,\sigma_2,\sigma_3)\mathcal{P}(\sigma_1,\sigma_2,\sigma_3) \tag{5.4.5}$$

$$\mathcal{P}(\sigma_1,\sigma_2,\sigma_3) = \sum_{s_1\vdash n}\sum_{s_2\vdash n}\sum_{s_3\vdash n}\sum_{\gamma_1,\gamma_2}\frac{d_{s_1}}{n!}\frac{d_{s_2}}{n!}\frac{d_{s_3}}{n!}\tilde{C}^{\gamma_1\gamma_2}_{s_1s_2s_3}(\sigma_1,\sigma_2,\sigma_3)\mathcal{P}^{\gamma_1\gamma_2}_{s_1s_2s_3} \tag{5.4.6}$$

These formulas provide the clearest way to understand the relation between the permutation and representation theory bases.

Now, in the permutation basis the gauge invariant operators close the following algebra

$$\mathcal{O}(\sigma_1,\sigma_2,\sigma_3)\mathcal{O}(\rho_1,\rho_2,\rho_3) = \mathcal{O}(\sigma_1\circ\rho_1,\sigma_2\circ\rho_2,\sigma_3\circ\rho_3) \tag{5.4.7}$$

$$\mathcal{P}(\sigma_1,\sigma_2,\sigma_3)\mathcal{P}(\rho_1,\rho_2,\rho_3) = \mathcal{P}(\sigma_1\circ\rho_1,\sigma_2\circ\rho_2,\sigma_3\circ\rho_3) \tag{5.4.8}$$

where $\sigma_i \in S_n$ and $\rho_i \in S_m$ for $i = 1, 2, 3$. Note that thanks to the way that we have ordered the fermions there are no -1 factors in this second equation.

We can now work out the details of this algebra in the representation basis. A straightforward computation shows

$$\mathcal{O}^{\gamma_1\gamma_2}_{r_1r_2r_3}\mathcal{O}^{\gamma_3\gamma_4}_{s_1s_2s_3} = \sum_{t_1\vdash n+m}\sum_{t_2\vdash n+m}\sum_{t_3\vdash n+m}\sum_{\gamma_5\gamma_6} f^{t_1t_2t_3;\gamma_1\gamma_2\gamma_3\gamma_4}_{r_1r_2r_3s_1s_2s_3;\gamma_5\gamma_6}\mathcal{O}^{\gamma_5\gamma_6}_{t_1t_2t_3} \tag{5.4.9}$$

where $r_i \vdash n$ and $s_i \vdash m$ for $i = 1, 2, 3$. The structure constants for this algebra are given by

$$\begin{aligned} f^{t_1t_2t_3;\gamma_1\gamma_2\gamma_3\gamma_4}_{r_1r_2r_3s_1s_2s_3;\gamma_5\gamma_6} &= \frac{d_{t_1}}{(n+m)!}\frac{d_{t_2}}{(n+m)!}\frac{d_{t_3}}{(n+m)!}\sum_{\sigma_1\in S_n}\sum_{\sigma_2\in S_n}\sum_{\sigma_3\in S_n}\sum_{\rho_1\in S_m}\sum_{\rho_2\in S_m}\sum_{\rho_3\in S_m} \\ &C^{\gamma_1\gamma_2}_{r_1r_2r_3}(\sigma_1,\sigma_2,\sigma_3)C^{\gamma_3\gamma_4}_{s_1s_2s_3}(\rho_1,\rho_2,\rho_3)C^{\gamma_5\gamma_6}_{t_1t_2t_3}(\sigma_1\circ\rho_1,\sigma_2\circ\rho_2,\sigma_3\circ\rho_2) \\ &= \frac{d_{t_1}n!m!}{(n+m)!d_{r_1}d_{s_1}}\frac{d_{t_2}n!m!}{(n+m)!d_{r_2}d_{s_2}}\frac{d_{t_3}n!m!}{(n+m)!d_{r_3}d_{s_3}}B^{\gamma_1}_a\circ B^{\gamma_3}_b B^{\gamma_5}_{ab}\;\; B^{\gamma_6}_{cd}B^{\gamma_2}_c\circ B^{\gamma_4}_d \end{aligned} \tag{5.4.10}$$

To get to the last line above, we have simply performed the sum over the σ_i and the ρ_i using the orthogonality relation (5.3.1.4). Remarkably, the structure constants are simply related to overlaps between branching coefficients! Computing these overlaps is a well defined problem in the representation theory of the symmetric group. Notice also that the structure constant, up to an overall factor, factorizes into a product of two overlaps of branching coefficients.

There is a similar algebra for the fermionic operators

$$\mathcal{P}^{\gamma_1\gamma_2}_{r_1r_2r_3}\mathcal{P}^{\gamma_3\gamma_4}_{s_1s_2s_3} = \sum_{t_1\vdash n+m}\sum_{t_2\vdash n+m}\sum_{t_3\vdash n+m}\sum_{\gamma_5\gamma_6} g^{t_1t_2t_3;\gamma_1\gamma_2\gamma_3\gamma_4}_{r_1r_2r_3s_1s_2s_3;\gamma_5\gamma_6}\mathcal{P}^{\gamma_5\gamma_6}_{t_1t_2t_3} \tag{5.4.11}$$

where the structure constants for this algebra are given by

$$\begin{aligned} g^{t_1t_2t_3;\gamma_1\gamma_2\gamma_3\gamma_4}_{r_1r_2r_3s_1s_2s_3;\gamma_5\gamma_6} &= \frac{d_{t_1}}{(n+m)!}\frac{d_{t_2}}{(n+m)!}\frac{d_{t_3}}{(n+m)!}\sum_{\sigma_1\in S_n}\sum_{\sigma_2\in S_n}\sum_{\sigma_3\in S_n}\sum_{\rho_1\in S_m}\sum_{\rho_2\in S_m}\sum_{\rho_3\in S_m} \\ &\tilde{C}^{\gamma_1\gamma_2}_{r_1r_2r_3}(\sigma_1,\sigma_2,\sigma_3)\tilde{C}^{\gamma_3\gamma_4}_{s_1s_2s_3}(\rho_1,\rho_2,\rho_3)\tilde{C}^{\gamma_5\gamma_6}_{t_1t_2t_3}(\sigma_1\circ\rho_1,\sigma_2\circ\rho_2,\sigma_3\circ\rho_2) \\ &= \frac{d_{t_1}n!m!}{(n+m)!d_{r_1}d_{s_1}}\frac{d_{t_2}n!m!}{(n+m)!d_{r_2}d_{s_2}}\frac{d_{t_3}n!m!}{(n+m)!d_{r_3}d_{s_3}}\tilde{B}^{\gamma_1}_a\circ\tilde{B}^{\gamma_3}_b\tilde{B}^{\gamma_5}_{ab}\;\;\tilde{B}^{\gamma_6}_{cd}\tilde{B}^{\gamma_2}_c\circ\tilde{B}^{\gamma_4}_d \end{aligned} \tag{5.4.12}$$

Again, the structure constants are simply related to overlaps between branching coefficients.

The existence of an algebraic structure for the gauge invariant operators has a remarkable consequence: we are able to solve the free theory exactly. To make this point, write the algebraic structure in a condensed notation as follows

$$\mathcal{O}^A\mathcal{O}^B = f^{AB}_C\mathcal{O}^C \tag{5.4.13}$$

with repeated indices summed. At the risk of being pedantic, A stands for two multiplicity labels (γ_1, γ_2 say) and three Young diagrams (r_1, r_2, r_3 say). Using this product repeatedly we find

$$\langle\mathcal{O}^{A_1}\mathcal{O}^{A_2}\mathcal{O}^{A_3}\cdots\mathcal{O}^{A_n}\rangle = f^{A_1A_2}_{C_1}f^{C_1A_3}_{C_2}\cdots f^{C_{n-2}A_n}_{C_{n-1}}\langle\mathcal{O}^{C_{n-1}}\rangle \tag{5.4.14}$$

so that the computation of an n-point correlation function is reduced to the computation of a one point function. We have already computed the most general one point function in the previous section. Of course, the structure constants of the algebra need to be evaluated and this is non-trivial. However, it does mean that the problem of solving the free tensor model has been reduced entirely to a problem in S_n representation theory. This simplification is highly non-trivial. There is a completely parallel argument for the fermionic tensor model.

5.5 Collective Field Theory

We have now constructed the complete set of gauge invariant variables and an algebra that these gauge invariants close. In this section we would like to construct a (collective) field theory governing the dynamics of these variables. Our discussion is guided by the dynamics of a single hermitian matrix $X = X^\dagger$ and we will review some relevant background before we consider the collective field theory relevant for the tensor model.

A complete set of gauge invariant variables for the one matrix model is provided by the Schur polynomials[143]

$$\chi_R(X) = \frac{1}{n!}\sum_{\sigma\in S_n}\chi_R(\sigma)\mathrm{Tr}(\sigma X) \tag{5.5.1}$$

These variables again close an interesting algebra, given by

$$\chi_R(X)\chi_S(X) = \sum_T g_{RST}\chi_T(X) \tag{5.5.2}$$

where g_{RST} are the Littlewood-Richardson coefficients. If we tried to quantize the Schur polynomial variables, it would be a mistake to treat them as independent, as the above algebra proves. In the case of a single matrix it is clear how we should proceed: one can select a smaller set of variables that are independent

$$\phi_n = \mathrm{Tr}(X^n) \tag{5.5.3}$$

where we should restrict $n \leq N$. The complete set of gauge invariant variables, the Schur polynomials, are polynomials in the ϕ_n. This is an important point: the ϕ_n are the set of variables that are independent and by considering polynomials in these variables, we recover the complete set of gauge invariant operators. In the large N limit, it is sensible to simply ignore the constraint $n \leq N$[120, 121]. We can then consider the field

$$\phi_k = \mathrm{Tr}(e^{ikX}) \tag{5.5.4}$$

or its Fourier transform, $\phi(x)$. The dynamics of this field, which is local in the emergent dimension x, is captured in the Das-Jevicki-Sakita Hamiltonian[120, 121, 56].

We now want to explore the possibility that there is a similar description possible for tensor models. Our first task is to identify the smaller set of independent variables which are independent and which we will quantize. Further, by considering polynomials in these variables, we should reconstruct the complete set of gauge invariant operators.

It proves convenient to work in the permutation basis

$$\bar{\Phi} \cdot \sigma_1 \circ \sigma_2 \circ \sigma_3 \cdot \Phi = \bar{\Phi}^{IJK} \Phi_{\sigma_1(I)\sigma_2(J)\sigma_3(K)} \tag{5.5.5}$$

These invariants were first counted by Geloun and Ramgoolam in [136]. They have identified the number of invariants with the series A110143 on the OEIS website. This sequence counts the number of orbits obtained when S_n acts on $S_n \times S_n$ via conjugacy, i.e. for $g \in S_n$ and $(x, y) \in S_n \times S_n$ we have $g(x, y) = (gxg^{-1}, gyg^{-1})$. The number of invariants grows extremely rapidly

$$1, 4, 11, 43, 161, 901, 5579, 43206, 378360, 3742738, ... \tag{5.5.6}$$

A useful way to label the invariants, following [136], is by bipartite cubic graphs with edges labeled by the gauge group the corresponding index belongs to.

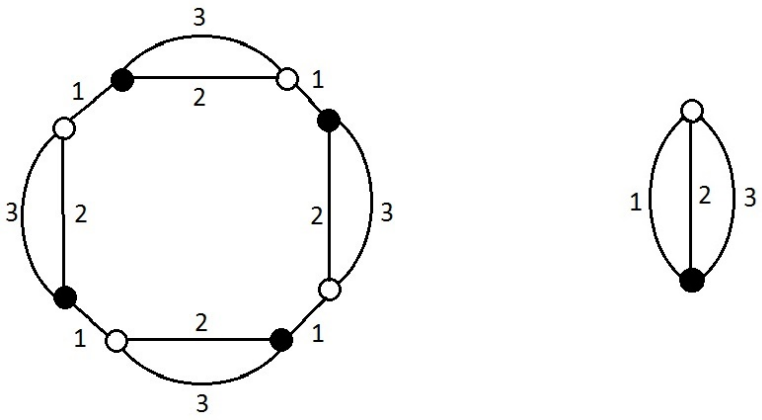


Figure 14: The above figures label gauge invariant operators in the tensor model gauge theory. Black dots correspond to $\bar{\phi}^{ijk}$'s and white dots to ϕ_{ijk}s. A line labeled by i is a gauge index for $U(N_i)$. The operator on the left corresponds to $\bar{\phi}^{i_1 j_1 k_1} \phi_{i_2 j_1 k_1} \bar{\phi}^{i_2 j_2 k_2} \phi_{i_3 j_2 k_2} \bar{\phi}^{i_3 j_3 k_3} \phi_{i_4 j_3 k_3} \bar{\phi}^{i_4 j_4 k_4} \phi_{i_1 j_4 k_4}$ and the operator on the right corresponds to $\bar{\phi}^{ijk} \phi_{ijk}$.

In the language of graphs it is easy to identify the smaller set of independent variables: they are the variables that correspond to connected graphs. The number of connected graphs can be counted using the plethystic logarithm and is identified with the series A057005 on the OEIS website[136]. The number of independent variables still grows extremely rapidly

$$1, 3, 7, 26, 97, 624, 4163, 34470, 314493, 3202839, 35704007, 433460014, ... \tag{5.5.7}$$

This growth seems to be too rapid to manage. We will now argue that we can restrict the dynamics to an even smaller set of variables. To describe the smaller set of variables, it is useful to consider

$$T^{i_1}{}_{i_2} = \bar{\phi}^{i_1 jk} \phi_{i_2 jk} \tag{5.5.8}$$

T is a matrix on the vector space that carries the fundamental of $U(N_1)$. It thus makes sense to take powers of T

$$(T^n)^{i_1}{}_{i_2} = T^{i_1}{}_j T^j{}_k \cdots T^l{}_{i_2} \tag{5.5.9}$$

The smaller set of gauge invariants that we consider is given by

$$\phi_n = \mathrm{Tr}(T^n) \tag{5.5.10}$$

The Hamiltonian of the tensor model quantum mechanics we consider is given by

$$H = -\frac{\partial}{\partial \bar{\phi}^{ijk}} \frac{\partial}{\partial \phi_{ijk}} + \frac{1}{4} \bar{\phi}^{ijk} \phi_{ijk} \tag{5.5.11}$$

The coefficient of the second term has been chosen to ensure that the equal time two point function is given by (5.3.1.1). The kinetic terms of the Hamiltonian, when rewritten in terms of the new (collective) variables are

$$-\frac{\partial}{\partial \bar{\phi}^{ijk}} \frac{\partial}{\partial \phi_{ijk}} = -\sum_{n,m} \Omega(n,m) \frac{\partial}{\partial \phi_n} \frac{\partial}{\partial \phi_m} + \sum_n \omega(n) \frac{\partial}{\partial \phi_n} \tag{5.5.12}$$

where[29]

$$\Omega(n,m) = \frac{\partial \phi_n}{\partial \bar{\phi}^{ijk}} \frac{\partial \phi_m}{\partial \phi_{ijk}} = nm\phi_{n+m-1} \tag{5.5.13}$$

$$\omega(n) = -\frac{\partial}{\partial \bar{\phi}^{ijk}} \left(\frac{\partial \phi_n}{\partial \phi_{ijk}} \right) = -\sum_{r=0}^{n-2} \phi_r \phi_{n-r-1} - N_2 N_3 m \phi_{m-1} \tag{5.5.14}$$

It is nontrivial that $\Omega(n,m)$ and $\omega(n)$ can be expressed in terms of the ϕ_n. This implies that the Hamiltonian itself can be expressed in terms of this smaller set of variables, and hence that it is consistent with the dynamics to restrict to this smaller set of variables. When written in terms of the new variables, the Hamiltonian

$$H = -\sum_{n,m} \Omega(n,m) \frac{\partial}{\partial \phi_n} \frac{\partial}{\partial \phi_m} + \sum_n \omega(n) \frac{\partial}{\partial \phi_n} + \frac{1}{4} \phi_1 \tag{5.5.15}$$

is not hermitian. This simply reflects the fact that in the new variables the inner product is accompanied by a non-trivial Jacobian $J[\phi]$. Performing a similarity transformation to trivialize the measure, we arrive at a manifestly hermitian Hamiltonian[120, 121, 56]

$$H = \Pi \Omega \Pi + \frac{1}{4} \left(\omega + \frac{\partial \Omega}{\partial \phi} \right) \Omega^{-1} \left(\omega + \frac{\partial \Omega}{\partial \phi} \right) + \phi_1 - \frac{1}{2} \frac{\partial \omega}{\partial \phi} - \frac{1}{2} \frac{\partial^2 \Omega}{\partial \phi \partial \phi} \tag{5.5.16}$$

where we have used an obvious matrix notation and have introduced the momentum $\Pi(n)$ conjugate to ϕ_n

$$\Pi_n = -i \frac{\partial}{\partial \phi_n} \tag{5.5.17}$$

[29]Note that these expressions are almost identical to the answers for the Hermitian one matrix model which are $\Omega(n,m) = nm\phi_{n+m-2}$ and $\omega(n) = -\sum_{r=0}^{n-2} \phi_r \phi_{n-r-2}$.

As we have commented above, the variables ϕ_n that we have employed in the description so far are a natural generalization of the variables (5.5.3) used in the matrix model. The variables (5.5.3) are essentially the eigenvalues of the matrix model, so that it is natural to interpret the gauge invariant variables constructed out of $T^i{}_j$ as providing an eigenvalue like description of the tensor model. Just as in the matrix case, the quantum mechanical system develops an extra dimension. To see how this happens, we can explore the range of the eigenvalues of T. In the case of a single matrix, the change to eigenvalues induces a Van der Monde determinant which produces a repulsion between the eigenvalues ensuring they spread out to produce a macroscopic emergent geometry at large N. To get some insight into what is happening in the case of the tensor model, we compute the one point functions

$$\langle \mathrm{Tr}(T^k)\rangle = \langle \bar\Phi \cdot (k) \circ \mathbf{1} \circ \mathbf{1} \cdot \Phi\rangle = \sum_{\sigma\in S_k} N_1^{C((k)\sigma)} N_2^{C(\sigma)} N_3^{C(\sigma)} \tag{5.5.18}$$

In the above (k) is a k-cycle which, for concreteness, we take to be $(123\cdots k)$. Lets study the limit that $N_i \to \infty$ holding $\frac{N_2}{N_3}$ fixed and taking $\alpha = \frac{N_2 N_3}{N_1}$ fixed. In this large N_i limit the above sum is then dominated by a nontrivial class of diagrams. For example

$$\begin{aligned}
\langle \mathrm{Tr}(T)\rangle &= N_1N_2N_3 = \alpha N_1^2 \\
\langle \mathrm{Tr}(T^2)\rangle &= N_1^2N_2N_3 + N_1N_2^2N_3^2 = (\alpha+\alpha^2)N_1^3 \\
\langle \mathrm{Tr}(T^3)\rangle &= N_1^3N_2N_3 + 3N_1^2N_2^2N_3^2 + N_1N_2^3N_3^3 + N_1N_2N_3 \\
&= (\alpha + 3\alpha^2 + \alpha^3 + \frac{\alpha}{N_1^2})N_1^4 \\
\langle \mathrm{Tr}(T^4)\rangle &= N_1^4N_2N_3 + 6N_1^3N_2^2N_3^2 + 6N_1^2N_2^3N_3^3 + N_1N_2^4N_3^4 + 5N_1^2N_2N_3 + 5N_1N_2^2N_3^2 \\
&= N_1^5\left(\alpha + 6\alpha^2 + 6\alpha^3 + \alpha^4 + \frac{5\alpha}{N^2} + \frac{5\alpha^2}{N^2}\right) \\
\langle \mathrm{Tr}(T^5)\rangle &= N_1^5N_2N_3 + 10N_1^4N_2^2N_3^2 + 20N_1^3N_2^3N_3^3 + 10N_1^2N_2^4N_3^4 + N_1N_2^5N_3^5 \\
&\quad +15N_1^3N_2N_3 + 40N_1^2N_2^2N_3^2 + 15N_1N_2^3N_3^3 + 8N_1N_2N_3 \\
&= N_1^6\Big(\alpha + 10\alpha^2 + 20\alpha^3 + 10\alpha^4 + \alpha^5 + \frac{15\alpha + 40\alpha^2 + 15\alpha^3}{N_1^2} + 8\frac{\alpha}{N_1^4}\Big) \\
\langle \mathrm{Tr}(T^k)\rangle &\sim N_1^{k+1}
\end{aligned} \tag{5.5.19}$$

The growth with k as N_1^{k+1} is a clear indication that the eigenvalues of T are spreading out and are potentially able to generate a new dimension. To construct the field theory in this extra dimension, it is useful to introduce the field

$$\phi(x) = \int \frac{dk}{2\pi}\, e^{-ikx}\, \phi_k \qquad \phi_k = \mathrm{Tr}(e^{ikT}) \tag{5.5.20}$$

Notice that $\phi(x)$ is nothing but the density of eigenvalues of the T matrix and consequently

$$\mathrm{Tr}(T^n) = \int dx \phi(x) x^n \tag{5.5.21}$$

The momentum dual to $\phi(x)$ is $\pi(x) = \frac{1}{i}\frac{\delta}{\delta\phi(x)}$ and similarly $\pi_k = \frac{1}{i}\frac{\delta}{\delta\phi_k}$. To perform the change of variables, note that the kinetic terms in the tensor model Hamiltonian can be written as

$$-\frac{\partial}{\partial\bar\phi^{ijk}}\frac{\partial}{\partial\phi_{ijk}} = -T^i{}_l \frac{\partial}{\partial T^j{}_l}\frac{\partial}{\partial T^i{}_j} - N_2N_3\frac{\partial}{\partial T^i{}_i}$$

$$= -\int dk \int dk' \; \Omega_{k,k'} \, \pi_k \, \pi_{k'} + \int dk \; \omega_k \, \pi_k \tag{5.5.22}$$

where

$$\begin{aligned} \Omega_{k,k'} &= T^i{}_l \frac{\partial \phi_k}{\partial T^j{}_l} \frac{\partial \phi_{k'}}{\partial T^i{}_j} = -kk' \mathrm{Tr}(T \, e^{i(k+k')T}) \\ &= ikk' \frac{\partial}{\partial k} \phi_{k+k'} \end{aligned} \tag{5.5.23}$$

and

$$\begin{aligned} \omega_k &= -T^i{}_l \frac{\partial}{\partial T^j{}_l} \left(\frac{\partial \phi_k}{\partial T^i{}_j} \right) - N_2 N_3 \frac{\partial \phi_k}{\partial T^i{}_i} \\ &= k \int_0^1 d\tau \; \phi_{\tau k} i \frac{\partial}{\partial \tau} \phi_{(1-\tau)k} - ikN_2N_3\phi_k \end{aligned} \tag{5.5.24}$$

To obtain these results, we have used the formula

$$\frac{\partial}{\partial M^i{}_j} (e^{-ikM})^k_l = (-ik) \int_0^1 d\tau (e^{-i\tau kM})^k{}_i (e^{-i(1-\tau)kM})^j{}_l \tag{5.5.25}$$

In position space we obtain

$$\Omega(x,x') = \frac{\partial}{\partial x} \frac{\partial}{\partial x'} \left(x\phi(x)\delta(x-x') \right) \tag{5.5.26}$$

and

$$\omega(x) = 2 \frac{\partial}{\partial x} \fint dy \; \phi(x)\phi(y) \frac{x}{x-y} + (N_2N_3 - N_1) \frac{\partial \phi(x)}{\partial x} \tag{5.5.27}$$

It is interesting to note that the formula for $\Omega(x,x')$ is identical to the formula obtained from the radial sector of multi matrix models, and that the formula for $\omega(x)$ is very similar - see [25, 27, 28, 29]. This easily leads to the following Hamiltonian (we have dropped constant terms)

$$\begin{aligned} H &= \int dx \left[\frac{\partial \pi}{\partial x} \, x\phi(x) \, \frac{\partial \pi}{\partial x} + \frac{\phi(x)}{4x} \left(\fint dy \; \frac{2x\phi(y)}{x-y} \right)^2 + \frac{(N_2N_3 - N_1)^2}{4x} \phi(x) + \frac{x}{4}\phi(x) \right] \\ &\quad -\mu \int dx \, \phi(x) \end{aligned} \tag{5.5.28}$$

where the last term above enforces the constraint $\int dx \phi(x) = N_1$. To get this result, we used

$$\int dx \fint dy \, \phi(x)\phi(y) \frac{x+y}{x-y} = 0 \tag{5.5.29}$$

As we explain in Appendix L, the Hamiltonian can be written as

$$H = \int dx \frac{\partial \pi}{\partial x} x\phi(x) \frac{\partial \pi}{\partial x} + V_{\text{eff}} \tag{5.5.30}$$

where the effective potential is

$$V_{\text{eff}} = \int dx \left[\frac{\pi^2 x}{3}\phi^3 + \frac{(\alpha-1)^2 N_1^2}{4x}\phi(x) + \frac{x}{4}\phi(x) - \mu\phi(x) \right] \tag{5.5.31}$$

The classical field should minimize the effective potential, which leads to the following classical collective equation of motion

$$\begin{aligned} 0 = \frac{\delta V_{\text{eff}}}{\delta\phi(x)} &= \pi^2 x\phi^2 + \frac{(1-\alpha)^2 N_1^2}{4x} + \frac{x}{4} - \mu \\ \Rightarrow \phi(x) &= \frac{1}{\pi}\sqrt{\frac{\mu}{x} - \frac{1}{4} - \frac{(1-\alpha)^2 N_1^2}{4x^2}} \end{aligned} \tag{5.5.32}$$

The chemical potential μ should be fixed by requiring that

$$\int_{x_-}^{x_+} dx\phi(x) = N_1 \tag{5.5.33}$$

where the limits of integration are

$$x_\pm = 2\mu \pm \sqrt{4\mu^2 - N_1^2(1-\alpha)^2} \tag{5.5.34}$$

As a test of this classical solution, we would like to show that it reproduces the correct large N_1 correlators. To simplify the analysis that follows, we will set $\alpha = 1$. In this case, after solving for μ we have the density

$$\phi(x) = \frac{1}{\pi}\sqrt{\frac{N_1}{x} - \frac{1}{4}} \qquad x_+ = 4N_1 \quad x_- = 0 \tag{5.5.35}$$

A simple computation now gives

$$\begin{gathered} \int_0^{\frac{N_1}{4}} x\phi(x)dx = N_1^2 \qquad \int_0^{\frac{N_1}{4}} x^2\phi(x)dx = 2N_1^3 \\ \int_0^{\frac{N_1}{4}} x^3\phi(x)dx = 5N_1^4 \qquad \int_0^{\frac{N_1}{4}} x^4\phi(x)dx = 14N_1^5 \qquad \int_0^{\frac{N_1}{4}} x^5\phi(x)dx = 42N_1^6 \end{gathered} \tag{5.5.36}$$

in complete agreement with (5.5.19). This provides a nice test of classical collective solution.

5.6 Summary and Outlook

Motivated by the close connection of tensor models to the SYK model, we have considered the problem of counting and then constructing the gauge invariant operators of tensor models. Bosonic tensor models have already been considered in the literature, and the results we have obtained are consistent with what is already known. Our results for fermionic vector models are novel. Using the operators that have been constructed, we have exhibited an interesting algebra

underlying the gauge invariant operators of the tensor model: the gauge invariant operators define a ring. We have written closed formulas for the structure constants of this ring. As we have explained, this algebraic structure allows us to express arbitrary correlation functions as one point functions, which we have computed explicitly. Consequently, once the structure constants of the algebra are known, the free theory has been solved exactly. We have expressed these structure constants as overlaps of branching coefficients so that their computation is now a well defined problem in the representation theory of the symmetric group.

To study the large N dynamics of tensor model quantum mechanics we have identified a smaller set of gauge invariant operators that has lead to an eigenvalue like description. The system admits a collective field theory description which is similar but not identical to the collective field theory of a singe hermitian matrix. Our collective description shares all the good features of previous collective descriptions. Two such features are

1. The collective description manifests the fact that the tensor model quantum mechanics has emergent dimensions. Further, it is very attractive and highly non-trivial that the collective dynamics in this emergent dimension is local.

2. The loop expansion parameter of the collective field theory is not $\hbar$ of the quantum mechanics, but rather it is $\frac{1}{N_1}$ with N_1 set by the tensor model gauge group. Consequently the classical equations of motion of the collective field theory yield the answer obtained by summing the complete set of Feynman diagrams that contribute at large N_1. For our tensor model example we have explicitly demonstrated this.

The above two features are highly suggestive of holography, which claims that a local (at large N_1) higher dimensional classical system is dual to the large N limit of the gauge theory.

There are a number of future directions that should be pursued. The fermionic tensor model rather than the bosonic tensor model appears to be more relevant to the problem of understanding holography. It would be interesting to develop the collective field theory of the fermionic model. Specifically, it would be fascinating if such a description could be developed for the Witten-Gurau model, which is of most relevance for SYK. Perhaps the most interesting question to ask is if we can enlarge the space of gauge invariants to get a genuinely larger space than the loop space of a single matrix model, such that the enlarged space is still manageable? It seems that tensor models maybe good toy models with which to explore holography.

6 Conclusions

We have studied holography in a number of different settings. We looked at understanding the link between eigenvalue dynamics and supergravity in Chapter 3, focusing on the $SU(2)$ sector of $\mathcal{N} = 4$ SYM. We looked for new integrable subsectors of the CFT in Chapter 4 by attaching open string to LLM geometries and studying the emergent gauge theory. Lastly we looked at improving our understanding of the relationship between gravity and a strongly coupled CFT by studying the gauge invariants in tensor models in Chapter 5.

One of our primary goals in Chapter 3 was to show we could successfully describe a sector of the two matrix model with eigenvalue dynamics. The observables in this sector were the BPS operators. We found we were able to reproduce genuine multimatrix correlators, a non-trivial test that our eigenvalue prescription works. We studied the dual BPS geometries and attempted to extend the results of [12], who showed that the eigenvalues of the single matrix model condense on a surface that defines the boundary conditions for non-singular solutions. We were able to do this at large N. One of the key ideas used the restricted Schur polynomials to construct a free fermion wave function. The reduction to eigenvalues required the use of a non-trivial Jacobian. This wavefunction was essentially an educated guess and it would be insightful if we could derive this in future work. This would make the link between eigenvalue dynamics and supergravity geometries more complete.

In Chapter 4 we were looking to find new integrable subsectors of the CFT. We studied excitations of LLM geometries. Young diagrams were an important tool as they label the CFT operators but also have a natural identification in the dual theory. Excitations are Young diagrams added to a background Young diagram representing the LLM geometry. We argue these excitations are localised on the brane worldvolume and that they are open strings. This gives rise to an emergent gauge theory which is $\mathcal{N} = 4$ SYM with gauge group $U(N_{eff})$ in the planar limit. We showed this by matching the anomalous dimensions and OPE coefficients which vanish in the planar limit. An interesting question arises from this study which is whether the emergent gauge theory is dual to an $AdS_5 \times S^5$ geometry in some limit. This would provide evidence that there are new holographic dualities.

In Chapter 5 we tasked ourselves with the construction of the complete set of gauge invariant operators for fermionic and bosonic tensor models. The construction of these operators is important for our understanding of holography and tensor models themselves have found application in holography via the SYK model. The results we obtained for the bosonic model is consistent with the literature and is a good indication of the reliability of our results for the fermionic model. We were able to compute correlation functions by exploiting the algebraic structure of the operators. This means we can solve the free theory once we know the structure constants. At large N we constructed a collective description which has two features promising for holography. These were the fact that the emergent dimensions in the tensor model quantum mechanics became manifest and the dynamics there is local. Secondly, we showed that the loop expansion parameter is $\frac{1}{N_1}$ and not $\hbar$ which is what we have when we study gravity at strong coupling. This is originally what motivated studies of gauge invariant observables in a collective field theory.

A persistent theme in this thesis has been the identification of ways to simplify complicated questions. In doing so, we have been able to make definite statements and find compelling evidence to motivate further study. For example, our goal to find integrability beyond the planar limit by studying excitations of new geometries found traction in the organisation of operators in terms of background dependent and independent terms, which allowed us to treat certain excitations of new geometries as if they were excitations of the vacuum. This is unexpected: new geometry backgrounds should be much more complicated than the vacuum yet we are able to relate them. Another example was identifying a class of operators of the two matrix model whose correlation functions could be replicated with eigenvalue dynamics. Lastly, we studied tensor models instead of matrix models to further our understanding of gauge invariants and holography. The implications of such simplifications are not only technical. They pose deep questions about our understanding of holography.

These types of questions are as important as our results. Beyond a specialised research question, our goal is to understand quantum gravity which means we must understand holography. This is a long term project and so our research must bridge what we know with what we can learn. What we have seen is that there are many ways to approach the gauge/gravity duality. This thesis primarily develops the picture at large N in the CFT and uses the fact that the mapping between CFT operators and supergravity geometries is well understood. For future work it would strengthen our results and improve our understanding to construct the dual gravity argument for the work in Chapter 4: we could study new integrable subsectors in the gravity. The work in Chapter 3 supports the connection between eigenvalue dynamics and supergravity and motivates a study of more supergravity backgrounds to support the results and deepen our understanding. The results of Chapter 5 are highly suggestive of holography since the gravitational description that emerges at strong coupling for a CFT had $\frac{1}{N}$ as a loop counting parameter. It would be interesting to look at formulating the dynamics of the eigenvalue description in terms of the density of eigenvalues which would have $\frac{1}{N}$ as a coupling. The eigenvalue argument we have made is at weak coupling but work by Berenstein and collaborators makes for compelling evidence at strong coupling. It is insightful to note that the results in this thesis using eigenvalue dynamics is valid for correlators of operators dual to states of large energy. In this sense we find a course grained description unlike the work achieved in Chapter 4 which used excitations of low energy such that the planar limit of the emergent theory agrees with $\mathcal{N} = 4$ SYM. Finally this work looked at free, weak and strong coupling in the CFT.

The technical achievements of this thesis relied on the use of group representation theory. This allowed us to simplify computations but it also had a natural interpretation in terms of the gauge/gravity duality which comes from the Young diagram labelling. This is non-trivial and it would be worthwhile to pursue studies in holography with this in mind.

A Inequivalent, Irreducible Representations

For any group, there are a finite number of inequivalent irreducible representations (irreps). These representations are the building blocks of the representation theory of the group and any representation in the group can be built out of some combination of irreps. This is why they are useful to study. In general, there are an infinite number of representations of any group, $\mathcal{G}$, and we cannot hope to list all of them.

A matrix representation of $\mathcal{G}$ is a map, $\Gamma_R(\cdot)$, from $\mathcal{G}$ to the group of matrices $GL(n,\mathbb{R})$ or $GL(n,\mathbb{C})$ such that, for $\forall g_1, g_2 \in \mathcal{G}$, the following relation is satisfied.

$$\Gamma_R(g_1)\cdot\Gamma_R(g_2) = \Gamma_R(g_1\cdot g_2) \tag{A.1}$$

This means that group composition is realised as matrix multiplication of the representations. This ensures that multiplication of two or more group elements yields another element of the group (by the group composition axiom, $g_1\cdot g_2 \in \mathcal{G}$). When two representations are related by

$$\widetilde{\Gamma}_R(g) = M^{-1}\Gamma_R(g)M \tag{A.2}$$

we say that they are equivalent representations, for all $g\in\mathcal{G}$ and M is any invertible matrix. One can see that $\widetilde{\Gamma}_R(g)$ is indeed a representation of the group by checking it obeys (A.1), which it does. Since there are an infinite number of invertible matrices M, there are an infinite number of representations equivalent to the representation $\Gamma_R(g)$. We can shorten this list by considering only the inequivalent representations of a group. However, there are still an infinite number of these.

Similar matrices have the same eigenvalues. We could use this to check to see whether two representations are equivalent. However, finding the eigenvalues of a matrix is not a simple problem, especially for large matrices. Computing the trace of a matrix is a much simpler problem. However, two matrices having equal traces does not imply they have the same eigenvalues. What we can consider instead is $\Gamma^n_R(g)$. If this representation is a d dimensional matrix then

$$\mathrm{Tr}(\Gamma^n_R(g)) = \sum_{i=1}^{d}\lambda_i^n$$

where the λ_i are the eigenvalues of $\Gamma_R(g)$. Now if $\mathrm{Tr}(\Gamma^n_R(g)) = \mathrm{Tr}(\widetilde{\Gamma}^n_R(g))$ for all n, then $\Gamma_R(g)$ and $\widetilde{\Gamma}_R$ have the same eigenvalues. What we have shown is that if the set of matrices N_i (i can be any number larger than 1) are equivalently related to $\widetilde{N}_i$ by $\widetilde{N}_i = M^{-1}N_iM$, then they satisfy the condition $\mathrm{Tr}(N_i^n) = \mathrm{Tr}(\widetilde{N}_i^n)\ \ \forall n$. However, the converse is not necessarily true. This is because the invertible matrix M is arbitrary in this case (i.e.: can be a different invertible matrix for each N_i). If we want the converse statement to be true then we need to strengthen our condition for testing for equivalent matrices. Now we consider an arbitrary product of matrices. For example

$$\mathrm{Tr}([N_1N_2\ldots N_8]^n) = \mathrm{Tr}([\widetilde{N}_1\widetilde{N}_2\ldots\widetilde{N}_8]^n)$$

This condition needs M to be the same for each of the N_i equivalent to some $\widetilde{N}_i$. If these matrices are representations of a group, then we can use the defining equation of a representation (A.1)

to rewrite it in the more compact form

$$\mathrm{Tr}(\Gamma_R(g)) = \mathrm{Tr}(\widetilde{\Gamma}_R(g)) \tag{A.3}$$

This is the condition that tells us when two representations, $\Gamma_R(g)$ and $\widetilde{\Gamma}_R(g)$, are equivalent. The trace of the representation of a group is denoted by

$$\mathrm{Tr}(\Gamma_R(g)) \equiv \chi_R(g)$$

and is called the character of group element g in representation R. Finally, we can say that two representations are equivalent if they have the same character.

Two group elements, g_1 and g_2, have the same character when they obey the equivalence relation

$$g_1 = g^{-1} g_2 g$$

We say these group elements are conjugate. This equivalence relation partitions the group into conjugacy classes. All elements in the same conjugacy class then will have the same character.

We understand what it means for representations to be equivalent. Now we need to learn what it means for a representation to be reducible. Recall that we are looking for the inequivalent, irreducible representations as this list is finite. If a representation can be written as the direct sum of two other representations, then it is reducible. Any representation that is equivalent to a block diagonal representation is the direct sum of two other representations. Thus any representation that is equivalent to a block diagonal representation is called a reducible representation. This block diagonal representation has at least two invariant subspaces. Each block in the diagonal will act in a different subspace such that the subspaces are not mixed by the action of the group (so subspaces are invariant). An irreducible representation is one which has no invariant subspaces under the action of the group. The number of inequivalent, irreducible representations is equal to the number of conjugacy classes. This number is finite for finite groups.

B Symmetric group and Representation Theory

The symmetric group, S_n is a group of operations

$$S_n = \{g_1, g_2, \dots g_p\}$$

such that each g_i; $i = 1, \dots p$ is a permutation of any number of objects between 1 and n. The order of this group is $p = n!$. For example, the group S_2 has $2! = 2$ elements. There are two objects we can permute: we say these objects are 1 and 2. This is standard notation so whenever we talk about the symmetric group we are talking about permuting the numbers $1, \dots n$. The kinds of permutations we can write down for S_2 is the swap (12) (which is also its inverse) and the identity, $\mathbb{1} = (1)(2)$ – no swap. This notation is called cycle notation and it is spelled out for (12) as follows:

$$1 \to 2 \quad 2 \to 1$$

In cycle notation each object is followed by its image and the last object's image in a cycle is the first object. In S_3 we have the group element (123). This permutes all three objects such that

$$1 \to 2 \quad 2 \to 3 \quad 3 \to 1$$

This a cycle of length three. We can decompose this into a product of 2 cycles, $(\cdot\cdot)$, as follows

$$(123) = (12)(23)$$

We consider the right action of the group so that we read the right hand side of the above equation as (starting with 1)

$$1 \to 2 \quad 2 \to 3 \quad 3 \to 2 \to 1$$

Any k-cycle (a cycle of length k) can be decomposed into a product of 2-cycles (called transpositions) by noticing that

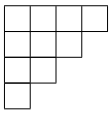
$$(g_1 g_2 \dots g_{n-1} g_n) = (g_1 g_2)(g_2 \dots g_n g_{n-1}) \tag{B.1}$$

and repeatedly applying it. Further, we can decompose any cycle into the the product of adjacent 2-cycles. This is a product of 2-cycles of the form $(p-1, p)$ where $p \leq n$ in S_n. For example, we can write the identity in S_2 as the product of an adjacent 2 cycle and its inverse $(12)(12) = \mathbb{1}$. We can see statement holds by using (B.1) and noting that any 2-cycle can be written as the product of adjacent transpositions. For example $(13) = (12)(23)(12)$. Later we will use this decomposition to form matrix representations of the action of group elements. These adjacent transpositions are sufficient to build the representation of the whole group because we can form any element in the group by taking the relevant product of a number of these adjacent transpositions.

Now that we have understood what is meant by cycle structure, we can introduce some new notation that will represent the cycle structure of group elements in S_n. These representations are partitions of n. That is, a set of positive integers $[n_1, n_2, \dots, n_k]$ such that $n_1 \geq n_2 \geq \dots \geq n_k$

and $n_1+n_2+\cdots+n_k = n$. By representing group elements in this way (by their cycle structure), we are partitioning the group and each partition has a finite number of group elements in it. Partitions are often visualised by Young diagrams.

Young diagrams of shape R consist of n boxes arranged in rows and columns. We say $R \vdash n$. The Young diagrams are left justified so that the number of boxes in each column is always greater than the number of boxes in the column to the right. Similarly, the number of boxes in each row is always greater than or equal to the number of boxes in the row beneath it. For example

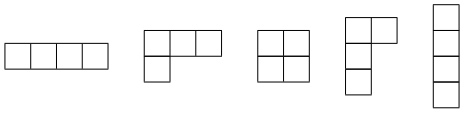


The first row has n_i boxes. Since $n_1 + n_2 + n_3 + n_4 = n$ we see that this Young diagram is representing a partition of a group element in S_{10}. So the number of boxes in the Young diagram tells us to which group the particular element represented belongs to. The structure of the Young diagram has a deeper interpretations as well. Each row represents a cycle in the group. The above Young diagram represents the cycle $(\cdot\cdot\cdot\cdot)(\cdot\cdot\cdot)(\cdot\,\cdot)(\cdot)$. So Young diagrams partition group elements according to their cycle structure. These partitions are called conjugacy classes.

Elements in the same conjugacy class $(g_1,\, g_2)$ obey the equivalence relation

$$g_1 = g^{-1} g_2 g$$

for any g in the same group. In the previous section, we saw that two group elements that are conjugate have the same character ($\chi_R(g) = \mathrm{Tr}(\Gamma_R(g))$. Young diagrams label representations of the symmetric group that are given by a set of matrices $\Gamma_R(g)$ that act on the vector space $V_R^{S_n}$. These representations are the inequivalent, irreducible representations of the group which we can see since they partition the group elements into conjugacy classes. For example, S_4 has the following possible Young diagrams:



So S_4 has five irreps or, equivalently, five conjugacy classes.

We can fill in the numbers $1, \ldots, n$ into the empty boxes of a Young diagram. The convention we use is that numbers in each row must decrease rightwards and numbers in each column must decrease downwards. By filling in the numbers $1, \ldots n$ into the empty boxes of a Young diagram, we form what is called a Young tableaux. When these label elements of a (complete) basis of $V_R^{S_n}$, they are called Young-Yamanouchi symbols. The number of Young-Yamanouchi states, $|R\rangle$, a representation, R, has is equal to the dimension of the Young diagram. In order to calculate the dimension of a Young diagram, we need to know two things. The first is the the number of boxes and the second is the hook lengths of each box. The hook length of a box x is calculated by drawing a horizontal line going rightwards from the box and a vertical line going downwards till the end of the Young diagram. The number of boxes these lines cross, including the starting box is the hook length. We denote the product of the hook lengths in

Young diagram R as $\prod_{x\in R}\text{hook}(x) \equiv \text{hooks}_R$. The dimension of a Young diagram is defined as

$$d_R = \frac{n!}{\text{hooks}_R} \tag{B.2}$$

For the Young diagram



the dimension is $d_R = \frac{4!}{4\cdot 2\cdot 1\cdot 1} = 3$. This means this representation has three associated Young-Yamanouchi states i.e.: we can fill the numbers 1, 2, 3 and 4 into the empty boxes in three ways:

$$|1\rangle = \begin{array}{|c|c|}\hline 4&3\\\hline 2\\\cline{1-1} 1\\\cline{1-1}\end{array}, \quad |2\rangle = \begin{array}{|c|c|}\hline 4&2\\\hline 3\\\cline{1-1} 1\\\cline{1-1}\end{array}, \quad |3\rangle = \begin{array}{|c|c|}\hline 4&1\\\hline 3\\\cline{1-1} 2\\\cline{1-1}\end{array} \tag{B.3}$$

We are almost ready to see how to calculate the matrix representations of elements in a group in a particular irrep. We now introduce the content of a box in Young diagram R. Each box x in row i and column j has content $c_x = j - i$. For example, consider the following Young diagram with contents filled in.

0	1	2	3
−1	0	1	
−2	−1		
−3			

Earlier we said we wanted to consider permutations which were a product of adjacent 2-cycles. We will consider the action of adjacent 2-cycles on our Young-Yamanouchi states. This sufficient because representations satisfy $\Gamma_R(g_1g_2) = \Gamma_R(g_1)\Gamma_R(g_2)$ where g_1 and g_2 are elements of the group. We will consider the action of $\Gamma_R(12)$ on the Young-Yamanouchi states given in (B.3). We denote the Young diagram after a swap, $(k, k+1)$, by $R_{(k,k+1)}$. Matrix elements of adjacent transpositions are specified by

$$\Gamma_R((k,k+1))|R\rangle = \frac{1}{c_k - c_{k+1}}|R\rangle + \sqrt{1 - \frac{1}{(c_k - c_{k+1})^2}}|R_{(k,k+1)}\rangle \tag{B.4}$$

Then

$$\begin{aligned}
\Gamma_{\begin{array}{|c|c|}\hline&\\\hline\\\cline{1-1}\\\cline{1-1}\end{array}}((12))|1\rangle &= -|1\rangle \\
\Gamma_{\begin{array}{|c|c|}\hline&\\\hline\\\cline{1-1}\\\cline{1-1}\end{array}}((12))|2\rangle &= -\frac{1}{3}|2\rangle + \frac{\sqrt{8}}{3}|3\rangle \\
\Gamma_{\begin{array}{|c|c|}\hline&\\\hline\\\cline{1-1}\\\cline{1-1}\end{array}}((12))|3\rangle &= |3\rangle + \frac{\sqrt{8}}{3}|2\rangle
\end{aligned}$$

which yields the matrix representation

$$\Gamma_R((12)) = \begin{pmatrix} -1 & 0 & 0 \\ 0 & -\frac{1}{3} & \frac{\sqrt{8}}{3} \\ 0 & \frac{\sqrt{8}}{3} & -\frac{1}{3} \end{pmatrix}$$

C Schur Polynomials

In [7], the exact two point function of Schur polynomials in the free field limit was calculated to be

$$\langle \chi_R(Z)\chi_S^\dagger(Z)\rangle = \delta_{RS} f_R \tag{C.1}$$

Since this correlator is diagonal in the Young diagram labels, it is only nonzero when $R = S$. The f_R denoted the products of weights in a Young diagram R. The weight of a box x is $N + j - i$. This is the content of a box x plus N. The result in [7] was obtained by exploiting the link between the symmetric group and the unitary group. The quantity f_R appears in the definition of the dimension of irreps of the unitary group:

$$Dim_R = \frac{f_R}{\text{hooks}_R}$$

This insight reduces our computations of Section 2.1.3 drastically. For example

$$\langle \chi_{\square\square}(Z)\chi_{\square\square}^\dagger(Z)\rangle = N(N+1)(N+2) \tag{C.2}$$

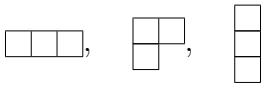
where

$$\chi_{\square\square}(Z) = \frac{1}{6}\left((\text{Tr}(Z))^3 + 3(\text{Tr}(z))(\text{Tr}(Z^2)) + 2\text{Tr}(Z^3)\right)$$

This demonstrates the effectiveness of this language to describe quantum gravity: it hints that we can study non-perturbative physics by summing all the ribbon graphs. In this section we define Schur polynomial labelled by Young diagram R and use it to reproduce (C.1).

We start off by making some comments about the unitary group, $U(N)$ since the action of our complex matrix model is invariant under the $U(N)$ symmetry. The irreps of $U(N)$ are labelled by Young diagrams. Unlike the symmetric group, S_n, where the number of boxes was restricted to n, the number of boxes in an irrep of $U(N)$ can have any number of boxes but the number of rows must be $\leq N$. There are many connections between $U(N)$ and S_n and these form what is known as the Schur-Weyl or Frobenius-Schur duality. States of $U(N)$ are labelled by Gelfan-Tsetlin patterns. This labelling chooses basis states that are simultaneous eigenstates of the matrix J_z. Thus, this basis is a natural choice for studying angular momentum. We will not go into details about the construction of these states but we note that they are related to Young diagrams in that they label states according to how they transform under a chain of subgroups.

Consider the vector space $V_N^{\otimes 3}$. The dimension of this vector space is N^3. There are three possible Young diagrams we can draw:



The dimensions of each of these in the S_n representation is 1, 2, 1 respectively and $\frac{N(N+1)(N+2)}{6}$, $\frac{N(N+1)(N-1)}{3}$, $\frac{N(N-1)(N-2)}{6}$ respectively. States are labelled by both the Young-Yamanouchi symbols and the Gelfand-Tsetlin patterns such that the total number of states is

$$1 \times \frac{N(N+1)(N+2)}{6} + 2 \times \frac{N(N+1)(N-1)}{3} + 1 \times \frac{N(N-1)(N-2)}{6} = N^3$$

as required. So the multiplicity of the $U(N)$ representations we obtain is organised by irreps of the symmetric group.
There are three operators we can construct for $n = 3$ and they are

$$\mathrm{Tr}(Z^3) \quad \mathrm{Tr}(Z^2)\mathrm{Tr}(Z) \quad \mathrm{Tr}(Z)^3$$

These operators are related to the shape of the Young diagrams. That is, they are related to the cycle structure of elements in S_n. For example, the 3-cycle is represented by $\square\square$ and corresponds to $\mathrm{Tr}(Z^3)$. The 2-cycle is represented by $\begin{smallmatrix}\square\square\\\square\end{smallmatrix}$ and corresponds to $\mathrm{Tr}(Z^2)\mathrm{Tr}(Z)$.

The Schur polynomial is defined as follows.

$$\chi_r(Z) \equiv \frac{1}{n!}\sum_{\sigma\in S_n}\chi_R(\sigma)Z^{i_1}_{i_{\sigma(1)}}Z^{i_2}_{i_{\sigma(2)}}\dots Z^{i_n}_{i_{\sigma(n)}} \tag{C.3}$$

Here R is a Young diagram of n boxes (labels an irrep pf the symmetric group), and $\chi_R(\sigma)$ is the character of $\sigma \in S_n$ in irrep R. The Schur polynomial $\chi_R(U)$ is the character of an element $U \in SU(N)$ in irrep R.

We can construct a projection operator onto an irrep R. This projector is defined as

$$P_R = \frac{1}{n!}\sum_{\sigma\in S_n}\chi_R(\sigma)\sigma \tag{C.4}$$

and $\mathrm{Tr}(P_R) = Dim_R$. We can rewrite our Schur polynomial in terms of this projection operator.

$$\begin{aligned}\chi_R(Z) &= \frac{1}{d_R}\left(\frac{d_R}{n!}\sum_{\sigma\in S_n}\chi_R(\sigma)\sigma Z^{i_1}_{i_{\sigma(1)}}Z^{i_2}_{i_{\sigma(2)}}\dots Z^{i_n}_{i_{\sigma(n)}}\right)\\ &= \frac{1}{d_R}\mathrm{Tr}\left(P_R Z^{\otimes n}\right)\end{aligned} \tag{C.5}$$

One last insight we need is that summing over the Wick contractions in a correlation function can be understood as the problem of summing over permutations. We have that

$$\langle Z^I_J(Z^\dagger)^K_L\rangle = \sum_{\sigma\in S_n}\sigma^I_L(\sigma^{-1})^K_J \tag{C.6}$$

This shorthand notation keeps track of the indices under matrix multiplication and can be expanded as $Z^I_J = Z^{i_1}_{j_1}Z^{i_2}_{j_2}\dots Z^{i_N}_{j_n}$ and similarly for the other matrices.

Now we are ready to show (C.1) holds.

$$\begin{aligned}
\langle \chi_R(Z)\chi^\dagger_Z(Z)\rangle &= \frac{1}{d_R d_S}(P_R)^I_J(P_S)^K_L\langle (Z^{\otimes n})^J_I (Z^{\dagger\otimes n})^L_K\rangle \\
&= \frac{1}{d_R d_S}(P_R)^I_J(P_S)^K_L \sum_{\sigma\in S_n}(\sigma^{-1})^J_K(\sigma)^L_I \\
&= \frac{1}{d_R d_S}\sum_{\sigma\in S_n}\mathrm{Tr}(P_R\sigma^{-1}P_S\sigma) \\
&= \frac{1}{d_R d_S}\sum_{\sigma\in S_n}\mathrm{Tr}(P_R P_S) \qquad\qquad \because P_S\sigma = \sigma P_S \\
&= \frac{\delta_{RS}n!}{d_R d_S}\mathrm{Tr}(P_R) = \frac{\delta_{RS}n!}{d_R d_S}Dim_R \\
&= \delta_{RS} f_R
\end{aligned} \tag{C.7}$$

where we have used the fact that the order of the group S_n is $n!$ in the second last line and the definitions of Dim_R and d_R to get the last line.

For the restricted Schur polynomials, the relevant projection operator (for the two matrix case) is

$$P_{R,(r,s)} = \frac{1}{n!}\frac{1}{m!}\sum_{\sigma_1\in S_n}\sum_{\sigma_2\in S_m}\chi_r(\sigma_1)\chi_s(\sigma_2)\Gamma_R(\sigma_1\sigma_2) \tag{C.8}$$

In terms of the projection operator we can write the restricted Schur polynomial as

$$\chi_{R,(r,s)\vec{\mu}}(Z^{\otimes n}Y^{\otimes m}) = \frac{1}{n!m!}\sum_{\sigma\in S_{n+m}}\mathrm{Tr}_{(r,s)\vec{\mu}}(\Gamma_R(\sigma))\mathrm{Tr}(\sigma Y^{\otimes m}\otimes Z^{\otimes n} = \mathrm{Tr}(P_{R,(r,s)\vec{\mu}}Z^{\otimes n}Y^{\otimes m}) \tag{C.9}$$

We call it the restricted Schur polynomial because we replace the usual character of our irreps with an object called the restricted character. This encodes the way we have partitioned the Young diagram R into $n+m$, where $r\vdash n$ and $s\vdash m$ are subspaces of R. In each of these subspaces we must consider S_n and S_m separately such that we study permutations in $S_n\times S_m$. This comes from the following logic.

We are working $V_N^{\otimes n+m}$. In the single matrix model, the following action of the permutations $\sigma\in S_n$ left $Z^{\otimes n}$ invariant.

$$(\sigma)^I_J Z^{\otimes n}(\sigma^{-1})^K_L = (Z^{\otimes n})^I_L \tag{C.10}$$

When we consider two complex matrix models, we have the same invariance holding for the product $Z^{\otimes n}Y^{\otimes m}$, but now $\sigma\in S_n\times S_m$. This is because we cannot swap Zs and Ys without changing the structure. Our permutations must act separately on each type of field so that we restrict to the subgroup $S_n\times S_m$. From (C.10) and using the cyclicity of the trace we obtain the relation

$$\mathrm{Tr}(\rho Z^{\otimes n}Y^{\otimes m}) = \mathrm{Tr}(\sigma^{-1}\rho\sigma Z^{\otimes n}Y^{\otimes m}) \tag{C.11}$$

This allows us to define a notion of restricted conjugate. Two elements g_1 and g_2 in S_{n+m} are restricted conjugate to one another if they satisfy the relation

$$g_1 = \sigma^{-1}g_2\sigma \tag{C.12}$$

for $\sigma \in S_n \times S_m$. The is like the equivalence relation, conjugate to, which we used when classifying irreps in Appendix *A* but with the added restriction that σ is in the subgroup. When studying single matrix models, we saw that the number of conjugacy classes was equal to the number of irreps and that this was equal to the number of physical observables. Now, in our multi matrix model, we have that the number of restricted conjugacy classes is equal to the number of physical observables.

A complete set of functions on the restricted conjugacy class are given by taking a restricted trace of the matrix irrep of the group element. The restricted trace is a trace over the subspace. The restricted character is defined as the restricted trace of a group element.

$$\chi_{R,(r,s)\vec{\mu}}(\sigma) = \mathrm{Tr}_{R,(r,s)\vec{\mu}}(\Gamma_R(\sigma)) \tag{C.13}$$

We label multiplicities with $\vec{\mu}$. Row and column indices in the restricted trace are traced over different subspaces (S_n and S_m). Note that the projectors here are not projection operators. In general, $\vec{\mu} \neq \vec{\nu}$ and we have that

$$P_{R,(r,s)\mu_1\mu_2} P_{T,(t,u)\nu_1\nu_2} = \mathcal{A}\delta_{RT}\delta_{rt}\delta_{su}\delta_{\mu_2\nu_1} P_{R,(r,s)\mu_1\nu_2} \tag{C.14}$$

where $\mathcal{A}$ is a number. The product of two projection operators is either zero, or one of the projectors, $P_R P_T = \delta_{RT} P_R$, by definition of a projection operator. Multiplicities label different copies of a representation. The projector on the right hand side of (C.14) has multiplicity labels that are different to the projectors on the left hand side, hence these objects are all different. However, if the multiplicity labels are the same, then these objects are projection operators. In general, they are not and we call them intertwining maps as they map us between different copies of the irrep. To illustrate:

$$\Gamma_{(r,s)\mu_1}(\sigma) P_{R,(r,s)\vec{\mu}} = P_{R,(r,s)\vec{\mu}} \Gamma_{(r,s)\mu_2}(\sigma) \tag{C.15}$$

D Gauss Graph Operators

Gauss graph operators are labelled by graphs consisting of nodes and oriented edges which start and end on nodes. The nodes correspond to rows of the Young diagram so that each eigenvalue is represented by a node in the graph. The Y fields are represented by edges so that there is one edge per field. The number of edges that start on a node must be equal to the number of edges ending on a node. If an edge stretched between two different nodes, this would be an interaction between the two eigenvalues. Since we are considering non-interacting fermions, we can only have edges starting and ending on the same node (see figure 15).

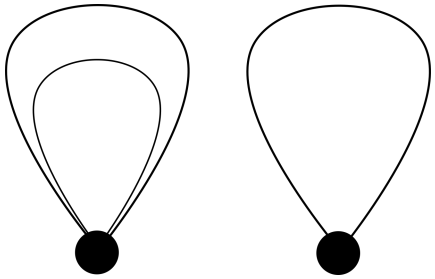


Figure 15: Gauss graph with two nodes and 3 edges

These particular Gauss graphs correspond to BPS operators. Thus we see that a fermion description of the two matrix model will describe BPS operators.

When the dilatation operator acts on the restricted Schur polynomials in the displaced corners approximation ($n >> m$), it factors into a separate action on each of the symmetric group labels: $r \vdash n$ and $s \vdash m$ which partition the Z and Y fields respectively. For the Gauss graph operators, this action is diagonal on the Y fields. This problem was solved using a double coset ansatz ([37]) which labelled the eigenoperators with Gauss graphs. The translation between the Young diagram and the Gauss graphs is achieved by replacing rows with nodes and representing the Y fields with oriented edges, with the condition that each graph has have the same number of outgoing and ingoing edges. BPS operators are labelled by graphs that have no edges stretching between different nodes. In this way edges are excitations of the giant gravitons, represented by nodes, with a number of ways to perform the excitation for a given m: we can permute the edges on a given node. For each permutation σ our Gauss graph operator is

$$O^{\vec{m}}_{R,r}(\sigma) = \frac{|H|}{\sqrt{m!}} \sum_{j,k} \sum_{s\vdash m} \sum_{\mu_1,\mu_2} \sqrt{d_s} \Gamma^{(s)}_{jk}(\sigma) B^{s\to 1_H}_{j\mu_1} B^{s\to 1_H}_{k\mu_2} O_{R,(r,s)\mu_1\mu_2} \tag{D.1}$$

where H is the product of symmetric groups $S_{m_1} \times S_{m_2} \times \cdots \times S_{m_p}$ and each m_i counts the number of Y fields in a row on the Young diagram or edges on a node. The normalised restricted Schur polynomial appears on the right hand side and branching coefficients for irrep $s \vdash m$ of S_m to a copy (labelled by the multiplicity index) of the trivial irrep of H. BPS operators correspond to the identity permutation because we cannot permute edges on the nodes to form

a new, distinct graph. Thus

$$\begin{aligned}
O^{BPS}_{R,r,\vec{m}} &= \frac{|H|}{\sqrt{m!}} \sum_{j,k} \sum_{s} \sum_{\mu_1\mu_2} \sqrt{d_s}\delta_{jk} B^{s\to 1_H}_{j\mu_1} B^{s\to 1_H}_{k\mu_2} O_{R,(r,s)\mu_1\mu_2} \\
&= \frac{|H|}{\sqrt{m!}} \sum_{s} \sum_{\mu} \sqrt{d_s} O_{R,(r,s)\mu\mu} \\
&= \frac{|H|}{\sqrt{m!}} \sum_{s} \sum_{\mu} \sqrt{\frac{m!}{\text{hooks}_s}} \sqrt{\frac{\text{hooks}_s \text{hooks}_r}{f_R \text{hooks}_R}} \frac{1}{n!m!} \sum_{\sigma\in S_{n+m}} \text{Tr}(P_{R,(r,s)\mu\mu}\Gamma^{(R)}(\sigma))\text{Tr}(\sigma Y^{\otimes m} Z^{\otimes n}) \\
&= \frac{|H|}{n!m!} \sqrt{\frac{\text{hooks}_r}{\text{hooks}_R f_R}} \sum_{\sigma\in S_{n+m}} \text{Tr}(\sum_{s} \sum_{\mu} P_{R,(r,s)\mu\mu}\Gamma^{(R)}(\sigma))\text{Tr}(\sigma Y^{\otimes m} Z^{\otimes n}) \qquad \text{(D.2)}
\end{aligned}$$

where $\Gamma^{(s)}_{jk}(1) = \delta_{jk}$ and the branching coefficients are orthogonal in the multiplicity index for $j = k$.

E Ratios of Hooks

The hook $H_R(i,j)$ of the box in row i and column j of R is the set of boxes (a,b) with $a=i$ and $b \geq j$ or $a \geq i$ and $b=j$. The hook-length $h_R(i,j)$ is the number of boxes in the hook $H_R(i,j)$. To visualize the hook associated to a given box, imagine an elbow with its joint in the box and one arm exiting R by moving to the right through the row of the box and one arm exiting by moving down through the column. The hook length is the number of boxes the elbow passes through. We use hooks_R to denote the product of hook lengths for each box in R. In this Appendix we want to derive a formula for the ratio

$$\frac{\text{hooks}_{+R}}{\text{hooks}_{+r}} \tag{E.1}$$

$+r$ is obtained from $+R$ by removing a total of $|R|-|r|$ boxes. All of these boxes are located close to corner i of Young diagram B.

Start by removing a single box from $+R$ to obtain the Young diagram $+R'$. Consider the ratio

$$\frac{\text{hooks}_{+R}}{\text{hooks}_{+R'}} \tag{E.2}$$

Imagine that the box that was removed comes from row a and column b of R. Denote the length of row a by l_a and the length of column b by l_b. The numbers a, b, l_a, l_b are all much smaller than $\sqrt{N}$. Most hook lengths in the numerator will equal the hook lengths in the denominator. The only hook lengths that don't match are lengths for hooks that enter or exit through the box that is removed. After many cancellations we find

$$\frac{\text{hooks}_{+R}}{\text{hooks}_{+R'}} = \prod_{j=1}^{i} \frac{L(j,i)-b+l_B}{L(j,i)-N_j-b+l_b} \prod_{l=i+1}^{C} \frac{L(i+1,l)-a+l_a}{L(c+1,l)-M_l-a+l_a} \frac{\text{hooks}_R}{\text{hooks}_{R'}} \tag{E.3}$$

where

$$L(c,d) = \sum_{k=c}^{d} (N_k + M_k) \tag{E.4}$$

and N_k and M_k are defined in Figure 12. These numbers specify the background Young diagram. In the large N limit this result can be simplified to

$$\frac{\text{hooks}_{+R}}{\text{hooks}_{+R'}} = \eta_B \frac{\text{hooks}_R}{\text{hooks}_{R'}} \left(1 + O\left(\frac{1}{N}\right)\right) \tag{E.5}$$

where

$$\eta_B = \prod_{j=1}^{i} \frac{L(j,i)}{L(j,i)-N_j} \prod_{l=i+1}^{C} \frac{L(i+1,l)}{L(c+1,l)-M_l} \tag{E.6}$$

Notice that η_B is independent of a and b, at large N. If we have removed two boxes from $+R$ to obtain $+R''$, we can use the above result to compute

$$\frac{\text{hooks}_{+R}}{\text{hooks}_{+R''}} = \frac{\text{hooks}_{+R}}{\text{hooks}_{+R'}} \frac{\text{hooks}_{+R'}}{\text{hooks}_{+R''}}$$

$$
\begin{aligned}
&= \left(\eta_B \frac{\text{hooks}_R}{\text{hooks}_{R'}}\right)\left(\eta_B \frac{\text{hooks}_{R'}}{\text{hooks}_{R''}}\right)\left(1+O\left(\frac{1}{N}\right)\right) \\
&= (\eta_B)^2 \frac{\text{hooks}_R}{\text{hooks}_{R''}}\left(1+O\left(\frac{1}{N}\right)\right)
\end{aligned} \tag{E.7}
$$

At large N, every time we remove a box from $+R$ it results in a factor of η_B in the ratio of hooks lengths. We have to remove $|R|-|r|$ boxes from R to obtain r, so that we find

$$
\frac{\text{hooks}_{+R}}{\text{hooks}_{+r}} = \frac{\text{hooks}_R}{\text{hooks}_r}(\eta_B)^{|R|-|r|}\left(1+O\left(\frac{1}{N}\right)\right) \tag{E.8}
$$

which is the identity (4.2.1.10) used in section 4.2.3.

F Ratios of Factors

Recall that f_R denotes the product of the factors of each box in R and that a box in row i and column j has factor $N - i + j$. In this Appendix we will compute the ratio of the product of factors for a Young diagram $+R$ and Young diagram B. $+R$ is obtained by attaching a smaller Young diagram R to the Young diagram B. The argument is rather simple and most easily illustrated with an explicit example.

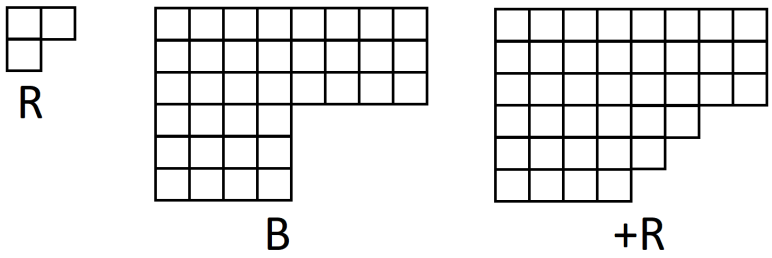


Figure 16: An example showing Young diagrams R, B and $+R$. The Young diagram $+R$ is obtained by stacking R next to B.

Consider the Young diagrams shown in Figure 16 above. It is simple to see that

$$f_R = N(N-1)(N+1) \tag{F.1}$$

and

$$\frac{f_{+R}}{f_B} = (N+\delta)(N+\delta-1)(N+\delta+1) \tag{F.2}$$

where $\delta = 1 = 5 - 4$. In general, if the top most and left most box of R is added to row a and column b of B, we will have $\delta = b - a$.

G Delocalised Trace Structures are Preserved

In this appendix we compute correlation functions of delocalised operators. Our results suggest that, in general, there is no simple relationship between correlation functions of delocalised operators and correlation functions of operators in the planar limit, even in the free CFT. The results of our computation do however provide evidence that mixing between different trace structures is suppressed, even for the delocalised operators.

To keep the discussion simple consider operators constructed from a single field Z. This will already probe aspects of the operator mixing issue. As a simple warm up example, consider delocalised excitations constructed by starting with operators of the form $\mathrm{Tr}(\sigma_1 Z^{\otimes n_1})\mathrm{Tr}(\sigma_2 Z^{\otimes n_2})$. To construct a delocalised excitation, begin by writing

$$\begin{aligned}\mathrm{Tr}(\sigma_1 Z^{\otimes n_1}) &= \sum_{R_1 \vdash n_1} \chi_{R_1}(\sigma_1)\chi_{R_1}(Z) \\ \mathrm{Tr}(\sigma_2 Z^{\otimes n_2}) &= \sum_{R_2 \vdash n_2} \chi_{R_2}(\sigma_2)\chi_{R_2}(Z)\end{aligned} \tag{G.1}$$

The delocalised excitation is given by

$$O^{(B)}(\sigma_1,\sigma_2) = \sum_{R_1,R_2} \chi_{R_1}(\sigma_1)\chi_{R_2}(\sigma_2)\chi_{+(R_1,R_2)}(Z) \tag{G.2}$$

The Young diagram $+(R_1,R_2)$ is obtained by adding R_1 at the ith inward pointing corner and adding R_2 at the jth inward pointing corner. This corresponds to localizing $\mathrm{Tr}(\sigma_1 Z^{\otimes n_1})$ at the ith corner and localizing $\mathrm{Tr}(\sigma_2 Z^{\otimes n_2})$ at the jth corner. It is now rather simple to evaluate the correlator

$$\begin{aligned}&\langle O^{(B)}(\sigma_1,\sigma_2)(x_1)O^{(B)}(\tau_1,\tau_2)^\dagger(x_2)\rangle_B \\ &= \sum_{R_1\vdash n_1, R_2\vdash n_2} \chi_{R_1}(\sigma_1)\chi_{R_2}(\sigma_2)\chi_{R_1}(\tau_1)\chi_{R_2}(\tau_2)\frac{f_{+(R_1,R_2)}}{f_B|x_1-x_2|^{2n_1+2n_2}} \\ &= \sum_{R_1\vdash n_1} \chi_{R_1}(\sigma_1)\chi_{R_1}(\tau_1)\frac{f_{R_1}(N_{\mathrm{eff},1})}{|x_1-x_2|^{2n_1}} \sum_{R_2\vdash n_2} \chi_{R_2}(\sigma_2)\chi_{R_2}(\tau_2)\frac{f_{R_2}(N_{\mathrm{eff},2})}{|x_1-x_2|^{2n_2}} \\ &= \langle \mathrm{Tr}(\sigma_1 Z^{\otimes n_1})(x_1)\mathrm{Tr}(\tau_1 Z^{\otimes n_1})(x_2)\rangle_{N\to N_{\mathrm{eff},1}} \langle \mathrm{Tr}(\sigma_2 Z^{\otimes n_2})(x_1)\mathrm{Tr}(\tau_2 Z^{\otimes n_2})(x_2)\rangle_{N\to N_{\mathrm{eff},2}}\end{aligned} \tag{G.3}$$

In the above expression, $f_R(M)$ means the product of the factors of Young diagram R with N replaced by M. Further $N_{\mathrm{eff},1}$ is the factor of the first box added to corner i and $N_{\mathrm{eff},2}$ is the factor of the first box added to corner j. The above result implies that the delocalised correlator has factorized into two factors, one for each corner on which the operator is located. Each factor is a correlation function. The value of N is replaced by an effective value of N for each corner. It is worth emphasizing that the expressions on the last line of (G.3) are exact. This result implies that trace mixing is even more constrained for the delocalised excitation than it is in the planar limit. Indeed, in the planar limit we will have mixing if the trace structure of $\mathrm{Tr}(\sigma_1 Z^{\otimes n_1})\mathrm{Tr}(\sigma_2 Z^{\otimes n_2})$ matches the trace structure of $\mathrm{Tr}(\tau_1 Z^{\otimes n_1})\mathrm{Tr}(\tau_2 Z^{\otimes n_2})$. For

the delocalised excitation we will only have mixing if the trace structure of $\mathrm{Tr}(\sigma_1 Z^{\otimes n_1})$ matches $\mathrm{Tr}(\tau_1 Z^{\otimes n_1})$ and the trace structure of $\mathrm{Tr}(\sigma_2 Z^{\otimes n_2})$ matches $\mathrm{Tr}(\tau_2 Z^{\otimes n_2})$.

There is a second type of delocalised excitation we could consider: a single trace operator that is itself delocalised. As an example, consider a single trace operator that is distributed between corners i and j. To write such a loop we introduce the space time independent auxiliary field $\mathcal{X}^a_b$, which has two point function

$$\langle \mathcal{X}^a_b \mathcal{X}^c_d \rangle = \delta^a_d \delta^c_b \tag{G.4}$$

Using this auxiliary field we can split any single trace operator into two traces, that reassemble to give a single trace when the average over $\mathcal{X}$ is performed. For example, we can replace

$$\mathrm{Tr}(Y^5) \quad \longrightarrow \quad \mathrm{Tr}(Y^2\mathcal{X})\mathrm{Tr}(Y^3\mathcal{X}) \tag{G.5}$$

Performing the average over $\mathcal{X}$, we recover our original loop

$$\langle \mathrm{Tr}(Y^2\mathcal{X})\mathrm{Tr}(Y^3\mathcal{X})\rangle = (Y^2)^b_a\ (Y^3)^d_c \langle \mathcal{X}^a_b \mathcal{X}^c_d\rangle = \mathrm{Tr}(Y^5) \tag{G.6}$$

The advantage of splitting things in this way, is that we can now follow exactly the same logic that we used for the first example above. We will take this to be the definition of the delocalised single trace operator. For the general operator constructed from Ys, the resulting expression is of the form[30]

$$O_A(Y) = \sum_{R^1,R^2,r^1,r^2} a^{(A)}_{R^1,R^2,r^1,r^2} \chi_{R^1,(r^1,\square)}(Y,\mathcal{X})\chi_{R^2,(r^2,\square)}(Y,\mathcal{X}) \tag{G.7}$$

The single extra box in the labels for the restricted Schur polynomial represents the auxiliary $\mathcal{X}$ field. We can now, following the example we studied above, attach R_1 and R_2 to different corners and in this way obtain the delocalised single trace operator. For operators that involve more than two corners, we would need to introduce more than one auxiliary field. Concretely, for the case we consider, we have

$$O^{(B)}_A \ = \sum_{R^1,R^2,r^1,r^2} a^{(A)}_{R^1,R^2,r^1,r^2}\ \chi_{+(R^1,R^2),\left(+(r^1_1,r^1_2),\square\times\square\right)}(Z,Y,\mathcal{X}) \tag{G.8}$$

The notation $\square\times\square$ is just to reflect the fact that we have not organized the auxiliary fields into representations of S_2. We can now average over $\mathcal{X}$ in (G.8) to obtain an operator that does not depend on the auxiliary fields. This averaging is easily performed using the methods developed in [144]. It is straight forward, but tedious and messy, to check that mixing between different trace structures of these delocalised excitations is also suppressed.

Lets illustrate the above construction with the simplest possible example: we consider two delocalised operators. The first, O_A, is given by placing $\mathrm{Tr}(Y)$ at corner i and $\mathrm{Tr}(Y)$ at corner j. The second, O_B, is obtained by distributing $\mathrm{Tr}(Y^2)$ between the two corners. When the background is not present, the relevant correlators are

$$\langle \mathrm{Tr}(Y^2)(x_1)\mathrm{Tr}(Y^{\dagger 2})(x_2)\rangle \ = \ \frac{2N^2}{|x_1-x_2|^4}$$

[30] Imagine that our operator is constructed using n Zs. The restricted Schur polynomials needed for this computation involve restricting S_{n+1} to S_n. There is no need for multiplicity labels when studying this restriction.

$$\begin{aligned}\langle \mathrm{Tr}(Y)^2(x_1)\mathrm{Tr}(Y^\dagger)^2(x_2)\rangle &= \frac{2N^2}{|x_1-x_2|^4}\\ \langle \mathrm{Tr}(Y)^2(x_1)\mathrm{Tr}(Y^{\dagger 2})(x_2)\rangle &= \frac{2N}{|x_1-x_2|^4}\end{aligned} \tag{G.9}$$

It is clear that the last correlator, which mixes different trace structures, is down by a factor of N. If we had normalized the two point functions to one, the last correlator above vanishes at large N which shows that different trace structures don't mix. The delocalised operator with $\mathrm{Tr}(Y)$ at corner i and $\mathrm{Tr}(Y)$ at corner j is obtained by adding a single box at corner i of B and a single box at corner j. Denote the factor of the box added at corner i by $N_{\mathrm{eff},1}$ and the factor of the box added at corner j by $N_{\mathrm{eff},2}$. It is a simple matter to find

$$\langle O_A^{(B)}(x_1)O_A^{(B)}(x_2)^\dagger\rangle = \eta_B\tilde{\eta}_B\frac{N_{\mathrm{eff},1}N_{\mathrm{eff},2}}{|x_1-x_2|^4} \tag{G.10}$$

in complete agreement with (G.3). The coefficient $\eta_B\tilde{\eta}_B$ is an order 1 number that arises from computing the ratios of hooks. After averaging over the $\mathcal{X}$ fields we find that $O_B^{(B)}(x_2)$ is a sum of two terms. One is clearly leading and has coefficient $\sqrt{1-\frac{1}{(N_{\mathrm{eff},1}-N_{\mathrm{eff},2})^2}}$. The subleading term have coefficient $\frac{1}{N_{\mathrm{eff},1}-N_{\mathrm{eff},2}}$. The leading term involves a twisted character in the notation of [62], while the subleading term is a normal restricted character. We find that both terms contribute to the correlator

$$\langle O_B^{(B)}(x_1)O_B^{(B)}(x_2)^\dagger\rangle = \eta_B\tilde{\eta}_B\frac{N_{\mathrm{eff},1}N_{\mathrm{eff},2}}{|x_1-x_2|^4} \tag{G.11}$$

while only the subleading term contributes to the mixed correlator

$$\langle O_A^{(B)}(x_1)O_B^{(B)}(x_2)^\dagger\rangle = \eta_B\tilde{\eta}_B\frac{N_{\mathrm{eff},1}N_{\mathrm{eff},2}}{(N_{\mathrm{eff},1}-N_{\mathrm{eff},2})|x_1-x_2|^4} \tag{G.12}$$

Since $N_{\mathrm{eff},1}-N_{\mathrm{eff},2}$ is of order N, this clearly demonstrates the suppression. Although there is little doubt that mixing between different trace structures is suppressed for the general delocalised excitations, at this point in time we do not have a simple general argument for this conclusion.

H Localised and Delocalised Mixing at One Loop

In this appendix we study a simple example of mixing between a localised and a delocalzied operator at one loop. Since we don't want a selection rule to prevent the operators from mixing, we need to consider operators that differ in the placement of at most one box. To make the computation as transparent as possible choose particularly simple operators. Our goal is to show that this mixing is of order N^{-1}. This is a simple illustration that the mixing between a delocalised operator and a local operator, is suppressed at large N.

The local operator that we consider is $O_{+\square\!\square,(+\square\square,\square\square)}(Z,Y)$. The representation $\square\!\square$ produces $(+\square\square,\square\square)$ once upon restricting from S_4 to $S_2\times S_2$ so that there is no need for multiplicity labels. Lets assume that this excitation is localised at corner i. For the delocalised operator, we assume that we have $(\square\!\square,(\square\square,\square))$ at corner i and $\square,(\cdot,\square)$ at corner j. For this example we can evaluate the matrix element (4.3.1.3) exactly. The result is

$$N_{+\square\!\square,(+\square\square,\square\square);+\left(\square\!\square_{\,i},\square_j\right),(+\square\square_i,\left(\square_i,\square_j\right))}=\frac{\lambda_{\text{eff,i}}}{4\pi}\sqrt{\frac{N_{\text{eff,i}}}{N_{\text{eff,j}}}}\frac{1}{N_{\text{eff,j}}-N_{\text{eff,i}}}\left(1+O\left(\frac{1}{N}\right)\right) \tag{H.1}$$

where $N_{\text{eff,i}}$ is the factor of the first box added at corner i, $N_{\text{eff,j}}$ is the factor of the first box added at corner j and $\lambda_{\text{eff,i}}\equiv g_{YM}^2 N_{\text{eff,i}}$. The fact that this mixing is of order N^{-1} is in perfect accord with the arguments of section 4.3.2.

I Correcting the Planar Limit

The emergent gauge theory has 't Hooft coupling $g^2_{YM}N_{\rm eff}$ with g^2_{YM} the coupling of the original CFT. It is natural to ask if (non-planar) higher genus corrections are suppressed by powers of N or powers of $N_{\rm eff}$. This Appendix gives a discussion of the issue.

The article [145] studied excitation of the annulus LLM background, with boundary condition given by a single black annulus (of area N) with a central white disk (of area M). The Young diagram describing this geometry has a total of N rows and M columns. A simple and clean argument shows that the 1/2 BPS correlators, with excitations constructed using only Z fields, admit an expansion with $N_{\rm eff}^{-2}$ playing the role of the genus counting parameter[145]. In the 1/2 BPS sector, this result generalizes to multi ring geometries and again the genus counting parameter is $N_{\rm eff}^{-2}$.

To go beyond the half BPS sector the result (4.2.3.13) can be used. After rescaling the fields which are not Z fields, by a factor of $1/\sqrt{\eta_B}$, we find a product of two terms

$$\langle O_A(x_1)O_B(x_2)^\dagger\rangle_B \;=\; F_{AB}(N_{\rm eff})\frac{1}{|x_1-x_2|^{2J}}\left(1+O\left(\frac{1}{N}\right)\right) \tag{I.1}$$

The first factor on the RHS above admits an expansion in $N_{\rm eff}^{-1}$. The second factor does not. Thus, in general our amplitude can't be developed as a series in the two small parameters $\lambda_{\rm eff}$ and $N_{\rm eff}^{-2}$.

J Check of Counting Formulas

In this section we will explore the counting formulas obtained in Section 5.2. First consider the counting at infinite N. It is rather easy to use characters of the symmetric group to compute the Kronecker coefficients and then sum the squares of the coefficients, to compute the number of bosonic gauge invariant operators (N_b) and the number of fermionic gauge invariants operators (N_f). The results are shown in Table 1.

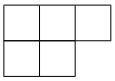
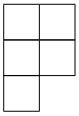
n	1	2	3	4	5	6
N_b	1	4	11	43	161	901
N_f	1	4	11	43	161	901

Table 1: The number of bosonic N_b or fermionic N_f gauge invariant tensors constructed using n fields. This counting is for gauge group ranks $N_1 = N_2 = N_3 = \infty$.

Note that the number of fermionic gauge invariant operators is equal to the number of bosonic gauge invariant operators. This fact is easily explained: every time we have a non-zero bosonic Kronecker coefficient, there is a corresponding non-zero fermionic Kronecker coefficient. This is easily proved using the well known property of characters of the symmetric group

$$\chi_{R^T}(\sigma) = \text{sgn}(\sigma)\chi_R(\sigma) \tag{J.1}$$

where R^T is the transposed Young diagram, i.e. the Young diagram obtained from R by swapping rows and columns. For example

$R =$  $\Rightarrow \quad R^T =$  (J.2)

Recall that 1^n represents the Young diagram with a single column of n boxes. Use n to denote the Young diagram that has a single row of n boxes. The proof is as follows

$$\begin{aligned}
g_{r_1,r_2,r_3,n} &= \frac{1}{n!}\sum_{\sigma\in S_n}\chi_{r_1}(\sigma)\chi_{r_2}(\sigma)\chi_{r_3}(\sigma)\chi_n(\sigma) \\
&= \frac{1}{n!}\sum_{\sigma\in S_n}\chi_{r_1}(\sigma)\chi_{r_2}(\sigma)\chi_{r_3}(\sigma) \\
&= \frac{1}{n!}\sum_{\sigma\in S_n}\chi_{r_1^T}(\sigma)\chi_{r_2^T}(\sigma)\chi_{r_3^T}(\sigma)(\text{sgn}(\sigma))^3 \\
&= \frac{1}{n!}\sum_{\sigma\in S_n}\chi_{r_1^T}(\sigma)\chi_{r_2^T}(\sigma)\chi_{r_3^T}(\sigma)\text{sgn}(\sigma) \\
&= \frac{1}{n!}\sum_{\sigma\in S_n}\chi_{r_1^T}(\sigma)\chi_{r_2^T}(\sigma)\chi_{r_3^T}(\sigma)\chi_{1^n}(\sigma) \\
&= g_{r_1^T,r_2^T,r_3^T,1^n}
\end{aligned} \tag{J.3}$$

Since the set of non-zero Kronecker coefficients are the same for the bosonic and the fermionic tensor models, and the number of gauge invariant operators is equal to the sum of the squares of these coefficients, this proves that the number of gauge invariant operators one can construct in bosonic tensor models equals the number of gauge invariant operators one can construct in fermionic tensor models.

The argument above has been for rank $d = 3$ tensors. It is clear that the above proof goes through for rank d tensors with d odd, since in this case $(\mathrm{sgn}(\sigma))^d = \mathrm{sgn}(\sigma)$. For even d however, the above proof does not go through: in this case $(\mathrm{sgn}(\sigma))^d = 1$. However, a simple variant of the proof does work: for rank four for example, it is simple to prove that

$$g_{r_1,r_2,r_3,r_4,n} = g_{r_1^T,r_2^T,r_3^T,r_4,1^n} \tag{J.4}$$

We have verified this equality explicitly for $n \leq 6$ and ranks $d \leq 8$, which is a nice check of the above arguments.

At finite N the number of fermionic and bosonic gauge invariant operators no longer matches. Recall that for a general rank d tensor model the gauge group is $U(N_1) \times U(N_2) \times \cdots \times U(N_d)$. As soon as n exceeds any of the N_i, it is possible to have Young diagrams $r \vdash n$ whose number of rows is greater than at least one of the N_i. In this case, the corresponding operator vanishes and it is for this reason that we must put a cut off on the number of rows. For example, for the bosons we have

$$N_b = \sum_{r_i \vdash n \; l(r_i) \leq N_i} g^2_{r_1\, r_2\, r_3\, 1} \tag{J.5}$$

The proof breaks because we can have, for example, $l(r_1) < N_1$ and $l(r_1^T) > N_1$. In Table 2 we have given the finite N counting for rank 3 tensors with $N_1 = N_2 = N_3 = 5$.

n	1	2	3	4	5	6
N_b	1	4	11	43	92	70
N_f	1	4	11	43	87	20

Table 2: The number of bosonic N_b or fermionic N_f gauge invariant tensors constructed using n fields. Here $N_1 = N_2 = N_3 = 5$.

Notice that there are more bosonic gauge invariant operators than there are fermionic gauge invariant operators. This is in fact rather general: the Kronecker coefficients relevant for the bosonic gauge invariants are mostly short and wide Young diagrams. On the other hand, the Kronecker coefficients relevant for the fermionic gauge invariants are mostly tall and thin Young diagrams. In fact, for the fermionic tensor model, there is some value of n beyond which there are no new gauge invariants. In Table 3 we have shown the finite N counting for rank 3 tensors with $N_1 = N_2 = N_3 = 3$. For $n \geq 6$ there are no gauge invariant operators.

For the first few values of n, it is possible to explicitly construct the gauge invariant operators. For $n = 1$ there is a single bosonic and a single fermionic gauge invariant operator

$$\bar{\phi}^{ijk}\phi_{ijk} \qquad\qquad \bar{\psi}^{ijk}\psi_{ijk} \tag{J.6}$$

n	1	2	3	4	5	6
N_b	1	4	11	12	151	18
N_f	1	4	11	8	41	0

Table 3: The number of bosonic N_b or fermionic N_f gauge invariant tensors constructed using n fields. Here $N_1 = N_2 = N_3 = 3$.

For $n = 2$ we have the following bosonic operators

$$\begin{array}{ll} \bar{\phi}^{i_1 j_1 k_1}\bar{\phi}^{i_2 j_2 k_2}\phi_{i_1 j_1 k_1}\phi_{i_2 j_2 k_2} & \bar{\phi}^{i_2 j_1 k_1}\bar{\phi}^{i_1 j_2 k_2}\phi_{i_1 j_1 k_1}\phi_{i_2 j_2 k_2} \\ \bar{\phi}^{i_1 j_2 k_1}\bar{\phi}^{i_2 j_1 k_2}\phi_{i_1 j_1 k_1}\phi_{i_2 j_2 k_2} & \bar{\phi}^{i_1 j_1 k_2}\bar{\phi}^{i_2 j_2 k_1}\phi_{i_1 j_1 k_1}\phi_{i_2 j_2 k_2} \end{array} \tag{J.7}$$

which nicely matches the counting given above. There is an identical set of operators for the fermions. For $n = 3$ we have the following bosonic operators

$$\begin{array}{ll} \bar{\phi}^{i_1 j_1 k_1}\bar{\phi}^{i_2 j_2 k_2}\bar{\phi}^{i_3 j_3 k_3}\phi_{i_1 j_1 k_1}\phi_{i_2 j_2 k_2}\phi_{i_3 j_3 k_3} & \bar{\phi}^{i_1 j_1 k_1}\bar{\phi}^{i_2 j_2 k_3}\bar{\phi}^{i_3 j_3 k_2}\phi_{i_1 j_1 k_1}\phi_{i_2 j_2 k_2}\phi_{i_3 j_3 k_3} \\ \bar{\phi}^{i_1 j_1 k_1}\bar{\phi}^{i_2 j_3 k_2}\bar{\phi}^{i_3 j_3 k_2}\phi_{i_1 j_1 k_1}\phi_{i_2 j_2 k_2}\phi_{i_3 j_3 k_3} & \bar{\phi}^{i_1 j_1 k_1}\bar{\phi}^{i_2 j_3 k_3}\bar{\phi}^{i_3 j_2 k_2}\phi_{i_1 j_1 k_1}\phi_{i_2 j_2 k_2}\phi_{i_3 j_3 k_3} \\ \bar{\phi}^{i_1 j_1 k_2}\bar{\phi}^{i_2 j_2 k_3}\bar{\phi}^{i_3 j_3 k_1}\phi_{i_1 j_1 k_1}\phi_{i_2 j_2 k_2}\phi_{i_3 j_3 k_3} & \bar{\phi}^{i_1 j_1 k_2}\bar{\phi}^{i_2 j_3 k_1}\bar{\phi}^{i_3 j_2 k_3}\phi_{i_1 j_1 k_1}\phi_{i_2 j_2 k_2}\phi_{i_3 j_3 k_3} \\ \bar{\phi}^{i_1 j_2 k_1}\bar{\phi}^{i_2 j_3 k_3}\bar{\phi}^{i_3 j_1 k_2}\phi_{i_1 j_1 k_1}\phi_{i_2 j_2 k_2}\phi_{i_3 j_3 k_3} & \bar{\phi}^{i_1 j_2 k_1}\bar{\phi}^{i_2 j_3 k_2}\bar{\phi}^{i_3 j_1 k_3}\phi_{i_1 j_1 k_1}\phi_{i_2 j_2 k_2}\phi_{i_3 j_3 k_3} \\ \bar{\phi}^{i_1 j_2 k_3}\bar{\phi}^{i_2 j_3 k_1}\bar{\phi}^{i_3 j_1 k_2}\phi_{i_1 j_1 k_1}\phi_{i_2 j_2 k_2}\phi_{i_3 j_3 k_3} & \bar{\phi}^{i_1 j_2 k_2}\bar{\phi}^{i_2 j_3 k_3}\bar{\phi}^{i_3 j_1 k_1}\phi_{i_1 j_1 k_1}\phi_{i_2 j_2 k_2}\phi_{i_3 j_3 k_3} \end{array} \tag{J.8}$$

which matches the counting given above. The set of fermionic operators is again the same.

K Examples of Operators and Correlators

In the previous Appendix we have written down some of the gauge invariant operators in the permutation basis. In this Appendix we will write down some operators in the representation theory basis. We will then explore correlators of gauge invariant operators, in both bases.

For $n = 2$ fields, there are no multiplicities, so these labels are dropped. There is a total of four gauge invariant operators that can be defined. We will give the complete set of gauge invariant operators, since this will allow us to test that they are indeed orthogonal and have the correct two point function. The operators are given by

$$\begin{aligned}\mathcal{O}_{\square\square,\square\square,\square\square} &= 2\bar{\phi}^{i_1j_1k_1}\bar{\phi}^{i_2j_2k_2}\phi_{i_1j_1k_1}\phi_{i_2j_2k_2} + 2\bar{\phi}^{i_2j_1k_1}\bar{\phi}^{i_1j_2k_2}\phi_{i_1j_1k_1}\phi_{i_2j_2k_2} \\ &\quad +2\bar{\phi}^{i_1j_2k_1}\bar{\phi}^{i_2j_1k_2}\phi_{i_1j_1k_1}\phi_{i_2j_2k_2} + 2\bar{\phi}^{i_1j_1k_2}\bar{\phi}^{i_2j_2k_1}\phi_{i_1j_1k_1}\phi_{i_2j_2k_2} \end{aligned} \tag{K.1}$$

$$\begin{aligned}\mathcal{O}_{\begin{smallmatrix}\square\\\square\end{smallmatrix},\begin{smallmatrix}\square\\\square\end{smallmatrix},\square\square} &= 2\bar{\phi}^{i_1j_1k_1}\bar{\phi}^{i_2j_2k_2}\phi_{i_1j_1k_1}\phi_{i_2j_2k_2} - 2\bar{\phi}^{i_2j_1k_1}\bar{\phi}^{i_1j_2k_2}\phi_{i_1j_1k_1}\phi_{i_2j_2k_2} \\ &\quad -2\bar{\phi}^{i_1j_2k_1}\bar{\phi}^{i_2j_1k_2}\phi_{i_1j_1k_1}\phi_{i_2j_2k_2} + 2\bar{\phi}^{i_1j_1k_2}\bar{\phi}^{i_2j_2k_1}\phi_{i_1j_1k_1}\phi_{i_2j_2k_2} \end{aligned} \tag{K.2}$$

$$\begin{aligned}\mathcal{O}_{\begin{smallmatrix}\square\\\square\end{smallmatrix},\square\square,\begin{smallmatrix}\square\\\square\end{smallmatrix}} &= 2\bar{\phi}^{i_1j_1k_1}\bar{\phi}^{i_2j_2k_2}\phi_{i_1j_1k_1}\phi_{i_2j_2k_2} - 2\bar{\phi}^{i_2j_1k_1}\bar{\phi}^{i_1j_2k_2}\phi_{i_1j_1k_1}\phi_{i_2j_2k_2} \\ &\quad +2\bar{\phi}^{i_1j_2k_1}\bar{\phi}^{i_2j_1k_2}\phi_{i_1j_1k_1}\phi_{i_2j_2k_2} - 2\bar{\phi}^{i_1j_1k_2}\bar{\phi}^{i_2j_2k_1}\phi_{i_1j_1k_1}\phi_{i_2j_2k_2} \end{aligned} \tag{K.3}$$

$$\begin{aligned}\mathcal{O}_{\square\square,\begin{smallmatrix}\square\\\square\end{smallmatrix},\begin{smallmatrix}\square\\\square\end{smallmatrix}} &= 2\bar{\phi}^{i_1j_1k_1}\bar{\phi}^{i_2j_2k_2}\phi_{i_1j_1k_1}\phi_{i_2j_2k_2} + 2\bar{\phi}^{i_2j_1k_1}\bar{\phi}^{i_1j_2k_2}\phi_{i_1j_1k_1}\phi_{i_2j_2k_2} \\ &\quad -2\bar{\phi}^{i_1j_2k_1}\bar{\phi}^{i_2j_1k_2}\phi_{i_1j_1k_1}\phi_{i_2j_2k_2} - 2\bar{\phi}^{i_1j_1k_2}\bar{\phi}^{i_2j_2k_1}\phi_{i_1j_1k_1}\phi_{i_2j_2k_2} \end{aligned} \tag{K.4}$$

A simple but tedious computation confirms (5.3.1.8) and (5.3.1.9). Some sample computations are

$$\langle \mathcal{O}_{\square\square,\square\square,\square\square} \rangle = 2N_1(N_1+1)N_2(N_2+1)N_3(N_3+1) \tag{K.5}$$

$$\langle \mathcal{O}_{\square\square,\square\square,\square\square}\mathcal{O}_{\square\square,\square\square,\square\square} \rangle = 32N_1(N_1+1)N_2(N_2+1)N_3(N_3+1) \tag{K.6}$$

$$\langle \mathcal{O}_{\square\square,\square\square,\square\square}\mathcal{O}_{\square\square,\square\square,\begin{smallmatrix}\square\\\square\end{smallmatrix}} \rangle = 0 \tag{K.7}$$

For $n = 2$, the complete set of fermionic operators in the representation basis is given by

$$\begin{aligned}\mathcal{P}_{\begin{smallmatrix}\square\\\square\end{smallmatrix},\begin{smallmatrix}\square\\\square\end{smallmatrix},\begin{smallmatrix}\square\\\square\end{smallmatrix}} &= 2\bar{\psi}^{i_1j_1k_1}\bar{\psi}^{i_2j_2k_2}\psi_{i_2j_2k_2}\psi_{i_1j_1k_1} - 2\bar{\psi}^{i_1j_2k_1}\bar{\psi}^{i_2j_1k_2}\psi_{i_2j_2k_2}\psi_{i_1j_1k_1} \\ &\quad -2\bar{\psi}^{i_1j_1k_2}\bar{\psi}^{i_2j_2k_1}\psi_{i_2j_2k_2}\psi_{i_1j_1k_1} - 2\bar{\psi}^{i_2j_1k_1}\bar{\psi}^{i_1j_2k_2}\psi_{i_2j_2k_2}\psi_{i_1j_1k_1} \end{aligned} \tag{K.8}$$

$$\begin{aligned}\mathcal{P}_{\begin{smallmatrix}\square\\\square\end{smallmatrix},\square\square,\square\square} &= 2\bar{\psi}^{i_1j_1k_1}\bar{\psi}^{i_2j_2k_2}\psi_{i_2j_2k_2}\psi_{i_1j_1k_1} - 2\bar{\psi}^{i_2j_1k_1}\bar{\psi}^{i_1j_2k_2}\psi_{i_2j_2k_2}\psi_{i_1j_1k_1} \\ &\quad +2\bar{\psi}^{i_1j_2k_1}\bar{\psi}^{i_2j_1k_2}\psi_{i_2j_2k_2}\psi_{i_1j_1k_1} + 2\bar{\psi}^{i_1j_1k_2}\bar{\psi}^{i_2j_2k_1}\psi_{i_2j_2k_2}\psi_{i_1j_1k_1} \end{aligned} \tag{K.9}$$

$$\mathcal{P}_{\square\square,\begin{smallmatrix}\square\\\square\end{smallmatrix},\square\square} = 2\bar{\psi}^{i_1j_1k_1}\bar{\psi}^{i_2j_2k_2}\psi_{i_2j_2k_2}\psi_{i_1j_1k_1} + 2\bar{\psi}^{i_2j_1k_1}\bar{\psi}^{i_1j_2k_2}\psi_{i_2j_2k_2}\psi_{i_1j_1k_1}$$
$$-2\bar{\psi}^{i_1j_2k_1}\bar{\psi}^{i_2j_1k_2}\psi_{i_2j_2k_2}\psi_{i_1j_1k_1} + 2\bar{\psi}^{i_1j_1k_2}\bar{\psi}^{i_2j_2k_1}\psi_{i_2j_2k_2}\psi_{i_1j_1k_1} \tag{K.10}$$

$$\mathcal{P}_{\square\square,\square\square,\begin{smallmatrix}\square\\\square\end{smallmatrix}} = 2\bar{\psi}^{i_1j_1k_1}\bar{\psi}^{i_2j_2k_2}\psi_{i_2j_2k_2}\psi_{i_1j_1k_1} + 2\bar{\psi}^{i_2j_1k_1}\bar{\psi}^{i_1j_2k_2}\psi_{i_2j_2k_2}\psi_{i_1j_1k_1}$$
$$+2\bar{\psi}^{i_1j_2k_1}\bar{\psi}^{i_2j_1k_2}\psi_{i_2j_2k_2}\psi_{i_1j_1k_1} - 2\bar{\psi}^{i_1j_1k_2}\bar{\psi}^{i_2j_2k_1}\psi_{i_2j_2k_2}\psi_{i_1j_1k_1} \tag{K.11}$$

Some sample computations confirming (5.3.2.4) and (5.3.2.5) are

$$\langle \mathcal{P}_{\begin{smallmatrix}\square\\\square\end{smallmatrix},\begin{smallmatrix}\square\\\square\end{smallmatrix},\begin{smallmatrix}\square\\\square\end{smallmatrix}} \rangle = 2N_1(N_1-1)N_2(N_2-1)N_3(N_3-1) \tag{K.12}$$

$$\langle \mathcal{P}_{\begin{smallmatrix}\square\\\square\end{smallmatrix},\begin{smallmatrix}\square\\\square\end{smallmatrix},\begin{smallmatrix}\square\\\square\end{smallmatrix}} \mathcal{P}_{\begin{smallmatrix}\square\\\square\end{smallmatrix},\begin{smallmatrix}\square\\\square\end{smallmatrix},\begin{smallmatrix}\square\\\square\end{smallmatrix}} \rangle = 32N_1(N_1-1)N_2(N_2-1)N_3(N_3-1) \tag{K.13}$$

$$\langle \mathcal{P}_{\begin{smallmatrix}\square\\\square\end{smallmatrix},\begin{smallmatrix}\square\\\square\end{smallmatrix},\begin{smallmatrix}\square\\\square\end{smallmatrix}} \mathcal{P}_{\begin{smallmatrix}\square\\\square\end{smallmatrix},\begin{smallmatrix}\square\\\square\end{smallmatrix},\square\square} \rangle = 0 \tag{K.14}$$

L Identities Needed to Derive the Collective Field Theory Hamiltonian

Using the identity

$$\oint dy \frac{e^{-iky}}{x-y} = \epsilon(k)\pi i e^{-ikx} \tag{L.1}$$

we find

$$\oint dy \ \frac{2x\, e^{-iky}}{y-x} = 2x\epsilon(k)\pi i e^{-ikx} \tag{L.2}$$

Our main goal in this Appendix is to explain how to rewrite the term

$$T_1 = \int dx \frac{\phi(x)}{x} \oint dy_1 \frac{2x\phi(y_1)}{y_1 - x} \oint dy_2 \frac{2x\phi(y_2)}{y_2 - x} \tag{L.3}$$

in a manifestly local form. This is the only term in the Hamiltonian that is not manifestly local. Use the Fourier transform

$$\phi(x) = \int \frac{dk}{2\pi} e^{-ikx} \phi_k \tag{L.4}$$

to write (this is the only non-local term in the Hamiltonian)

$$\begin{aligned} T_1 &= \int \frac{dk_1}{2\pi} \int \frac{dk_2}{2\pi} \int \frac{dk_3}{2\pi} \int dx \phi_{k_1} \phi_{k_2} \phi_{k_3} 4x e^{-ik_1 x} \oint dy_1 \frac{e^{-ik_2 y_1}}{y_1 - x} \oint dy_2 \frac{e^{-ik_3 y_2}}{y_2 - x} \\ &= \int \frac{dk_1}{2\pi} \int \frac{dk_2}{2\pi} \int \frac{dk_3}{2\pi} \int dx \phi_{k_1} \phi_{k_2} \phi_{k_3} 4x e^{-ik_1 x} \left[\pi i \epsilon(k_2) e^{-ik_2 x}\right] \left[\pi i \epsilon(k_3) e^{-ik_3 x}\right] \\ &= -4\pi^2 \int \frac{dk_1}{2\pi} \int \frac{dk_2}{2\pi} \int \frac{dk_3}{2\pi} \int dx \phi_{k_1} \phi_{k_2} \phi_{k_3} x e^{-i(k_1+k_2+k_3)x} \epsilon(k_2)\epsilon(k_3) \end{aligned} \tag{L.5}$$

The expression on the last line can be manipulated, by renaming variables into

$$\begin{aligned} &-\frac{4\pi^2}{3} \int \frac{dk_1}{2\pi} \int \frac{dk_2}{2\pi} \int \frac{dk_3}{2\pi} \int dx \phi_{k_1} \phi_{k_2} \phi_{k_3} x e^{-i(k_1+k_2+k_3)x} (\epsilon(k_1)\epsilon(k_2) + \epsilon(k_1)\epsilon(k_3) + \epsilon(k_2)\epsilon(k_3)) \\ &= \frac{4\pi^2}{3} \int \frac{dk_1}{2\pi} \int \frac{dk_2}{2\pi} \int \frac{dk_3}{2\pi} \phi_{k_1} \phi_{k_2} \phi_{k_3} (i\partial_{k_1} \delta(k_1 + k_2 + k_3))(\epsilon(k_1)\epsilon(k_2) + \epsilon(k_1)\epsilon(k_3) + \epsilon(k_2)\epsilon(k_3)) \end{aligned} \tag{L.6}$$

Because of the delta function, one or two of the k_i's must be positive so that

$$\epsilon(k_1)\epsilon(k_2) + \epsilon(k_1)\epsilon(k_3) + \epsilon(k_2)\epsilon(k_3) = -1 \tag{L.7}$$

and we now find

$$T_1 = \frac{4\pi^2}{3} \int \frac{dk_1}{2\pi} \int \frac{dk_2}{2\pi} \int \frac{dk_3}{2\pi} \phi_{k_1} \phi_{k_2} \phi_{k_3} (i\partial_{k_1} \delta(k_1 + k_2 + k_3)) = \frac{4\pi^2}{3} \int dx x \phi^3(x) \tag{L.8}$$

so that, remarkably, this term is local and it gives rise to a cubic interaction!

References

[1] N. N. Bogoliubov and O.S. Parasiuk. On the Multiplication of Propagators in Quantum Field Theory. *Acta Math*, **97**:227–326, (1957). 3

[2] K. Hepp. Proof of the Bogoliubov-Parasiuk Theorem on Renormalisation. *Comm. Math. Phys.*, **2**:301–326, (1966). 3

[3] W. Zimmermann. Local Operator Products and Renormalisation in Quantum Field Theory. In *S. Deser, et al.*, Proceedings of the 1970 Brandeis Summer Institute in Theoretical Physics, pages 399–589, (1970). 3

[4] J.Maldacena. The Large N Limit of Superconformal Field Theories and Supergravity. *Adv. Theor. Math. Phys.*, **2**:231–252, (1998). 4, 54, 77, 106, 107

[5] G. 't Hooft. A Planar Diagram Theory for Strong Interactions. *Nucl. Phys. B*, **72**(461), (1974). 6, 10, 54

[6] J. Maldacena and A. Zhiboedov. Constraining Conformal Field Theories with a Higher Spin Symmetry. *J. Phys.*, **A46**(214011), (2013). 19

[7] S. Corley, A. Jevicki, and S. Ramgoolam. Exact Correlators of Giant Gravitons from Dual N=4 SYM Theory. *Adv. Theor. Math. Phys.*, **5**(4):809–839, (2001). 32, 54, 55, 56, 77, 78, 79, 81, 133

[8] J. McGreevy, L. Susskind, and N. Toumbas. Invasion of the Giant Gravitons from Anti de Sitter Space. *JHEP*, **0006**(008), (2000). 36, 37, 54, 78

[9] M. Green, J. Schwarz, and E. Witten. *Superstring Theory: Volume 2*. Cambridge University Press, (1987). 49

[10] D. Cerdeno and C. Munoz. An introduction to supergravity. In *Proceedings of the Corfu Summer Institute on Elementary Particle Physics*. JHEP Proceedings, (1998). 51

[11] R. de Mello Koch, D. Gossman, L. Nkumane, and L. Tribelhorn. Eigenvalue dynamics for multimatrix models. *Phys. Rev. D*, **96**(026011), (2017). 54

[12] H. Lin, O. Lunin, and J. M. Maldacena. Bubbling AdS space and 1/2 BPS geometries. *JHEP*, **0410**(025), (2004). 54, 55, 73, 77, 78, 81, 101, 102, 107, 126

[13] V. Balasubramanian et al. Giant Gravitons in Conformal Field Theory. *JHEP*, **0204**(034), (2002). 54, 77, 107

[14] A. Hashimoto, S. Hirano, and N. Itzhaki. Large branes in AdS and their field theory dual. *JHEP*, **0008**(051), (2000). 54, 55, 78

[15] M. T. Grisaru, R. C. Myers, and O. Tafjord. Susy and goliath. *JHEP*, **0008**(040), (2000). 54, 78

[16] D. Berenstein. A Toy Model for the AdS/CFT Correspondence. *JHEP*, **0407**(018), (2004). 54, 55, 56, 58, 77, 107

[17] E. Brezin, C. Itzykson, G. Parisi, and J. B. Zuber. Planar diagrams. *Commun. Math. Phys.*, **59**(35), (1978). 54, 55, 56

[18] J. Ginibre. Statistical Ensembles of Complex, Quaternion and Real Matrices. *J. Math. Phys.*, **6**(440), (1965). 54, 55, 56, 61

[19] A. Jevicki and B. Sakita. The quantum collective field method and its application to the planar limit. *Nucl. Phys. B*, **165**(511), (1980). 54

[20] A. Jevicki and B. Sakita. Collective field approach to the large N limit: Euclidean field theories. *Nucl. Phys. B*, **185**(89), (1981). 54

[21] K. Demeterfi, A. Jevicki, and J. P. Rodrigues. Scattering amplitudes and loop corrections in collective string field theory. *Nucl. Phys. B*, **362**(173), (1991). 54

[22] K. Demeterfi, A. Jevicki, and J. P. Rodrigues. Scattering amplitudes and loop corrections in collective string field theory 2. *Nucl. Phys. B*, **365**(499), (1991). 54

[23] K. Demeterfi, A. Jevicki, and J. P. Rodrigues. Perturbative results of collective string field theory. *Mod. Phys. Lett. A*, **6**(3199), (1991). 54

[24] A. Donos, A. Jevicki, and J. P. Rodrigues. Matrix model maps in AdS/CFT. *Phys. Rev. D*, **72**(125009), (2005). 54

[25] M. Masuku and J. P. Rodrigues. Laplacians in polar matrix coordinates and radial fermionization in higher dimensions. *J. Math. Phys.*, **52**(032302), (2011). 55, 123

[26] Y. Kimura, S. Ramgoolam, and D. Turton. Free particles from brauer algebras in complex matrix models. *JHEP*, **1005**(052), (2010). 55

[27] M. Masuku and J. P. Rodrigues. How universal is the Wigner distribution? *J. Phys. A*, **45**(085201), (2012). 55, 123

[28] M. Mulokwe M. Masuku and J. P. Rodrigues. Large N matrix hyperspheres and the gauge-gravity correspondence. *JHEP*, **1512**(035), (2015). 55, 123

[29] M. Masuku and J. P. Rodrigues. De Alfaro, Fubini and Furlan from multi matrix systems. *JHEP*, **1512**(175), (2015). 55, 123

[30] C. Kristjansen, J. Plefka, G. W. Semenoff, and M. Staudacher. A new double scaling limit o f$N = 4$ super Yang-Mills theory and PP wave strings. *Nucl. Phys. B*, **643**(3), (2002). 55, 61

[31] Y. Takayama and A. Tsuchiya. Complex matrix model and fermion phase space for bubbling AdS geometries. *JHEP*, **0510**(004), (2005). 55

[32] V. Balasubramanian, D. Berenstein, B. Feng, and M. X. Huang. D-branes in Yang-Mills theory and emergent gauge symmetry. *JHEP*, **0503**(006), (2005). 57, 78, 107

[33] R. Bhattacharyya, S. Collins, and R. d. M. Koch. Exact multi-matrix correlators. *JHEP*, **0803**(044), (2008). 57, 78, 79, 81, 84, 85, 87

[34] R. Bhattacharyya, R. de Mello Koch, and M. Stephanou. Exact Multi-Restricted Schur Polynomial Correlators. *JHEP*, **0806**(101), (2008). 57, 78, 79, 81, 85

[35] V. De Comarmond, R. de Mello Koch, and K. Jefferies. Surprisingly simple spectra. *JHEP*, **1102**(006), (2011). 57, 79, 95

[36] R. de Mello Koch, M. Dessein, and D. Giataganas et al. Giant Graviton Oscillators. *JHEP*, **1007**(009), (2011). 57, 58, 70, 83, 104, 107

[37] R. de Mello Koch and S. Ramgoolam. A double coset ansatz for integrability in AdS/CFT. *JHEP*, **1206**(083), (2012). 57, 70, 83, 104, 107, 137

[38] D. Berenstein. Large N BPS states and emergent quantum gravity. *JHEP*, **0601**(125), (2006). 58, 76

[39] D. Berenstein and R. Cotta. Aspects of emergent geometry in the AdS/CFT context. *Phys. Rev. D*, **74**(026006), (2006). 58, 76

[40] D. Berenstein and R. Cotta. A Monte-Carlo study of the AdS/CFT correspondence: An exploration of quantum gravity effects. *JHEP*, **0704**(071), (2007). 58, 75, 76

[41] D. Berenstein, R. Cotta, and R. Leonardi. Numerical tests of AdS/CFT at strong coupling. *Phys. Rev. D*, **78**(025008), (2008). 58, 76

[42] D. Berenstein. A strong coupling expansion for $N = 4$ SYM theory and other SCFT's. *Int. J. Mod. Phys. A*, **23**(2143), (2008). 58, 76

[43] D. Berenstein and Y. Nakada. The shape of emergent quantum geometry from an $N = 4$ SYM minisuperspace approximation. *arXiv:1001.4509 [hep-th]*, 2010. 58, 76

[44] D. Berenstein. Sketches of emergent geometry in the gauge/gravity duality. *Fortsch. Phys.*, **62**(776), (2014). 58, 76

[45] V. Balasubramanian, J. de Boer, V. Jejjala, and J. Simon. The library of Babel: On the origin of gravitational thermodynamics. *JHEP*, **0512**(006), (2005). 58, 75

[46] S.E.Vazquez. Reconstructing 1/2 BPS space-time metrics from matrix models and spin chains. *Phys. Rev. D*, **75**(125012), (2007). 58

[47] H. Y. Chen, D. H. Correa, and G. A. Silva. Geometry and topology of bubble solutions from gauge theory. *Phys. Rev. D*, **76**(026003), (2007). 58, 101

[48] R. de Mello Koch. Geometries from Young diagrams. *JHEP*, **0811**(061), (2008). 58, 67, 78

[49] S. Lee, S. Minwalla, M. Rangamani, and N. Seiberg. Three point functions of chiral operators in $D = 4$, $N = 4$ SYM at large N. *Adv. Theor. Math. Phys.*, **2**(697), (1998). 59

[50] S. Corley and S. Ramgoolam. Finite factorization equations and sum rules for BPS correlators in $N = 4$ SYM theory. *Nucl. Phys. B*, **641**(131), (2002). 61

[51] R. C. Myers and O. Tafjord. Superstars and giant gravitons. *JHEP*, **0111**(009), (2001). 67

[52] A. Donos. A description of 1/4 BPS configurations in minimal type IIB SUGRA. *Phys. Rev. D*, **75**(025010), (2007). 71, 72

[53] A. Donos. BPS states in type IIB SUGRA with SO(4) x SO(2)(gauged) symmetry. *JHEP*, **0705**(072), (2007). 71

[54] B. Chen, S. Cremonini, A. Donos, F. L. Lin, H. Lin, J. T. Liu, D. Vaman, and W. Y. Wen. Bubbling AdS and droplet descriptions of BPS geometries in IIB supergravity. *JHEP*, **0710**(003), (2007). 71

[55] O. Lunin. Brane webs and 1/4-BPS geometries. *JHEP*, **0809**(028), (2008). 71, 72

[56] S. R. Das and A. Jevicki. String field theory and physical interpretation of $D = 1$ strings. *Mod. Phys. Lett. A*. 75, 107, 119, 121

[57] D. Berenstein. Strings on conifolds from strong coupling dynamics, part I. *JHEP*, **0804**(002), (2008). 76

[58] D. E. Berenstein and S. A. Hartnoll. Strings on conifolds from strong coupling dynamics: Quantitative results. *JHEP*, **0803**(072), (2008). 76

[59] D. E. Berenstein, M. Hanada, and S. A. Hartnoll. Multi-matrix models and emergent geometry. *JHEP*, **0902**(010), (2009). 76

[60] R. de Mello Koch, P. Diaz, and H. Soltanpanahi. Non-planar anomalous dimensions in the sl(2) sector. *Phys. Lett. B*, **713**(509), (2012). 76, 88, 107

[61] R. de Mello Koch, P. Diaz, and N. Nokwara. Restricted Schur Poynomials for Fermions and Integrability in the su(2-3) Sector. *JHEP*, **1303**(173), (2013). 76, 88, 107

[62] J. Smolic R. de Mello Koch and M. Smolic. Giant Gravitons – with Strings Attached (I). **0706**(074), (2007). 76, 79, 84, 107, 111, 144

[63] J. Smolic R. de Mello Koch and M. Smolic. Giant Gravitons – with Strings Attached (II). *JHEP*, **0709**(049), (2007). 76, 79

[64] D. Bekker, R. de Mello Koch, and M. Stephanou. Giant gravitons - with strings attached III. *JHEP*, **0802**(029), (2008). 76

[65] R. de Mello Koch, H. Jia-Hui, and L. Tribelhorn. Exciting LLM Geometries. *JHEP*, **1807**(146), (2018). 77

[66] J. A. Minahan and K. Zarembo. The Bethe ansatz for $\mathcal{N} = 4$ super Yang-Mills. *JHEP*, **0303**(013), (2003). 77

[67] N. Gromov, V. Kazakov, S. Leurent, and D. Volin. Quantum spectral curve for planar $\mathcal{N} = 4$ super-Yang-Mills theory. *Phys. Rev. Lett.*, **112**(011602), (2014). 77

[68] N. Beisert *et al.* Review of AdS/CFT integrability: An overview. *Lett. Math. Phys.*, **99**(3), (2012). 77

[69] S. S. Gubser, I. R. Klebanov, and A. M. Polyakov. Gauge theory correlators from non-critical string theory. *Phys. Lett. B*, **428**(105), (1998). 77

[70] E. Witten. Anti-de Sitter space and holography. *Adv. Theor. Math. Phys.*, **2**(253), (1998). 77

[71] D. Berenstein, D. H. Correa, and S. E. Vazquez. All loop BMN state energies from matrices. *JHEP*, **0602**(048), (2006). 77

[72] D. M. Hofman and J. M. Maldacena. Giant magnons. *J. Phys. A*, **39**(13095), (2006). 77

[73] N. Beisert. The SU(2—2) dynamic S-matrix. *Adv. Theor. Math. Phys.*, **12**(945), (2008). 77

[74] E. Brezin, C. Itzykson, G. Parisi, and J. B. Zuber. Planar diagrams. *Commun. Math. Phys.*, **59**(35), (1978). 77

[75] R. de Mello Koch, C. Mathwin, and H. J. R. van Zyl. LLM Magnons. *JHEP*, **1603**(110), (2016). 78, 79, 80, 82, 94, 95

[76] R. de Mello Koch, M. Kim, and H. J. R. Zyl. Integrable Subsectors from Holography. *JHEP*, **1805**(198), (2018). 78, 79, 80, 82, 95

[77] V. Balasubramanian, M. x. Huang, T. S. Levi, and A. Naqvi. Open strings from $\mathcal{N} = 4$ super Yang-Mills. *JHEP*, **0208**(037), (2002). 78

[78] D. Berenstein and A. Miller. Code subspaces for LLM geometries. *Class. Quant. Grav.*, **35**(065003), (2018). 78

[79] D. Berenstein and A. Miller. Superposition induced topology changes in quantum gravity. *JHEP*, **1711**(121), (2017). 78

[80] H. Lin and K. Zeng. Detecting topology change via correlations and entanglement from gauge/gravity correspondence. *J. Math. Phys.*, (**59**), (2018). 78

[81] J. Simon. Correlations vs connectivity in $\mathcal{R}$-charge. *JHEP*, **1810**(048), (2018). 78, 101

[82] R. de Mello Koch, N. H. Tahiridimbisoa, and C. Mathwin. Anomalous dimensions of heavy operators from magnon energies. *JHEP*, **1603**(156), (2016). 79, 95, 107

[83] Y. Kimura. Correlation functions and representation bases in free $\mathcal{N} = 4$ super Yang-Mills. *Nucl. Phys. B*, **865**(568), (2012). 79, 107

[84] T. W. Brown. Permutations and the Loop. *JHEP*, **0806**. 79

[85] M. Kim and H. J. R. van Zyl. Semiclassical SL(2) strings on LLM backgrounds. *Physics Letters B*, **784**, (2018). 80, 95

[86] D. Garner, S. Ramgoolam, and C. Wen. Thresholds of large N factorization in CFT_4: exploring bulk spacetime in AdS_5. *JHEP*, **1411**(076), (2014). 86

[87] R. de Mello Koch, G. Kemp, B. A. E. Mohammed, and S. Smith. Nonplanar integrability at two loops. *JHEP*, **1210**(144), (2012). 98

[88] R. de Mello Koch, T. K. Dey, N. Ives, and M. Stephanou. Hints of integrability beyond the planar limit: Nontrivial backgrounds. *JHEP*, **1001**(014), (2010). 101

[89] H. Lin, A. Morisse, and J. P. Shock. Strings on bubbling geometries. *JHEP*, **1006**(055), (2010). 101

[90] P. Diaz, H. Lin, and A. Veliz-Osorio. Graph duality as an instrument of gauge-string correspondence. **57**(052302), (2016). 101

[91] S. Ryu and T. Takayanagi. Holographic derivation of entanglement entropy from AdS/CFT. *Phys. Rev. Lett.*, **96**(181602), (2006). 101

[92] M. Van Raamsdonk. Building up spacetime with quantum entanglement. *Gen. Rel. Grav.*, **42**(2323), (2010). [Int. J. Mod. Phys. D **19**, 2429 (2010)]. 101

[93] W. Carlson, R. de Mello Koch, and H. Lin. Nonplanar integrability. *JHEP*, **1103**(105), (2011). 104, 107

[94] R. de Mello Koch and M. Kim. in progress. 104

[95] B. Eden, Y. Jiang, D. le Plat, and A. Sfondrini. Colour-dressed hexagon tessellations for correlation functions and non-planar corrections. *JHEP*, (170), (2018). 105

[96] T. Bargheer, J. Caetano, T. Fleury, S. Komatsu, and P. Vieira. Handling handles I: Nonplanar integrability. *arXiv:1711.05326 [hep-th]*, 2017. 105

[97] B. Eden, Y. Jiang, M. de Leeuw, T. Meier, D. l. Plat, and A. Sfondrini. Positivity of hexagon perturbation theory. *JHEP*, **1811**(097), (2018). 105

[98] V. Balasubramanian, J. de Boer, V. Jejjala, and J. Simon. Entropy of near-extremal black holes in AdS_5. *JHEP], volume =* **0805***, number = 067, year = (2008).* 105

[99] R. Fareghbal, C. N. Gowdigere, A. E. Mosaffa, and M. M. Sheikh-Jabbari. Nearing extremal intersecting giants and new decoupled sectors in $\mathcal{N} = 4$ SYM. *JHEP*, **0808**(070), (2008). 105

[100] T. Harmark, K. R. Kristjansson, and M. Orselli. Matching gauge theory and string theory in a decoupling limit of AdS/CFT. *JHEP*, **0902**(027), (2009). 105

[101] J. de Boer, M. Johnstone, M. M. Sheikh-Jabbari, and J. Simon. Emergent IR dual 2d CFTs in charged AdS_5 black holes. *Phys. Rev. D*, **85**(084039), (2012). 105

[102] M. Johnstone andM. M. Sheikh-Jabbari, J. Simon, and H. Yavartanoo. Near-extremal vanishing horizon AdS_5 black holes and their CFT duals. *JHEP*, **1304**(045), (2013). 105

[103] R. de Mello Koch, D. Gossman, and L. Tribelhorn. Gauge invariants, correlators and holography in bosonic and fermionic tensor models. *JHEP*, **1709**(011), (2017). 106

[104] A. Kitaev. A simple model of quantum holography. *talks at KITP*. April 7 2015 and May 27 2015. 106

[105] S. Sachdev and J. Ye. Gapless spin fluid ground state in a random, quantum Heisenberg magnet. *Phys. Rev. Lett.*, **70**(3339), (1993). 106

[106] J. Polchinski and V. Rosenhaus. The spectrum in the Sachdev-Ye-Kitaev model. *JHEP*, **1604**(001), (2016). 106

[107] A. Jevicki, K. Suzuki, and J. Yoon. Bi-local holography in the SYK model. *JHEP*, **1607**(007), (2016). 106, 107

[108] J. Maldacena and D. Stanford. Remarks on the Sachdev-Ye-Kitaev model. *Phys. Rev. D*, **94**(106002), (2016). 106

[109] A. Jevicki and K. Suzuki. Bi-local holography in the SYK model: Perturbations. *JHEP*, **1611**(046), (2016). 106, 107

[110] J. Maldacena, S. H. Shenker, and D. Stanford. A bound on chaos. *JHEP*, **1608**(106), (2016). 106

[111] E. Witten. An SYK-like model without disorder. *arXiv:1610.09758 [hep-th]*, 2016. 106

[112] R. Gurau. The complete $1/N$ expansion of an SYK–like tensor model. *Nucl. Phys. B*, **916**(386), (2017). 106

[113] I. R. Klebanov and G. Tarnopolsky. Uncolored random tensors, melon diagrams, and the Sachdev-Ye-Kitaev models. *Phys. Rev. D*, **95**(046004), (2017). 106

[114] F. Ferrari. The large D limit of planar diagrams. *arXiv:1701.01171 [hep-th]*, 2017. 106

[115] H. Itoyama, A. Mironov, and A. Morozov. Rainbow tensor model with enhanced symmetry and extreme melonic dominance. *Phys. Lett. B*, **771**(180), (2017). 106

[116] S. Carrozza and A. Tanasa. $O(N)$ random tensor models. *Lett. Math. Phys.*, **106**(1531), (2016). 106

[117] J. Yoon. SYK models and SYK-like tensor models with global symmetry. *JHEP*, **1007**(183), (2017). 106

[118] R. Gurau. Invitation to random tensors. *SIGMA*, **12**(094), (2016). 106

[119] R. Gurau. The 1/N expansion of colored tensor models. *Annales Henri Poincare*, **12**(829), (2011). 106

[120] A. Jevicki and B. Sakita. The quantum collective field method and its application to the planar limit. *Nucl. Phys. B*, **165**(511), (1980). 106, 119, 121

[121] A. Jevicki and B. Sakita. Collective field approach to the large N limit: Euclidean field theories. *Nucl. Phys. B*, **185**(89), (1981). 106, 119, 121

[122] S. Corley, A. Jevicki, and S. Ramgoolam. Exact correlators of giant gravitons from dual $\mathcal{N} = 4$ SYM theory. *Adv. Theor. Math. Phys.*, **5**(809), (2002). 107, 108

[123] S. Corley and S. Ramgoolam. Finite factorization equations and sum rules for BPS correlators in $\mathcal{N} = 4$ SYM theory. *Nucl. Phys. B*, **641**(131), (2002). 107, 108

[124] R. de Mello Koch, G. Kemp, and S. Smith. From large N nonplanar anomalous dimensions to open spring theory. *Phys. Lett. B*. 107

[125] R. de Mello Koch and J. P. Rodrigues. Systematic 1/N corrections for bosonic and fermionic vector models without auxiliary fields. *Phys. Rev. D*, **54**(7794), (1996). 107

[126] S. R. Das and A. Jevicki. Large N collective fields and holography. *Phys. Rev. D*, **68**(044011), (2003). 107

[127] I. R. Klebanov and A. M. Polyakov. AdS dual of the critical O(N) vector model. *Phys. Lett. B*, **550**(213), (2002). 107

[128] R. de Mello Koch, A. Jevicki, K. Jin, and J. P. Rodrigues. AdS_4/CFT_3 construction from collective fields. *Phys. Rev. D*, **83**(025006), (2011). 107

[129] R. de Mello Koch, A. Jevicki, J. P. Rodrigues, and J. Yoon. Canonical formulation of $O(N)$ vector/higher spin correspondence. *J. Phys. A*, **48**(105403), (2015). 107

[130] S. R. Das, A. Jevicki, and K. Suzuki. Three dimensional view of the SYK/AdS duality. *JHEP*, **1709**(017), (2017). 107

[131] W. Fu, D. Gaiotto, J. Maldacena, and S. Sachdev. Supersymmetric Sachdev-Ye-Kitaev models. *Phys. Rev. D*, **95**(069904), (2017). 107

[132] C. Peng, M. Spradlin, and A. Volovich. A supersymmetric SYK-like tensor model. *JHEP*, **1705**(062), (2017). 107

[133] M. Spradlin C. Pen and and A. Volovich. Correlators in the $\mathcal{N} = 2$ supersymmetric SYK model. *JHEP*, **1710**(202), 2017. 107

[134] J. Murugan, D. Stanford, and E. Witten. More on supersymmetric and 2d analogs of the SYK model. *JHEP*, **1708**(146), 2017. 107

[135] J. Yoon. Supersymmetric SYK model: Bi-local collective superfield/supermatrix formulation. *JHEP*, **1710**(172), 2017. 107

[136] J. Ben Geloun and S. Ramgoolam. Counting tensor model observables and branched covers of the 2-sphere. *arXiv:1307.6490 [hep-th]*, 2013. 107, 110, 120

[137] A. Mironov and A. Morozov. Correlators in tensor models from character calculus. *Phys. Lett. B.*, **774**, number = 063, year = 2017. 107

[138] R. de Mello Koch and S. Ramgoolam. From matrix models and quantum fields to Hurwitz space and the absolute Galois group. *arXiv:1002.1634 [hep-th]*, 2010. 107

[139] P. Diaz and S. J. Rey. Orthogonal bases of invariants in tensor models. *JHEP*, **1802**(089), 2018. 107, 112

[140] J. F. Willenbring M.W. Hero. Stable Hilbert series as related to the measurement of quantum entanglement. *Discrete Math.*, **309**(23-24), (2009). 107, 112

[141] J. Pasukonis and S. Ramgoolam. Quivers as calculators: Counting, correlators and Riemann surfaces. *JHEP*, **1304**(094), (2013). 111

[142] P. Mattioli and S. Ramgoolam. *Phys. Rev. D*, **93**(Permutation Centralizer Algebras and Multi-Matrix Invariants), (2016). 117

[143] A. Jevicki. Nonperturbative collective field theory. *Nucl. Phys. B*, **376**(75), (1992). 119

[144] R. de Mello Koch, N. Ives, and M. Stephanou. Correlators in nontrivial backgrounds. *Phys. Rev. D*, **79**(026004), (2009). 143

[145] R. de Mello Koch, T. K. Dey, N. Ives, and M. Stephanou. Correlators of operators with a large $\mathcal{R}$-charge. *JHEP*, **0908**(083), (2009). 146